

RadarConf'22

2022 IEEE RADAR CONFERENCE



... Where Radar Innovation Never Sleeps



Radar Summer School

Saturday March 19th 2022

Sunday March 20th 2022



Daily Schedule

Saturday, March 19th

Time	Title	Instructor
8:45 – 9:00	Opening Ceremony	Nathan Goodman
9:00 - 10:00	The Story of Radar: The Interwar Years	Greg Coxson
10:00 – 10:30	Break	
10:30 - 12:00	Introduction to Radar Systems	Justin Metcalf
12:00 – 13:45	Break	
13:45 – 14:45	Estimation and Detection	Christ Richmond
15:00 – 16:00	Radar Imaging	Armin Doerry
16:00 – 16:30	Break	
16:30 – 17:30	Low Cost Radar Demonstration	John Stralka and Frank Robey

Sunday, March 20th

Time	Title	Instructor
9:00 - 10:00	Target Tracking	James Nesteroff
10:15 – 11:15	Space Time Adaptive Processing	William Melvin
11:15 – 11:45	Break	
11:45 – 12:45	Meteorological Radars	Pavlos Kollias
12:45 – 14:30	Break	
14:30 – 15:30	Digital Array Radars	Kenneth O'Haver
15:30 – 16:00	Break	
16:00 – 17:00	Low Cost Radar Demonstration	John Stralka and Frank Robey

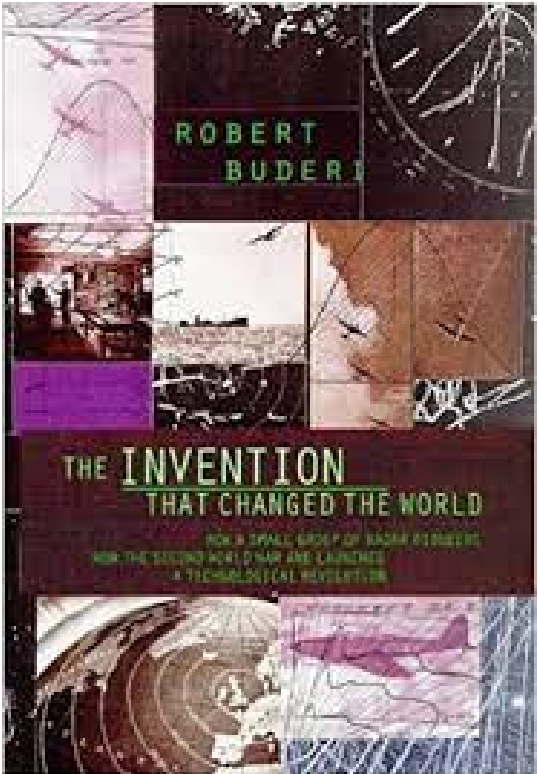
Story of Radar – The Interwar Years

Greg Coxson, ECE Department
United States Naval Academy
Annapolis, Maryland

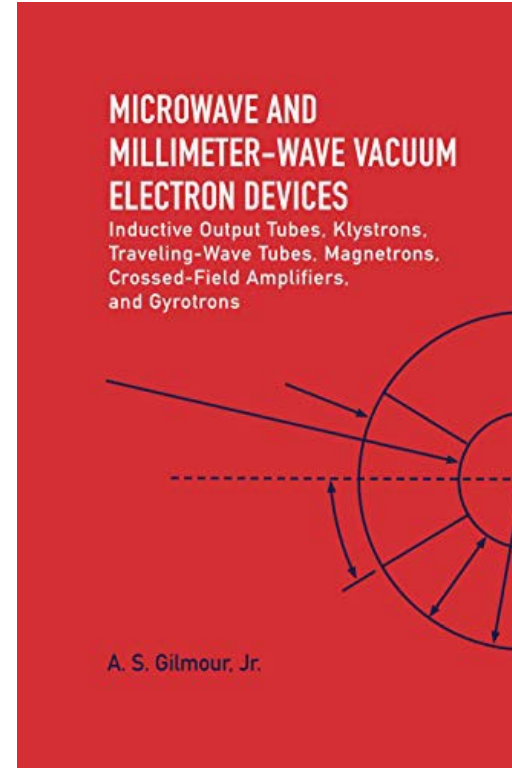
The Interwar Years Make a Terrific Radar Story

- Numerous accidental discoveries
 - Each time, met with inability to gain financial backing
- Then, 1933 and the German threat
 - Necessity led to serendipity and success
 - .. and funding!
- The radar story often centers on events in Great Britain
 - Others contributed, as well
 - Let's review the well-told story of Radar
 - Then, back up and fill in some of the background figures and developments

Recommended Resources



Robert Buderi
“The Invention that Changed the World”
(Simon & Schuster, 1998)

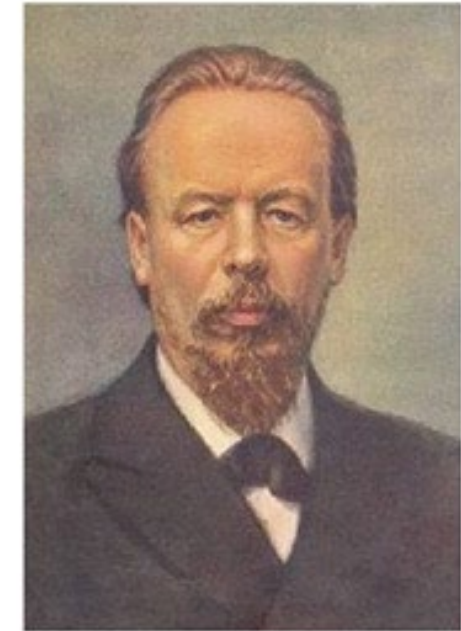


A.S. Gilmour
“Microwave and Millimeter-Wave Devices”
(ArTech House, 2020)

An Early Detection by Beat Frequency

Alexander Stepanovich Popov (1859-1906)

- 1897: Noted interference beat caused in a radio communication set by passage of a vessel between two ships
- conceived of a system to detect objects remotely



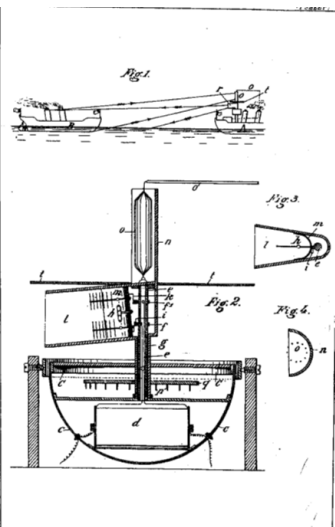
Изобретатель радио профессор
Александр Степанович Попов (1859 – 1905)

Radar was an Invention ``In the Air'' ..

1904 -- First Radar Patent



Christian Hülsmeyer
(German inventor;
1881-1957)



First Radar Patent, 1904

Hülsmeyer:

- ``One ship can detect another ship using radio waves!''
At night or in fog!
Can be used for collision avoidance in harbors!
- Conducted public demonstrations
Germany, Holland
- Patented his device in several countries (1904)
But the invention failed to attract sponsors, and
It withered on the vine

1922 -- Serendipity on the Potomac

In the **autumn of 1922**, A.H. Taylor and L.C. Young of the Navy's Aircraft Radio Laboratory (ARL), soon to be part of the new Naval Research Lab, demonstrated detection of a wooden ship using a CW wave-interference radar, at Haynes Point in Washington DC.



Taylor (1879-1961)
and Young (1891-1981)

1930 – Hyland Unexpectedly Detects Aircraft

Young with the assistance of associate engineer **Lawrence ("Pat") Hyland** began field testing high-frequency beams used to guide aircraft. During calibration, after briefly testing new direction-finding equipment at Bolling Field, a **Vought Corsair** flying overhead noticeably influenced the signals being read by Young.

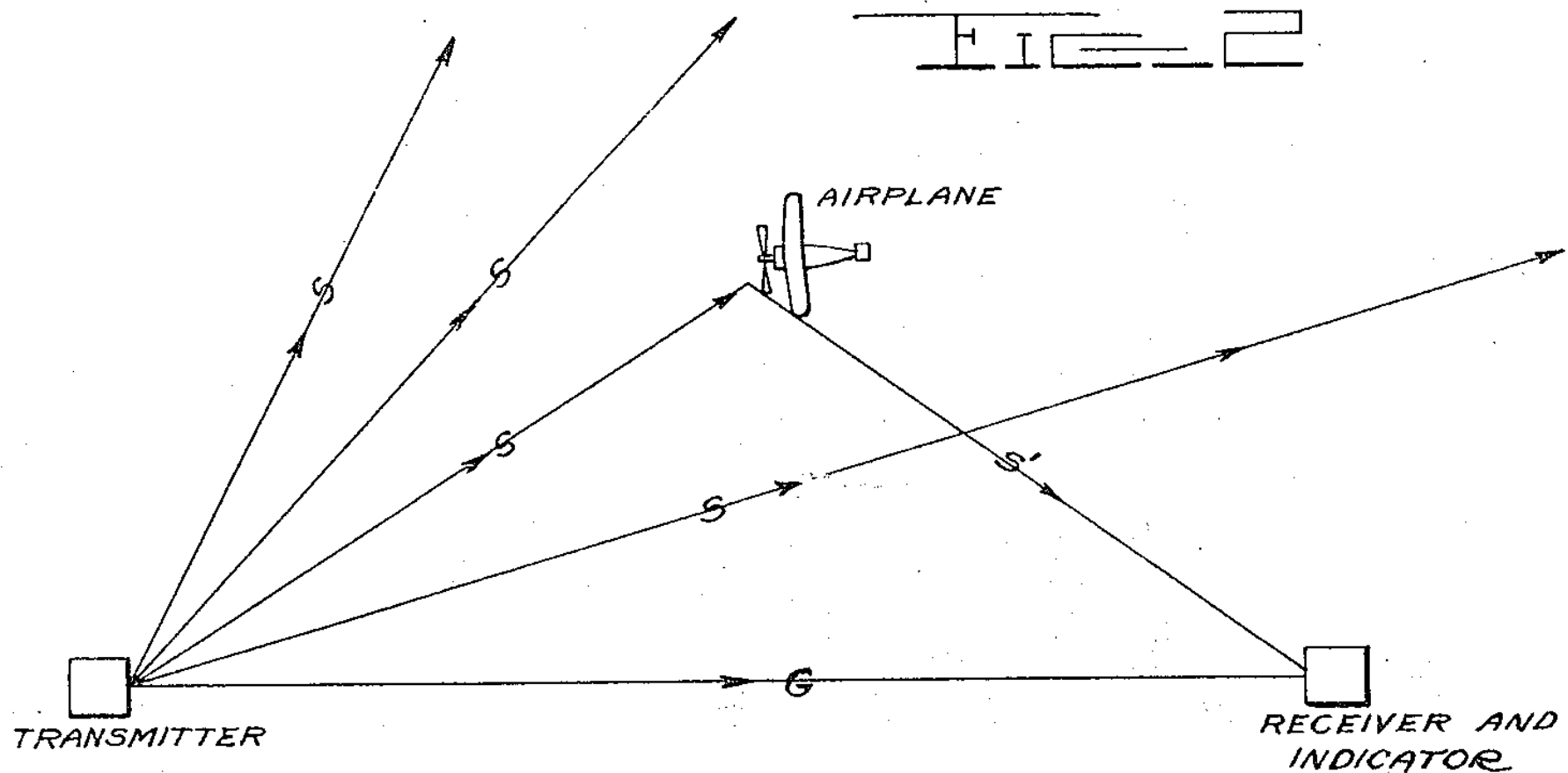


Pat Hyland
(1897-1989)



Vought O2U Corsair

Figure from US1981884 ("System for Detecting Objects by Radio"), Filed 6/13/1933 by NRL's A.H. Taylor



.. But Not Allowed to Land

Hulsmeyer:

- ``One ship can detect another ship using radio waves!''
 - At night or in fog!
 - Can be used for collision avoidance in harbors!
- Conducted public demonstrations
 - Germany, Holland
- Patented his device in several countries (1904)
- After all that, the invention failed to attract sponsors
 - It withered on the vine.

Taylor (after Haynes Point, 1922)

So emphatic was Taylor, he penned a letter to the Bureau of Engineering explaining in detail their discovery and its **practical use in identifying enemy vessels regardless of darkness, fog or other visual inhibitors**, particularly for use in safeguarding Navy vessels traveling miles apart on open waters.

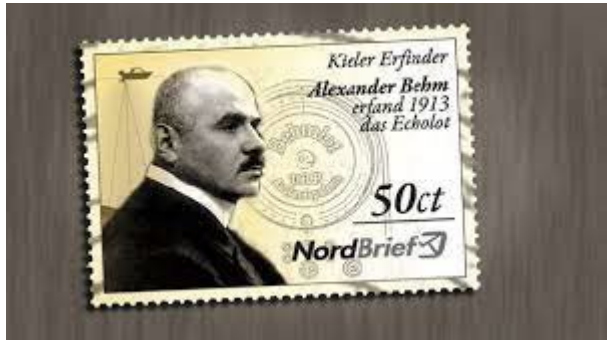
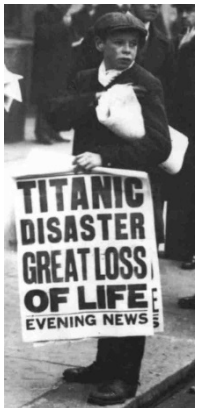
Unfortunately, neither the Navy nor the Bureau showed interest, and Taylor and Young shelved the project in favor of more demanding projects.

1936 – Finally, Funding (for Taylor)

Taylor had never stopped arguing for work on radio detection of aircraft.

In **June, 1936**, a demonstration for a group of visiting admirals included Adm. Harold R. Stark, Chief of Naval Operations and Rear Adm. Harold G. Bowen, Chief of the Bureau of Engineering — later to become one of radar's most enthusiastic supporters — **resulted in the problem of radio detection being awarded the necessary funding and the highest possible priority within the Naval Research Laboratory.**

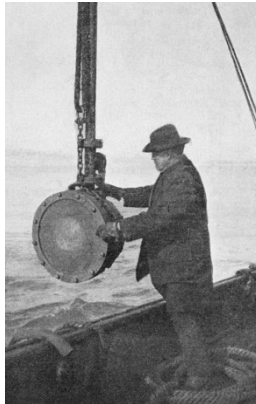
Sonar Attracts More Interest



Alexander Behm
(1880-1952) – Echo
Sounder (1913)



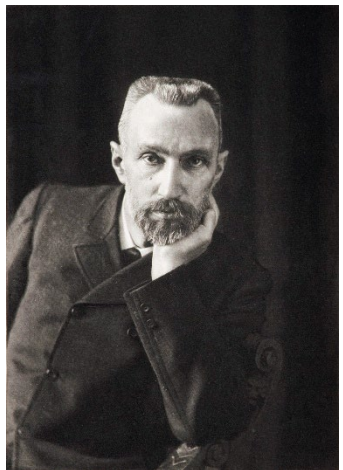
Lewis Nixon
(1861-1941) – one
of first sonar-like
devices (1906)



Reginald
Fessenden
(1866-1932)
Fessenden
Oscillator
(1912)



Robert Boyle
(1883-1955)



Pierre Curie
(1859-1906)

Paul Langevin
(1872-1946) – first
device for sonar
detection of
submarines (1915)

The Terrifying Legacy of World War I

Strategic bombing during World War I introduced air attacks intended to panic civilian targets, and led in 1918 to the amalgamation of British army and navy air services into the Royal Air Force.



"The bomber will always get through" was a phrase used by Stanley Baldwin in a 1932 speech "A Fear for the Future" given to the British Parliament. His speech stated that contemporary bomber aircraft had the performance necessary to conduct a strategic bombing campaign that would destroy a country's cities and **there was little that could be done in response.**



Before the advent of radar, the only practicable means of aircraft detection was acoustic. A network of acoustic detectors was built in the 1920s and 1930s on the south and east coasts of the UK. Some still remain.

In calm air conditions, detection ranges of up to 25 km were achievable.

“A Terrible Process is astir. Germany is arming”*

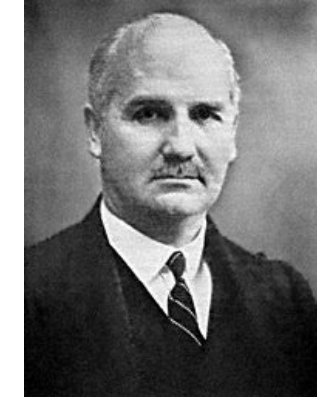


Sir Winston Churchill
(1874-1965)

The 1930s were Churchill’s “Wilderness Years”. Nonetheless, he advocated for developing military technology, especially to counter Germany’s concerning military build-up.

An appeaser is one who feeds a crocodile – hoping it will eat him last.

Let our advance worrying become advance thinking and planning.



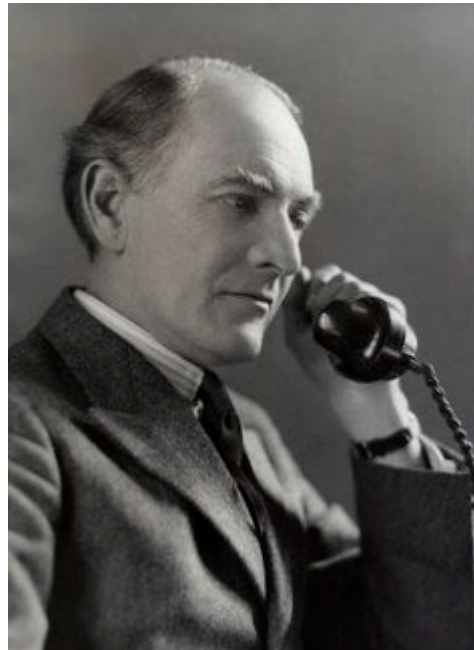
Frederick Lindemann
(1886-1957)

Churchill became PM in 1940 and named Lindemann his scientific advisor

*Churchill observation after **1932 road trip** in Europe, with Lindemann.

How About a Death Ray Against Air Threats?

H.E Wimperis, who had been instrumental in setting up the Committee for The Scientific Survey of Air Defence (CSSAD), suggested they ask Watson-Watt (whom he had known at university), to comment on reports of a German Death Ray based on radio.



H.E. ('Harry') Wimperis
(1876-1960)



Robert Watson-Watt
(1892-1973)

January, 1935 – Robert Watson Watt was working as a chief scientist at a meteorological station at Slough. He was known for his 1920s development of Huff-Duff (short for ‘‘High-Frequency Direction Finding’’)

Watson-watt to new assistant Arnold Wilkins:

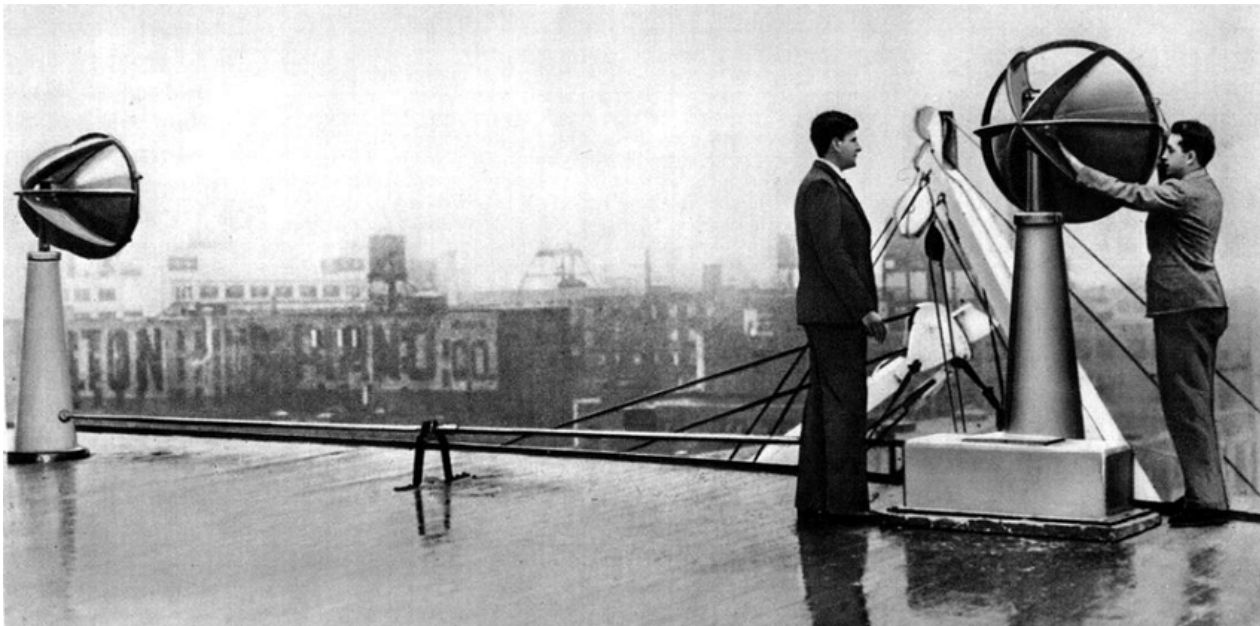
‘‘Please calculate the amount of High Frequency power which should be radiated to raise the temperature of eight pints of water from 98°F to 105°F at a distance of 5km and a height of 1km’’

Wilkins’s calculations showed that this would not work, but that it might be possible to detect an incoming aircraft at a distance of 5km.



'Skip' Wilkins
(1907-1985)

Unexpected Source of Inspiration



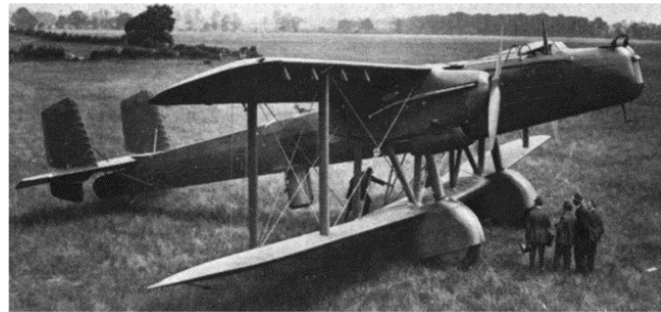
Obstacle detector radar on the deck of the S.S. Normandie, in New York harbor, 1935. It was designed for iceberg detection. (Henri Gutton* depicted on left)

* (Henri and Camille Gutton were father and son)

1935: News items about a French radio-based obstacle detection system on luxury liner SS Normandie were noticed independently by British (Randall and Boot at U. Birmingham) and American radar development teams (Robert Page at NRL; Irving Wolff at RCA). This spurred them to speed up their development efforts.

Skip is Johnny on the Spot -- The Daventry Experiment (26 February 1935)

For the critical proof of concept, Wilkins cobbled together a test system. Despite the damp weather .. success!



The target:
Handley Page
Heyford Bomber

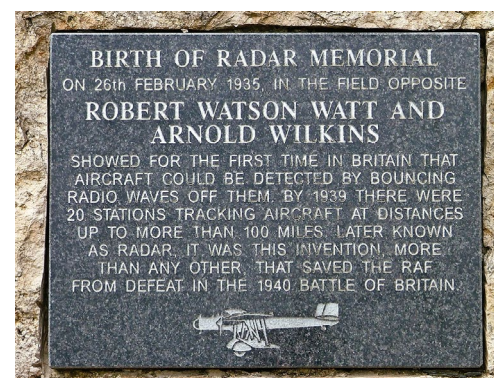


The test lab --
a converted
ambulance

The source -- a
BBC Short-Wave
Transmitter



The radio receiver



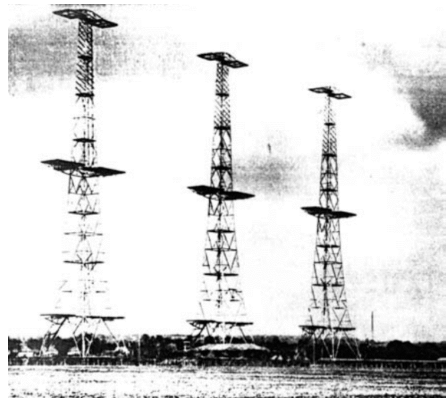
Daventry needed a cover story!

Paddy Heazell, **Most Secret – The Hidden History of Orford Ness** (The History Press, 2010):

Wilkins (to Watson-Watt, the day before the experiment): "These activities are going to arouse the curiosity of the Station. What must I say when people ask me what I am doing"

Watson-Watt: "Oh. Just say you are doing a DF [direction finding] experiment."

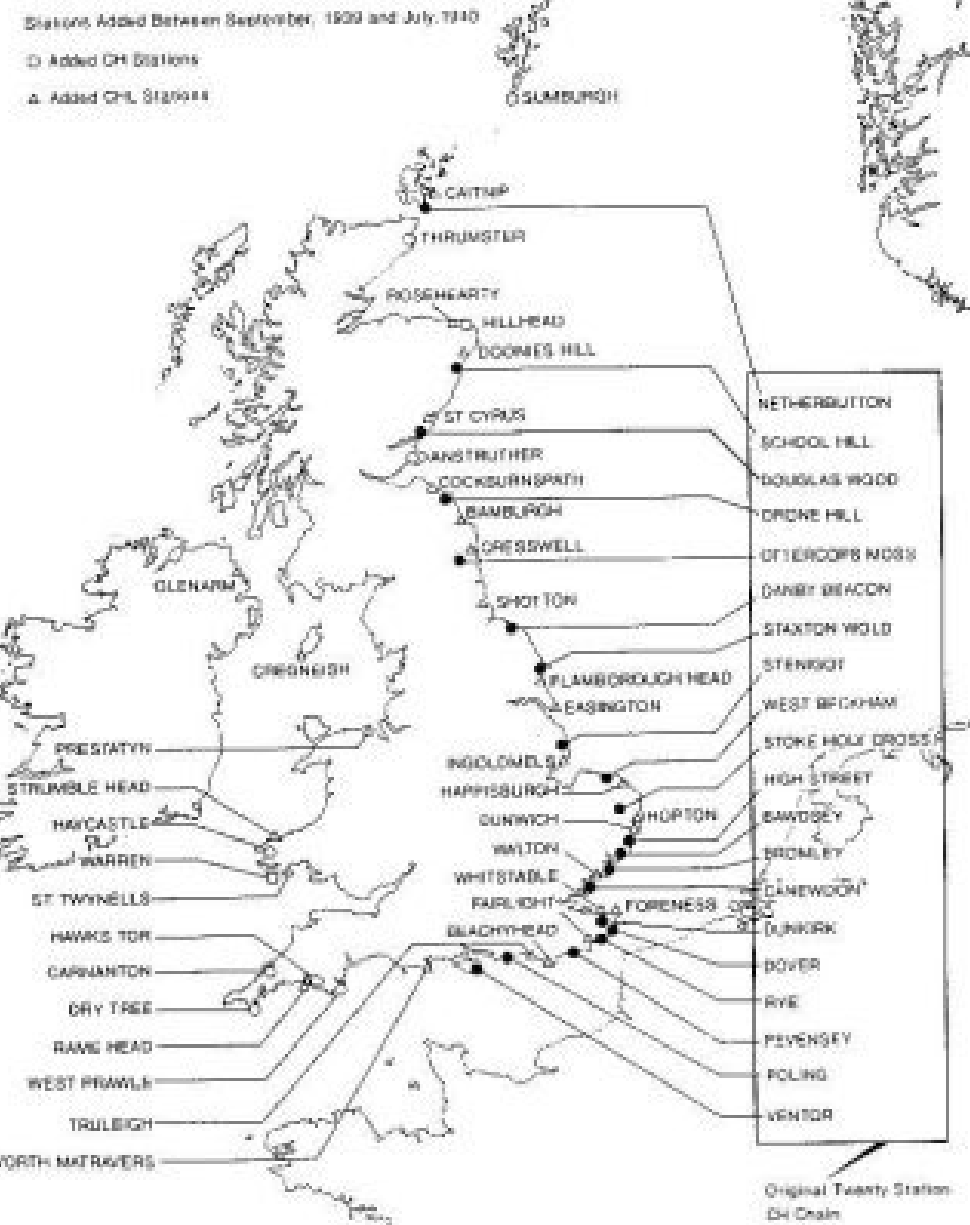
Chain Home Network



Bawdsey Manor

- HF (12-meter wavelength), rather than microwave!
- Long antenna (achieved by cable strung between towers)
- Wide beam
- Poor resolution

At the time, it was not yet possible to achieve high transmission power at microwave frequencies (hence the choice of HF)



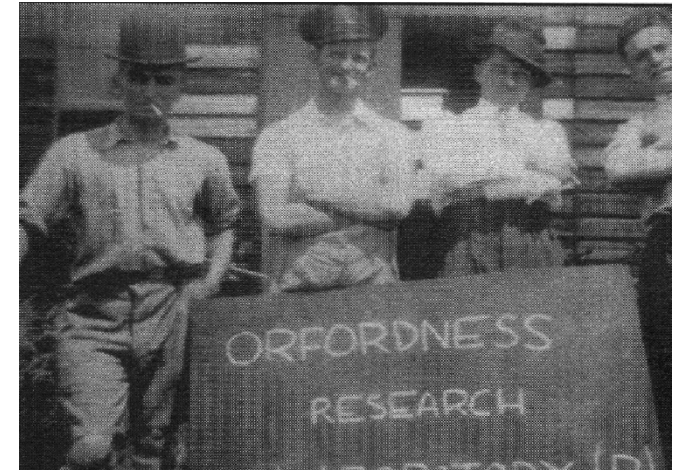
The Crown and Castle Pub – Birthplace (Aug 1936) of RDF2 (Project to Mount Radars on Night Fighters)

Watson-Watt met with his researchers at the local (Orford, Suffolk) Crown and Castle pub, and agreed that the best solution was to introduce a small radar that could be mounted in a night fighter .. Edward ("Taffy") Bowen asked to take on the project, and formed a small team to consider the problem in August 1936. **They gave the concept the name RDF2, as Chain Home was at that time known as RDF1.**

Watson-Watt's team had four young researchers (or "boffins"): A.P. ("Jimmy") Rowe, Edward ("Taffy") Bowen, Arnold ("Skip") Wilkins and L.H. Bainbridge Bell.



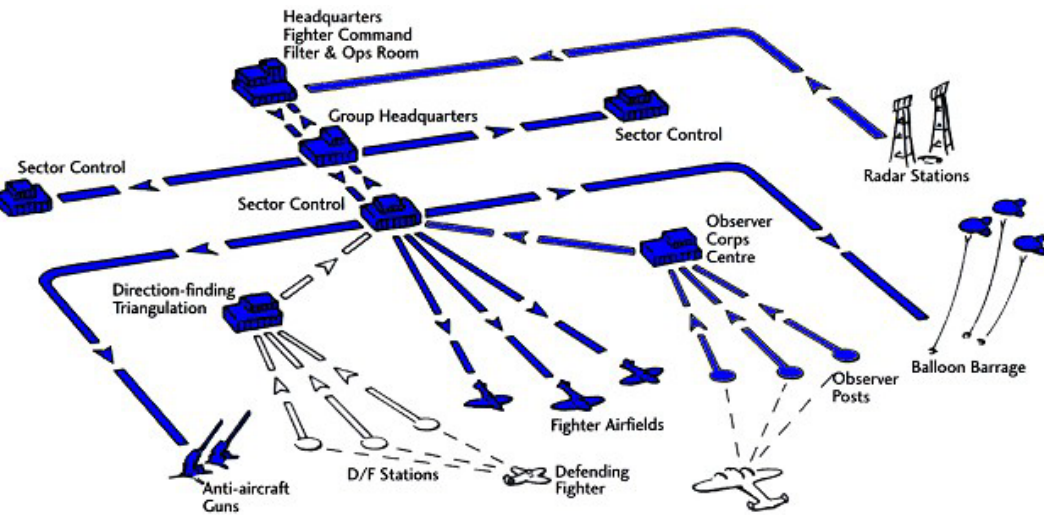
The Crown
And Castle,
Orford



The "boffins": Skip Wilkins is left center; Taffy Bowen is at the right. (from Paddy Heazell, Most Secret – the Hidden History of Orford Ness)

The Dowding System

July 1936 -- Hugh Dowding appointed commanding officer of the newly created Royal Air Force (RAF) Fighter Command. He was one of the most highly-placed persons in Britain who **did not agree with Baldwin's 1932 declaration that ``The bomber will always get through''.**



Dowding conceived and oversaw the development of the Dowding System. This consisted of an **integrated air defense system** featuring **Radar** (whose potential Dowding was among the first to appreciate)



Hugh Dowding
(1882-1970)

Then One February (1940) Night at U. of Birmingham ..

Anode block of the improved cavity magnetron of Randall and Boot



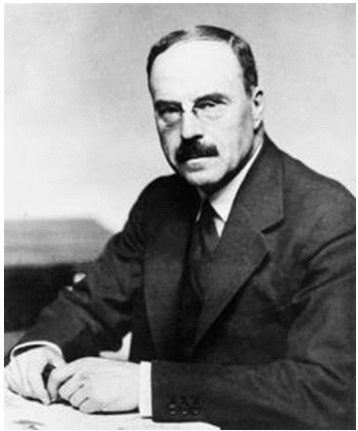
Generated microwave frequencies at 400 Watts (ultimately 50 kWatts, about 100 times the power of earlier variants of the cavity magnetron)

Sir John Turton Randall
(English physicist; 1905-1984) and
Henry Albert Howard ("Harry") Boot (English
physicist; 1917-1983)



The Tizard Mission (September 1940)

The objective of the mission was to cooperate in science and technology with the U.S., which was neutral and, in many quarters, unwilling to become involved in the war. The U.S. had greater resources for development and production, which Britain desperately wanted to use.



Sir Henry Thomas Tizard
(English chemist; 1885-1959)

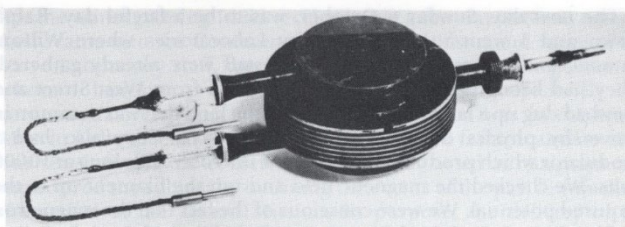


Figure 11.1 An external view of the actual magnetron taken to North America by the Tizard Mission in August 1940. This is probably the only example of the original batch of 12 still in existence; it is now on display in the Museum of the National Research Council, Ottawa.



Vannevar
Bush
(1890-1974)



Karl Compton
(MIT President;
1887-1954)



Alfred Lee
Loomis
(American
entrepreneur
and scientist;
1887-1975)



Admiral Harold
Gardiner Bowen
(Director of NRL;
1883-1965)

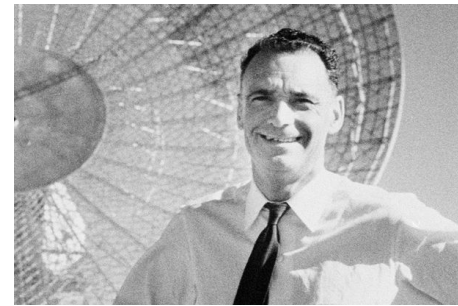
MIT's Radiation Lab

Approved October, 1940

- Lee DuBridge chosen as director
- First year funding of \$800K

Developed half of the new radar designs in WWII

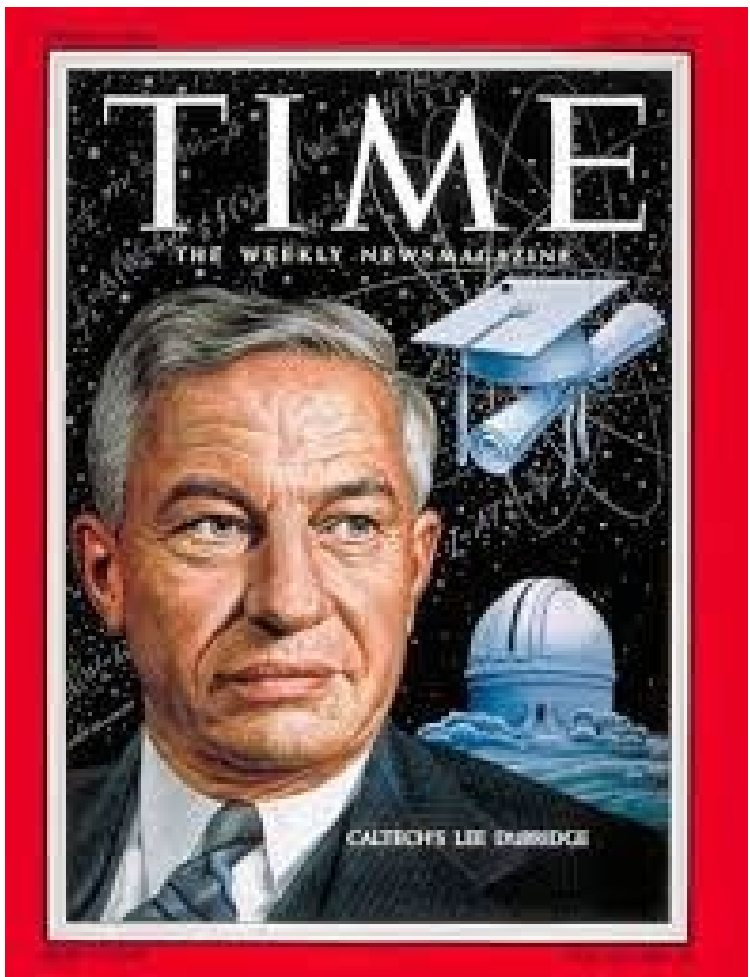
Provided 1 million cavity magnetrons



Edward ('Taffy')
Bowen
(1911-1991)

``In many ways it was more like a scientific convention than a research laboratory, except that it was a convention that kept running year after year. Here was the cream of American scientists, hell-bent on doing all they could for the war effort – **some fourteen months before America itself actually entered the war.**''

-- Eddie (''Taffy'') Bowen
(speaking about the Rad Lab)



Lee DuBridge (American educator and physicist; 1901-1994):

“The bomb may have ended the war, but radar won the war.”

Now Back Up a Bit

Radar development happened rapidly between 1936 and 1940

- This rapidity makes a good story, but misses some contributions
- Progress was on-going in the 1920s, 1930s:
 - Move to Higher Frequencies (''hyper-Frequency'', a.k.a. microwaves)
 - Components
 - Waveforms

Work was happening in different countries, and was done by under-appreciated inventors, engineers, military leaders, and mathematicians.

Push to Higher Frequencies

WWI: need for tightly directed transmissions secure from enemy ears

- Western Electric (the manufacturing subsidiary of AT&T):
 - Pushed the art of wireless transmission ahead by as much as a decade
 - **Researchers realized benefits of short waves**
 - Short waves start out more concentrated → greater portion of signal arrives at the destination
 - Also reduces power demands
 - They do not attenuate as much as thought
 - Higher frequencies suddenly attractive

1920s: Big players get involved in short-wave communication

- RCA, Westinghouse, Telefunken

1931 -- Signs of a Move toward Microwaves



1931 -- Microwave Comms Link Experiment

1.7 Giga-Hertz (18 cm)
Bidirectional
Calais, France to
Dover, UK
 $\frac{1}{2}$ Watt
40 km



Andre Clavier
(1894-1972)



1931 – William Blair Launches Project 88 (‘Position Finding by Means of Light’)

Blair was director of the Army Signal Corp Lab (SCL) at Fort Monmouth, NJ



William Blair (1874-1962)

Blair determines microwave signals are best for detecting aircraft.

Ft Monmouth would develop SCR-270, the “Pearl Harbor Radar”.

1933 – Serendipity Strikes Again

Mathematicians Sergei **Schelkunoff** (AT&T Bell Labs) and Sallie **Mead** (AT&T D&R) discover a mode in circular waveguides for which attenuation **decreases** with higher frequency. This helped inspire support for development of microwave-frequency waveguides.



Sallie Pero Mead
(1891-1983)



Sergei A. Schelkunoff
(1897-1992)

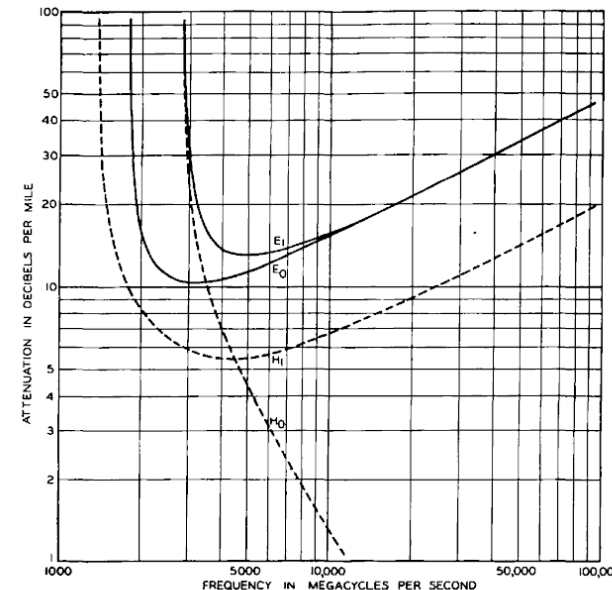


Fig. 7—Attenuations suffered by each of the more common types of waves in a hollow copper pipe 5 inches in diameter.

Components

Higher frequencies required innovations and component development:

- **Plumbing** -- Waveguides and antennas for microwave transmissions.
- **Power** – The Cavity Magnetron
- **Pulses** -- for accurate range estimates
- **Protection** – The duplexer was key to installing radars on air platforms

(Four P's)

Plumbing

Waveguides (and Antennas)

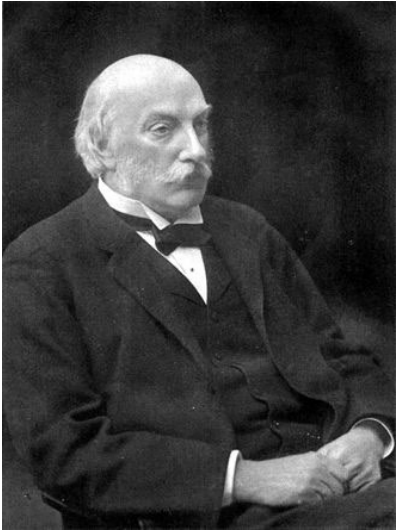
Early Waveguide Developments

- J.J. Thomson (1893): proposed the first structure for guiding waves.
- Oliver Lodge (1894): Experimental tests of waveguides.
- Lord Rayleigh (1897): Mathematical analysis of electromagnetic waves in a metal cylinder
- Lord Rayleigh (1877-1878): ``The Theory of Sound'' – full mathematical analysis of propagation modes.
- Jagadish Chandra Bose (1897): researched millimeter wavelengths (he used frequencies as high as 60 GHz!), using waveguides.
- Sommerfeld and Debye (1920s): studied dielectric waveguides.

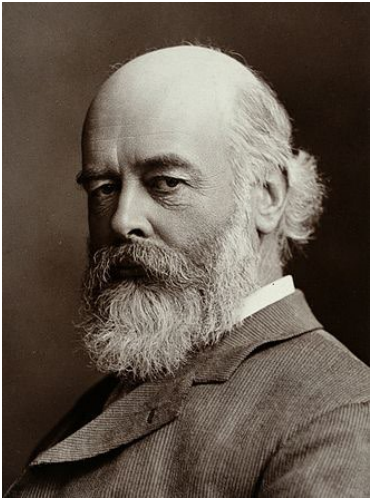
Waveguide Pioneers



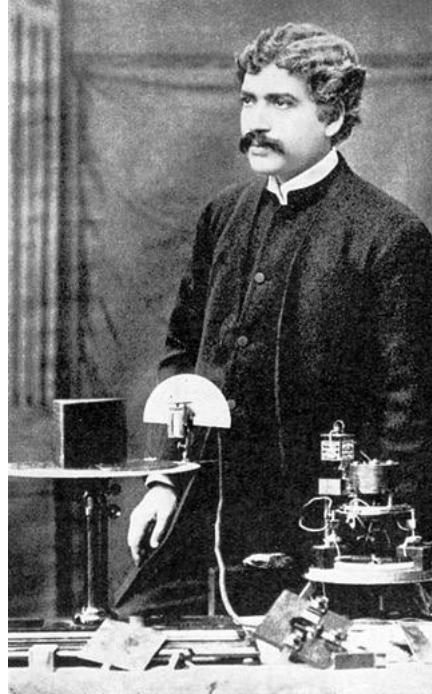
Sir Joseph John Thomson
(1856-1940)



John William Strutt,
3rd Baron Rayleigh
(1842-1919)



Sir Oliver Lodge
(1851-1940)



Jagadish Chandra Bose
(1858-1937)



Arnold Sommerfeld
(1868-1951)

Waveguide Research in Hiatus Until 1931 ..

.. waveguides needed for the low frequencies used for communications needed to have impractically large diameters. By the late 1920s, frequencies below 25 MHz were commonplace; researchers turned again to the higher frequencies.

Practical investigations resumed in 1931:

- George Southworth (AT&T D&R, then Bell Labs)
 - Wanted to revisit interesting phenomena from his Yale PhD work

Independently, practical investigations at MIT:

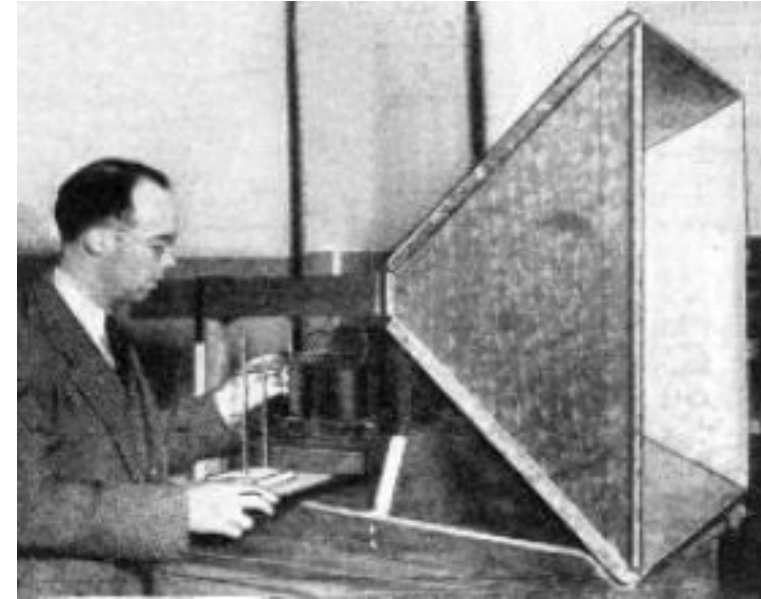
- Wilmer Barrow (MIT)

Waveguide Research – Southworth and Barrow



George Southworth
(1890-1972)
Waveguide
development
at Bell Labs.

“Send money” – first message sent through an air-filled waveguide (1933)



Wilmer Barrow (1903-1975). Invented waveguide (1936) and horn antenna (1938)

Power

The Cavity Magnetron

- Transmission Power at Microwave Frequencies

Albert Hull of GE (1920) – Inventor of the (Single-Anode) Magnetron



Albert Hull
(1880-1966)

Albert Hull (American physicist and electrical engineer) invented the magnetron, while working for General Electric Research Lab in Schenectady, New York

His driving motivation was to get around Lee DeForest patents on the Audion triode. Hull used a magnetic field, rather than electric field, to control current flow.

The magnetron alone is an oscillator. It needs enhancements in order to amplify a signal.

Magnetron Progress in 1920s and 1930s

Zacek and Habann –
Frequencies to 100 MHz
to 1 GHz

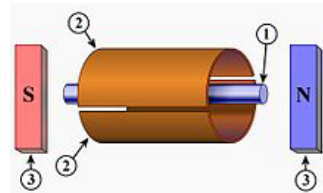


Photo
not
found

August Zacek
(Czech;
1886-1961)

Erich Habann
(German;
1892-1968)

Split-Anode Magnetron (1929)



Able to achieve 17 centimeters (1.76 GHz)

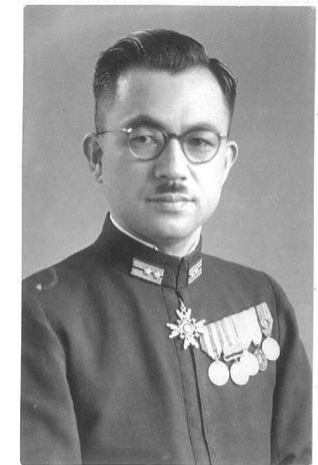


Kinjiro Okabe
(1896-1984)

Generated
world-wide
interest

Push-Pull Technique (1937)

Tsunio Ito &
Yoji Ito –
Enhancement
in Frequency
stability



Yoji Ito (1901-1955)

Magnetron development
by Japan was ahead
of England by WW II

French Developments

Emile Girardeau:

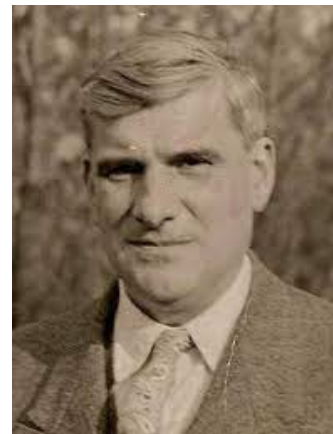
- Established CSF (Compagnie Generale de la telegraphie sans fil) General Research Labs.
- First to patent set of frequencies used by radar.

Maurice Ponte:

- With **H. Gutton**: French pioneers of resonant magnetron



Emile Girardeau
(1882-1970)



Henri Gutton
(1905-1984)



Maurice Ponte
(1902-1983)

1934 (by June): first decimetric (16 cm) radar.

Dutch/German Developments

- A. L. Samuel (Bell Labs)
 - Proposed the multiple-cavity concept
- Klaus Posthumus (Dutch)
 - Multiple-segment design (1934)
 - ``Paved the way'' for multi-cavity design.
 - **Limited to 10 Watts**
- Hans Holmann (German)
 - Multiple-cathode design (1935)
 - Worked with Posthumus at Philips (Netherlands)



Klaas Posthumus
(1902-1990)



Hans Hollmann
(1899-1960)

Russians – 300 Watt Power; Velocity-Modulation Concept

- Aleksereff and Malearoff
 - Magnetron with four internal cavities (1936)
 - 300 Watts
 - Published in 1940
- Dmitry Rozhansky
 - Concept of velocity modulation (1935)
 - Key to Klystron design
 - Did not build a device



Dmitry Rozhansky
(1888-1935)

The Klystron Story -- Before the Varians



Oskar Heil (1908-94) and Agnessa (Arsenjeva) Heil (1901-1991)

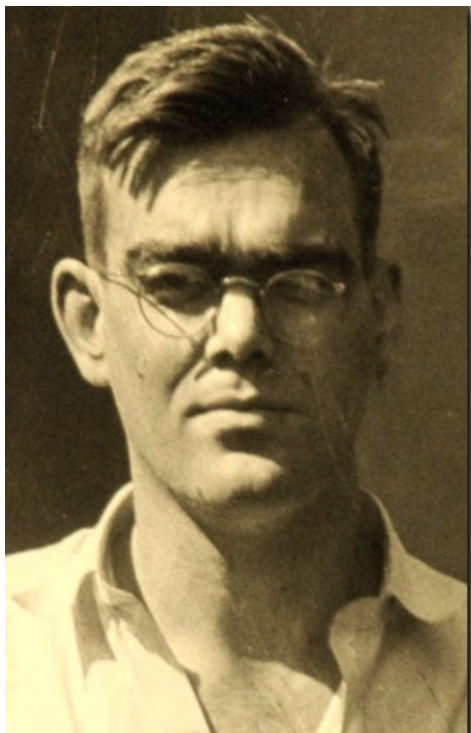
Arsenjeva-Heil, A.; Heil, O. (1935). "Eine neue Methode zur Erzeugung kurzer, ungedämpfter elektromagnetischer Wellen großer Intensität" [A new method for the generation of short, undamped electromagnetic waves of high intensity]. *Zeitschrift für Physik*

Velocity Modulation (1935) – concept but no device

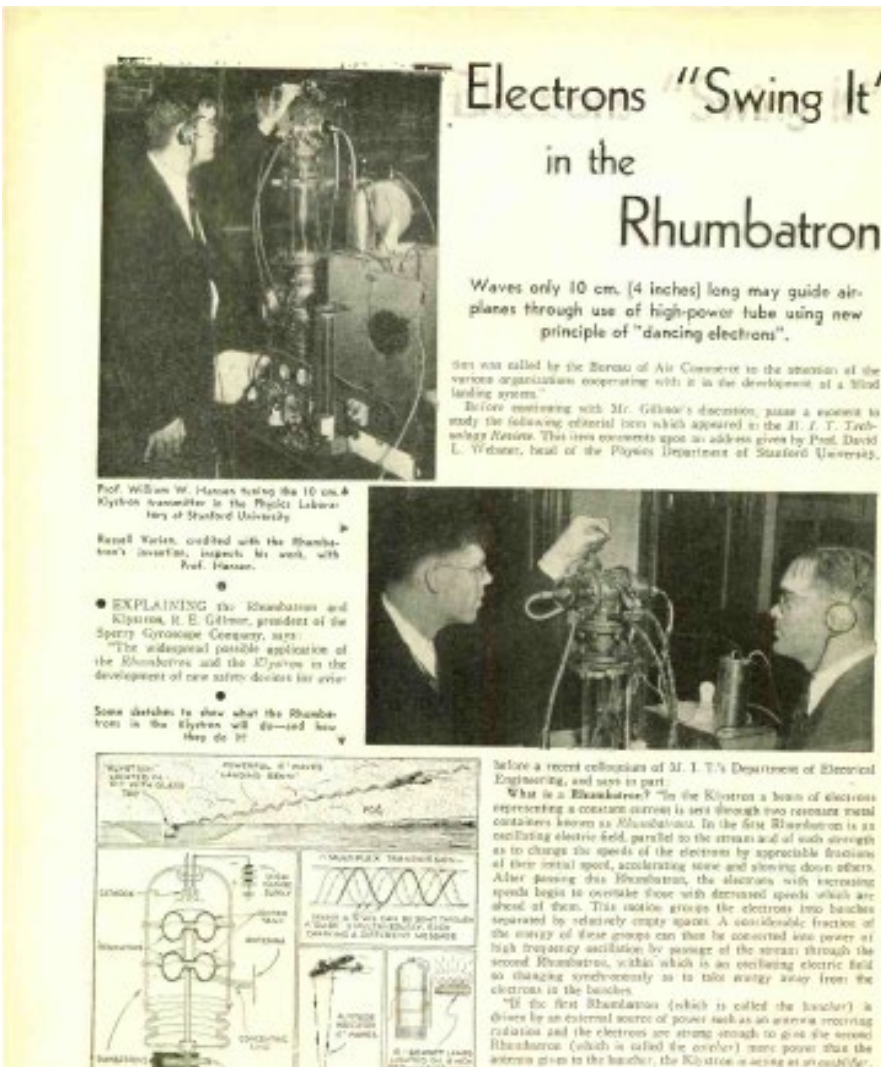


William Hansen (on the right) (1909-1949). Goal: high-power X-ray spectroscopy

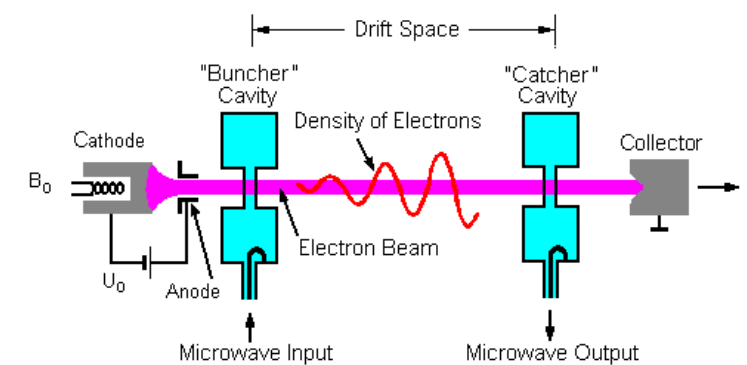
Hansen's Rhumbatron -- Essential Step to the Klystron



William Hansen
(1909-1949)



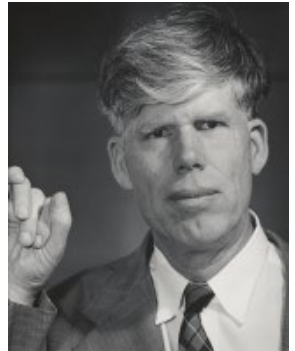
The Rhumba craze took off in 1931.



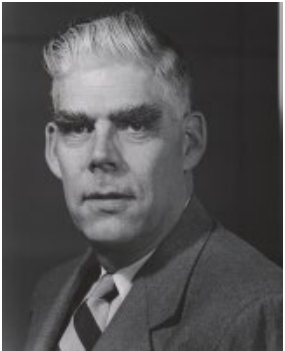
Klystron used two rhumbatrons
(for the Buncher and the Catcher)

Klystron on a Shoe-String (\$100)

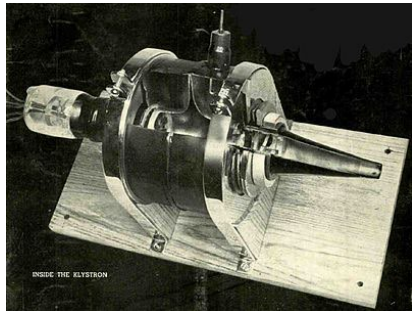
The **Varian brothers** were from an Irish-immigrant family of theosophists who helped found a Utopian society in Halcyon, California. They were interested in piloting private planes, and in **navigation**.



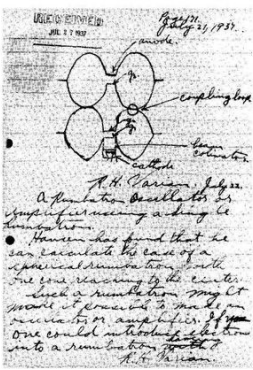
Russell Varian
(1898-1959) –
The Physicist



Sigurd Varian
(1901-1961) –
The Pilot



1940 Westinghouse
Klystron prototype.



Concept came to
Russell Varian in a
dream

“What we need is a **reliable beam** to bring planes down in weather like this”
(Sigurd Varian, after a touchy 1934 landing into Tampico airport in Mexico)



Sigurd Varian (on left)

“The klystron had been developed partly in an attempt to find a microwave power source for a **blind landing system**.”

They were also concerned about the German threat:
“[Sigurd] felt that Hitler could easily establish bases in Central America, from which his planes could fly into the United States at night, or at low elevations, and drop bombs, without ever being detected.”

The Cavity Magnetron of Randall and Boot

Klystron:

- Strength: Low losses and large heat dissipation
- Weakness: Small cathode limits number of electrons

Magnetron:

- Strength: Large cylindrical cathode and anode (can handle large numbers of electrons)
- Weakness: high losses, no way to dissipate large amounts of heat

Randall and Boot's key idea: Combine the two, and gain the best aspects of both.



Mark Olifant
(1901-2000)
Australian-born physicist, U. Birmingham. His 1939 research grant for short-wavelength radar led to Randall and Boot's cavity Magnetron.

Serendipity (Once Again) -- The Cavity Magnetron

A discovery in a lab at the University of Birmingham enabled the British to produce high-power signals at microwave frequencies ..

``The magnetron .. surged to life .. **On February 21, 1940** .. The physicists John Randall and Henry Boot huddled around a disembodied car headlight in a makeshift laboratory at the University of Birmingham. Suddenly, at the flick of a switch, power shot from a strange piece of gadgetry that resembled a pint-sized engine rotor with a series of cylindrical holes cut into its body .. As a small blue arc sizzled off the wires connecting the device to a headlamp, the six-watt car bulb shone brightly for an instant and burned out, overwhelmed by the energy coursing into it.''

(R. Buderi, *The Invention That Changed the World*)

400 Watts at 9.8 cm wavelengths

By 1941, engineers achieved power output of 100 kWatts.



Randall (center) and Boot (right) showing magnetron to Alfred Lee Loomis (left).

University of Birmingham

Pulses

- Early systems were continuous-wave
 - Relied on beat frequency to detect targets
- Key innovation:
 - Pulses for accurate delay estimation
 - Delay is then used to determine target range

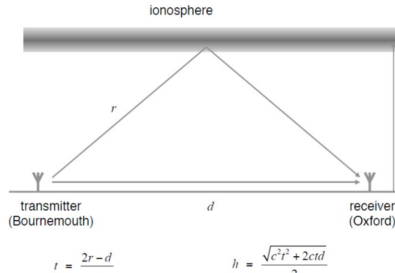
In December 1924, **Appleton and Barnett** in the UK used an FM radar (CW interference) technique to measure the height of the ionosphere. The following year **Breit and Tuve** in the US used a **pulse modulation** signal (suggested by Leo Young at NRL) for ranging.



Edward Appleton
(1892-1965)



Miles Aylmer
Fulton Barnett
(1901-1979)



Appleton, E.V. and Barnett, M.A.F., 'On some direct evidence for downward atmospheric reflection of electric rays', Proc. Roy. Soc., Vol.109, pp261-641, December 1925. (experiments at end of 1924)



Gregory Breit
(1899-1981)



Merle Tuve
(1901-1982)



Leo Young

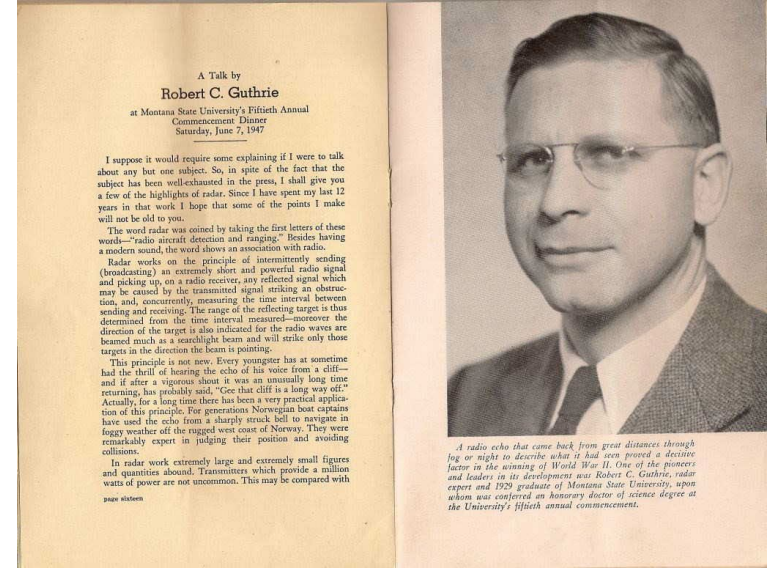
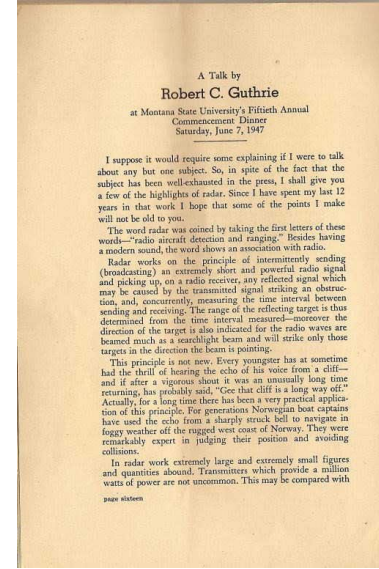
NRL – Radio Detection Using Pulses

1934: first radio-detection system to incorporate pulses

- Not in the European nations threatened with bombing, but in the United States
 - Dr. Robert Page of NRL (working under direction of Taylor and Young)
 - Robert Guthrie, his technician



Robert Morris Page
(1903-1992)



Robert Chilton Guthrie
(1906-1999)

I suppose it would require some explaining if I were to talk about any but one subject. So, in spite of the fact that the subject has been well-examined in the press, I shall give you a few of the highlights of radar. Since I have spent my last 12 years in that work I hope that some of the points I make will not be old to you.

The word "radar" was coined by taking the first letters of these words—"radio detection and ranging." Besides having a modern sound, the word shows an association with radio.

Radar works on the principle of sending out a powerful radio signal (broadcasting) and picking up with a radio receiver, any reflected signal which may be caused by the transmitted signal striking an obstruction, and, more correctly, measuring the time interval between sending and receiving the signal after it reflects off a target, thus determined from the time interval measured—moreover the direction of the target is also indicated for the radio waves are beamed out as a series of pulses and will strike only those targets in the path of the beam is pointing.

This principle is not new. Every youngster has at sometime had the thrill of hearing the echo of his voice off a cliff and if he has done it often it will usually long time returning, has probably said, "Gee that cliff is a long way off." Actually, for a long time there has been a very practical application of this principle. The Vikings, for instance, some boatmen have used the echo from a sharply struck bell to navigate in foggy weather off the rugged west coast of Norway. They were remarkably expert in judging their position and avoiding collisions.

In radar work extremely large and extremely small figures and quantities abound. Transmitters which provide a million watts of power are not uncommon. This may be compared with page sixteen

A radio echo that came back from great distance through fog or night to describe what it is seen proves a decisive factor in radar. One of the pioneers and leaders in its development was Robert C. Guthrie, radar expert and 1929 graduate of Montana State University, upon whom was conferred an honorary doctor of science degree at the University's fifteenth annual commencement.

Page's Pulse Modulation

John Page, "The Development of Radar":

"Leo C. Young suggested radio pulses. But no one had the technology to transmit or receive signals in this manner. My father was assigned the task of inventing something, anything, that might demonstrate whether this was feasible. He not only succeeded, but also quickly went to high frequencies and high power, never dreamed possible in the 1930's, to get equipment small enough and powerful enough to work aboard ships."

"He used the most powerful ham radio transmitter tubes of the day (Eimac, Palo Alto, CA) and got 10-20 times the rated power out of them by designing circuits that turned them on and off for milliseconds at a time in a sequenced, 6-tube ring oscillator."

With Developers Aware of Importance as Weapon—

RADAR RESEARCH PUSHED FERVENTLY DURING DECADE OF PEACE

EDITORIAL NOTE: The basic principle of radar, the radio "eyes" of the armed forces, was discovered in 1922 by Dr. Albert Hoyt Taylor, then at the Naval Research Laboratory. He noticed that radio waves were deflected by passing ships despite fog or darkness. The Navy did nothing about his discovery, but with another less successful experiment, he invented CXAM in 1930. It was found that those same waves could detect airplanes a remarkable four miles away. John M. Brightower of the Associated Press takes up the story at that point in the story of its early development.

By JOHN M. BRIGHTOWER
Washington, D.C., by the
Associated Press

WASHINGTON, June 24.—At last month—June, 1930—the developers of radar realized that their discoveries had gone far beyond academic experiments.

Here was a method which might be used to intercept ships, to locate aircraft, to track ships at night, to locate planes and determine distance to

them they got into action.

Here was one of the greatest achievements in warfare since the original creation of the military uses of aircraft.

There followed several months of intensive experiments with aerial detection. Various radio equipments were tried until Dr. Albert Hoyt Taylor and his associates, including George Young, who was then director of the Naval Research Laboratory's aircraft radio section, spent weeks bounding waves off planes around the Naval Air Station and along the coast. The results were dramatic. About Vernon bedeviled on the Virginia side of the ocean. Much progress was made, but there was no need of the experiments, which he did with unrelenting energy, Taylor said.

AKRON DOMINATED

Then the war clouds, which happened to be very heavy, was over. The Navy, which had been slow to make use of radar, decided just to make sure that aircraft as well as planes could be picked up.

All this work was carried on with regularity, however, and in November the Kennedy-Garrison laboratory became the world's electric test, about 120 miles and these were required, comparatively simple apparatus, including two widely separated antennae—antennae, the other for receiving.

This angered Taylor considerably. He is a man who likes to design a machine exactly to suit it to a particular purpose. It is an attitude of the engineer.

The apparatus was entirely effective, however, and not too costly for use on land. At one time Taylor worked out a complete detection system for the city of Wash-

ington about the experiments and their possibilities to defense of the country against air attack was second in the Army in 1932.

Army research labs that of the Navy, was then started for funds, and no vigorous progress until the ones suggested by Taylor was made before 1940.

ARMY SYSTEM SET UP

The research and development undertaken by the Army signal corps eventually led to the series of radar production set up around the coastal frontiers of the United States to detect the presence of aircraft which may still be in flight.

This lets evaded the problem of what to do about intercepting the many ships against air attack. For a time the best brains of the research laboratory were baffled.

Young, however, continued to think about the problem.

For radio detection was then but one, and by official standards a minor, one of N.R.L.'s projects.

One day Ben C. Young, an associate of Taylor, showed him Taylor's writing a letter with a typewriter in radio detection.

"Remember the Remond-Hawley experiments?" he asked. "Why don't we do this thing with pulses?"

"Well," Taylor replied, "let's have you up there in the meantime. These are not too bad."

Thus began the Remond-Hawley experiments, which is probably why the pulse worked so well in those experiments. I doubt whether it would work on shipboards considering the complex apparatus and the short distances we must work with water.

But Taylor never was a man to reject an idea simply because he disagreed with it. He told Young to begin work on the pulse principle.

Young had a new line of research and worked hard at least alone for three or four months. His problem was typical of all those encountered, before and after, in radar development. The extremely short wavelength of the waves makes it difficult to observe and prove a technique for the pulse system of plane detection. He was convinced that only with pulses would a workable system be possible.

PAGE GETS ON STAFF

While Taylor's work was much longer than radar always, Young, however, got his first break. Young in his laboratory worked almost day and night to observe and prove a technique for the pulse system of plane detection. He was convinced that only with pulses would a workable system be possible.

"After three or four months, during which Young was more or less alone," Taylor says, "I told him we had to have some help. And that's when I hired Mr. Page on. He'd been working on the project for me and I knew that he gave him an excellent record, and he wanted on."

"Page has made more contributions to modern radar than any other man."

While Taylor, Young, and many others in the laboratory were veterans, Robert H. Young was a youngster, but a brilliant worker, passionately devoted to physics. He had gone directly to Michigan State University, St. Paul, Minn., in 1927. Jean M. Gagnard, physicist and personal friend of Robert H. Young, had given Page such a

REPORT GIVES RESULTS

Sent in November, 1938, Taylor

had made a comprehensive report

to the Navy's Bureau of Engineering, of which Young was then assistant chief, entitled "Radio-Electric Signals From Moving Objects."

The paper told about detection of ships and planes, how and why they were detected and what the tactical possibilities were.

The admiral at the Navy experimen-

tal did not have to crawl

like a worm in a

water tank,

but

he

had

the

ability

to

see

the

ship

and

the

plane

and

the

boat

and

the

aircraft

and

Contributions Elsewhere

France

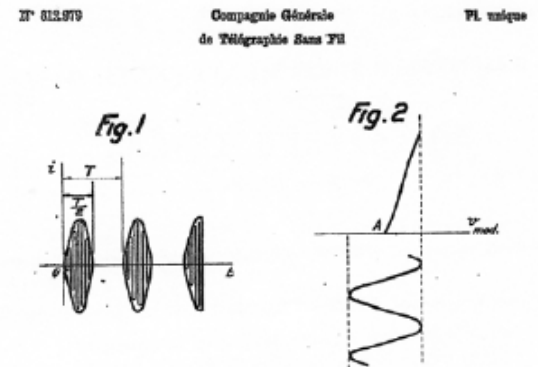
- (Jan'y 1936): Pulse principle patented by Henri Gutton and Maurice Ponte
 - French patent #812,979 ("Perfectionnement a la detection des obstacles par ondes electromagnetiques")
- (April 1937): Maurice Elie (SFR):
 - pulse-modulating transmitter tubes.

29 jan 1936



Japan:

- (1941): Initiated pulse radar ("thanks to" German reports of British radars).



Protection

- The duplexer was needed for protecting the sensitive receiver from the powerful transmitter
- Key to placing Transmitter and Receiver in close proximity
 - Critical for putting radar on air platforms
 - Also important for ship radar

Dr. Page at NRL – Development of the Duplexer

John Page, "The Development of Radar":

``This **duplexer solution** to a vexing problem (blinding and destabilizing a sensitive receiver) **came to my father while in a Sunday morning church service** (he certainly wasn't paying attention to the minister). The idea so impressed him that he stopped off at the Laboratory and recorded the idea into his workshop log books. His assistant* went to work on it immediately, and several days later a working prototype was installed and tested in a wave guide. It worked the first time. ''

``After the British invented the magnetron it was combined with the duplexer, allowing high power and even higher frequency equipment to be installed on board British fighter-bombers. This was just in the nick of time to break the back of the German wolf packs in the Atlantic. ''

* Almost certainly Robert Chilton Guthrie

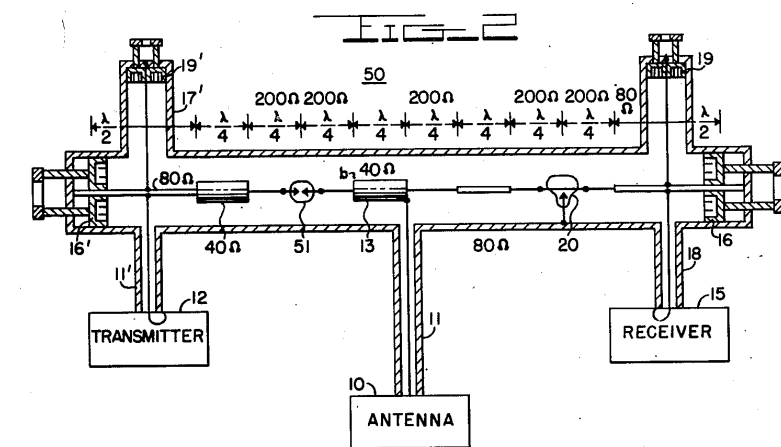
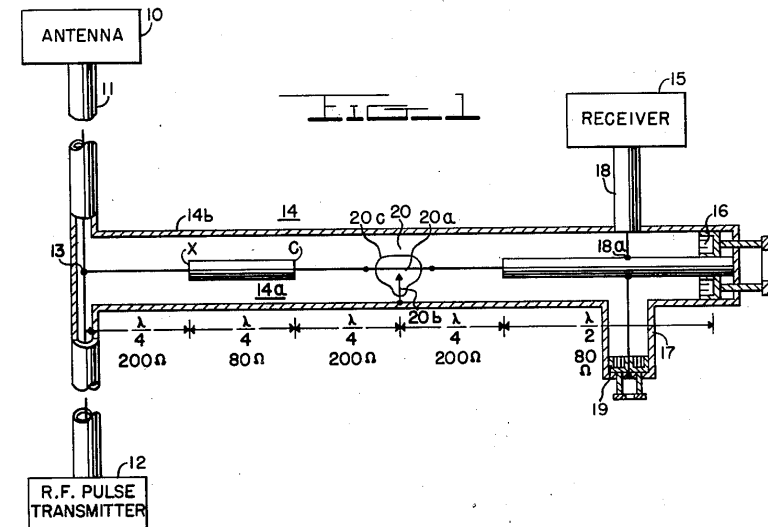
June 27, 1950

R. M. PAGE

2,512,673

Page's Antenna Duplexer

- Antenna duplexer, based on gas discharge
 - Part of the invention disclosed in patent US2512673 (granted in 1948).
 - First tested (USS Leahy) and installed on Navy vessels



INVENTOR.
ROBERT M. PAGE

BY

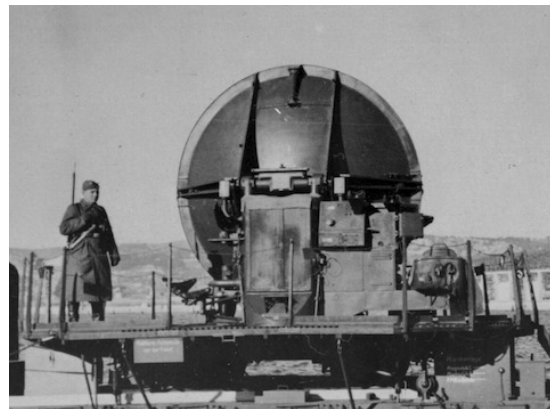
mckayes

ATTORNEY

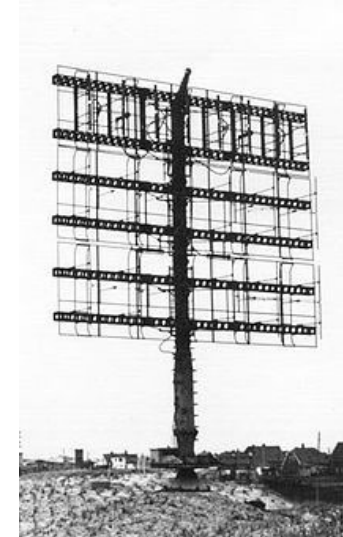
Radar Systems Come Together

Germany, Of Course

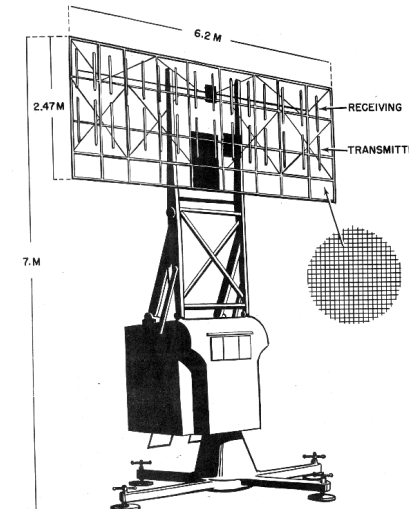
- 1933: Hitler takes power
- Funkmesstechnik -- remote radio measuring technology)
 - Operational by WWII:
 - Freya: 2.4m wavelength radar for aircraft detection; 80-km range
 - Seetakt: 80-cm wavelength radar; ship detection; 14-km range
 - Wurzberg ground radar; 4000 manufactured



Wurzberg
ground-based
Radar



Freya early warning
radar antenna



Seetakt
shipboard
Radar

1934: Dr. Rudolph Kuhnhold

Dr. Rudolph Kuhnhold

- ``Brilliant'' German engineer
- Owned GEMA (Gesellschaft fur Elektroakustische und Mechanische Apparate)

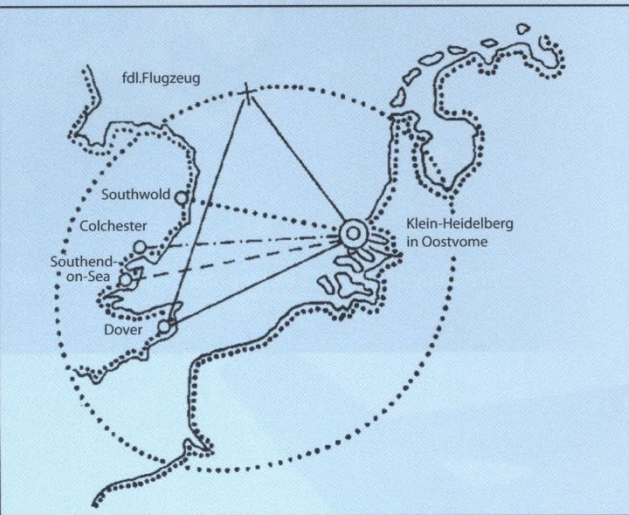
Experimental radio-detection system at Pelzerhaken (east of Kiel)

- 700-Watt transmitter
- 600 MHz
- March 20: Detected Hesse battleship in Kiel Harbor
 - 600 yards range

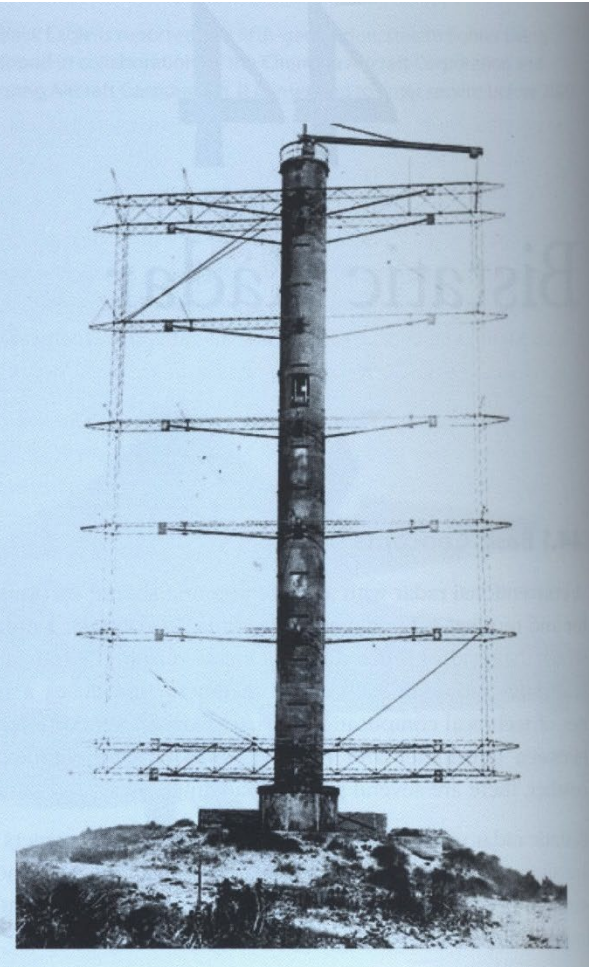


Hessen battleship passing under
Levensau Bridge at Kiel Harbor

Klein Heidelberg



THE FIRST OPERATIONAL BISTATIC RADAR, IN THE MODERN SENSE, WAS THE German WW2 bistatic system *Klein Heidelberg*. This exploited transmissions from the British Chain Home radar stations on the east coast of England, which made it completely undetectable and therefore immune to jamming and countermeasures. In fact the Allies did not find out about it until November 1944. It achieved reported detection ranges of Allied aircraft of more than 400 km and was undoubtedly decades ahead of its time.



Passive radar system,
which used the signals
from Chain Home.

Image from Stimson, "Introduction to Airborne Radar"

USSR:

Pavel K. Oshchepkov (1908-1992)

- **1933:** Began development of a *razvedyvat'l'naya elektromagnitnaya stantsiya* (reconnaissance electromagnetic station)



P.K. Oshchepkov,
circa 1935

- Russia had production radars available by the German invasion in June 1941
- Production radars and development radars used for air defense of Leningrad and Moscow
- German invasion displaced Russian radar facilities, reduced development

France – (1934) Bi-Static CW Detection of Aircraft

First patent of an operational radio-detection apparatus using centimetric waves (1934).

- Detected coastlines and ships at 10 to 12 nautical miles.

Pierre David and **Camille Gutton** study of aircraft detection

- Assisted by French Army SEMT (directed by Major **Paul Labat**)
- Inspired by NRL work
- June 27: success with 5-meter wavelength, 50 Watt power, plane at 5000 meter altitude, 7 to 8 kilometers distant
- Short-wave bistatic Continuous-Wave



L-to-R: Pierre David,
Paul Labat, C. Lange

UK -- First Airborne Radar

Air-to-Surface Vessel (ASV) Mark II

- First aircraft mounted radar of any sort to be used operationally
- Airborne sea-surface search radar developed by the UK's Air Ministry
- Developed between late 1937 and early 1939, following the accidental detection of ships in the English Channel by an experimental air-to-air radar

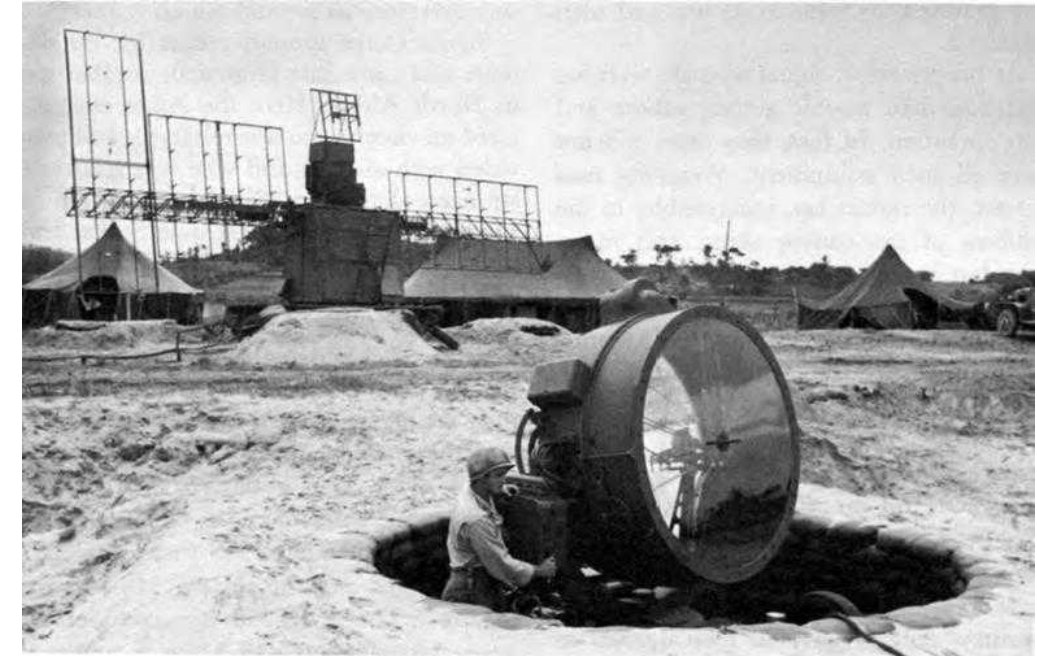
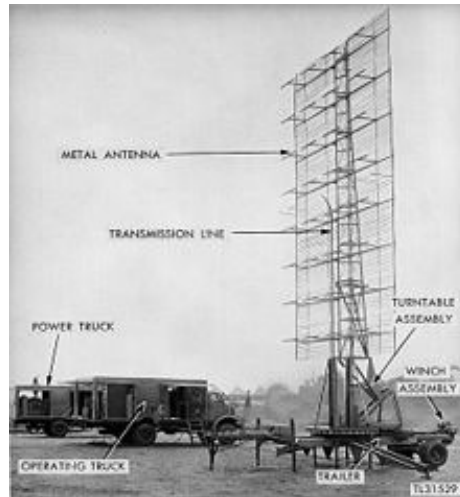


Transmitter above
The cockpit; receiver
on the right side of the
cockpit

U.S. -- Ft. Monmouth (Army) -- Searchlight Control Radar (SCR)

- SCR-268 – detected aircraft at 7 miles on 14 December 1936
- SCR-270

SCR-270



SCR-268 radar system deployed to North Africa

U.S. -- SCR-270 Was An Early Warning Radar

The **SCR-270** (Signal Corps Radio model 270) was one of the first operational early-warning radars. It was the U.S. Army's primary long-distance radar throughout World War II and was deployed around the world. It is also known as the **Pearl Harbor Radar**, since it was a SCR-270 set that detected the incoming raid about half an hour before the attack commenced.

December 7, 1941 – although the radars worked, the Japanese still caught the U.S. by surprise.

KERMIT A. TYLER, 96

Pearl Harbor figure never shook 'don't worry about it' comment

BY DENNIS MCLELLAN

"Don't worry about it." Those words, which he uttered on a peaceful Sunday morning in 1941 on the Hawaiian island of Oahu, were heard by Kermit A. Tyler, then the young 28-year-old officer on duty at the Fort Shafter radar information center in Honolulu.

Mr. Tyler was the Army Air Forces' first lieutenant on temporary duty at Fort Shafter's radar information center on the morning of Dec. 7, 1941, when a radar operator on the northern tip of the island reported that he and another private were seeing an unusually large "blip" on their radar screen, indicating a large number of aircraft about 132 miles away and fast approaching.

"Don't worry about it," Tyler told the radar operator, thinking it was a flight of U.S. B-17 bombers that was due in from the mainland.

Instead, the blip on the radar screen was the first wave of more than 350 Japanese fighters, torpedo bombers, dive bombers and horizontal bombers whose surprise attack on Pearl Harbor and the island's main airfields shortly before 8 a.m. plunged the United States into World War II.

"I wake up at nights sometimes and think about it," Mr. Tyler said in a 2007 interview with the *Star Ledger* of Newark, N.J. "But I don't feel guilty. I did all I could that morning."

Mr. Tyler, who suffered two strokes within the last two years, died Jan. 23 at his home in San Diego at age 96.

He was a hero, no doubt about it," Mr. Tyler's widow, Mrs. Mary Tyler, said. "He flew combat missions in the Pacific. He retired from the Air Force as a lieutenant colonel in 1960 and earned a degree in education from San Diego State University. He then launched a career in real estate and later became a landlord."

But there always was the infamous role he played on Dec. 7, his words immortalized in history books, articles, documentaries and a 1970 movie about the attack on Pearl Harbor, "Tora! Tora! Tora!" Often asked if he regretted not receiving angry letters blasting him for not taking action that day, And audiences watching the Pearl Harbor documentary at the Pearl Harbor Visitor Center still groan when they hear Mr. Tyler's response to the radar report.

"He's certainly a footnote to the Pearl Harbor history and the movie," said Daniel Martinez, chief historian for the National Park Service at World War II Valor in the Pacific National Monument in Pearl Harbor.

Mr. Tyler, a fighter pilot assigned to the 78th Pursuit Squadron at Wheeler Field, was working the 4 to 8 a.m. shift as



Kermit A. Tyler was on duty at Fort Shafter's radar information center on Dec. 7, 1941.

the officer on duty at the Fort Shafter radar information center on Dec. 7, 1941.

"He was never trained for that job," Martinez said. "He had a walk-through the previous Wednesday but had never spent a full day there."

The commanding general of Wheeler Field wanted young pilots to learn as much about the radar system as possible, so they'd be more effective at intercepting enemy planes," Martinez added. Mr. Tyler was selected to be an observer-trainee in the radar information center.

Congressional committees and military inquiries that looked into what happened at Pearl Harbor did not find Mr. Tyler at fault, Martinez said.

Although the two radar operators thought the "blip" on their screens represented about 50 planes, Martinez said, they never volunteered that information to Tyler.

And, he said, there was indeed a flight of planes flying in from Hickam Field over to San Francisco, and they were due to land at Hickam Field at 8 a.m.

"We look for simple answers, and Kermit Tyler fit in as the fall guy for the attack," that he was not responsible, Martinez said. Mr. Tyler occasionally received angry letters blasting him for not taking action that day.

And audiences watching the Pearl Harbor documentary at the Pearl Harbor Visitor Center still groan when they hear Mr. Tyler's response to the radar report.

Mr. Tyler was born April 21, 1913, in Oelwein, Iowa, and later moved with his family to Long Beach, Calif. He attended junior college in Long Beach and spent several years in the Civilian Conservation Corps before being accepted into the Army for cadet flying training in 1936.

He was preceded in death by his wife, Mary, in 2007, and a son.

Survivors include three children; three grandchildren; and a great-granddaughter.

— Los Angeles Times

Obituary of Kermit Tyler
(1913-2010)

U.S. – Navy's CXAM (Delivered by RCA, 1940)

The **CXAM** radar system was the first production radar system deployed on United States Navy ships.

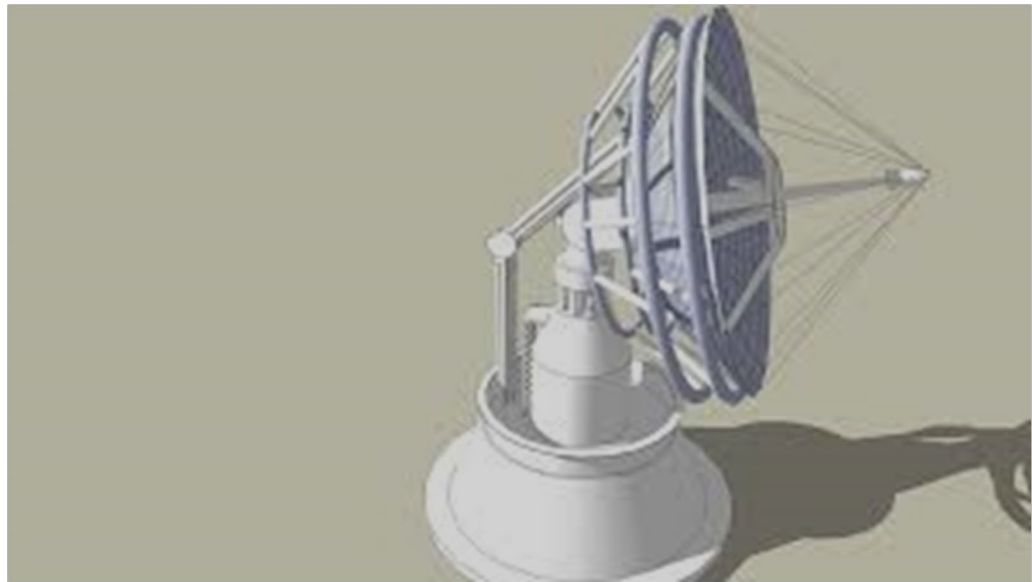
CXAM:

- Mid-high VHF frequency band of 200 MHz.
- It followed earlier prototype systems, e.g. the NRL radar installed in April 1937 on the destroyer *Leary*;
- its successor, the XAF, installed in December 1938 on the battleship *New York*
- CXZ -- first RCA-designed system, installed in December 1938 or January 1939 on the battleship *Texas*.



World War II and Radar

- The power that radar conferred on armed forces was clear to all nations that fought in WW II





2022 IEEE Radar Summer School: Introduction to Radar Systems

Justin Metcalf^{1,2}

¹*Advanced Radar Research Center, University of Oklahoma, Norman, Oklahoma, USA*

²*School of Electrical and Computer Engineering, University of Oklahoma, Norman, OK, USA*



Radar: What is it Good For?



- **RADAR: Radio Detection and Ranging**
 - Observed by Hertz in 1886 to verify Maxwell's equations
 - Patented Hülsmeyer in Germany in 1904 to detect ships
- Some applications of radar
 - Weather
 - Air traffic control
 - Air target detection & tracking
 - » Ground based, air based
 - Ground moving target detection and tracking
 - Near earth object detection and tracking
 - » Space junk!
 - Automotive
 - » Adaptive cruise control
 - » Autonomous driving enabler
 - Over the horizon radar
- Imaging
 - » Surveillance
 - » Oil spill detection
 - » Hydrology
 - » Ocean currents
 - » Ice sheet thickness
 - » Biomedical
- Ground penetrating radar
 - » Underground tunnel detection
 - » Buried object detection



Radar Features



- Radar systems are as varied as the applications
- Intrinsic radar sensor advantages:
 - Active illuminator → day or night,
 - RF frequencies → all-weather capability
 - Long range with large area/volumetric coverage and fast scan times
- Disadvantages:
 - Resolution – bound by bandwidth and frequency
 - Aggregate target signal degrades as R^4 → high dynamic range requirement
- Radar provides *direct* measurements of
 - Range
 - Range rate (i.e., velocity)
 - Angle (elevation and azimuth)



Outline



- **Radar phenomenology – motivates our system design**
 - **Antenna overview**
 - **Radar range equation**
- **Overview of radar signals**
 - **Range resolution and simple pulses**
 - **Pulse compression waveforms and linear frequency modulated (LFM) waveforms**
 - **Doppler effect**
- **Basic components of a radar system**
 - **Transmit (waveform generation and high power amplification)**
 - **Mixing**
 - **Noise and receive amplifying**
 - **Sampling and processing considerations**



Radar Phenomenology



Propagating Electromagnetic (EM) Waves



- Radar antenna couples an electromagnetic (EM) wave into the environment
- An EM wave propagating outward from a source varies by:

$$E(R, t) \propto \frac{1}{R} \cos(\Omega t - KR) = \text{Re} \left\{ \frac{1}{R} e^{-jKR} e^{j\Omega t} \right\}$$

- The magnitude of the electric field decays linearly with radial distance from the source
- This causes *spreading loss* which is a fundamental driver of radar system design!

The phase varies with time as a function of a *center frequency* (given here in angular units)

Complex envelope

The phase varies with radial distance from the source as a function of a *wavenumber K*



Wavenumber and Attenuation



- At a particular *instant in time* the electric field as a function of range is proportional to:

$$E(R) \propto \frac{1}{R} \cos(\Omega t - KR) = Re \left\{ \frac{1}{R} e^{-jKR} e^{j\Omega t} \right\} = Re \left\{ \frac{1}{R} e^{-jK_r R} e^{-K_i R} e^{j\Omega t} \right\}$$

Wavenumber $K = 2\pi/\lambda$
in direction of propagation

phase propagation

Carrier wave attenuation

A purple arrow points from the text "in direction of propagation" to the term e^{-jKR} in the first equation.

- In general, the wavenumber is **complex**, so $K = K_r - jK_i$
- The term $\exp(-K_i R)$ is an attenuation **in addition** to any spreading loss
- The power density of the wave is therefore reduced by an additional:

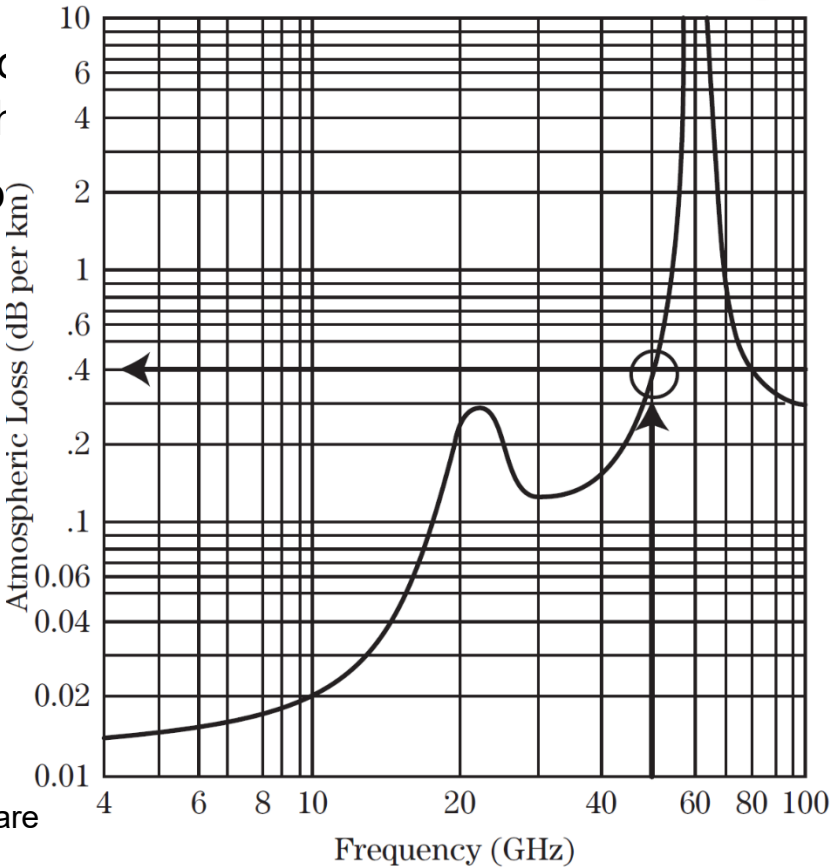
$$[\exp(-K_i R)]^2 = \exp(-2K_i R)$$



Attenuation



- Let $\kappa_e = 2K_i$ be called the extinction coefficient. Power is reduced by $\exp(-2\kappa_e)$ for every unit length
- Atmospheric losses are one factor for choosing frequency
 - Attenuation can be good or bad...
 - Typically given in dB/km



Atmospheric attenuation at Sea level.

Source: David Adamy, "Electronic Warfare Pocket Guide", 2011



Antenna Emissions



- Waves generated by a real source are the sum of the spherical waves from all its infinitesimal source components





Antenna Emissions



- Waves generated by a real source are the sum of the spherical waves from all its infinitesimal source components





Antenna Emissions



- Waves generated by a real source are the sum of the spherical waves from all its infinitesimal source components
- In the far field, these components combine to form a (mostly) spherical wavefront:

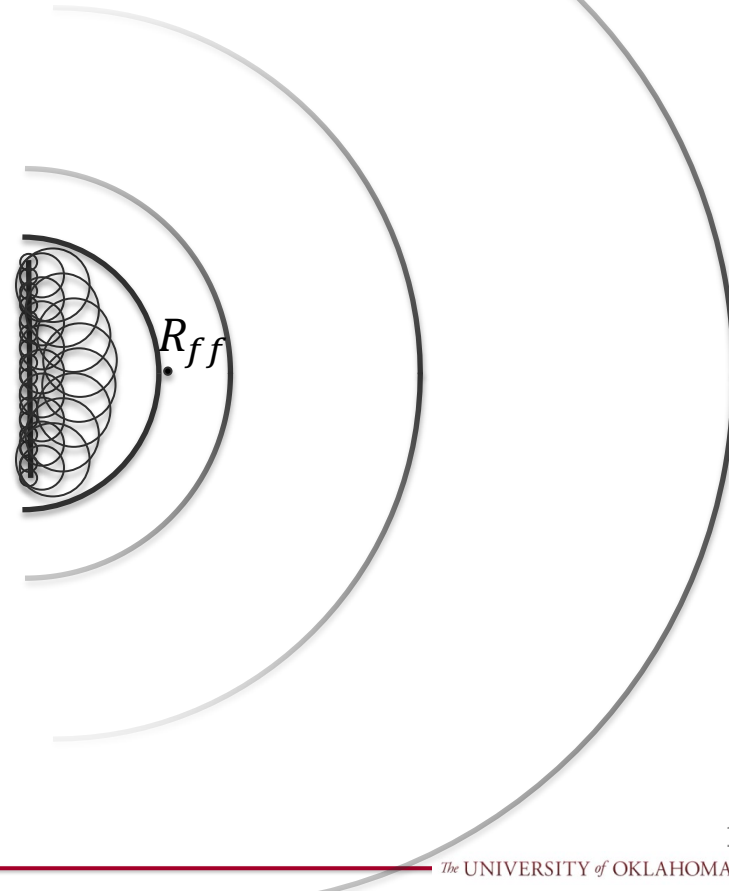




Far Field Assumption



- Waves generated by a real source are the sum of the spherical waves from all its infinitesimal source components
- In the far field, these components combine to form a (mostly) spherical wavefront:
 - Rule of Thumb:
 - where D is the *physical size* of the source
 - Note the dependence on both the physical size of the antenna and the wavelength of the emission!

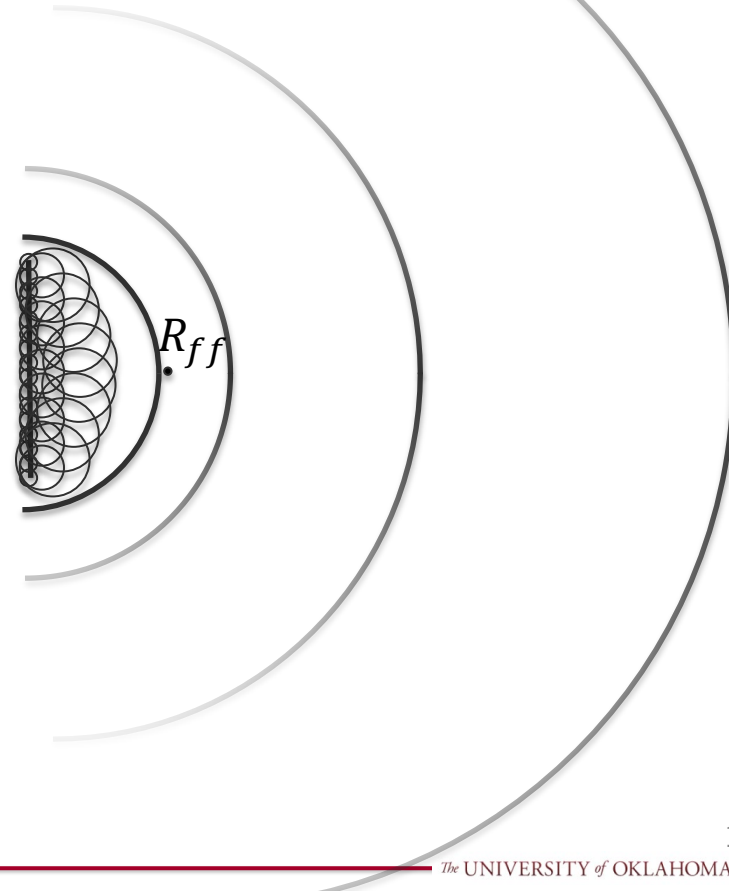




Plane Wave Assumption



- Sphere is eventually so big that it appears planar to a finite target
 - Rule of Thumb:
$$R \geq 2.5L^2/\lambda$$
 - where L is the size of the target
 - Important for phased array antennas
- We will focus on plane waves/far field, but some applications must consider near-field effects (e.g., some ground-penetrating radars)





Antenna Directivity



- Far-field antenna radiation pattern is the Fourier transform of the aperture current distribution
- The **directivity pattern** of an antenna is

$$D(\theta, \phi) = \frac{U(\theta, \phi)}{U_0}$$

Intensity of the antenna
Intensity of an (unrealizable)
isotropic radiator

- We can rearrange as:

$$U(\theta, \phi) = \frac{P_{TX}}{4\pi} D(\theta, \phi)$$

Radiated transmit power
evenly distributed around 4π
steradians

Radiation intensity depends
on both transmitted power and
antenna

Directivity is dependent on
antenna only



Average Directivity and Antenna Metrics



- It can be shown that

$$\frac{1}{4\pi} \int_0^{2\pi} \int_0^\pi D(\theta, \phi) \sin \theta d\theta d\phi = 1$$

- In other words, the *average directivity of any antenna must be unity*
- In general, the fundamental antenna metrics are

- The maximum value of the directivity pattern, called gain G
 - Mainlobe (i.e., the angles where the gain is achieved) beamwidth Ω_A

» 3 dB
» Null-to-null

- Sidelobe level

$$\Omega_A = \iint_{\text{main lobe}} \sin \theta d\theta d\phi$$

- Desired to have low sidelobes, high gain, and *appropriate* beamwidth



Beamwidth and Gain



- It can be shown that

$$G\Omega_A = 4\pi \rightarrow G = \frac{4\pi}{\Omega_A}$$

Beamwidth of isotropic radiator (in steradians)

Beamwidth of antenna (in steradians)

- Increasing gain directly means we *decrease* the beamwidth
- Narrow beams provide a radar
 - High gain
 - Better angular information and reduced multiplicative interference (e.g., clutter)
 - Slow scan times
- Wide beams
 - Low gain
 - Fast scan
 - Can be improved through synthetic apertures...stay tuned!



Transmit and Receive Considerations



- Radar typically requires large energy-on-target
 - Large transmit power
 - High gain
 - We will explore the reasons why momentarily!
- Transmit sidelobes must be minimized
 - Can cause strong interference across wide area
 - Illuminate targets outside the main beam
- Directionality of radar sets it apart from mobile radio services
 - Mobile communications typically use omnidirectional antennas
- Receive gain is often expressed in terms of antenna *effective area*

$$G = \frac{4\pi A_e}{\lambda^2}$$



Gain Approximations



- Beamwidths are often measured as the 3 dB beamwidth
 - The angle span where the main beam is $\geq 1/2$ of its peak value
 - Angles are referred to as θ_3, ϕ_3
- Common gain approximation for linear/rectangular aperture is:

$$G \approx \frac{26,000}{\theta_3 \phi_3} \text{ (}\theta_3, \phi_3 \text{ in degrees)} = \frac{7.9}{\theta_3 \phi_3} \text{ (}\theta_3, \phi_3 \text{ in radians)}$$

- Ignores antenna efficiency
- Beamwidth for ideal linear/rectangular antenna aperture is:

$$\theta_3 = 2 \sin^{-1} \left(\frac{1.4\lambda}{\pi D_y} \right) \approx 0.886 \frac{\lambda}{D_y} \text{ radians}$$



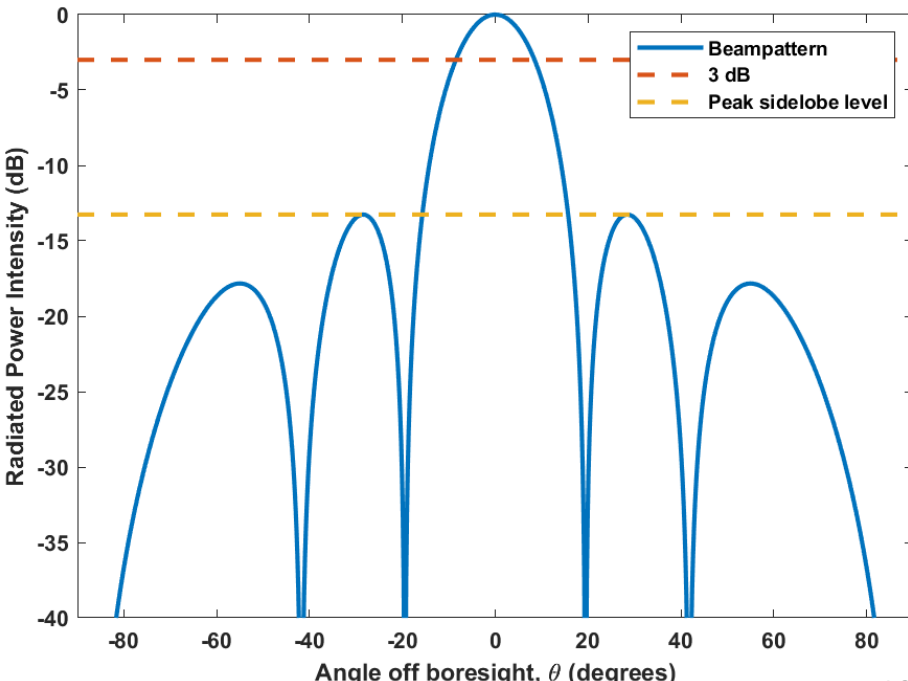
Example Power Pattern: Uniform Current Source



- For example, consider a 10 GHz (X-band, 3 cm wavelength) idealized uniform current source antenna
- For a $D_y = 9$ cm antenna, the normalized pattern is:

$$E(\theta) = \text{sinc} \left[\left(\frac{D_y}{\lambda} \right) \sin \theta \right]$$
$$= \text{sinc}[3 \sin \theta]$$

- We are *ignoring* the ϕ component for the purposes of this example
- We are also ignoring antenna efficiency
- Note: $D_y = 3\lambda$





Example Power Pattern: Uniform Current Source



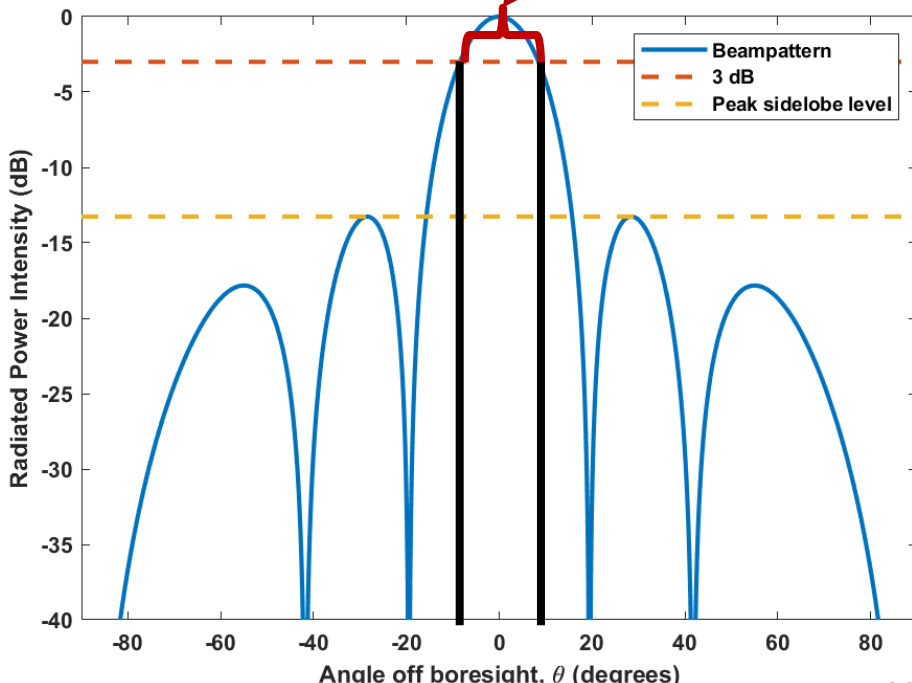
- For example, consider a 10 GHz (X-band, 3 cm wavelength) idealized uniform current source antenna
- For a $D_y = 9$ cm antenna, the normalized pattern is:

$$E(\theta) = \text{sinc} \left[\left(\frac{D_y}{\lambda} \right) \sin \theta \right]$$
$$= \text{sinc}[3 \sin \theta]$$

– We are *ignoring* the ϕ component for the purposes of this example

- Note: $D_y = 3\lambda$

$$\theta_3 \approx \left(\frac{180}{\pi} \right) 0.886 \frac{\lambda}{D_y} \approx 17 \text{ degrees}$$





Example Power Pattern: Uniform Current Source

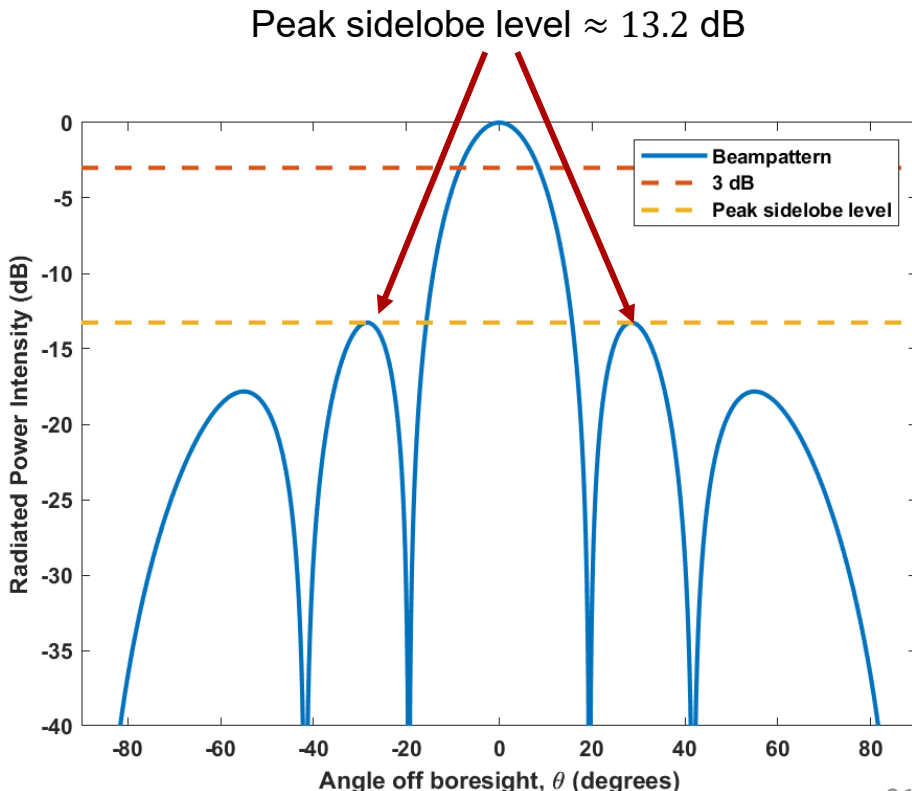


- For example, consider a 10 GHz (X-band, 3 cm wavelength) idealized uniform current source antenna
- For a $D_y = 9$ cm antenna, the normalized pattern is:

$$E(\theta) = \text{sinc} \left[\left(\frac{D_y}{\lambda} \right) \sin \theta \right]$$
$$= \text{sinc}[3 \sin \theta]$$

– We are *ignoring* the ϕ component for the purposes of this example

- Note: $D_y = 3\lambda$





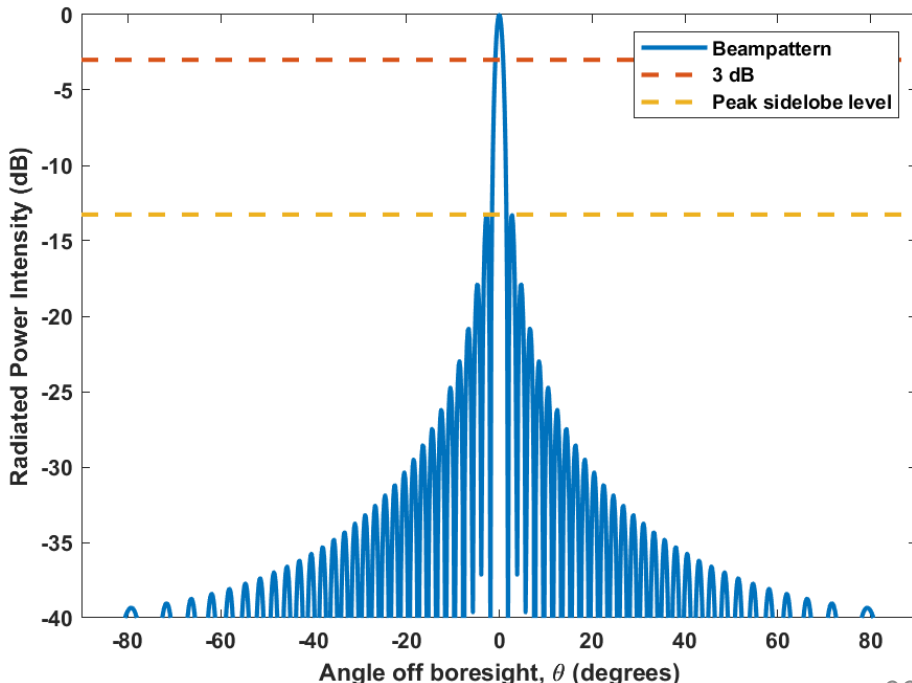
Example Power Pattern: Uniform Current Source



- For example, consider a 10 GHz (X-band, 3 cm wavelength) idealized uniform current source antenna
- For a $D_y = 90$ cm antenna, the normalized pattern is:

$$E(\theta) = \text{sinc} \left[\left(\frac{D_y}{\lambda} \right) \sin \theta \right]$$
$$= \text{sinc}[(30) \sin \theta]$$

- Note: now $D_y = 30\lambda$





Example Power Pattern: Uniform Current Source

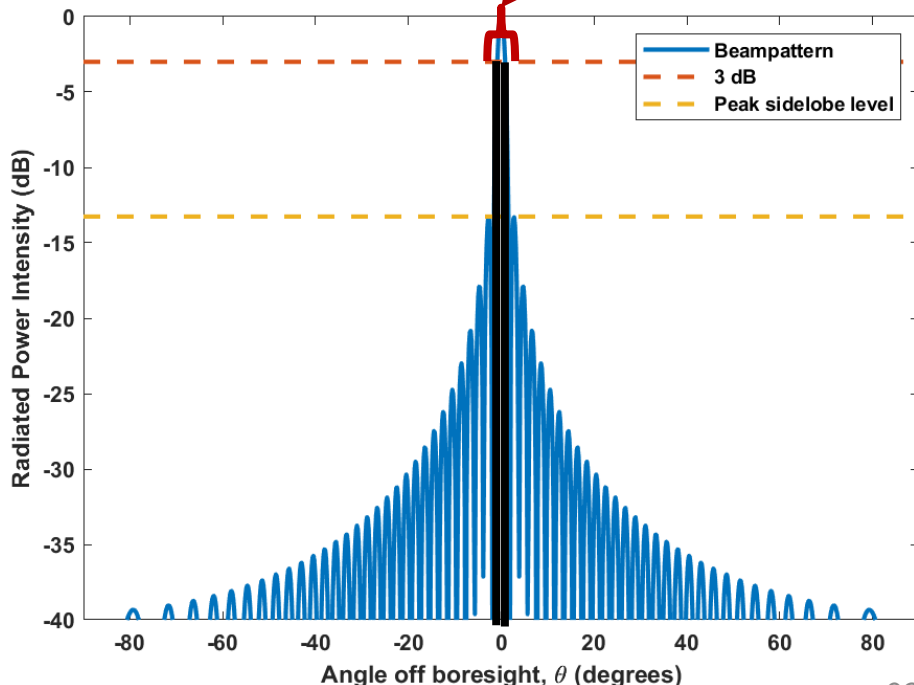


- For example, consider a 10 GHz (X-band, 3 cm wavelength) idealized uniform current source antenna
- For a $D_y = 90$ cm antenna, the normalized pattern is:

$$E(\theta) = \text{sinc} \left[\left(\frac{D_y}{\lambda} \right) \sin \theta \right]$$
$$= \text{sinc}[(30) \sin \theta]$$

- Note: now $D_y = 30\lambda$

$$\theta_3 \approx \left(\frac{180}{\pi} \right) 0.886 \frac{\lambda}{D_y} \approx 1.7 \text{ degrees}$$





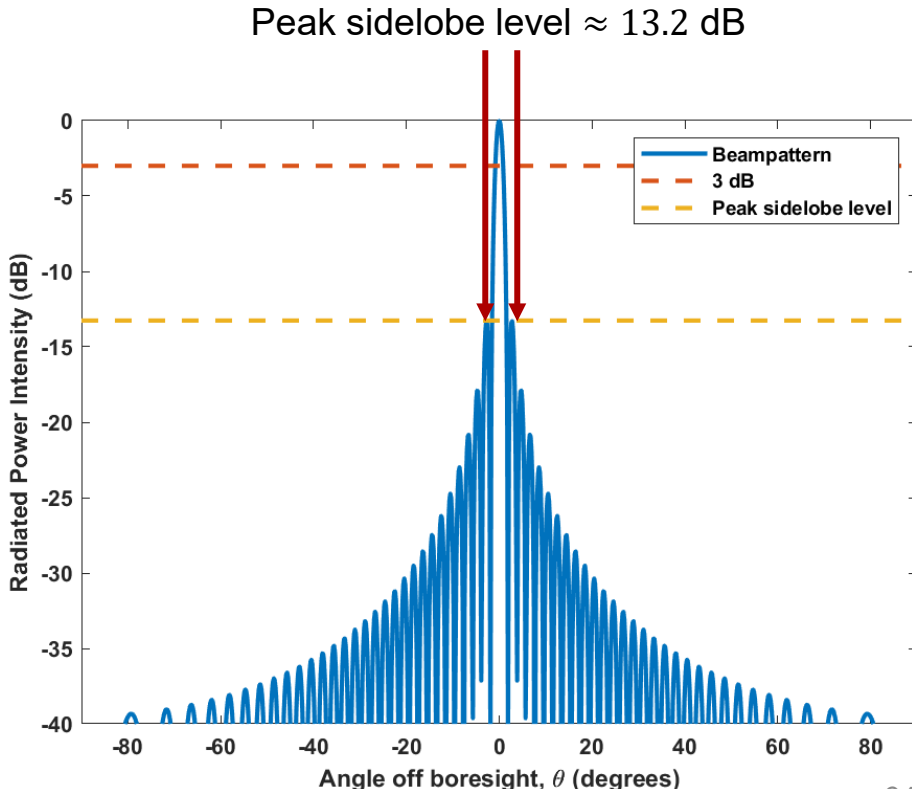
Example Power Pattern: Uniform Current Source



- For example, consider a 10 GHz (X-band, 3 cm wavelength) idealized uniform current source antenna
- For a $D_y = 90$ cm antenna, the normalized pattern is:

$$E(\theta) = \text{sinc} \left[\left(\frac{D_y}{\lambda} \right) \sin \theta \right]$$
$$= \text{sinc}[(30) \sin \theta]$$

- Note: now $D_y = 30\lambda$
- Peak sidelobe level depends on aperture shape – not electrical size!

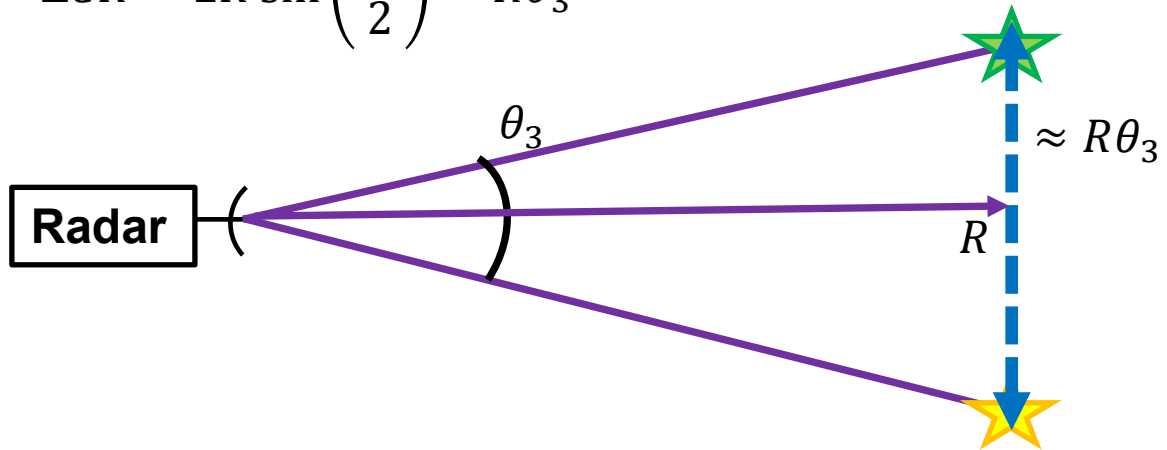




Angular Resolution

- The angular resolution of a radar is approximately equal to

$$\Delta CR = 2R \sin\left(\frac{\theta_3}{2}\right) \approx R\theta_3$$



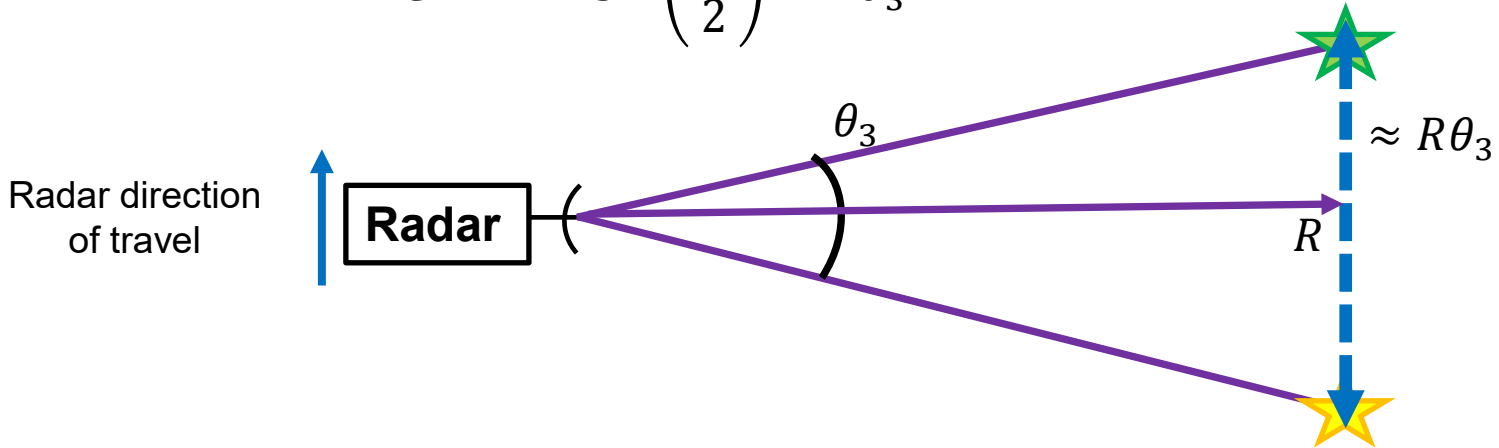
- Important: the angular resolution is **range dependent!**



Angular Resolution

- The angular resolution of a radar is approximately equal to

$$\Delta CR = 2R \sin\left(\frac{\theta_3}{2}\right) \approx R\theta_3$$



- Important: the angular resolution is **range dependent!**
- Particularly if the radar is moving perpendicular to the direction of illumination the angular resolution is known as the *cross-range* resolution



3-D Resolution Cell

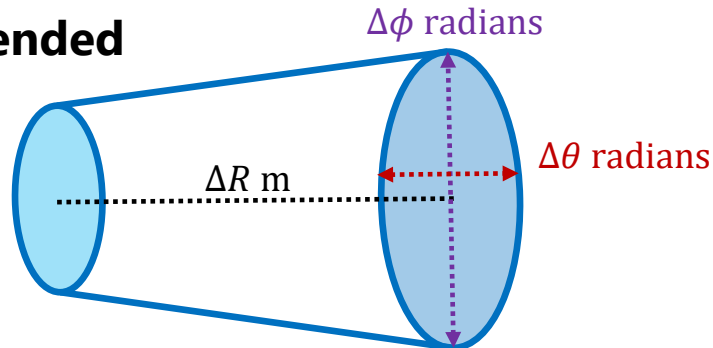


- The radar is taking measurements defined in three dimensions: radial range R , azimuth angle θ , and elevation angle ϕ
- The total volume is defined by the subtended solid angle and range resolution
- The approximate volume is:

$$\Delta V = \pi \left(\frac{R\theta_3}{2} \right) \left(\frac{R\phi_3}{2} \right) \Delta R = \frac{\pi}{4} R^2 \theta_3 \phi_3 \Delta R$$

Area of ellipse

Very small compared to rest of expression



- Note that we can approximate as:

$$\Delta V \approx R^2 \theta_3 \phi_3 \Delta R = (R\theta_3)(R\phi_3)\Delta R = \Delta\theta_3 \Delta\phi_3 \Delta R$$

- We will consider the range resolution ΔR soon



3-D Resolution Cell

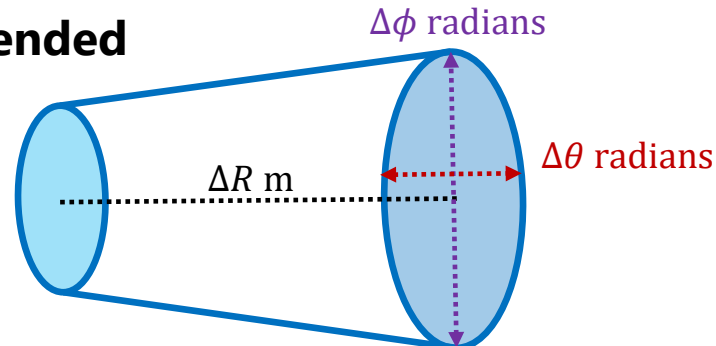


- The radar is taking measurements defined in three dimensions: radial range R , azimuth angle θ , and elevation angle ϕ
- The total volume is defined by the subtended solid angle and range resolution
- The approximate volume is:

$$\Delta V = \pi \left(\frac{R\theta_3}{2} \right) \left(\frac{R\phi_3}{2} \right) \Delta R = \frac{\pi}{4} R^2 \theta_3 \phi_3 \Delta R$$

Area of ellipse

Very small compared to rest of expression



- This volume increases with R^2
- At a given sample the receiver will collect energy from *all scatterers* contained within a resolution cell of size $\Delta\theta_3\Delta\phi_3\Delta R$



Radar Range Equation



- The **radar range equation** is a *deterministic* model relating the received power from a target reflection to the transmitted power
- Incorporates most system parameters to *bound* the received signal power
 - Fundamental relation for basic system design and analysis
- Let's build this classic equation...



Transmitted Power Density



- If a signal of P_t watts is transmitted *isotropically*, the power **density** at range R is

$$\frac{P_t}{4\pi R^2} \text{ W/m}^2$$

- Note that this is a **power** quantity, not an amplitude/voltage
 - P_t is set by the amplifier chain in the transmitter
- If an antenna with gain G is used (where G is ratio of peak antenna power to isotropic gain) is used instead, the power density in direction of peak gain becomes

$$Q_t = \frac{P_t G_t}{4\pi R^2} \text{ W/m}^2$$

- If the target is in a different direction than the peak, then the power density is reduced according to the beampattern of the antenna



Example Tx Power Density: S-Band Radar



- Consider a radar with a
 - Square antenna 1 m on each side
 - Transmit power of 1 kW
 - Center frequency of 3 GHz (S-Band)
- Assume there is a target
 - Isotropic RCS of 1 m^2
 - Radial range of 5 km
- Consider the spherical spreading radiation *from the radar to the target*





Example Tx Power Density: X-Band Radar



- Consider a radar with a
 - Square antenna 1 m on each side
 - Transmit power of 1 kW
 - Center frequency of 10 GHz (X-Band)
- Assume there is a target
 - Isotropic RCS of 1 m^2
 - Radial range of 5 km
- Consider the spherical spreading radiation *from the radar to the target*

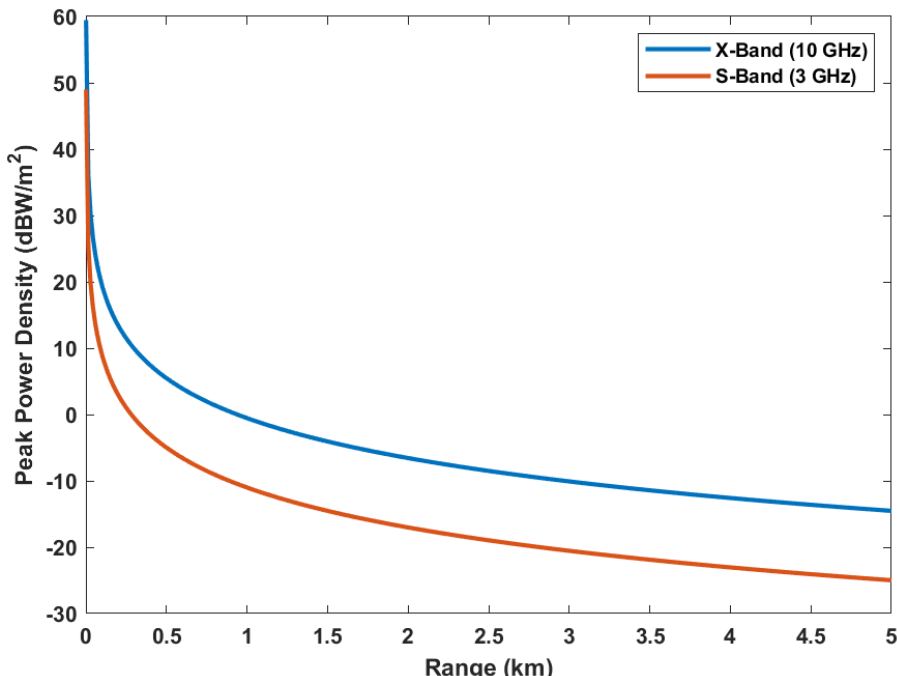




X-Band and S-Band Power vs. Range



- X-band system has ~10 dB more gain than S-band for same antenna footprint
 - Spreading losses only
 - X-band will suffer more atmospheric loss than S-band
- Note extreme power loss – from 1 meter to 5 km the radar suffers from 79 dB of spreading loss
 - Nearly 8 orders of magnitude!
- Now the radiation needs to get back to the radar...





Target Backscatter Power



- Suppose a stationary target exists at range R
 - The incident RF energy is scattered by the target in all directions
 - Portion of the power reflected toward the radar receiver is called the backscatter
- Recall the units of power density is W/m^2
- Assume the energy of the target backscatter equals that incident on an *area of σm^2* , known as the *radar cross section (RCS)* of the target
- The backscattered *power (not density)* is then

$$P_b = \frac{P_t G_t \sigma}{4\pi R^2} \text{ W}$$

- The RCS is not the physical cross-sectional area of the actual target
- It is an *equivalent area* that is highly dependent on target type/shape



Defining Radar Cross Section



- The radar cross section (RCS) is the fictional area that accounts for the backscattered power from the target, P_b

$$P_b = \sigma Q_t \text{ W}$$

- Therefore, as P_b must satisfy

$$Q_b = \frac{P_b}{4\pi R^2} \frac{\text{W}}{\text{m}^2} = \frac{\sigma Q_t}{4\pi R^2} \frac{\text{W}}{\text{m}^2} \rightarrow \sigma = 4\pi R^2 \frac{Q_b}{Q_t} \text{ m}^2$$

- Thus, RCS is the fictional area that accounts for the *relative* value of backscattered power density in terms of the incident power density
 - Note: assumes *isotropic* reradiation of backscatter!
 - RCS of real non-spherical targets is *highly* directional
 - Often described with a statistical model
- One big issue with the above equation for RCS...range dependence!



Range Independent RCS Definition



- To calculate the RCS we take the limit as $R \rightarrow \infty$ to remove dependence on range

$$\sigma = 4\pi \lim_{R \rightarrow \infty} \left[R^2 \frac{|\vec{E}^b|^2}{|\vec{E}^t|^2} \right]$$

Backscattered E-field amplitude

Transmitted E-field amplitude

The diagram shows the RCS formula $\sigma = 4\pi \lim_{R \rightarrow \infty} \left[R^2 \frac{|\vec{E}^b|^2}{|\vec{E}^t|^2} \right]$. A red arrow points from the text "Backscattered E-field amplitude" to the term $|\vec{E}^b|^2$. A blue arrow points from the text "Transmitted E-field amplitude" to the term $|\vec{E}^t|^2$.

- Therefore, RCS **only depends** on scatterer characteristics!



Received Target Power



- The reflection from the target travels to the receiver
- If the transmitter and receiver are at the same range, the power density at the receiver is therefore

$$Q_r = \frac{P_t G_t \sigma}{(4\pi)^2 R^4} \text{ W/m}^2$$

- Recall that the antenna has an **effective aperture** of $A_e \text{ m}^2$ to collect the backscattered radiation
- The received power is therefore

$$P_r = \frac{P_t G_t A_e \sigma}{(4\pi)^2 R^4} \text{ W}$$

- If the transmitter and receiver are separate it is a **bistatic system** and the transmit and receive propagation are treated separately



Received Target Power



- Recall that the gain can be related to effective aperture as:

$$G_r = \frac{4\pi}{\lambda^2} A_e$$

- The received power *prior to receive amplification* is therefore

$$P_r = \frac{P_t G_t G_r \lambda^2 \sigma}{(4\pi)^3 R^4} \text{ W}$$

- This is the ideal received power in a vacuum
- Real systems also suffer loss prior to sampling, denoted as L_s
 - Attenuation in cables, waveguides, circulators, etc.
- We've also discussed frequency dependent atmospheric loss



Example Rx Power Density: X-Band Radar



- Consider a radar with a
 - Square antenna 1 m on each side
 - Transmit power of 1 kW
 - Center frequency of 10 GHz (X-Band)
- Assume there is a target
 - Isotropic RCS of 1 m^2
 - Radial range of 5 km
- Consider the spherical spreading radiation *from the target back to the radar*

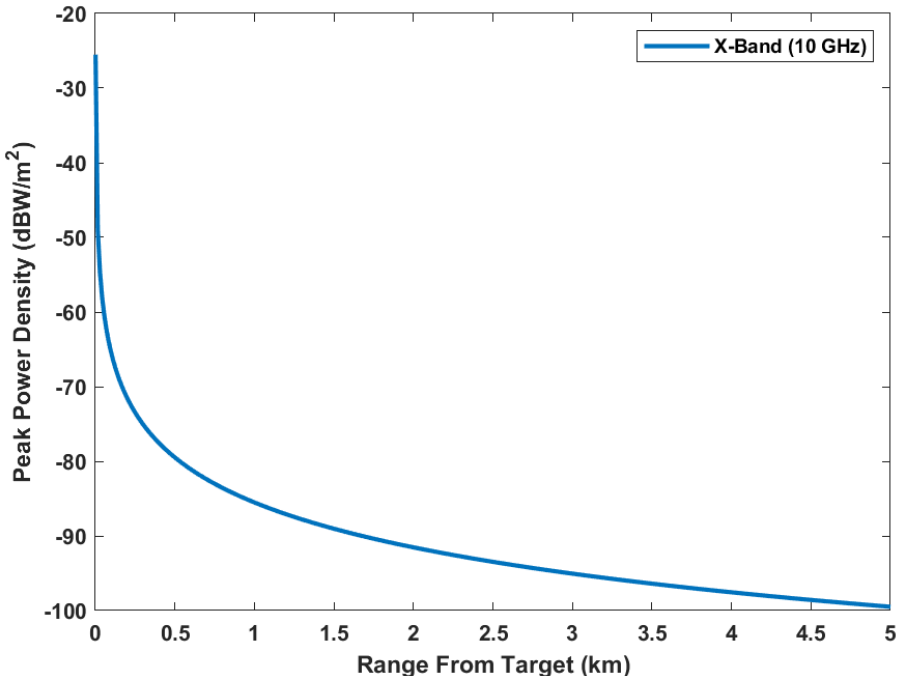




Example Return Power from 1 m^2 Target @ 5 km



- Recall the radar parameters:
 - Square antenna 1 m **on each side**
 - Transmit power of 1 kW
 - Center frequency of 10 GHz (**X-Band**)
- For a 1 kW transmission...the radar received 10^{-10} W in received power density
 - That is a **13 order of magnitude** difference for a target only 5 km from the radar!!



To achieve long range radar systems must have large average power and be able to detect very weak signals



Radar Signal Characteristics



Received Signal Components



- Received signal is a *superposition* of several components

- **Signal**

- Targets

- **Clutter**

- Surface (ground, sea)
 - Weather (clouds, rain)

Multiplicative components

- **Noise**

- External (cosmic noise)
 - Internal (shot, *thermal*)

- **Electromagnetic interference**

- TV stations
 - Cell phones
 - Other communication devices
 - Jamming
 - Other radars

Additive components



Simple Pulse Waveforms



- The ***simple pulse*** is a rectangular window at the carrier frequency of duration T_p and bandwidth B
 - For a rectangular pulse it can be shown that $T_p \approx \frac{1}{\beta}$
- It can be shown that the range resolution is

$$\Delta R \approx \frac{c}{2\beta}$$

- A ***long*** pulse has “narrow” bandwidth and ***poor*** range resolution
- A ***short*** pulse has “wide” bandwidth and ***good*** range resolution

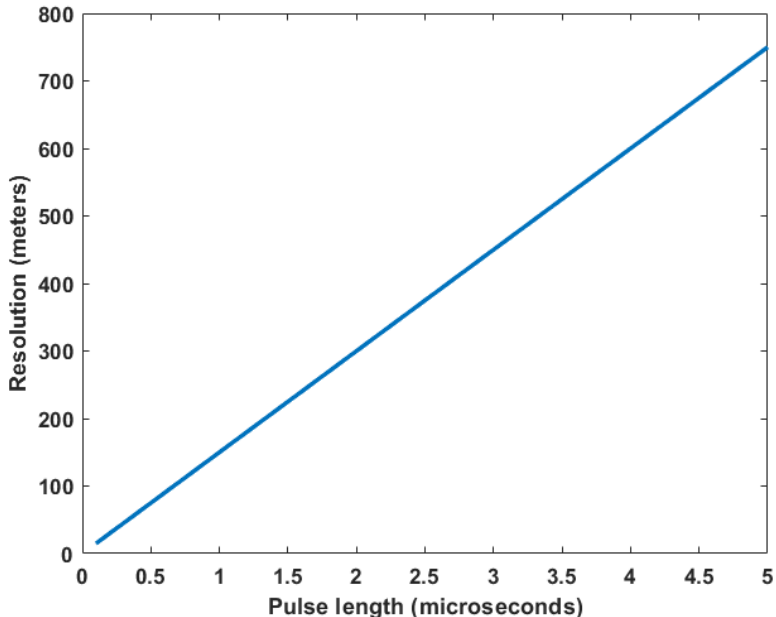
Simple pulses have an intrinsic tradeoff between resolution and energy



Range Resolution of a Simple Pulse



- Short pulses \Rightarrow high resolution
- Often a radar cannot transmit and receive at the same time
 - The radar is “blind” to the (at least) first range bin
- Most high-power amplifiers operate in *saturation* and therefore emit constant-amplitude waveforms
 - Short pulses therefore have lower *energy-on-target*
- To *decouple* range resolution and energy-on-target *pulse compression* waveforms are used



Range resolution as a function of pulse length



Pulse Compression Waveform



- A **pulse compression** radar waveform is a modulated pulse
- A **pulse compression waveform** is any waveform where $BT_p > 1$
- The range resolution of a pulse compression waveform is still

$$\Delta R \approx \frac{c}{2B}$$

- Therefore, the modulation **decouples** pulse duration and bandwidth
 - Pulse compression waveforms are “long” ($T_p > \frac{1}{B}$)
- Matched filtering **compresses** the long waveform and yields the resolution of a shorter pulse $T_c = \frac{1}{B}$
- Optimization of **phase coded** waveforms is an active area of research
 - BT_p “chips” of length T_c can be optimized to yield a desired autocorrelation
 - Time-bandwidth product BT_p is the **dimensionality** of the waveform optimization



Linear Frequency Modulated Waveform



- The linear frequency modulated (LFM) waveform is the most common pulse compression waveform
- The frequency function of the LFM is defined as:

$$f_{LFM}(t) = \pm \left(-\frac{B}{2} + \frac{B}{T_p} t \right)$$

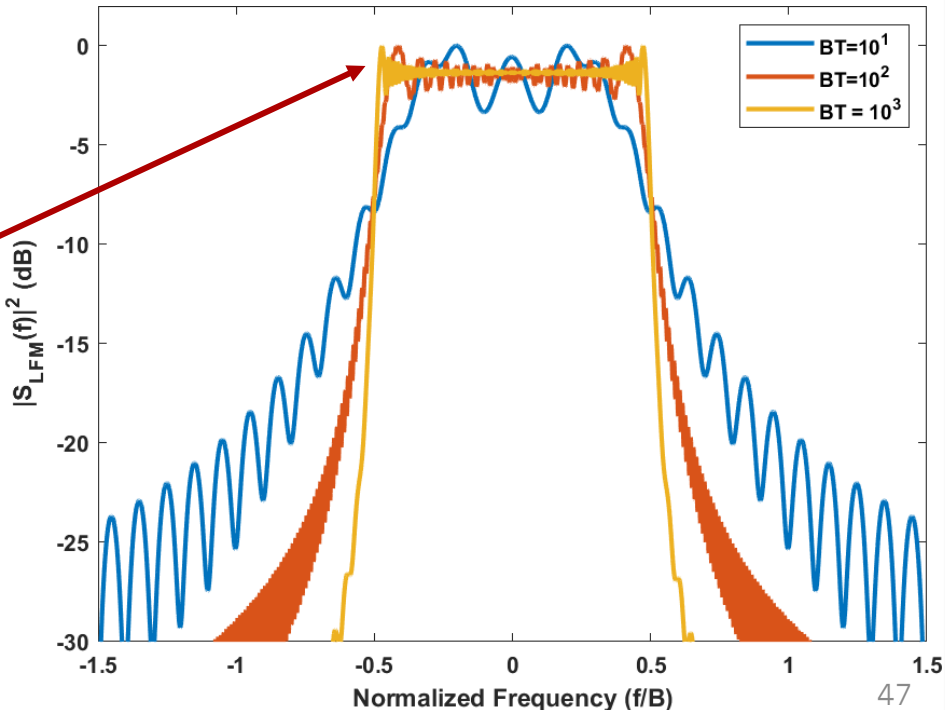
- The LFM therefore *sweeps* linearly across the frequency band $\left[-\frac{B}{2}, \frac{B}{2} \right]$
 - The *chirp rate* or slope of the sweep is $k = \frac{B}{T_p}$
 - The LFM is therefore a rectangular window in frequency
- The sign indicates the direction of the chirp
 - Negative sign results in a *downchirp* that sweeps from high to low frequency
 - Positive sign results in an *upchirp* that sweeps from low to high frequency



Consequences of Dimensionality



- The expression for the LFM waveform assumes a perfect rectangular window in frequency
 - Still has a finite time window!
- LFM *converges* to a rectangular frequency window with increasing BT_p
 - Jump discontinuity causes unavoidable ringing (Gibbs Phenomenon)
- LFM has sinc-like autocorrelation (i.e. range) sidelobes
 - Peak sidelobe level of ≈ -13 dB





Doppler Shift



- A target moving with a constant linear velocity *relative to the radar* will induce a frequency shift on the returned signal
- The *Doppler shift* in frequency is simply the frequency change – the difference between the new center frequency F and starting frequency F_0

$$F_D = F - F_0 = F_0 \left(\frac{c + \nu}{c - \nu} \right) - F_0 = F_0 \left[\frac{c + \nu}{c - \nu} - 1 \right] = \frac{2\nu}{c - \nu} F_0$$

- For $\nu \ll c$ (**most cases**):
 - Note that the Doppler shift depends on the center frequency of the radar!
- Measuring the Doppler shift provides
 - Information on target velocity
 - The primary discriminator for filtering ground clutter!



Radar Systems



General Radar System Tasks and Goals



- **Transmitter subsystem tasks**
 - Generate waveforms
 - Upconvert waveforms to carrier frequency
 - Condition signal – make sure we transmit a *clean and contained* signal!
 - Amplify the transmitted signal to an appropriate power level
 - Efficiently couple amplified signal to the environment via antenna
- **Receiver subsystem tasks**
 - Amplify received signal
 - Reject interference
 - Downconvert to baseband
 - All while maximizing dynamic range and minimizing noise contributions

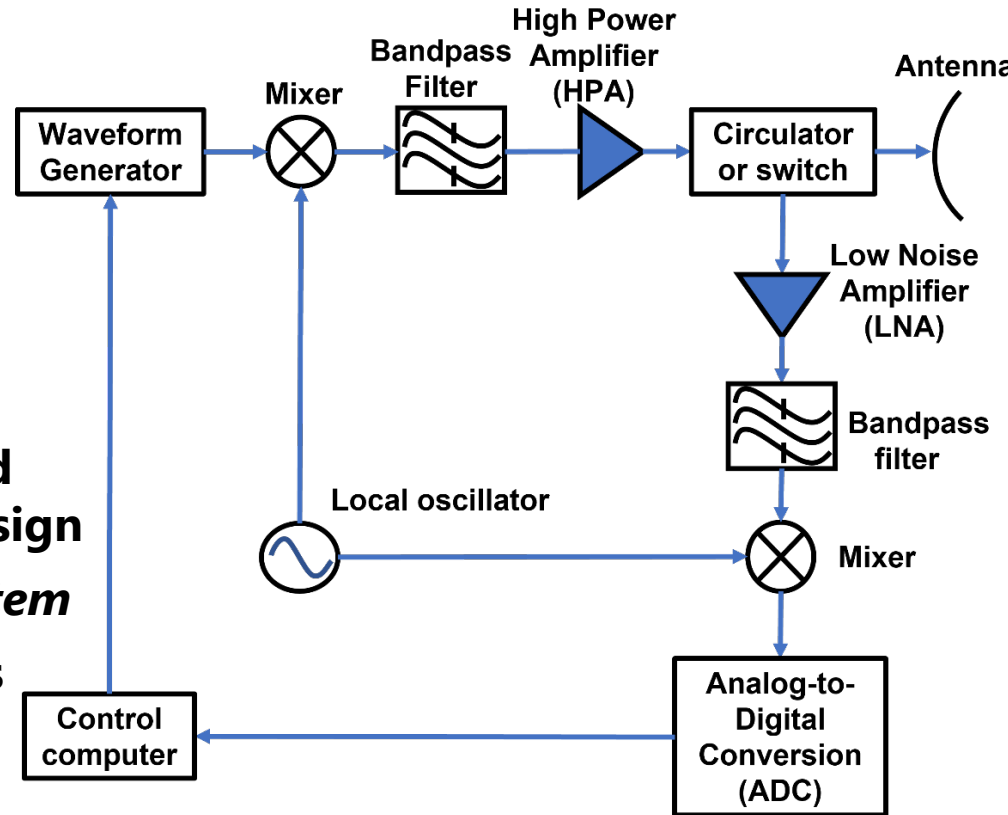


An Example System

- This is an ***illustrative*** system

- MANY variations exist!
- Usually, additional filters and amplifiers...
- May have additional downconversion stages

- We will use this system to demonstrate how radar goals and phenomenology drive system design
- Remember, radar is an ***active system***
- Consider two general subsystems
 - Transmit subsystem
 - Receive subsystem

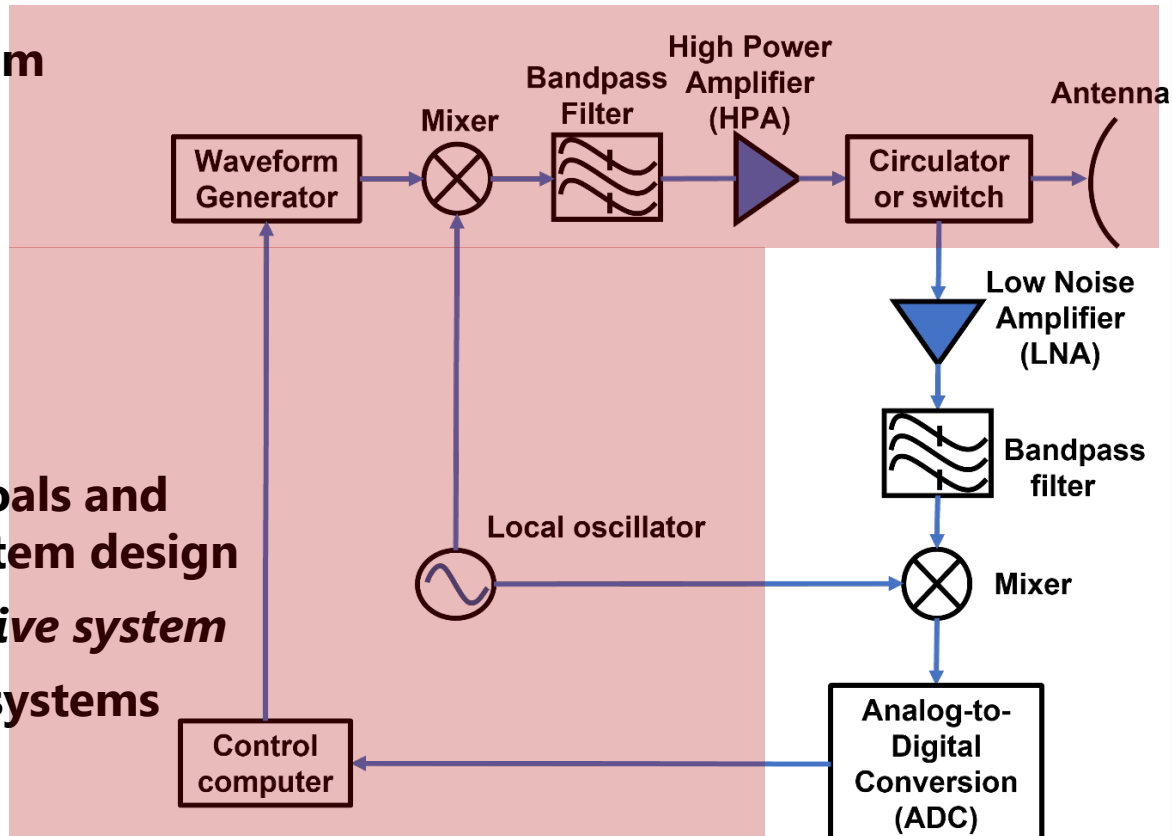




An Example System



- This is an ***illustrative*** system
 - MANY variations exist!
 - Usually, additional filters and amplifiers...
 - May have additional downconversion stages
- We will use this system to demonstrate how radar goals and phenomenology drive system design
- Remember, radar is an ***active system***
- Consider two general subsystems
 - Transmit subsystem
 - Receive subsystem

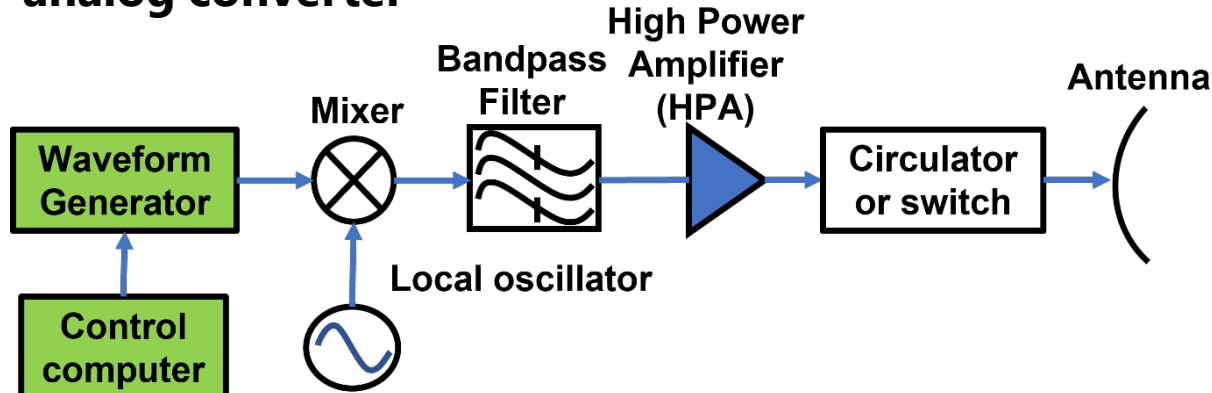




Radar Waveform Generation



- The transmitted waveform is generally a combination of:
 - Pulsed vs. continuous wave (CW)
 - Simple pulse or pulse compression waveform
- Pulsed waveforms use high peak power while CW waveforms rely on long integration times to offset low peak power
 - Dependent on HPA!
- Depending on digital-to-analog converter (DAC) capability, may be able to directly generate arbitrary waveforms at RF center frequency

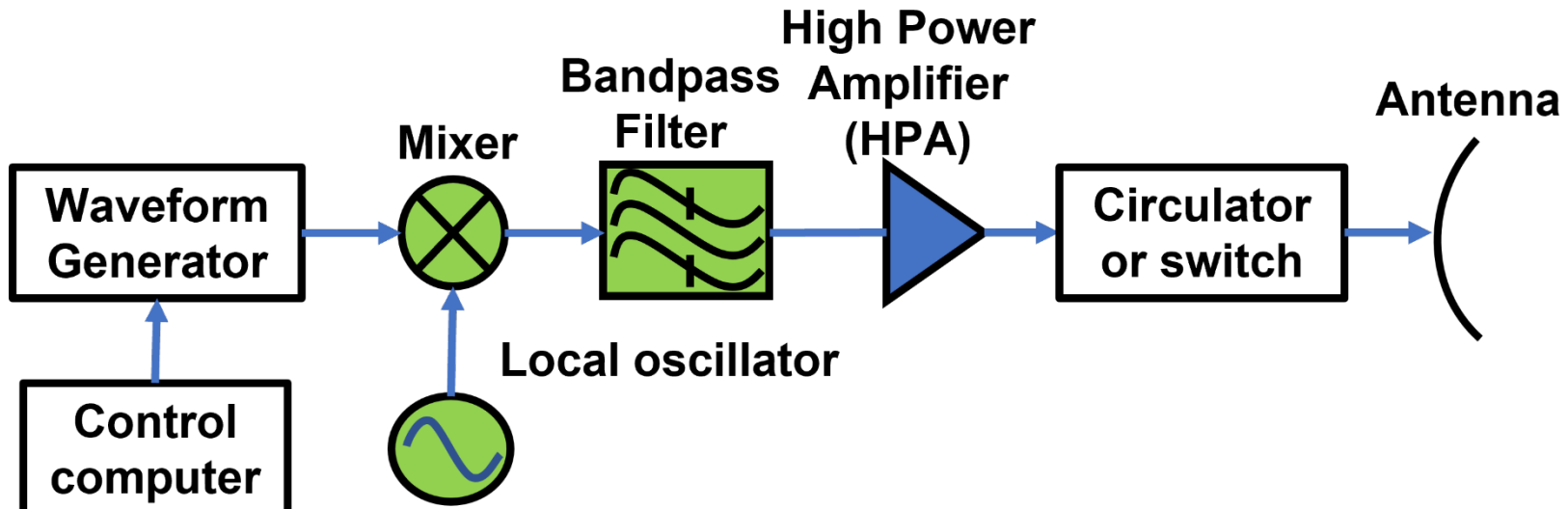




Mixing Process



- Recall that radars operate at a *carrier frequency* likely measured in GHz
 - Generating or receiving arbitrary signals at these frequencies is impractical!
 - In general, we need to *upconvert* an intermediate frequency or baseband signal to the desired carrier frequency



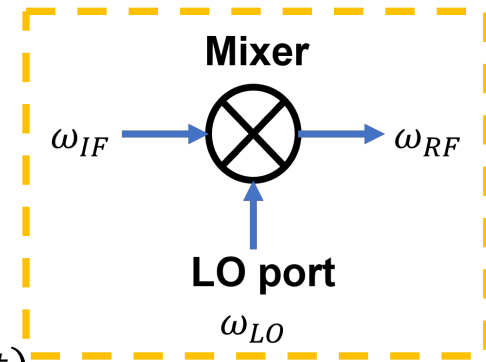


Mixing Process



- Mixers are *non-linear* devices that allow frequency modulation of signals
 - An ideal mixer is just a cosine multiplier!
- Assume that the radar waveform is a voltage sinusoid centered at an *intermediate frequency* ω_{IF}
- *Mixing* the waveform and a local oscillator (LO) at ω_{LO} yields:

$$\begin{aligned}v_{RF}(t) &= v_{IF}(t)v_{LO}(t) = \cos(\omega_{IF}t)\cos(\omega_{LO}t) \\&= \frac{1}{2}\cos[(\omega_{IF} - \omega_{LO})t] + \boxed{\frac{1}{2}\cos[(\omega_{IF} + \omega_{LO})t]}\end{aligned}$$



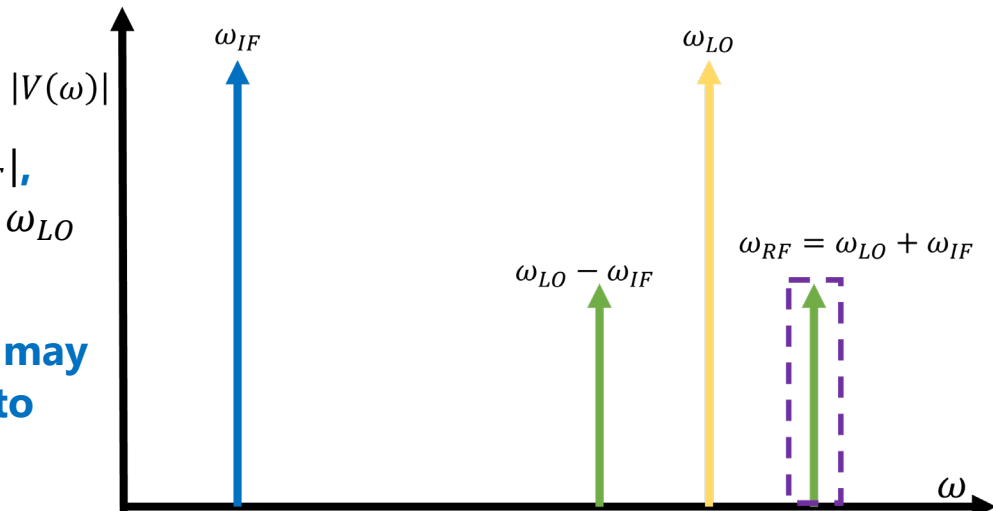
- Therefore, the *ideal* mixing process produces mixing product at our desired RF frequency $\omega_{RF} = \omega_{IF} + \omega_{LO}$



Mixing



- Unfortunately...mixers are never ideal!
- Can show from Taylor Series expansion the mixer produces *intermodulation products* at the following frequencies:
 - 1st order: ω_{LO} , ω_{RF}
 - 2nd order: $2\omega_{LO}$, $2\omega_{IF}$,
 $\omega_{LO} - \omega_{IF}$, $\omega_{RF} + \omega_{LO}$
 - 3rd order: $2\omega_{LO} - \omega_{IF}$, $|2\omega_{LO} - \omega_{RF}|$,
 $3\omega_{LO}$, $3\omega_{IF}$, $2\omega_{LO} + \omega_{IF}$, $2\omega_{IF} + \omega_{LO}$
 - ...and so on
 - Therefore, on transmit the mixer may be followed by a *bandpass filter* to remove these products

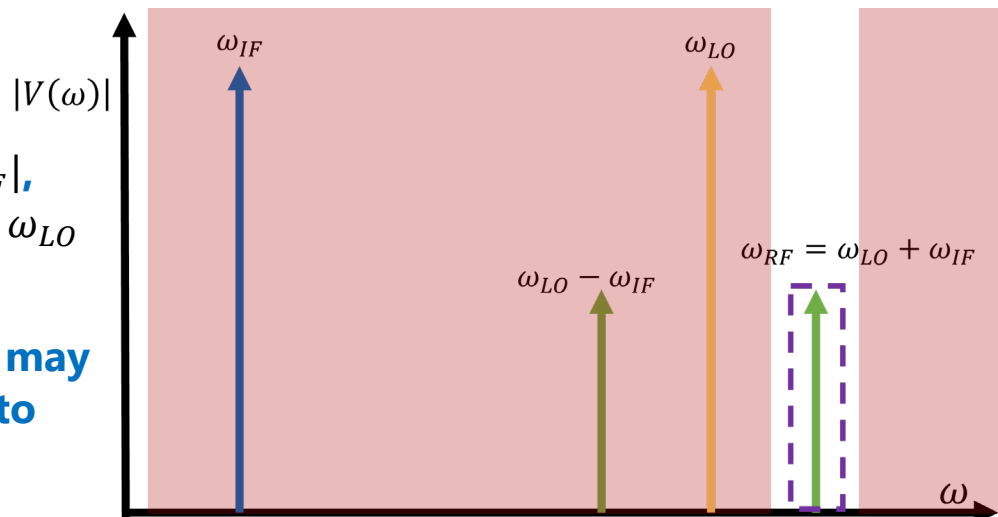




Mixing



- Unfortunately...mixers are never ideal!
- Can show from Taylor Series expansion the mixer produces *intermodulation products* at the following frequencies:
 - 1st order: ω_{LO} , ω_{RF}
 - 2nd order: $2\omega_{LO}$, $2\omega_{IF}$,
 $\omega_{LO} - \omega_{IF}$, $\omega_{RF} + \omega_{LO}$
 - 3rd order: $2\omega_{LO} - \omega_{IF}$, $|2\omega_{LO} - \omega_{RF}|$,
 $3\omega_{LO}$, $3\omega_{IF}$, $2\omega_{LO} + \omega_{IF}$, $2\omega_{IF} + \omega_{LO}$
 - ...and so on
 - Therefore, on transmit the mixer may be followed by a *bandpass filter* to remove these products

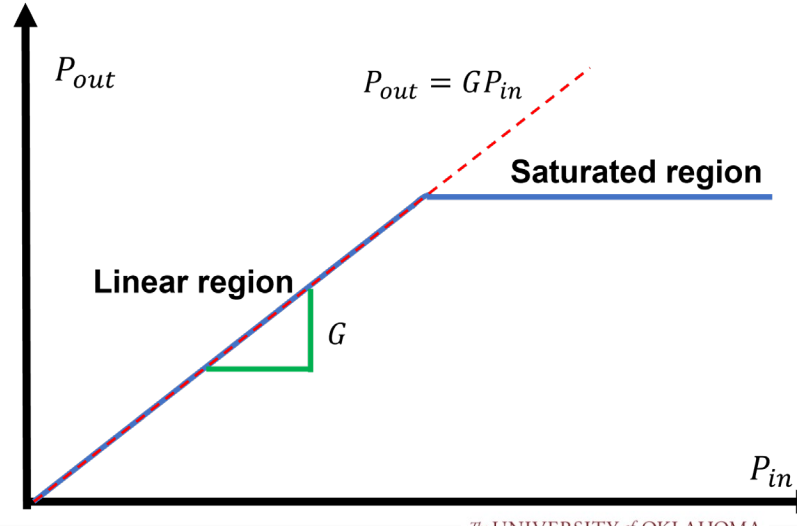




High Power Amplifiers (HPAs)



- The final signal is typically amplified prior to transmission by the antenna
- For power-efficiency (HPAs) typically operate in the *saturated region*
 - Traditionally vacuum tube based
 - Solid state becoming more common – especially on digital arrays
- Operating in saturated region → constant modulus waveforms
 - Amplitude modulated waveforms become distorted
- Amplifier considerations
 - Efficiency and heat dissipation
 - Peak power
 - Duty cycle and average power
 - Rise/fall time

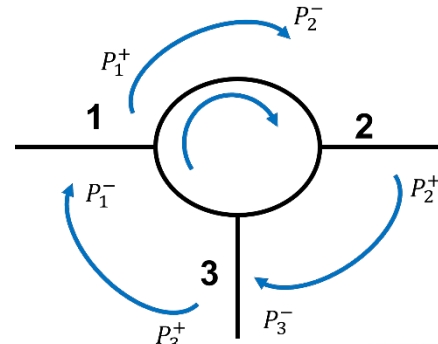




Antenna and Circulator/Switch



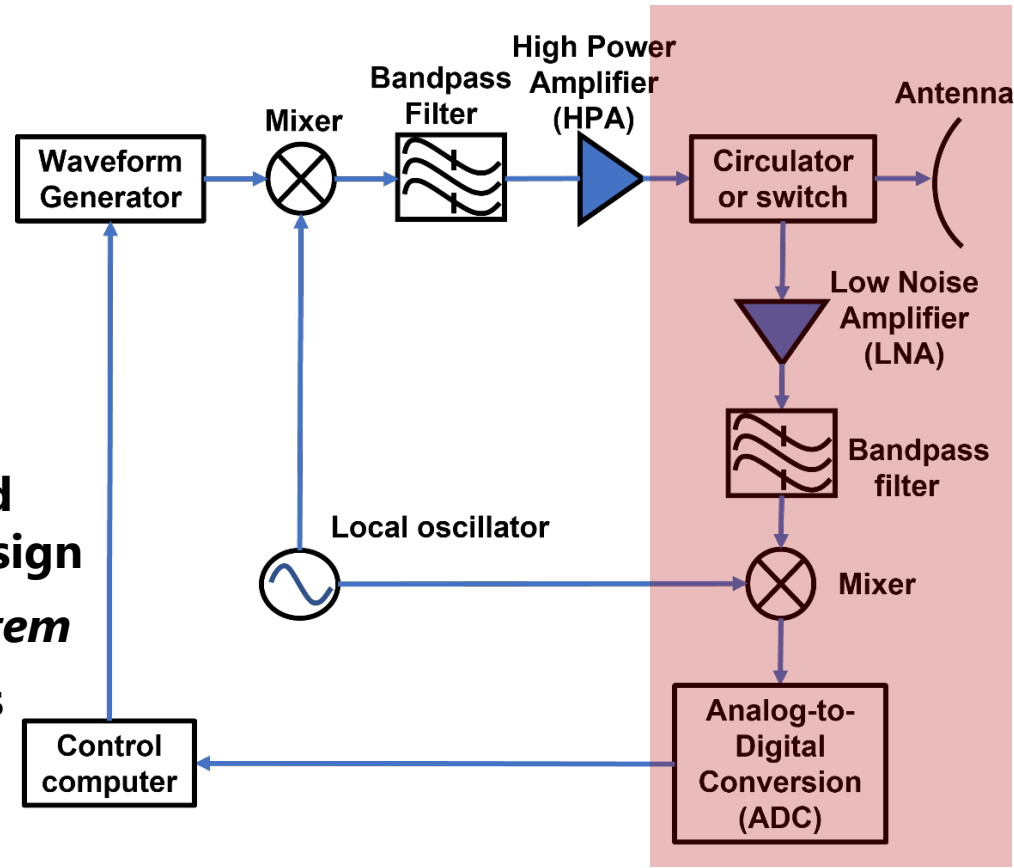
- We have already covered antenna basics
- Key problem: radars transmit a very strong signal to receive a very weak signal → requires receiver to be very sensitive
- Using a single or collocated antenna(s) causes transmit-receive coupling
 - Strong coupling can damage/destroy a sensitive receiver!
- Some possible mitigation techniques:
 - Circulators are non-reciprocal devices that pass a signal to the next port
 - High-speed switches can blank the receiver while transmitting
- Note: most high-power pulsed radars are *blind* when transmitting
 - No received information from range equal to pulse duration!





An Example System

- This is an ***illustrative*** system
 - MANY variations exist!
 - Usually, additional filters and amplifiers...
 - May have additional downconversion stages
- We will use this system to demonstrate how radar goals and phenomenology drive system design
- Remember, radar is an ***active system***
- Consider two general subsystems
 - Transmit subsystem
 - Receive subsystem





Thermal Noise



- All components warmer than absolute zero will generate *thermal noise*
- Noise power has a *power spectral density* of

$$S_n(F) = \frac{2k_b T R_s(hF/k_b T)}{\exp\left(\frac{hF}{k_b T}\right) - 1} = \frac{2R_s hF}{\exp\left(\frac{hF}{k_b T}\right) - 1}$$

- Where $h = 6.6254 \times 10^{-34}$ Joules · second (**Planck's constant**)
- And $k_b = 1.38 \times 10^{-23}$ Joules/°K (**Boltzmann's constant**) → temperature is in Kelvin
- Note: this is a *two-sided* power density (one sided power is twice this)
- Note that if $\frac{hF}{k_b T} \ll 1$ then $\exp\left(\frac{hF}{k_b T}\right) \approx 1 + \frac{hF}{k_b T}$
- Result is the expression:

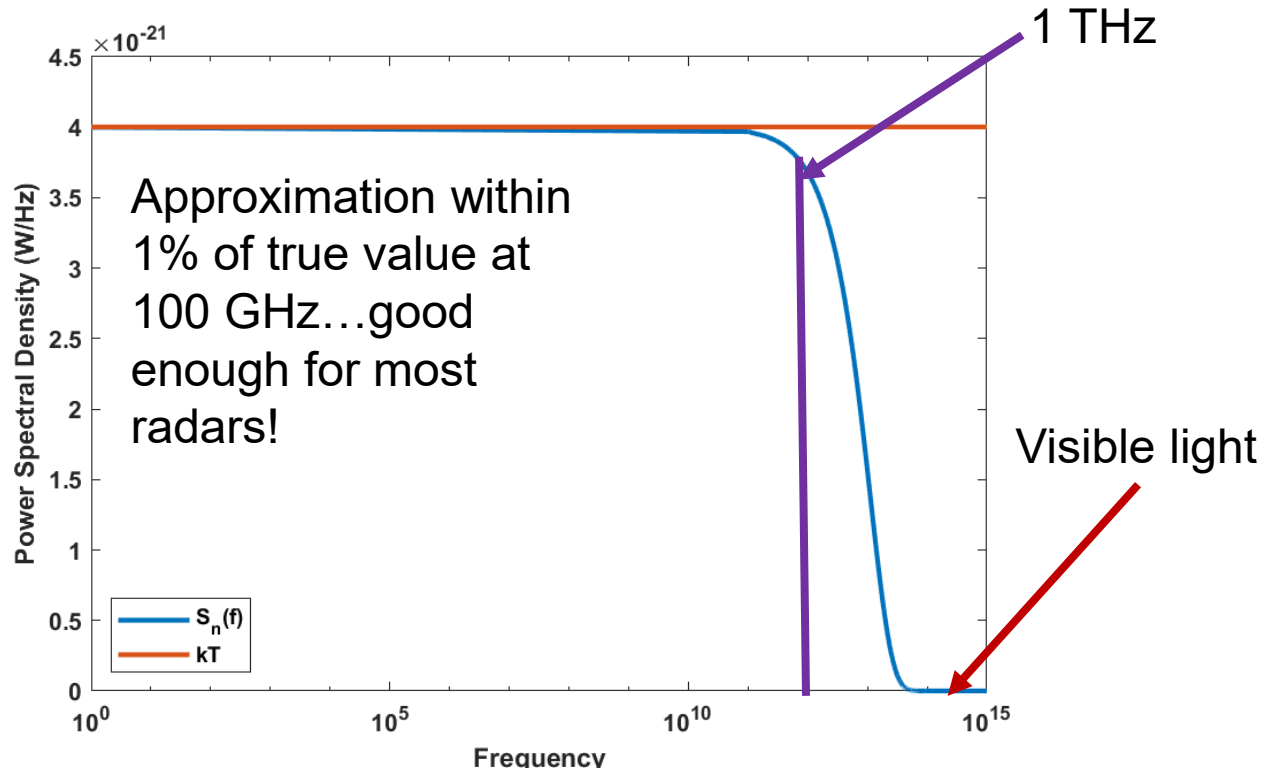
$$S_n(F) = 2R_s k_b T \text{ Joules} = 2R_s k_b T \frac{\text{W}}{\text{Hz}} \rightarrow P_n = k_b T B \text{ Watts}$$



Thermal Noise Approximation



- Plot for $T = 290^\circ\text{K}$ ($k_b T \approx 4 \times 10^{-21} \text{ W/Hz}$)





Component Signal to Noise Ratios



- The *input* signal-to-noise ratio (SNR) to a component at temperature T_s is defined as:

$$SNR_i = \frac{P_i}{k_b T_s B}$$

- Where P_i is the signal power we want to sample
 - And T_s is the *input or source* noise temperature
- The *output* SNR of the component is therefore:

$$SNR_o = \frac{GP_i}{Gk_b T_s B + P_{na}}$$

- Where G is the gain of the component (note: $G < 1 \rightarrow$ attenuation)
 - And P_{na} is the noise power added by the component
 - The total *output noise power* is therefore $Gk_b T_s B + P_{na}$



Noise Figure Definition



- The noise figure for a receiver component is defined as the ratio of the *input* signal-to-noise ratio (SNR) to the *output* SNR

$$F = \frac{SNR_i}{SNR_o} = \frac{\frac{P_i}{k_b T_s B}}{\frac{GP_i}{Gk_b T_s B + P_{na}}} = \frac{Gk_b T_s B + P_{na}}{Gk_b T_s B} = 1 + \frac{P_{na}}{Gk_b T_s B}$$

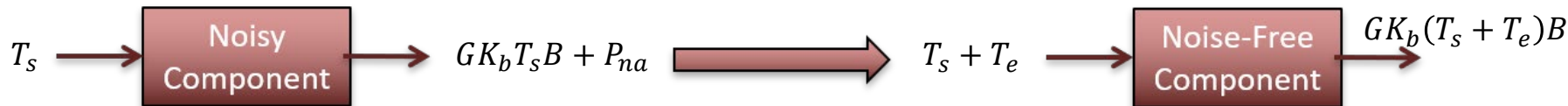
- Another way of thinking about the noise figure is it is the ratio of the *actual* total noise to the *minimum* ($T_s = T_0 = 290 \text{ } ^\circ\text{K}$) or standard noise
- This leads to the idea of *effective noise temperature*



Effective Noise Temperature



- We can model the component as an ideal, noise-free component, but with extra noise power on the input:



- The effective noise temperature T_e is therefore found from the expression:

$$P_{na} = Gk_b T_e B$$

- We can find the *operating noise figure* of the component as

$$F_{op} = 1 + \frac{P_{na}}{Gk_b T_s B} = 1 + \frac{Gk_b T_e B}{Gk_b T_s B} = 1 + \frac{T_e}{T_s} \rightarrow T_e = (F_{op} - 1)T_s$$



Operating Noise Figure



- The expression of the operating noise figure depends on the input temperature:

$$F_{op} = 1 + \frac{T_e}{T_s}$$

- If the source temperature is $T_s = T_0 = 290^{\circ}\text{K}$ (i.e. room temperature) then F_{op} is the “standard” noise figure:

$$F_{op} = 1 + \frac{T_e}{T_s} = 1 + \frac{T_e}{290}$$

- Effective temperature of a component depends on its physical temperature
 - A particular value of noise figure is only valid for a specific input temperature and operating temperature!



Multiple Components



- For N components in series, the combined noise figure is

$$F = F_1 + \frac{F_2 - 1}{G_1} + \frac{F_3 - 1}{G_1 G_2} + \dots + \frac{F_N - 1}{G_1 G_2 \dots G_{N-1}}$$

- What does that tell us about the importance of having a *low noise* amplifier as the first component in a receiver?
- Equivalently...

$$T_e = T_{e1} + \frac{T_{e2}}{G_1} + \frac{T_{e3}}{G_1 G_2} + \dots + \frac{T_{eN}}{G_1 G_2 \dots G_{N-1}}$$

- The noise figure of the receiver is a measure of how much noise is contributed to the signal by the receiver
- Typical “low” noise figures are 2-3 dB, can be above 10 dB
 - Noise figure tends to rise as a function of frequency
 - Corresponding effective temperatures are 170 °K – 2600 °K



Radar Range Equation – With Noise!



- Recall the radar range equation (now with a total system gain term added):

$$P_r = \frac{P_t G_t G_r \lambda^2 \sigma}{(4\pi)^3 L_s L_a R^4} \text{ W}$$

- Incorporating the output noise power gives us the signal-to-noise ratio:

$$SNR = \frac{GP_r}{N} = \frac{GP_t G_t G_r \lambda^2 \sigma}{(4\pi)^3 L_s L_a R^4} \frac{1}{Gk_b T_s BF} = \boxed{\frac{P_t G_t G_r \lambda^2 \sigma}{(4\pi)^3 k_b T_s BFL_s L_a R^4}}$$

- This equation is the *ultimate limiting factor* in radar performance
- If you do not have sufficient SNR – no amount of signal processing can save you!!!

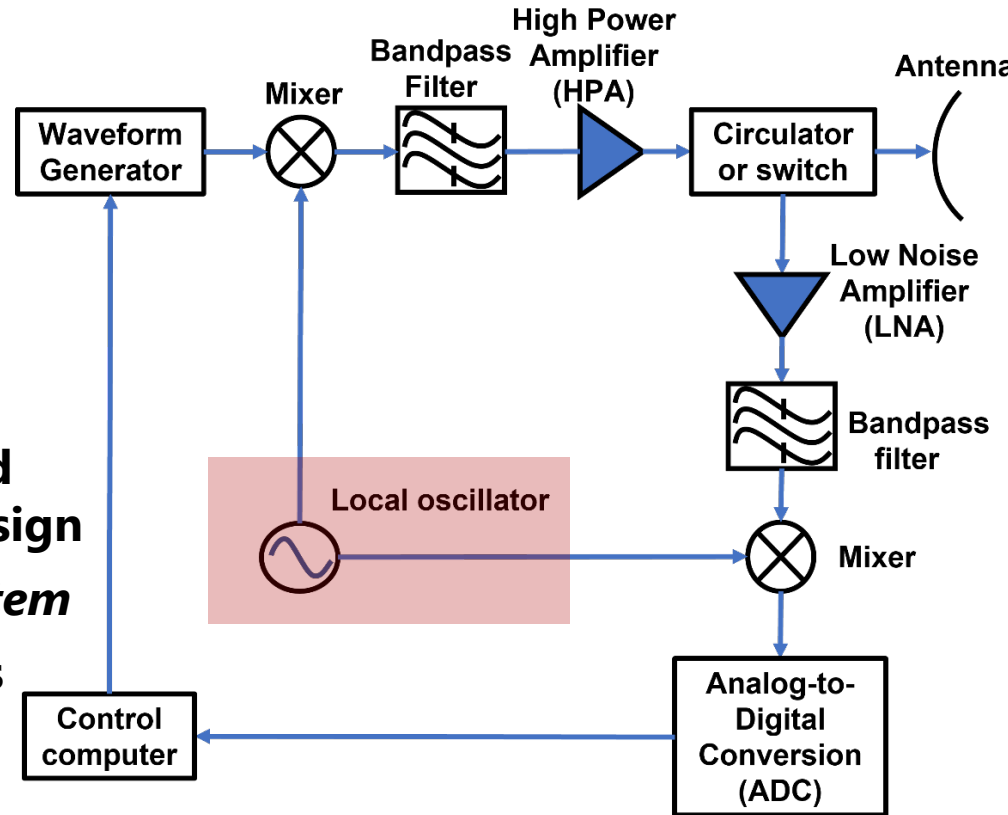


An Example System

- This is an ***illustrative*** system

- MANY variations exist!
 - Usually, additional filters and amplifiers...
 - May have additional downconversion stages

- We will use this system to demonstrate how radar goals and phenomenology drive system design
- Remember, radar is an ***active system***
- Consider two general subsystems
 - Transmit subsystem
 - Receive subsystem





Oscillators



- All mixers must be fed by a *local oscillator* (LO) to provide the reference to upconvert or downconvert the RF signal
- If the radar will perform Doppler processing the transmitted waveform and the received signal must be phase synchronous
- Oscillators are not perfect tones – the signal has *phase noise*
 - Need low phase noise for Doppler processing
 - Phase noise is a limiting factor for clutter cancellation
- Many different oscillator options!
 - Typical tradeoff is low-phase noise vs oscillator frequency tunability
 - Oscillators may be temperature sensitive

Oscillators are often an underappreciated...but critical component in radar system design



Sampling



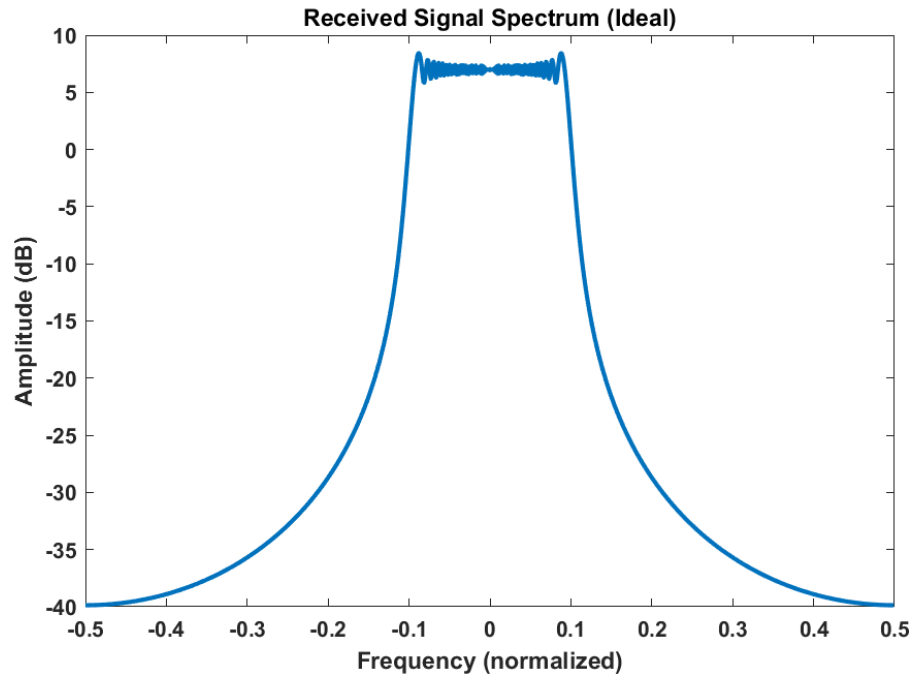
- If possible analog-to-digital conversion (ADC) is done at a *digital IF, f_{IF}*
 - All-real sampling with one ADC, but must sample at $> 2 \left(f_{IF} + \frac{B}{2} \right)$
- Downconversion process will add a DC bias due to LO leakage (first order mixing product)
- Alternative approach is *direct digital downconversion*
 - Demodulate directly to baseband
 - To represent non-symmetric signal centered at zero frequency must sample as complex value
 - Use two downconversion paths that are 90° out of phase (i.e., a sine and a cosine), known as in-phase and quadrature (or IQ)
 - Complex sampling with two ADCs sampling at $> B$
 - Problem: two paths may have slight amplitude or phase mismatch – **IQ imbalance!**



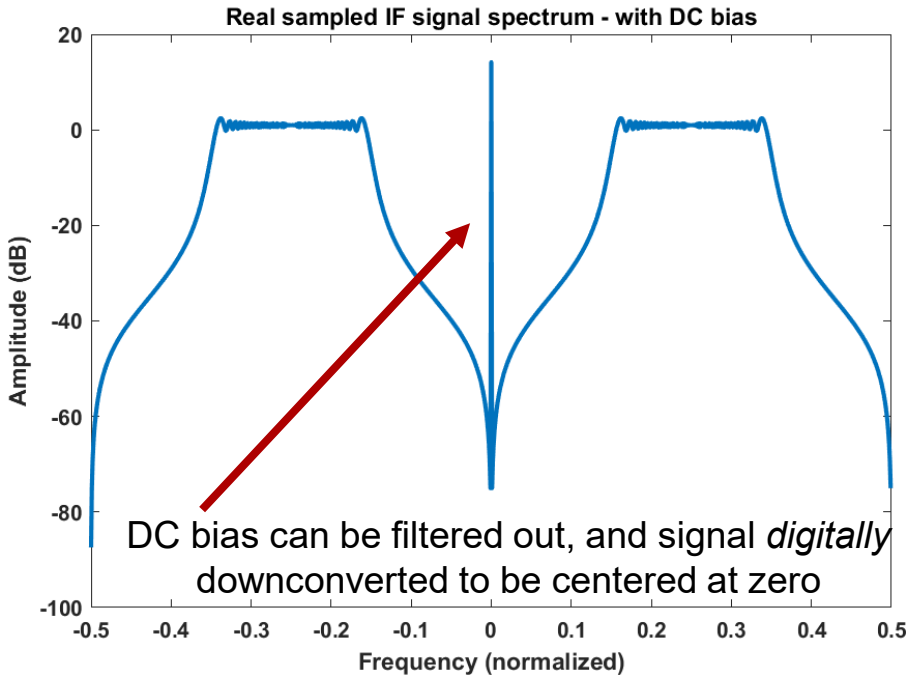
Digital IF Sampling



Ideal LFM spectrum: What we want!



All real sampling: what we get

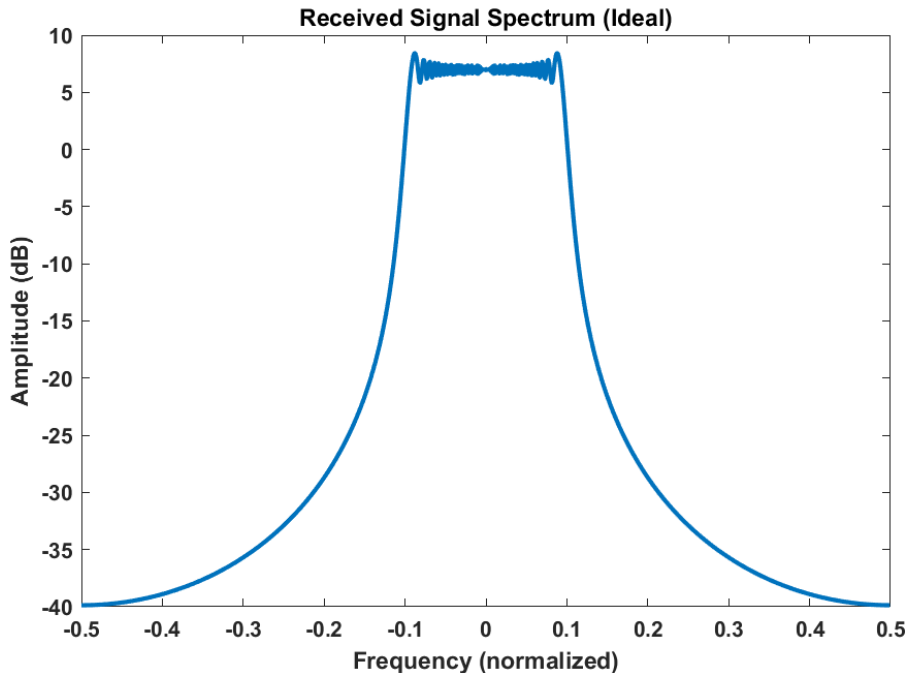




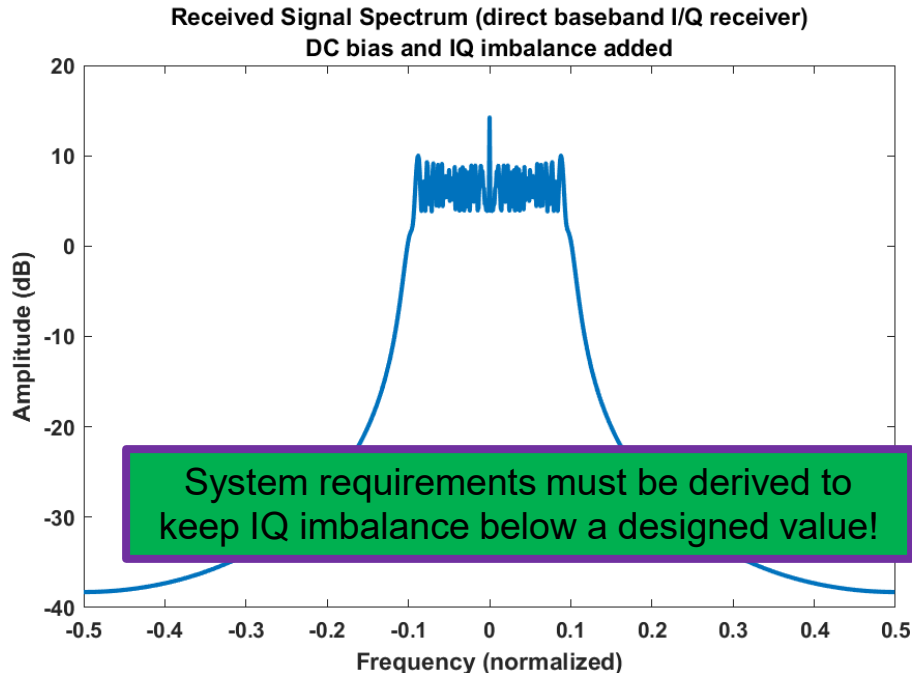
Direct Digital Downconversion



Ideal LFM spectrum: What we want!



Direct digital downconversion with errors: what we get





Parting Thoughts



- Key radar system trends we haven't covered include
 - Phased/digital arrays – stay tuned!
 - Software defined systems
- Radar system design is
 - Informed by physics and constrained by devices
 - Bound by requirements for cost, size, weight and power (C-SWaP)
- Radar signal processing is done on the *back-end* control computer
 - Task/mode-defined (e.g., imaging, detection, tracking, etc.)
- Backend computer systems are typically *heterogeneous*
 - Field programmable gate arrays (FPGAs) and application specific integrated circuits (ASICs) for basic digital signal processing on streaming data
 - Graphics processing units (GPUs) for embarrassingly parallelizable processing
 - General purpose CPUs for other processing



Advanced Radar Research Center

<http://arrc.ou.edu>



Backup



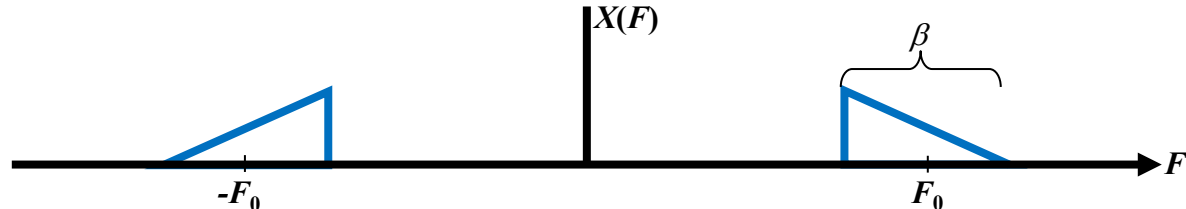
Sampling



- Consider a real bandpass signal:

$$x(t) = a(t) \cos(2\pi F_0 t + \theta(t))$$

- $a(t)$ is (potentially) time-varying signal envelope
- F_0 is center frequency
- $\theta(t)$ is (potentially) time-varying phase



- According to Nyquist criterion, to fully represent signal we need to sample at least at rate $F_s \geq 2(F_0 + \beta/2)$ where β is the bandwidth
 - At 10 GHz center frequency $\Rightarrow F_s \geq 20 \text{ GS/s}!!!$
 - We only care about sampling β



In-Phase and Quadrature



- We need a way to represent a signal – and sample it!

- Recall: $\cos(A + B) = \cos(A)\cos(B) - \sin(A)\sin(B)$

- Then:

$$\begin{aligned}x(t) &= a(t) \cos(2\pi F_0 t + \theta(t)) \\&= a(t) \cos(2\pi F_0 t) \cos[\theta(t)] - a(t) \sin(2\pi F_0 t) \sin[\theta(t)] \\&= x_I(t) \cos(2\pi F_0 t) - x_Q(t) \sin(2\pi F_0 t)\end{aligned}$$

- Where

- $x_I(t) = a(t) \cos[\theta(t)]$ is the *in-phase component*
 - $x_Q(t) = a(t) \sin[\theta(t)]$ is the *quadrature component*

- $x_I(t)$ and $x_Q(t)$ are what we actually want – these are the components that carry information

- Note these are lower frequency components relative to the carrier
 - This slow variation means we consider them to be *narrowband signals*



Complex Envelope



- Using Euler's identity, the complex envelope is defined as

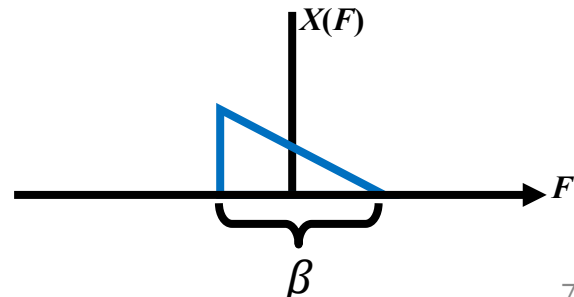
$$\tilde{x}(t) = x_I(t) + jx_Q(t) = a(t)\exp[j\theta(t)]$$

- Using the complex envelope, the original signal is:

$$x(t) = \text{Re}[\tilde{x}(t) \exp(j2\pi F_0 t)]$$

- While F_0 is important – especially with respect to components (mixers, amplifiers, antennas, etc.) and phenomenology (radar cross section, Doppler), the complex envelope is what we sample!
- The spectrum of $\tilde{x}(t)$ alone after we have mixed down to baseband is centered about

- Spectrum is non-symmetric – complex signal
- Highest frequency component is $\beta/2$
- Can sample complex samples at $F_s = \beta$!

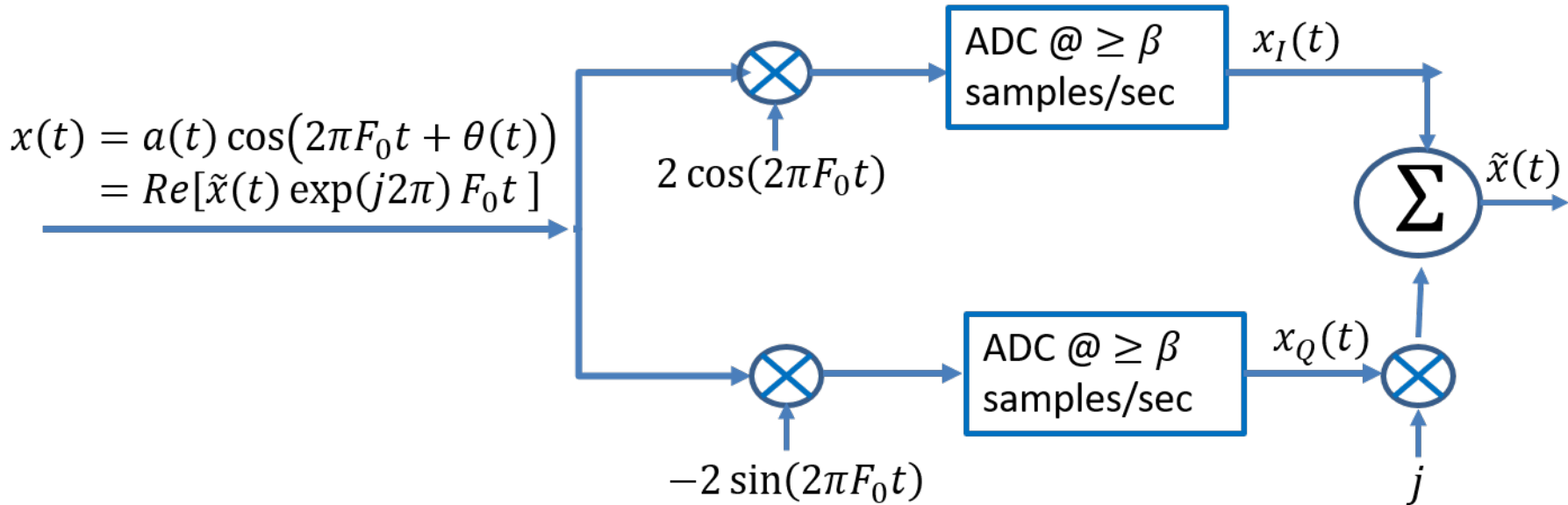




Obtaining Complex Envelope



- Great – now how do I get the complex envelope?
- Option 1: direct digital downconversion, or IQ demodulation
 - Mix down to baseband in two separate paths

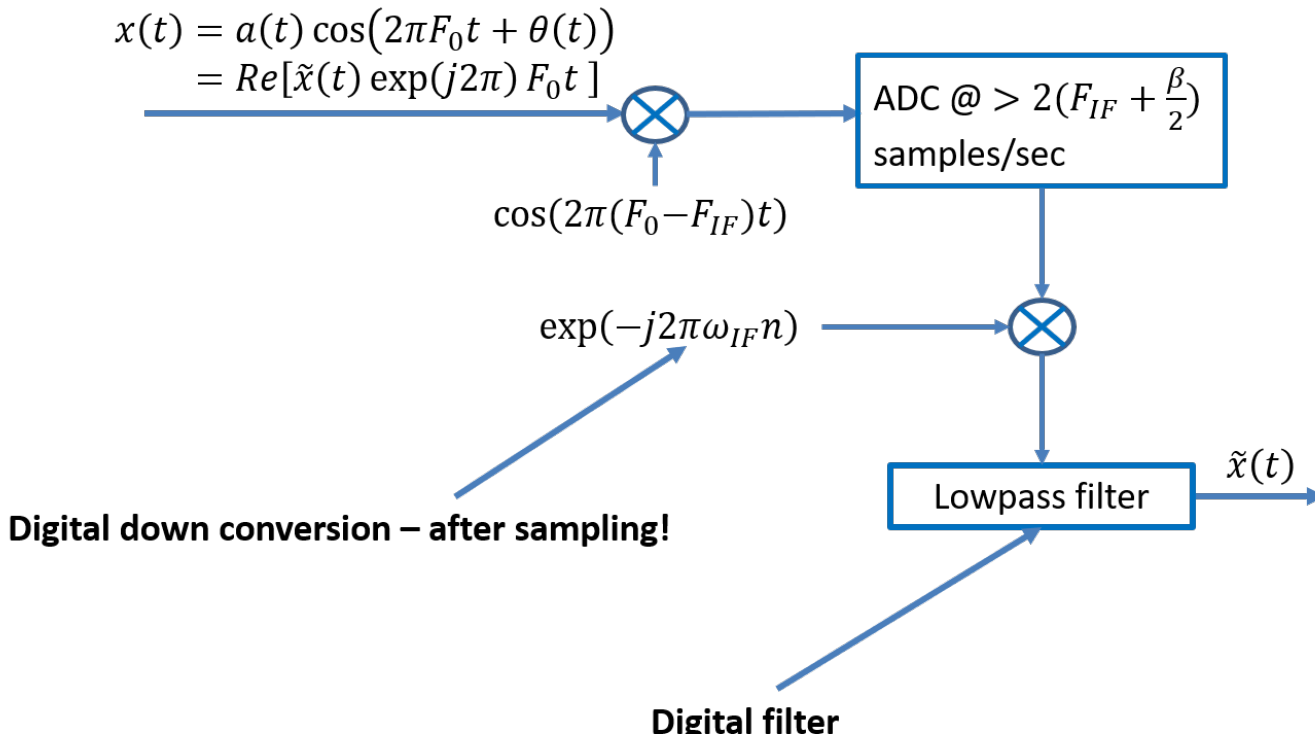




Digital IF Sampling



- Option 2: Digital IF sampling, also called low-IF or digital IQ sampling



Estimation and Detection

Christ D. Richmond

IEEE AESS Radar Summer School

March 19, 2022

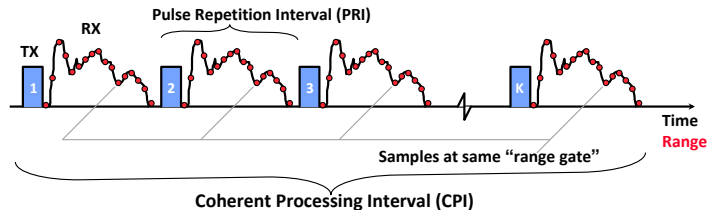


Table of contents

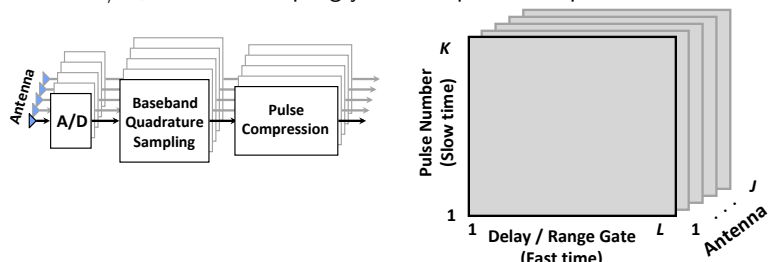
- 1 Pulsed-Doppler Radar Data
- 2 Parameter Estimation
 - Mean Squared Error (MSE)
 - Statistical Inference
 - Cramér-Rao Bound (CRB)
- 3 Maximum-Likelihood (ML) Parameter Estimation
 - ML Relation to CRB
- 4 Detection Theory
 - Statistical Hypothesis Testing
 - Probabilities of Detection (PD) and False Alarm (PFA)
- 5 Likelihood Ratio Test (LRT)
 - Neyman-Pearson (NP) Criterion
- 6 Generalized Likelihood Ratio Test (GLRT)
 - Practical Matters
 - GLRT Approach
- 7 Radar Processing Examples
 - Coherent Matched-Filter
 - Matched-Filter (MF)
 - Pre-Whitened Energy Detector
 - Geometric Observations and Whitening

Pulsed-Doppler Radar Data Collection

- Radar transmits pulsed waveform periodically (period is pulse repetition interval):



- In-Phase / Quadrature sampling yields complex envelope data:

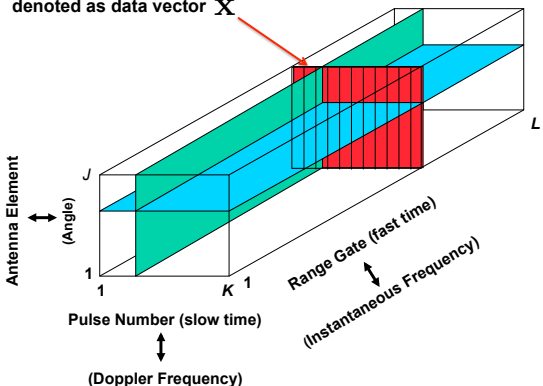


- Pulse compression improves SNR and aides delay alignment

Pulsed-Doppler Radar Data Cube: One CPI

- CPI of complex envelope data organized into of radar data cube.
- Cube has dimensions:
 - pulse (slow time)
 - delay/range (fast time)
 - space/antenna.
- Fourier transforms provide data space revealing Doppler/velocity and angle information.
- Each range bin is tested and processed individually for target presence. We denote the data in an individual range bin by the symbol x (a complex data vector).

A single range gate of data for space-time processing, denoted as data vector \mathbf{X}



Parameter Estimation: Mean Squared Error (MSE) Metric

- Mean squared error (MSE) is useful measure of estimation performance.
- Consider real scalar parameter θ having estimate $\hat{\theta}(\mathbf{x})$. The MSE is defined as

$$\text{MSE}(\theta) \triangleq E\{[\hat{\theta}(\mathbf{x}) - \theta]^2\} = \begin{cases} \int_{\Omega} [\hat{\theta}(\mathbf{x}) - \theta]^2 \cdot p(\mathbf{x}|\theta) d\mathbf{x}, & \text{if continuous } \mathbf{x} \\ \sum_{\Omega} [\hat{\theta}(\mathbf{x}) - \theta]^2 \cdot P(\mathbf{x}|\theta), & \text{if discrete } \mathbf{x} \end{cases}$$

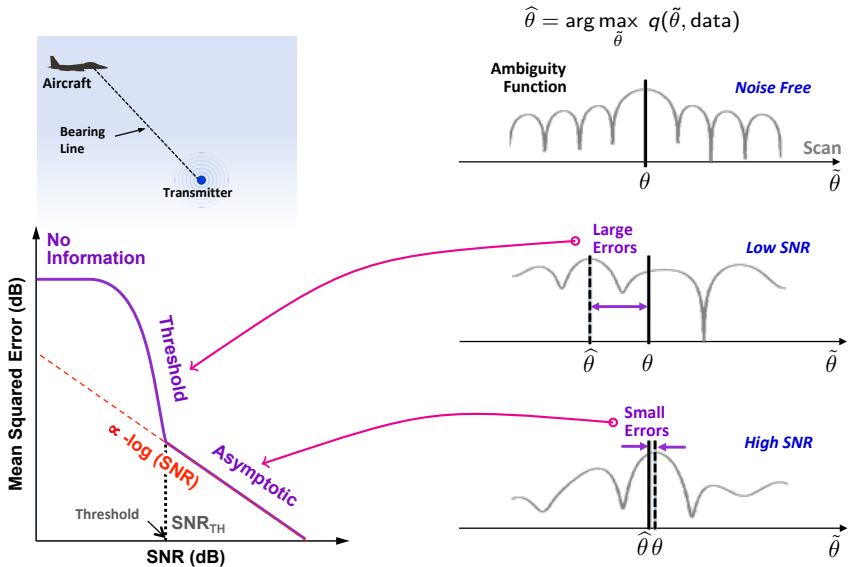
Averaging is over random data \mathbf{x} while conditioned on true parameter value θ .

- Note MSE can be rewritten as

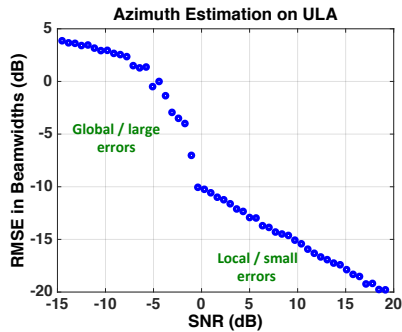
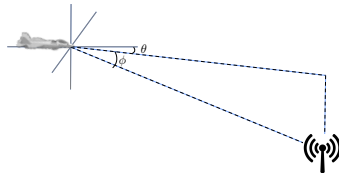
$$\begin{aligned} \text{MSE}(\theta) &= E\{(\hat{\theta} - \theta)^2\} = E\{(\hat{\theta} - E\{\hat{\theta}\}) + E\{\hat{\theta}\} - \theta)^2\} \\ &= E\{(\hat{\theta} - E\{\hat{\theta}\})^2\} + (E\{\hat{\theta}\} - \theta)^2 + 2E\{(\hat{\theta} - E\{\hat{\theta}\})(E\{\hat{\theta}\} - \theta)\} \\ &= E\{(\hat{\theta} - E\{\hat{\theta}\})^2\} + [E\{\hat{\theta}\} - \theta]^2 \\ &\triangleq \sigma_{\hat{\theta}}^2 + [\text{Bias}\{\hat{\theta}\}]^2. \end{aligned}$$

- The first term is recognized as the **variance** of $\hat{\theta}$.
- The second term is the square of the **bias** of estimator $\hat{\theta}$.
- Estimator MSE is given by sum of estimator variance and squared bias.
- If $E\{\hat{\theta}\} = \theta$ then estimator is **unbiased** and **variance = MSE**.

Mean Squared Error Performance: Nonlinear Estimation



Example: Direction-Of-Arrival Estimation

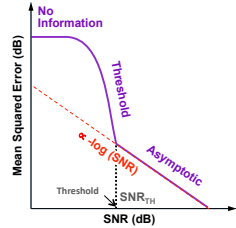


- Simulation details:
 - 18 element uniform linear array (ULA), $\lambda/2$ element spacing
 - 3dB Beamwidth $\simeq 7.2$ degs, search space [60 120] degs
 - 0dB white noise, true signal @ 90 degs (broadside)
- Characterization of MSE either focuses on local or both local and global errors
 - Small errors determined by estimator behavior local to global peak
 - Large errors determined by behavior over entire search space

Estimation Theory: Inference and Bounds

- Observe evidentiary data $\mathbf{x} = [x_1, x_2, \dots, x_N]^T$
- Assume model for data, i.e. $\mathbf{x} \sim p(\mathbf{x}|\theta)$ where θ is parameter
- Estimate parameter using observed data, i.e. determine $\hat{\theta}(\mathbf{x})$
- How well can we do?...i.e. is there a $\sigma^2(\theta)$ such that

$$\sigma^2(\theta) \leq E \left\{ [\hat{\theta}(\mathbf{x}) - \theta]^2 \right\} ?$$



- Yes, such are called **parameter bounds**
 - Some lower bound local errors only
 - Others lower bound both local and global errors

Cramér-Rao Bound: Real Scalar Parameters

- Recall scalar covariance inequality

$$1 \geq \frac{E^2\{\zeta\eta\}}{E\{\zeta^2\}E\{\eta^2\}} \implies E\{\zeta^2\} \geq \frac{E^2\{\zeta\eta\}}{E\{\eta^2\}} \text{ with equality iff. } \zeta \propto \eta$$

- Consider parameter estimate: $\hat{\theta} = \hat{\theta}(\mathbf{x})$, $E\{\hat{\theta}\} = \theta$, $\mathbf{x} \sim p(\mathbf{x}|\theta)$
- Choose random variables as: $\zeta = \hat{\theta} - \theta$, $\eta = \frac{\partial \ln p}{\partial \theta}$ (Score Function)
- Inequality can lower bound estimator mean squared error (MSE):

$$E\{(\hat{\theta} - \theta)^2\} \geq \frac{E^2\left\{(\hat{\theta} - \theta)\frac{\partial \ln p}{\partial \theta}\right\}}{E\left\{\left(\frac{\partial \ln p}{\partial \theta}\right)^2\right\}} = \frac{1}{E\left\{\left(\frac{\partial \ln p}{\partial \theta}\right)^2\right\}} = \text{CRB}(\theta)$$

Cramér-Rao
Bound
(CRB)
▶ Proof

- CRB given by inverse Fisher Information: $\text{FIM}(\theta) = E\left\{\left(\frac{\partial \ln p}{\partial \theta}\right)^2\right\}$
- CRB lower bounds MSE of all unbiased estimators, i.e. such that $E\{\hat{\theta}\} = \theta$.

Cramér-Rao Bound: Real Vector Parameters

- Let $\boldsymbol{\theta} = [\theta_1, \theta_2, \dots, \theta_M]^T$, $\hat{\boldsymbol{\theta}}(\mathbf{x}) = [\hat{\theta}_1(\mathbf{x}), \hat{\theta}_2(\mathbf{x}), \dots, \hat{\theta}_M(\mathbf{x})]^T$, assume $E\{\hat{\boldsymbol{\theta}}(\mathbf{x})\} = \boldsymbol{\theta}$
- Multivariate covariance inequality: $E\{\zeta \zeta^T\} \geq E\{\zeta \eta^T\} E^{-1}\{\eta \eta^T\} E\{\eta \zeta^T\}$
- Variable choice for ζ and η lower bounds estimator MSE matrix:

$$\zeta = \hat{\boldsymbol{\theta}} - \boldsymbol{\theta}, \quad \eta = \frac{\partial \ln p(\mathbf{x}|\boldsymbol{\theta})}{\partial \boldsymbol{\theta}} \implies E\{(\hat{\boldsymbol{\theta}} - \boldsymbol{\theta})(\hat{\boldsymbol{\theta}} - \boldsymbol{\theta})^T\} \geq \mathbf{CRB}(\boldsymbol{\theta})$$

- Fisher information matrix (FIM) and translation matrix:

$$\mathbf{J}(\boldsymbol{\theta}) \triangleq \underbrace{E\left\{ \frac{\partial \ln p(\mathbf{x}|\boldsymbol{\theta})}{\partial \boldsymbol{\theta}} \frac{\partial \ln p(\mathbf{x}|\boldsymbol{\theta})}{\partial \boldsymbol{\theta}}^T \right\}}_{E\{\eta \eta^T\}}, \quad \boldsymbol{\Xi}(\boldsymbol{\theta}) \triangleq \underbrace{E\left\{ \frac{\partial \ln p(\mathbf{x}|\boldsymbol{\theta})}{\partial \boldsymbol{\theta}} (\hat{\boldsymbol{\theta}} - \boldsymbol{\theta})^T \right\}}_{E\{\eta \zeta^T\}} = \mathbf{I}_M$$

- CRB lower bound for unbiased estimators given by:

$$E\{(\hat{\boldsymbol{\theta}} - \boldsymbol{\theta})(\hat{\boldsymbol{\theta}} - \boldsymbol{\theta})^T\} \geq \mathbf{CRB}(\boldsymbol{\theta}) = \mathbf{J}^{-1}(\boldsymbol{\theta}) \implies E\{[\hat{\theta}_i(\mathbf{x}) - \theta_i]^2\} \geq [\mathbf{J}^{-1}(\boldsymbol{\theta})]_{i,i}$$

Maximum-Likelihood (ML) Parameter Estimation

- Consider choosing estimator $\hat{\theta}(\mathbf{x})$ to minimize $\Pr(|\hat{\theta}(\mathbf{x}) - \theta| > \frac{\Delta}{2})$. Note that

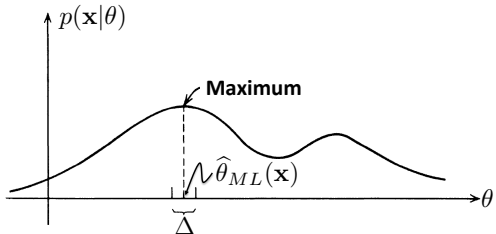
$$\begin{aligned}\Pr(|\hat{\theta}(\mathbf{x}) - \theta| > \frac{\Delta}{2}) &= \Pr(|\theta - \hat{\theta}(\mathbf{x})| > \frac{\Delta}{2}) = 1 - \Pr(|\theta - \hat{\theta}(\mathbf{x})| \leq \frac{\Delta}{2}) \\ &= 1 - \Pr(-\frac{\Delta}{2} \leq \theta - \hat{\theta}(\mathbf{x}) \leq \frac{\Delta}{2}) \\ &= 1 - \Pr(\hat{\theta}(\mathbf{x}) - \frac{\Delta}{2} \leq \theta \leq \hat{\theta}(\mathbf{x}) + \frac{\Delta}{2}) \\ &= 1 - \int d\mathbf{x} \int_{\hat{\theta}(\mathbf{x}) - \frac{\Delta}{2}}^{\hat{\theta}(\mathbf{x}) + \frac{\Delta}{2}} p(\mathbf{x}, \theta) d\theta = 1 - \int d\mathbf{x} \int_{\hat{\theta}(\mathbf{x}) - \frac{\Delta}{2}}^{\hat{\theta}(\mathbf{x}) + \frac{\Delta}{2}} p(\theta) p(\mathbf{x}|\theta) d\theta\end{aligned}$$

- Assume $\frac{\Delta}{2}$ is small $\implies \int_{\hat{\theta}(\mathbf{x}) - \frac{\Delta}{2}}^{\hat{\theta}(\mathbf{x}) + \frac{\Delta}{2}} p(\theta) p(\mathbf{x}|\theta) d\theta \simeq p(\hat{\theta}(\mathbf{x})) \cdot p(\mathbf{x}|\hat{\theta}(\mathbf{x})) \cdot \Delta$
 - Assume $p(\theta)$ is uniform over its support \mathcal{S}_θ , i.e. $p(\theta) = \mathcal{K}$ for all $\theta \in \mathcal{S}_\theta \implies$
- $$\Pr(|\hat{\theta}(\mathbf{x}) - \theta| > \frac{\Delta}{2}) \simeq 1 - \mathcal{K} \Delta \int p(\mathbf{x}|\hat{\theta}(\mathbf{x})) \cdot d\mathbf{x}$$
- Thus, to minimize $\Pr(|\hat{\theta}(\mathbf{x}) - \theta| > \frac{\Delta}{2})$ we must choose $\hat{\theta}(\mathbf{x})$ to maximize $p(\mathbf{x}|\hat{\theta}(\mathbf{x}))$ for each value of data measurement \mathbf{x} .

Maximum-Likelihood (ML) Parameter Estimation

- Maximum-likelihood (ML) estimator is therefore defined as

$$\begin{aligned}\hat{\theta}_{ML}(x) &= \arg \max_{\theta} p(x|\theta) \\ &= \arg \max_{\theta} \ln p(x|\theta)\end{aligned}$$



- $p(x|\theta)$ as function of parameter θ for fixed x is called a **likelihood function**.
- ML chooses as an estimate the value of θ in S_θ that **most likely** caused observed data x to occur, when compared to all other values of θ in S_θ .
 - Hence, the name "**maximum-likelihood**."
- It is sometimes convenient to maximizing the **natural logarithm of pdf**.
 - Maximization is equivalent since logarithm is a **one-to-one** mapping over non-negative numbers.

CRB Relationship to Maximum-Likelihood Estimation

- Maximum-Likelihood (ML) chooses parameter estimate such that:

$$\hat{\theta}_{ML} \triangleq \arg \max_{\theta} p(\mathbf{x}|\theta) = \arg \max_{\theta} \ln p(\mathbf{x}|\theta)$$

- ML search may be **highly nonlinear** (e.g. Doppler, delay, and angle in radar).
- Local behavior, however, often can be **linearized** via **Taylor's theorem**:

$$\frac{\partial \ln p(\mathbf{x}|\hat{\theta}_{ML})}{\partial \theta} = \frac{\partial \ln p(\mathbf{x}|\theta_T)}{\partial \theta} + \frac{\partial^2 \ln p(\mathbf{x}|\theta_T)}{\partial \theta^2} (\hat{\theta}_{ML} - \theta_T) + \text{h.o.t.}$$

where it is assumed that $\mathbf{x} \sim p(\mathbf{x}|\theta_T)$.

- When ML is local maximum then $\frac{\partial \ln p(\mathbf{x}|\hat{\theta}_{ML})}{\partial \theta} = 0$ and estimation error satisfies:

$$(\hat{\theta}_{ML} - \theta_T) \simeq - \left[E \left\{ \frac{\partial^2 \ln p(\mathbf{x}|\theta_T)}{\partial \theta^2} \right\} \right]^{-1} \frac{\partial \ln p(\mathbf{x}|\theta_T)}{\partial \theta}$$

- Recall covariance inequality obtains equality when $\zeta \propto \eta$, i.e. $(\hat{\theta} - \theta) \propto \frac{\partial \ln p}{\partial \theta}$
- Thus, if an estimator exists that obtains the CRB then it is ML

Maximum-Likelihood Estimation of Vector Parameter

- ML estimate of $\theta = [\theta_1, \dots, \theta_M]^T$ when $x \sim p(x|\theta)$ is given by

$$\hat{\theta}_{ML}(x) = \arg \max_{\theta \in S_\theta} p(x|\theta) \text{ where } S_\theta \text{ is support of } \theta.$$

- ML chooses θ in $S_\theta \subseteq \mathbb{R}^{M \times 1}$ that makes data x most likely to have occurred.
- Sometimes it's more convenient to use equivalent search of logarithm of pdf:

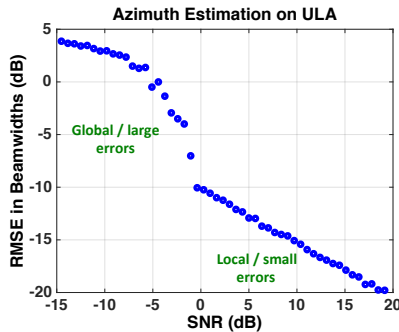
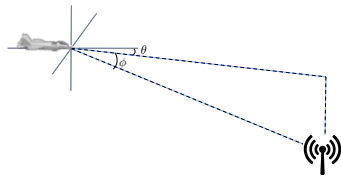
$$\hat{\theta}_{ML}(x) = \arg \max_{\theta \in S_\theta} \ln p(x|\theta) \text{ where } S_\theta \text{ is support of } \theta.$$

- Assuming $x \sim p(x|\theta_T)$, ML estimator error is asymptotically approximated as:

$$(\hat{\theta}_{ML} - \theta_T) \simeq - \left[E \left\{ \frac{\partial^2 \ln p(x|\theta_T)}{\partial \theta \partial \theta^T} \right\} \right]^{-1} \frac{\partial \ln p(x|\theta_T)}{\partial \theta}.$$

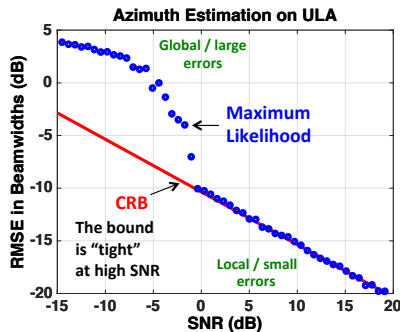
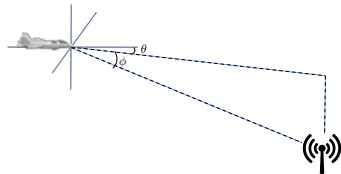
- Assuming $x \sim p(x|\theta_T)$, asymptotically $\hat{\theta}_{ML}(x) \sim \mathcal{N}(\theta_T, \text{CRB}(\theta_T))$.
 - ML is asymptotically **unbiased** and **efficient** (convergence guarantee)!
- Thus, if an estimator exists that obtains the CRB then it is ML

Example: Direction-Of-Arrival Estimation and the CRB



- Simulation details:
 - 18 element uniform linear array (ULA), $\lambda/2$ element spacing
 - 3dB Beamwidth $\simeq 7.2$ degs, search space [60 120] degs
 - 0dB white noise, true signal @ 90 degs (broadside)
- Characterization of MSE either focuses on local or both local and global errors
 - Small errors determined by estimator behavior local to global peak
 - Large errors determined by behavior over entire search space

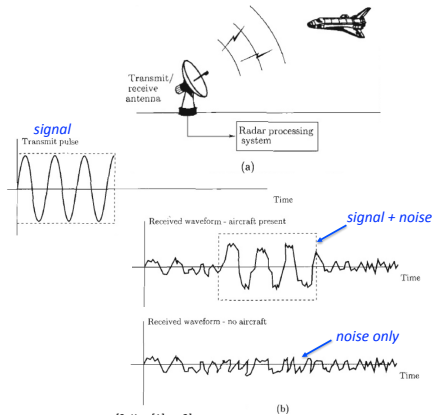
Example: Direction-Of-Arrival Estimation and the CRB



- Simulation details:
 - 18 element uniform linear array (ULA), $\lambda/2$ element spacing
 - 3dB Beamwidth ≈ 7.2 degs, search space [60 120] degs
 - 0dB white noise, true signal @ 90 degs (broadside)
- Characterization of MSE either focuses on local or both local and global errors
 - Small errors determined by estimator behavior local to global peak
 - Large errors determined by behavior over entire search space

Detection Theory in Signal Processing

- **Detection** is a common task for many systems, disciplines, and applications.
 - Radar/sonar (active), communication, medicine/biology, security, etc.
 - Common engineering exercise is looking for signals buried in “noise.”

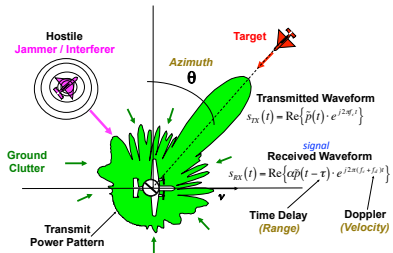
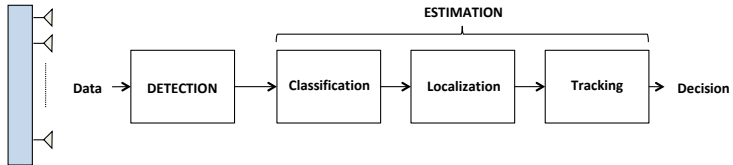


[S. Kay [1], p. 3]

Figure 1.1. Radar system (a) Radar (b) Radar waveforms.

Airborne Radar Example

- Signal **detection** is challenged by **interference** and additive **receiver noise**.
- After target is detected, it is desired to estimate **signal waveform parameters**.
 - Waveform parameters carry information about target (e.g. range from radar, velocity with respect to radar, bearing/elevation angle, reflective strength, etc.).
- Signal processing chain operations for **surveillance system** illustrated below:



The Detection Problem and Statistical Hypothesis Testing

- Detection is essentially an exercise in **binary hypothesis testing**.
- The **problem of detection** can be stated simply as follows:
 - ① Observe measured data
 - ② Use data to decide between two possible hypotheses:

H_0 : Null Hypothesis

H_1 : Alternative Hypothesis

where clearly, the two hypotheses are denoted H_0 and H_1 .

- Although not a requirement, traditionally the **null hypothesis** is chosen to be an event that is believed to be true in most cases.
- The **alternative hypothesis**, however, usually represents a rare event.
- Regarding our **radar example** it is reasonable to choose hypotheses as:

H_0 : Signal absent (noise only)

H_1 : Signal present (signal + noise)

The Detection Problem and Statistical Hypothesis Testing

- The decision between hypotheses will be based on **evidentiary measured data**.
- Denote this measured data by $\mathbf{x} = [x_1, x_2, \dots, x_N]^T$.
- Model each hypothesis by an appropriate data distribution¹:

$$\begin{aligned} H_0 &: \mathbf{x} \sim p(\mathbf{x}|H_0) \\ H_1 &: \mathbf{x} \sim p(\mathbf{x}|H_1) \end{aligned}$$

where $p(\mathbf{x}|H_k)$, $k = 0, 1$ are probability density functions (pdf).

- Given data \mathbf{x} and knowledge of pdfs $p(\mathbf{x}|H_k)$, $k = 0, 1$, we must decide which hypothesis has yielded this measured data.
 - Our decision rule should allow for **every** possible value of \mathbf{x} .
 - Ultimate goal is to **partition data measurement space** into **two sets**:
 - ① A set for deciding hypothesis H_0
 - ② and a set for deciding hypothesis H_1
 - Denote data measurement space by Ω . We seek to partition Ω into two sets.
 - It is useful to define a **decision rule function** $\phi(\mathbf{x})$ defined on Ω .

¹The notation here is the conventional one for conditional probabilities, i.e. $p(A|B)$ is the probability of event A given that event B has occurred.

Decision Rule $\phi(x)$: Partitioning Data Space

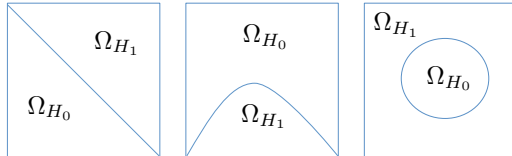
- Let $\phi(x)$ assume **only one** of two values: **0** or **1**. Specifically,
 - for $x \in \Omega$ that we wish to decide H_0 , the ϕ function will assume value 0;
 - for $x \in \Omega$ that we wish to decide H_1 , the ϕ function will assume value 1;
- Let partitions of Ω for H_k be denoted by Ω_{H_k} , $k = 0, 1 \Rightarrow$

$$\phi(x) = \begin{cases} 0, & x \in \Omega_{H_0}, \text{ Decide } H_0 \\ 1, & x \in \Omega_{H_1}, \text{ Decide } H_1. \end{cases}$$

Thus, $\phi(x)$ is effectively an **indicator function for the domain Ω_{H_1}** .

- $\phi(x)$ partitions data space Ω into two **mutually exclusive, collectively exhaustive** sets Ω_{H_0} and Ω_{H_1} where $\Omega_{H_0} \cap \Omega_{H_1} = \emptyset$ and $\Omega_{H_0} \cup \Omega_{H_1} = \Omega$.
- Example partitions of data space Ω are conceptually illustrated in Venn Diagrams:

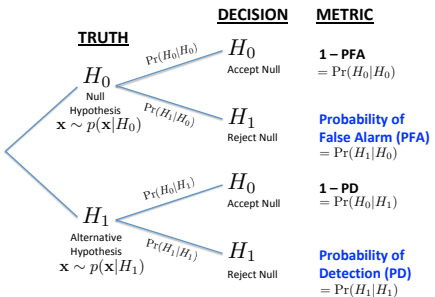
$$\Omega = \Omega_{H_0} \cup \Omega_{H_1}$$



where each square symbolizes entire data space Ω .

Probability Tree for Detection Problem

- Probability space tree for binary hypothesis testing:



– The probability of deciding hypothesis H_m when hypothesis H_k is true is denoted $\Pr(H_m|H_k)$ where $m = 0, 1; k = 0, 1$.

– Specifically, we read this as
 $\Pr(H_m|H_k) \stackrel{\triangle}{=} \Pr(\text{Decide } H_m \mid H_k \text{ is true});$

- $\Pr(H_1|H_1)$ is called the **probability of detection (PD)** and
- $\Pr(H_1|H_0)$ is called the **probability of false alarm (PFA)**.
- These probabilities will obviously depend on our chosen decision rule $\phi(\mathbf{x})$:

$$\Pr(H_1|H_1) = \int_{\Omega_{H_1}} p(\mathbf{x}|H_1) d\mathbf{x} = \int_{\Omega} \phi(\mathbf{x}) \cdot p(\mathbf{x}|H_1) d\mathbf{x} \stackrel{\triangle}{=} \text{PD}$$

$$\Pr(H_1|H_0) = \int_{\Omega_{H_1}} p(\mathbf{x}|H_0) d\mathbf{x} = \int_{\Omega} \phi(\mathbf{x}) \cdot p(\mathbf{x}|H_0) d\mathbf{x} \stackrel{\triangle}{=} \text{PFA}$$

Neyman-Pearson (NP) Criterion

- Neyman and Pearson (NP) suggested constraining probability of false alerts while maximizing the probability of detecting targets.
- NP strategy is well-suited for radar applications:
 - Radar applications often search over large volumes of air space, resulting in many repeated binary hypothesis tests (one for each resolution cell).
 - Computational capacity of hardware and other resources, however, often limit the number of detection alerts that can be considered per unit time.
 - Thus, it is practically useful to constrain the number of false alarms, while maximizing true detection.
- Consider the following Lagrangian objective function proposed by NP:

$$\begin{aligned}
 \mathcal{P}_{NP} &= PD + \eta \cdot (\tilde{\alpha} - PFA) = \Pr(H_1|H_1) + \eta \cdot [\tilde{\alpha} - \Pr(H_1|H_0)] \\
 &= \int_{\Omega} \phi(\mathbf{x}) p(\mathbf{x}|H_1) d\mathbf{x} + \eta \left(\tilde{\alpha} - \int_{\Omega} \phi(\mathbf{x}) p(\mathbf{x}|H_0) d\mathbf{x} \right) \\
 &= \eta \tilde{\alpha} + \int_{\Omega} \phi(\mathbf{x}) [p(\mathbf{x}|H_1) - \eta \cdot p(\mathbf{x}|H_0)] d\mathbf{x}.
 \end{aligned}$$

where PD is to be maximize and η is a Lagrange multiplier for the PFA constraint.

Optimal Neyman-Pearson Decision Rule

$$\mathcal{P}_{NP} = \eta \tilde{\alpha} + \int_{\Omega} \phi(\mathbf{x}) \cdot [p(\mathbf{x}|H_1) - \eta \cdot p(\mathbf{x}|H_0)] d\mathbf{x}$$

- Examining integrand, note that for any fixed value of $\eta > 0$:
 - \mathbf{x} such that $p(\mathbf{x}|H_1) = \eta \cdot p(\mathbf{x}|H_0)$ do not contribute to \mathcal{P}_{NP} ;
 - \mathbf{x} such that $p(\mathbf{x}|H_1) > \eta \cdot p(\mathbf{x}|H_0)$ increases value of \mathcal{P}_{NP} ;
 - \mathbf{x} such that $p(\mathbf{x}|H_1) < \eta \cdot p(\mathbf{x}|H_0)$ decreases value of \mathcal{P}_{NP} ;
- Recall that $\phi(\mathbf{x}) = 0$ or $\phi(\mathbf{x}) = 1$; includes or excludes contribution to integral.
- Thus, to maximize \mathcal{P}_{NP} the optimal decision rule $\phi(\mathbf{x})$ is one that excludes all regions of Ω which decrease overall value of \mathcal{P}_{NP} , i.e.

$$\phi_{NP}(\mathbf{x}, \eta) = \begin{cases} 0, & p(\mathbf{x}|H_1) < \eta \cdot p(\mathbf{x}|H_0) \\ 1, & p(\mathbf{x}|H_1) > \eta \cdot p(\mathbf{x}|H_0) \end{cases}$$

where the inherent dependence on threshold η has been denoted.

- We assumed that $\eta > 0$. It is clear now that $\eta \leq 0$ is nonsensical since it suggests choosing hypothesis H_1 all the time.
- Since threshold η is the Lagrange multiplier, it is chosen to meet desired PFA constraint, i.e. η is chosen such that

$$\text{PFA}(\eta) = \int_{\Omega} \phi_{NP}(\mathbf{x}, \eta) \cdot p(\mathbf{x}|H_0) d\mathbf{x} = \int_{\Omega_{H_1}(\eta)} p(\mathbf{x}|H_0) d\mathbf{x} = \tilde{\alpha}.$$

Likelihood Ratio Test (LRT)

- The optimal partitioning of data space Ω is given explicitly by

$$\Omega_{H_1}(\eta) = \{\mathbf{x} \in \Omega \mid p(\mathbf{x}|H_1) > \eta \cdot p(\mathbf{x}|H_0)\}, \quad \Omega_{H_0}(\eta) = \{\mathbf{x} \in \Omega \mid p(\mathbf{x}|H_1) < \eta \cdot p(\mathbf{x}|H_0)\}$$

- When both density functions are continuous and $p(\mathbf{x}|H_0)$ is non-zero, then NP rule $\phi_{NP}(\mathbf{x}, \eta)$ is equivalent to comparing the following test statistic to a threshold:

$$t_{LRT}(\mathbf{x}) \triangleq \frac{p(\mathbf{x}|H_1)}{p(\mathbf{x}|H_0)} \begin{matrix} H_1 \\ > \end{matrix} \eta. \quad \begin{matrix} H_0 \\ < \end{matrix} \quad \text{— This test statistic is called the likelihood ratio test (LRT).}$$

- It is remarkable that the optimal strategy for deciding between two simple hypotheses involves computing a single real scalar and comparing to a fixed threshold, independent of the original dimensionality of the data observation \mathbf{x} .
- Denote pdf of LRT statistic under hypothesis H_k as $p_{t_{LRT}|H_k}$, $k = 0, 1$.
 - PD and PFA of LRT are equivalently given by

$$PD_{NP}(\eta) = \int_{\eta}^{\infty} p_{t_{LRT}|H_1}(t|H_1) dt, \quad PFA_{NP}(\eta) = \int_{\eta}^{\infty} p_{t_{LRT}|H_0}(t|H_0) dt.$$

- It is often useful to plot $PD_{NP}(\eta)$ versus $PFA_{NP}(\eta)$ as the threshold η is varied. The resulting curve is known as a receiver operating characteristic (ROC) curve.

Remarks on Radar Detection

- So far we've assumed that the data distribution characterizing each hypothesis is unique and known perfectly, i.e. we assume we know $p(\mathbf{x}|H_0)$ and $p(\mathbf{x}|H_1)$.
 - Thus, each hypothesis is characterized by a **single** known distribution.
 - The binary hypothesis problem in this case is a **simple hypothesis testing**.
 - LRT yields optimal decision rule subject to Neyman-Pearson criterion.
- In practice, however, data distributions $p(\mathbf{x}|H_k)$, $k = 0, 1$ are not known perfectly.
- The radar return signal from a target depends on target orientation presented to radar, i.e. it's **radar cross section (RCS)**.
 - Unlikely, however, that target orientation will be known prior.
 - Target **radar detection problem** may be modeled as follows:

$$H_0 : \mathbf{x} \sim CN(\mathbf{0}, \mathbf{R}) = p(\mathbf{x}|H_0) \quad \text{Target absent}$$

$$H_1 : \mathbf{x} \sim CN(S \cdot \mathbf{v}, \mathbf{R}) = p(\mathbf{x}|H_1) \quad \text{Target present}$$

- vector \mathbf{v} is **target response vector** for specific range/delay τ , Doppler frequency f_d , and angle ϕ (i.e. for a particular resolution cell);
- complex amplitude S represents magnitude and phase of target return **reflectivity** determined by RCS target presents to radar at time of illumination.
- Target signal response can be modeled as a **parameterized mean** $\mu(\theta_t) = S \cdot \mathbf{v}(\tau, f_d, \phi)$ where the set of **signal parameters** is $\theta_t = [S, \tau, f_d, \phi]^T$.

Remarks on Radar Detection

- The colored noise is characterized by covariance \mathbf{R} .
- Let data covariance be parameterized by parameters θ_n , i.e. $\mathbf{R} = \mathbf{R}(\theta_n)$.
- Target parameters θ_t and noise parameters θ_n will be **unknown** in practice.
 - Hence, it is not possible to perfectly specify the data distributions, i.e. $p(\mathbf{x}|H_0, \theta_0)$ and $p(\mathbf{x}|H_1, \theta_1)$ where $\theta_0 = \theta_n$ and $\theta_1 = [\theta_t; \theta_n]$ cannot be specified because parameters θ_0 and θ_1 are unknown.
- Consequently, it is not possible to specify the optimal decision rule.
- The hypothesis testing problem can be stated as

$$H_0 : \mathbf{x} \sim p(\mathbf{x}|H_0, \theta_0) \quad \text{Null Hypothesis}$$

$$H_1 : \mathbf{x} \sim p(\mathbf{x}|H_1, \theta_1) \quad \text{Alternative Hypothesis}$$

where the hypotheses yield data distributions specified by parameters θ_0 and θ_1 .

- Methods for developing good decision rules when data distributions are not known perfectly are needed for practical application.

Generalized Likelihood Ratio Test (GLRT)

- LRT is optimal test for a simple hypothesis testing problem.
- When parameters θ_0 and θ_1 are known perfectly then LRT can be used:

$$t_{LRT}(\mathbf{x}) = \frac{p(\mathbf{x}|H_1, \theta_1)}{p(\mathbf{x}|H_0, \theta_0)} \begin{matrix} > \\ < \end{matrix} \eta.$$

H_1
 H_0

- Usually parameters θ_0, θ_1 are not known in practice, as in radar example.
- If estimates $\hat{\theta}_0, \hat{\theta}_1$ are available, then perhaps a good test can be formed:

$$\hat{t}_{LRT}(\mathbf{x}) = \frac{p(\mathbf{x}|H_1, \hat{\theta}_1)}{p(\mathbf{x}|H_0, \hat{\theta}_0)} \begin{matrix} > \\ < \end{matrix} \eta.$$

H_1
 H_0

- This is, of course, only approximates the optimal LRT.
- Most detection theory is attempting to approximate the LRT.
- Of course, test $\hat{t}_{LRT}(\mathbf{x})$ may perform well if our parameter estimates $\hat{\theta}_0, \hat{\theta}_1$ are “good enough.”

Generalized Likelihood Ratio Test (GLRT)

- The generalized likelihood ratio test (GLRT) takes the approach of \widehat{t}_{LRT} .
 - Specifically, GLRT uses maximum-likelihood (ML) estimates \Rightarrow

$$t_{GLRT}(\mathbf{x}) = \frac{\max_{\boldsymbol{\theta}_1} p(\mathbf{x}|H_1, \boldsymbol{\theta}_1)}{\max_{\boldsymbol{\theta}_0} p(\mathbf{x}|H_0, \boldsymbol{\theta}_0)} \begin{matrix} H_1 \\ > \\ < \\ H_0 \end{matrix} \eta.$$

- Sometimes logarithm of GLRT, an equivalent test, is easier to work with

$$\tilde{t}_{GLRT}(\mathbf{x}) = \max_{\boldsymbol{\theta}_1} \ln p(\mathbf{x}|H_1, \boldsymbol{\theta}_1) - \max_{\boldsymbol{\theta}_0} \ln p(\mathbf{x}|H_0, \boldsymbol{\theta}_0) \begin{matrix} H_1 \\ > \\ < \\ H_0 \end{matrix} \ln \eta = \tilde{\eta}.$$

- GLRT tends to work well in practice and is often considered the benchmark performer, although it is not guaranteed to be optimal **non-asymptotically**, i.e. with limited data.
- GLRT, however, is **guaranteed to converge** to the most powerful test in the limit of large amounts of data or high SNRs by virtue of the asymptotic properties of ML i.e. as $N \rightarrow \infty$ (or as SNR $\rightarrow \infty$); namely, $t_{GLRT}(\mathbf{x}) \rightarrow t_{LRT}(\mathbf{x})$.

Radar Example: Coherent Matched-Filter

- Consider binary hypothesis testing problem

$$\begin{aligned} H_0 &: \mathbf{x} = \mathbf{n}, & (\text{noise only}), & p(\mathbf{x}|H_0) = \mathcal{CN}(\mathbf{0}, \mathbf{R}) \\ H_1 &: \mathbf{x} = S\mathbf{v} + \mathbf{n}, & (\text{signal} + \text{noise}), & p(\mathbf{x}|H_1) = \mathcal{CN}(S\mathbf{v}, \mathbf{R}). \end{aligned}$$

- The log-likelihood ratio test (LRT) statistic follows as

$$\begin{aligned} \tilde{t}_{LRT} &= \ln p(\mathbf{x}|H_1) - \ln p(\mathbf{x}|H_0) = -(\mathbf{x} - S\mathbf{v})^H \mathbf{R}^{-1} (\mathbf{x} - S\mathbf{v}) + \mathbf{x}^H \mathbf{R}^{-1} \mathbf{x} \stackrel{\begin{matrix} > \\ < \end{matrix}}{\begin{matrix} H_1 \\ H_0 \end{matrix}} \tilde{\eta} \implies \\ \tilde{t}_{LRT} &= \operatorname{Re}(S^* \mathbf{v}^H \mathbf{R}^{-1} \mathbf{x}) \stackrel{\begin{matrix} > \\ < \end{matrix}}{\begin{matrix} H_1 \\ H_0 \end{matrix}} \tilde{\eta}. \end{aligned}$$

- Recall LRT is optimal test for **simple hypothesis testing** problem, i.e. perfect knowledge of $p(\mathbf{x}|H_0)$ and $p(\mathbf{x}|H_1)$ is assumed. Thus, perfect knowledge of parameters S , \mathbf{v} , and \mathbf{R} is assumed here.
- LRT is optimal test that maximizes probability of detection (PD) for a fixed probability of false alarm (PFA).
- It is noteworthy that LRT statistic can be written $\tilde{t}_{LRT} = \operatorname{Re}(\mathbf{w}_{LRT}^H \mathbf{x})$ where linear filter is $\mathbf{w}_{LRT} = S\mathbf{R}^{-1}\mathbf{v}$.
 - We recognize that $\mathbf{w}_{LRT} \propto \mathbf{R}^{-1}\mathbf{v}$, i.e. filter **maximizing output SNR**.

Radar Example: Matched-Filter (MF)

- Neyman-Pearson LRT assumes perfect knowledge of all parameters.
- The complex amplitude S in radar captures attenuation due to propagation losses and reflectivity of the target determined by its effective RCS at time of illumination.
- Thus, it is often unrealistic to assume perfect knowledge of S .
- Applying GLRT method to address an unknown S suggests the test

$$\tilde{t} = \ln \frac{\max_S p(\mathbf{x}|H_1)}{p(\mathbf{x}|H_0)} = \ln \max_S p(\mathbf{x}|H_1) - \ln p(\mathbf{x}|H_0) = \max_S \ln p(\mathbf{x}|H_1) - \ln p(\mathbf{x}|H_0)$$

where last equality follows because logarithm is one-to-one mapping.

- Thus, we have $\tilde{t} = [\max_S -(\mathbf{x} - S\mathbf{v})^H \mathbf{R}^{-1} (\mathbf{x} - S\mathbf{v})] + \mathbf{x}^H \mathbf{R}^{-1} \mathbf{x}$
 $= [\max_S -\mathbf{x}^H \mathbf{R}^{-1} \mathbf{x} - |S|^2 \mathbf{v}^H \mathbf{R}^{-1} \mathbf{v} + S^* \mathbf{v}^H \mathbf{R}^{-1} \mathbf{x} + \mathbf{x}^H \mathbf{R}^{-1} \mathbf{v} S] + \mathbf{x}^H \mathbf{R}^{-1} \mathbf{x}$
- Completing the square in $S \implies$

$$\tilde{t} = \left[\max_S -\mathbf{x}^H \mathbf{R}^{-1} \mathbf{x} - \mathbf{v}^H \mathbf{R}^{-1} \mathbf{v} \left| S - \frac{\mathbf{v}^H \mathbf{R}^{-1} \mathbf{x}}{\mathbf{v}^H \mathbf{R}^{-1} \mathbf{v}} \right|^2 + \frac{|\mathbf{v}^H \mathbf{R}^{-1} \mathbf{x}|^2}{\mathbf{v}^H \mathbf{R}^{-1} \mathbf{v}} \right] + \mathbf{x}^H \mathbf{R}^{-1} \mathbf{x}.$$

Clearly, to maximize over S one must choose $\hat{S}_{ML} = \frac{\mathbf{v}^H \mathbf{R}^{-1} \mathbf{x}}{\mathbf{v}^H \mathbf{R}^{-1} \mathbf{v}} \implies$

Radar Example: Matched-Filter (MF) Cont.

- Thus, GLRT statistic can be written

$$\tilde{t} = -\mathbf{x}^H \mathbf{R}^{-1} \mathbf{x} + \frac{|\mathbf{v}^H \mathbf{R}^{-1} \mathbf{x}|^2}{\mathbf{v}^H \mathbf{R}^{-1} \mathbf{v}} + \mathbf{x}^H \mathbf{R}^{-1} \mathbf{x} \implies \tilde{t} = \frac{|\mathbf{v}^H \mathbf{R}^{-1} \mathbf{x}|^2}{\mathbf{v}^H \mathbf{R}^{-1} \mathbf{v}} \triangleq t_{MF}.$$

- Thus, target detection is determined by thresholding t_{MF} , i.e.

$$t_{MF} = \frac{|\mathbf{v}^H \mathbf{R}^{-1} \mathbf{x}|^2}{\mathbf{v}^H \mathbf{R}^{-1} \mathbf{v}} \begin{matrix} H_1 \\ > \\ < \\ H_0 \end{matrix} \eta_{MF}.$$

- Note that statistic can be expressed as $t_{MF} = |\mathbf{w}_{MF}^H \mathbf{x}|^2$ where $\mathbf{w}_{MF} = a \mathbf{R}^{-1} \mathbf{v}$ and constant is $a = 1/\sqrt{\mathbf{v}^H \mathbf{R}^{-1} \mathbf{v}}$.
- This GLRT test statistic t_{MF} is sometimes called the **clairvoyant matched filter**.
- Only magnitude of output of filter \mathbf{w}_{MF} is used for detection.
 - Compare to coherent matched filter test \tilde{t}_{LRT} that uses magnitude and phase.

Radar Example: Pre-Whitened Energy Detector

- If target response vector \mathbf{v} is unknown along with S then GLRT method suggests

$$\tilde{t} = \ln \frac{\max_{S, \mathbf{v}} p(\mathbf{x}|H_1)}{p(\mathbf{x}|H_0)} = \ln \max_{S, \mathbf{v}} p(\mathbf{x}|H_1) - \ln p(\mathbf{x}|H_0) = \max_{S, \mathbf{v}} \ln p(\mathbf{x}|H_1) - \ln p(\mathbf{x}|H_0)$$

where last equality follows because logarithm is one-to-one mapping.

- Maximization over S was done in last example; thus continuing we have

$$\tilde{t} = \max_{\mathbf{v}} \left[-\mathbf{x}^H \mathbf{R}^{-1} \mathbf{x} + \frac{|\mathbf{v}^H \mathbf{R}^{-1} \mathbf{x}|^2}{\mathbf{v}^H \mathbf{R}^{-1} \mathbf{v}} \right] + \mathbf{x}^H \mathbf{R}^{-1} \mathbf{x} = \max_{\mathbf{v}} \frac{|\mathbf{v}^H \mathbf{R}^{-1} \mathbf{x}|^2}{\mathbf{v}^H \mathbf{R}^{-1} \mathbf{v}}.$$

- Considering change of variables $\mathbf{x}_0 = \mathbf{R}^{-1/2} \mathbf{x}$ and $\mathbf{v}_0 = \mathbf{R}^{-1/2} \mathbf{v} \implies$

$$\tilde{t} = \max_{\mathbf{v}_0} \frac{|\mathbf{v}_0^H \mathbf{x}_0|^2}{\|\mathbf{v}_0\|^2} \leq \|\mathbf{x}_0\|^2 \quad \text{where upper bound follows from Cauchy-Schwarz inequality.}^2$$

- Note that max only depends on the **direction** of \mathbf{v}_0 .
- Equality is obtained if and only if $\mathbf{v}_0 \propto \mathbf{x}_0 \implies$

$$\tilde{t} = \max_{\mathbf{v}_0} \frac{|\mathbf{v}_0^H \mathbf{x}_0|^2}{\|\mathbf{v}_0\|^2} = \|\mathbf{x}_0\|^2 = \mathbf{x}^H \mathbf{R}^{-1} \mathbf{x} \triangleq t_{ED}$$

- This GLRT test is sometimes referred to as a **prewhitened energy detector**.

²Cauchy-Schwarz inequality says for $\mathbf{a}, \mathbf{b} \in \mathbb{C}^N \implies 0 \leq \frac{|\mathbf{a}^H \mathbf{b}|^2}{\|\mathbf{a}\|^2 \cdot \|\mathbf{b}\|^2} \leq 1$.

Geometric Observations and Whitening

- With variable change $\mathbf{x}_0 = \mathbf{R}^{-1/2}\mathbf{x}$ and $\mathbf{v}_0 = \mathbf{R}^{-1/2}\mathbf{v}$, MF statistic can be written

$$t_{MF} = \frac{|\mathbf{v}_0^H \mathbf{x}_0|^2}{\|\mathbf{v}_0\|^2} \triangleq |\mathbf{u}_v^H \mathbf{x}_0|^2, \text{ where unit vector } \mathbf{u}_v = \frac{\mathbf{v}_0}{\|\mathbf{v}_0\|}.$$

- Note that multiplication by $\mathbf{R}^{-1/2}$ is a **whitening transformation**, i.e.

$$\mathbf{x} \sim \begin{cases} H_0 & : \mathcal{CN}(\mathbf{0}, \mathbf{R}) \\ H_1 & : \mathcal{CN}(S\mathbf{v}, \mathbf{R}) \end{cases} \implies \mathbf{x}_0 = \mathbf{R}^{-1/2}\mathbf{x} \sim \begin{cases} H_0 & : \mathcal{CN}(\mathbf{0}, \mathbf{I}_N) \\ H_1 & : \mathcal{CN}(S\mathbf{v}_0, \mathbf{I}_N) \end{cases}$$

- MF is a projection of measured whitened data \mathbf{x}_0 onto signal direction \mathbf{u}_v .
- Note that **total energy** in \mathbf{x}_0 is given by $\|\mathbf{x}_0\|^2 = t_{ED}$.
 - t_{ED} can be interpreted as **total energy** from **all directions**
 - To see this, define unitary matrix $\mathbf{U} = [\mathbf{u}_v | \mathbf{u}_{\perp,1} | \mathbf{u}_{\perp,2} | \cdots | \mathbf{u}_{\perp,N-1}]$ where last $N - 1$ columns are orthogonal to \mathbf{u}_v , and $\mathbf{U}\mathbf{U}^H = \mathbf{U}^H\mathbf{U} = \mathbf{I}_N \implies$

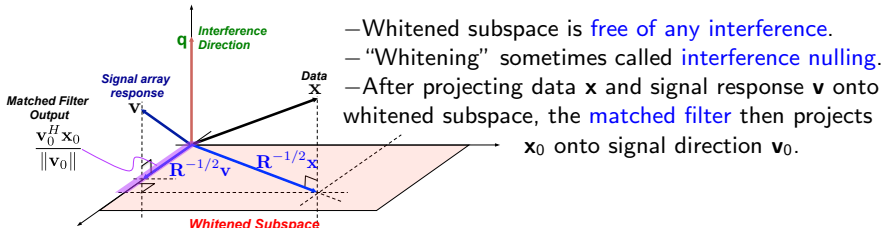
$$\|\mathbf{x}_0\|^2 = \mathbf{x}_0^H \mathbf{x}_0 = \mathbf{x}_0^H \mathbf{I}_N \mathbf{x}_0 = \mathbf{x}_0^H \mathbf{U} \mathbf{U}^H \mathbf{x}_0 = |\mathbf{u}_v^H \mathbf{x}_0|^2 + \sum_{i=1}^{N-1} |\mathbf{u}_{\perp,i}^H \mathbf{x}_0|^2$$

Geometric Observations and Whitening

- Regarding the whitening transformation, consider a covariance representing white noise plus a **directional interferer** with response \mathbf{q} (typical structure in radar):

$$\mathbf{R} = \mathbf{I}_N + \sigma_J^2 \mathbf{q} \mathbf{q}^H \implies \lim_{\sigma_J^2 \rightarrow \infty} \mathbf{R}^{-1} = \lim_{\sigma_J^2 \rightarrow \infty} \mathbf{I}_N - \frac{\mathbf{q} \mathbf{q}^H}{\frac{1}{\sigma_J^2} + \|\mathbf{q}\|^2} = \mathbf{I} - \mathbf{u}_q \mathbf{u}_q^H, \text{ where } \mathbf{u}_q = \frac{\mathbf{q}}{\|\mathbf{q}\|}.$$

- Limiting form of \mathbf{R}^{-1} is a **projection matrix** onto space orthogonal to the interferer response \mathbf{q} .
- Projection matrices have eigenvalues that are either unity or zero. Thus, $(\mathbf{I} - \mathbf{u}_q \mathbf{u}_q^H)^{-1/2} = \mathbf{I} - \mathbf{u}_q \mathbf{u}_q^H$, i.e. $\lim_{\sigma_J^2 \rightarrow \infty} \mathbf{R}^{-1} = \lim_{\sigma_J^2 \rightarrow \infty} \mathbf{R}^{-1/2} = \mathbf{I} - \mathbf{u}_q \mathbf{u}_q^H$.
- The change of variables $\mathbf{x}_0 = \mathbf{R}^{-1/2} \mathbf{x}$ and $\mathbf{v}_0 = \mathbf{R}^{-1/2} \mathbf{v}$ effectuates a projection onto the **space orthogonal to interference**:



Closing Remarks

- Radar signal processing is a mature field with new areas of growth.
- Estimation and Detection Theory play a fundamental role.
- Key topics covered:
 - Maximum-Likelihood (ML) Estimation
 - Cramér-Rao Bound (CRB)
 - Likelihood Ratio Test (LRT)
 - Generalized Likelihood Ratio Test (GLRT)
- These techniques can be applied to a wide spectrum of problems.

References

-  J. Ward, *Space-Time Adaptive Processing for Airborne Radar*, Technical Report 1015, Lexington, MA: Lincoln Labs, MIT, 1994.
-  Steven M. Kay, *Fundamentals of Statistical Signal Processing: Detection Theory*, Prentice-Hall, Inc., Englewood Cliffs, NJ, 1998.
-  Steven M. Kay, *Fundamentals of Statistical Signal Processing: Estimation Theory*, Prentice-Hall Inc., Englewood Cliffs, NJ, 1993.
-  H. L. Van Trees, K. L. Bell, and Z. Tian, *Detection, Estimation and Modulation Theory*, 2nd ed. Hoboken, NJ, USA: Wiley, 2013.
-  L. L. Scharf, *Statistical Signal Processing: Detection, Estimation, and Time Series Analysis*, Reading, MA, USA: Addison-Wesley, 1991.

Backup Slides

Regularity Conditions: Allow Order Reversal of Integration & Differentiation

- By linearity of integration we have

$$\begin{aligned} E \left\{ (\hat{\theta} - \theta) \frac{\partial \ln p}{\partial \theta} \right\} &= \int (\hat{\theta} - \theta) \frac{\partial \ln p}{\partial \theta} pdx \\ &= \int \hat{\theta} \cdot \frac{\partial \ln p}{\partial \theta} pdx - \theta \int \frac{\partial \ln p}{\partial \theta} pdx \end{aligned}$$

- Order reversal of integration / differentiation simplifies first term:

$$\begin{aligned} \int \hat{\theta} \cdot \frac{\partial \ln p}{\partial \theta} pdx &= \int \hat{\theta} \cdot \frac{1}{p} \frac{\partial p}{\partial \theta} \cdot pdx \\ &= \int \hat{\theta} \cdot \frac{\partial p}{\partial \theta} dx = \frac{\partial}{\partial \theta} \int \hat{\theta} \cdot pdx = \frac{\partial \hat{\theta}}{\partial \theta} = 1 \end{aligned}$$

- Lastly, order reversal shows that second term vanishes:

$$\begin{aligned} \int \frac{\partial \ln p}{\partial \theta} \cdot pdx &= \int \frac{1}{p} \frac{\partial p}{\partial \theta} \cdot pdx \\ &= \int \frac{\partial p}{\partial \theta} dx = \frac{\partial}{\partial \theta} \int pdx = \frac{\partial}{\partial \theta}(1) = 0 \end{aligned}$$

[◀ Return](#)

Radar Imaging

Dr. Armin Doerry

www.Doerry.us

Radar Image

The fundamental operation of radar is one of a ranging instrument.

- this is essentially a one-dimensional measurement

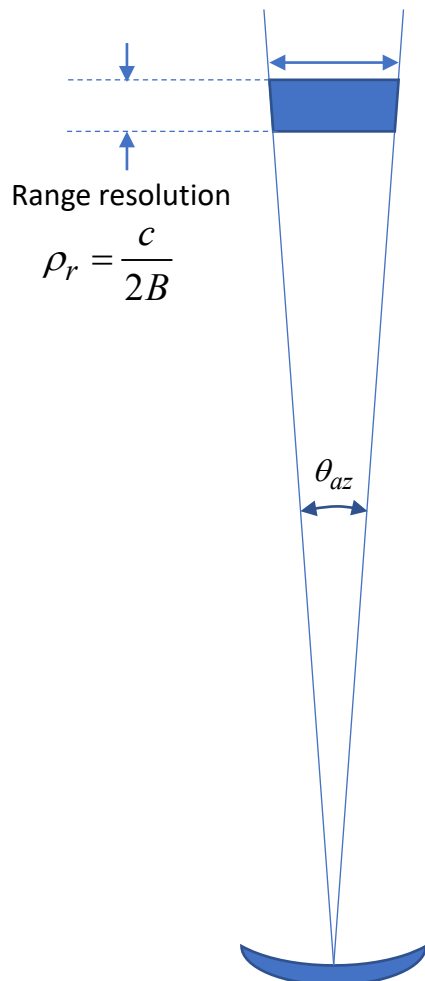
However, combining ranging with directional information yields a multi-dimensional product,

- an image is just a planar projection or rendering of this multi-dimensional data
- Directional information can be ascertained by a variety of techniques

Two basic classes of images

1. real-beam, or real-aperture
2. synthetic-beam, or synthetic-aperture

Real Beam Images



$$\rho_r = \frac{c}{2B}$$

Azimuth resolution
 $\rho_a = \theta_{az}r$

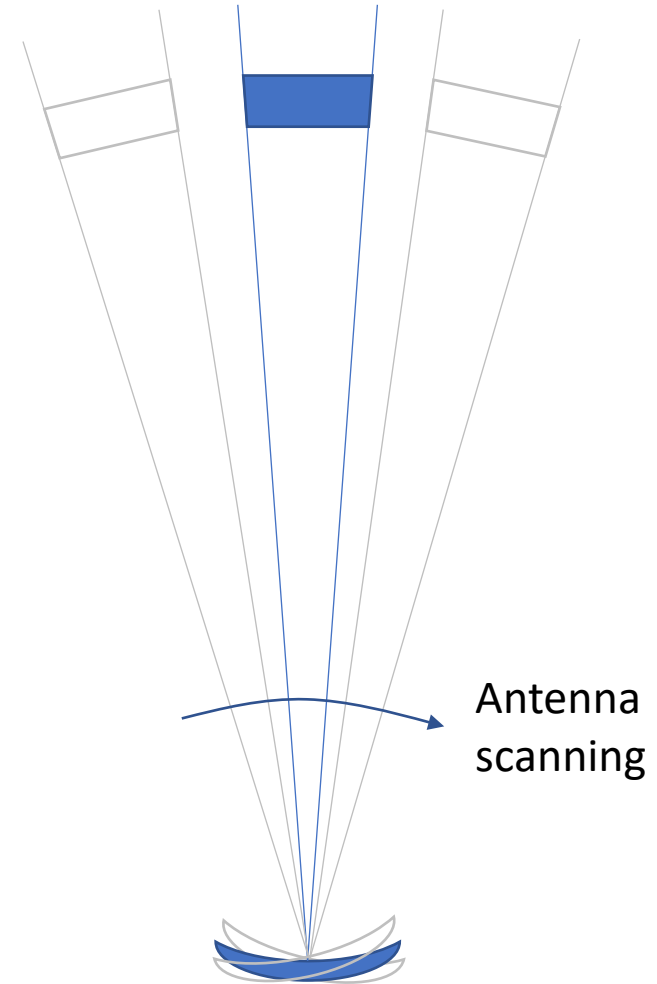
Range resolution is inversely proportional to waveform bandwidth, B .

Azimuth resolution is limited by only the antenna beamwidth θ_{az} and the operating range, r .

Any one beam direction yields a single range profile.

An image is created by assembling multiple range profiles with the antenna beam pointed in different directions, by “scanning” the antenna.

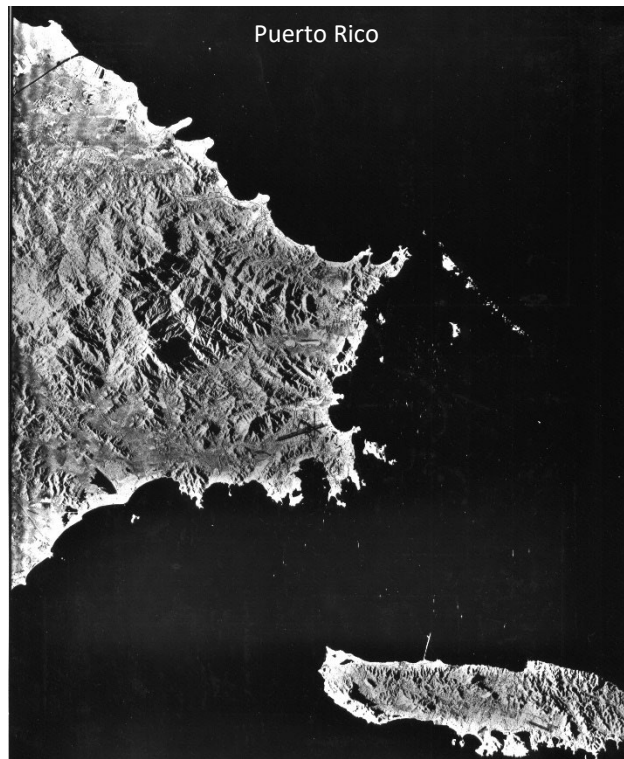
Scans may be angular or linear.



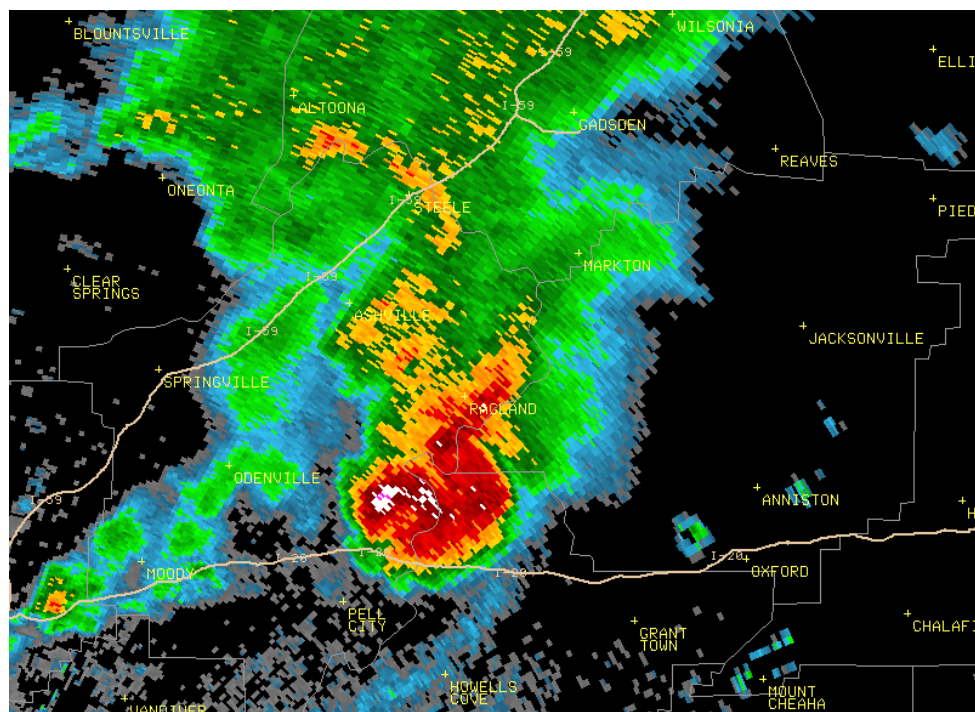
Real Beam Images

Common applications of real-beam radar imaging includes

1. Maritime search/navigation radar
2. Weather mapping radar
3. Side-Looking Airborne Radar (SLAR)



Courtesy USGS

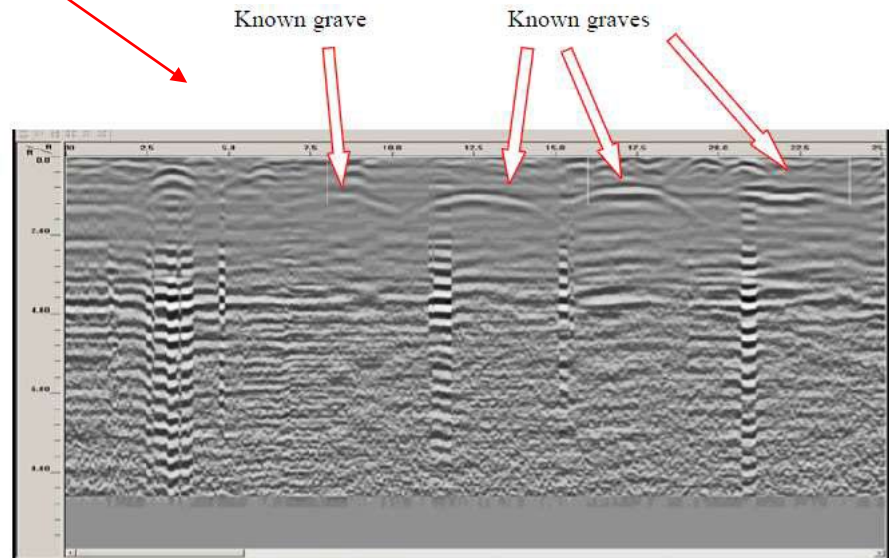
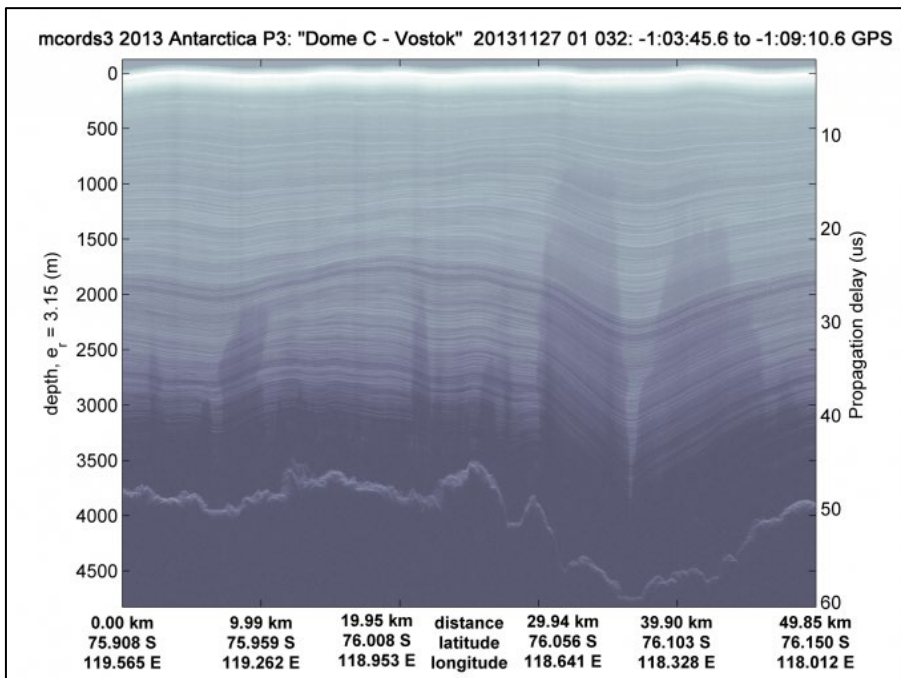
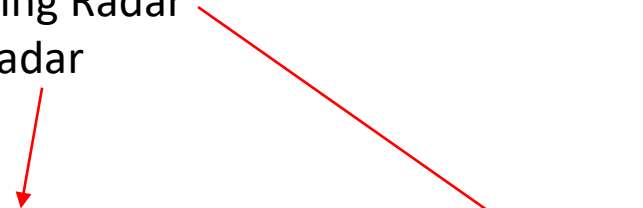


Courtesy National Weather Service

Real Beam Images

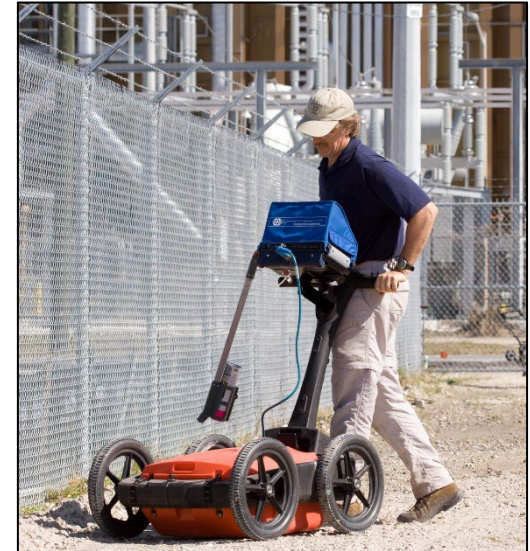
Profiling radar systems

- 4. Ground-Penetrating Radar
- 5. Ice-penetrating radar



Amari & Alsulaimani, 2016

Image Credit: CReSIS / Theresa Stumpf



Courtesy GeoView, Inc.

Real Beam Images

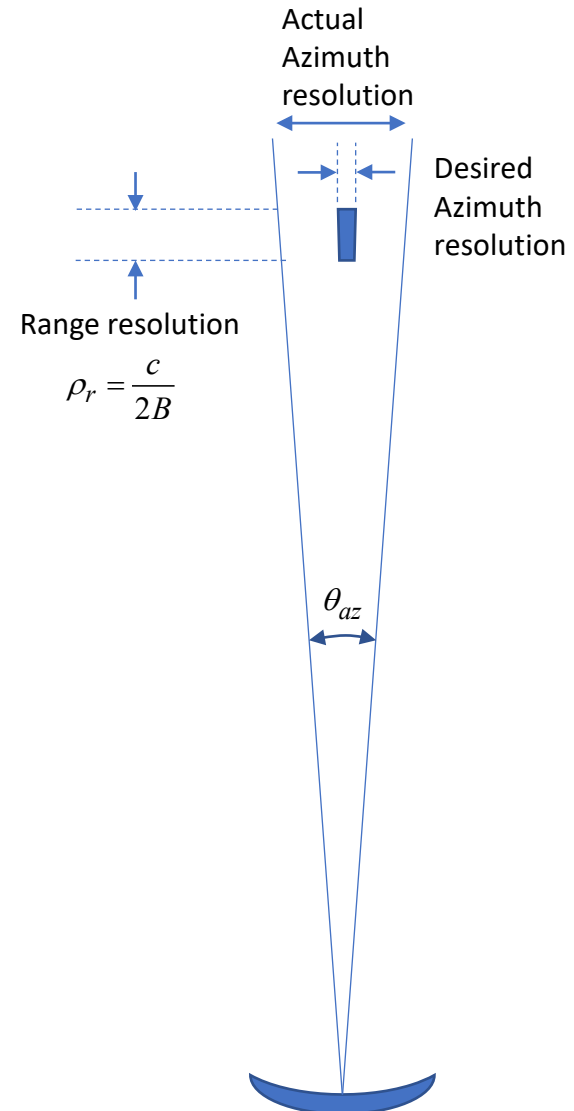
The fundamental problem for real-beam operation is that the angular resolution, and hence the spatial resolution at some range, is limited by the antenna beam, which can be quite wide, especially when antenna size is constrained, such as with airborne systems.

The question then becomes “Can we improve angular resolution to something finer than the real antenna’s beamwidth.

The answer is “Yes!”

The technique involves coherently processing data collected from multiple viewing angles

- Thereby synthesizing an antenna aperture much wider than the actual real-beam antenna
- Process in a manner similar to “tomography”



Aperture Synthesis

Consider a revolving turntable illuminated by a distant stationary radar in a 2-D geometry.

The turntable contains a single reflector located at coordinates (s_x, s_y) .

At long ranges, $r \approx r_{c0} + s_y$

Since the turntable is rotating, we also calculate a range rate, $\dot{r} \approx -s_x \dot{\theta}$

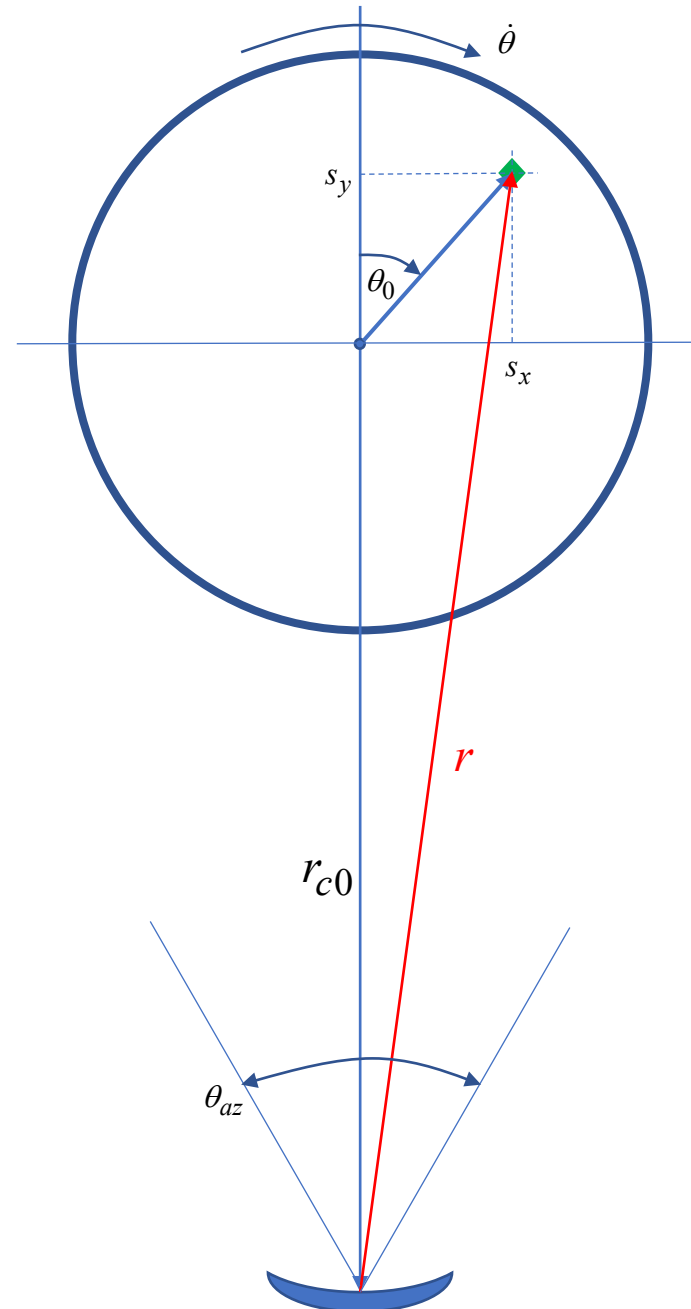
So, a range measure gives us the y-coordinate of the reflector,

$$s_y \approx r - r_{c0}$$

and a range-rate measure gives us the x-coordinate

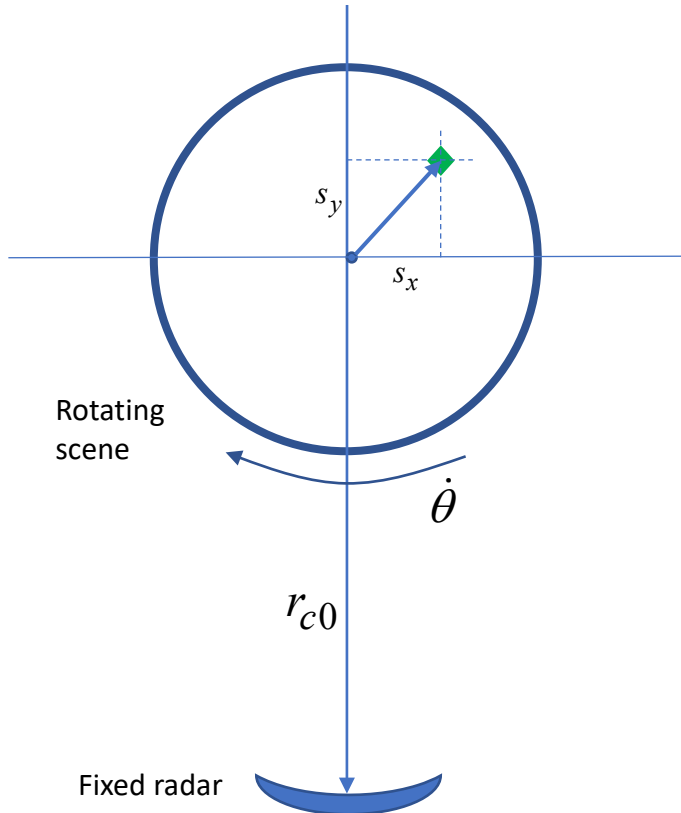
$$s_x \approx -\frac{\dot{r}}{\dot{\theta}} = -\frac{dr}{d\theta}$$

It's really range-rate in terms of an angle change



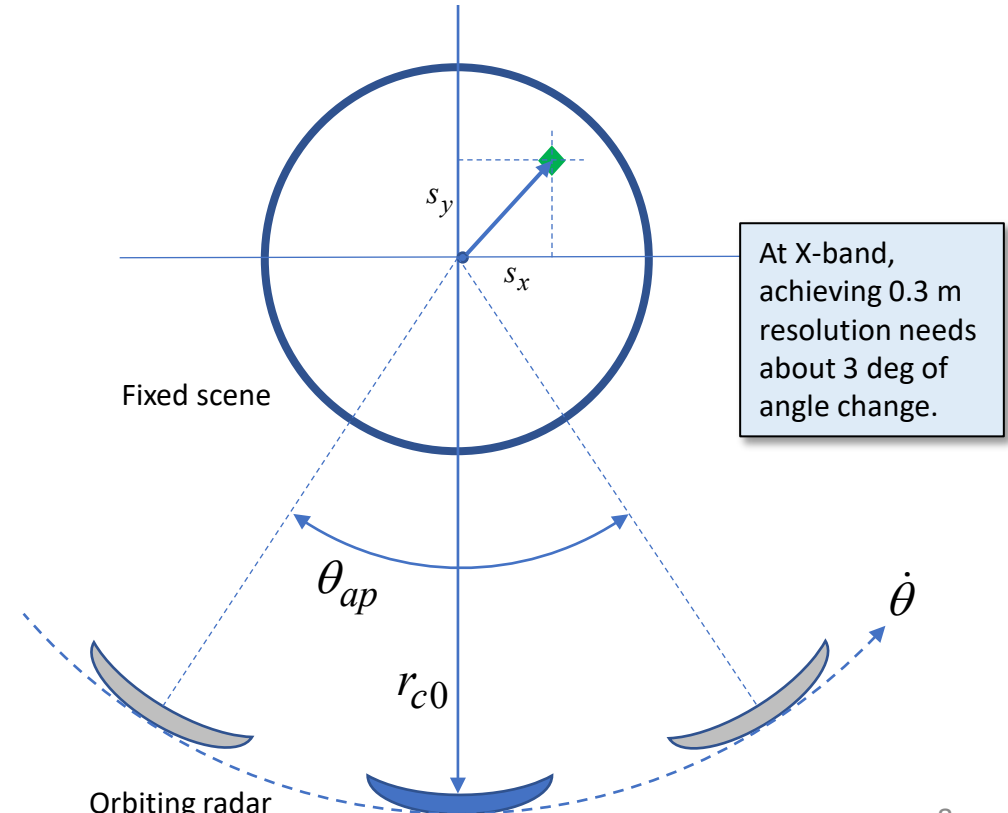
Aperture Synthesis

What's important is the relative motion between radar and target scene.



This can happen with

1. radar stationary and scene rotating
2. Scene stationary and radar orbiting
3. Both radar and target scene moving to effect a viewing aspect change



Aperture Synthesis

A moving radar reflector will manifest a Doppler shift in the radar echo proportional to the range-rate

$$f_D = -\frac{2}{\lambda} \dot{r}$$

Consequently, an azimuth (cross-range) span D_x of radar reflectors will occupy some Doppler bandwidth

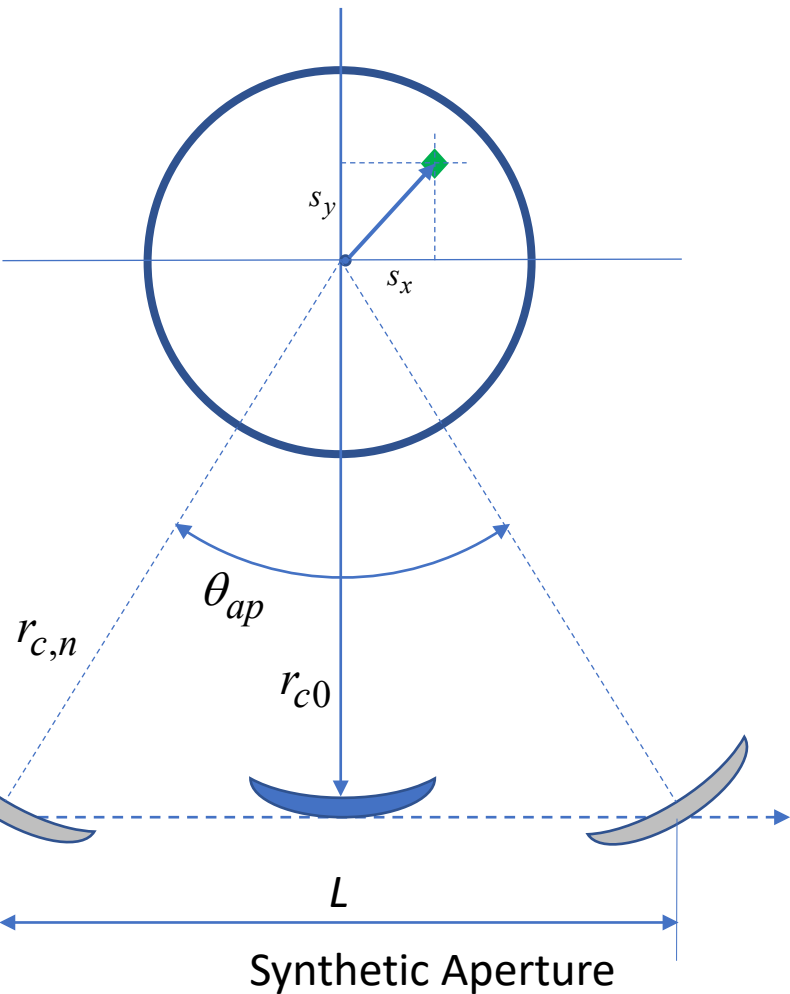
$$B_D = \frac{2}{\lambda} D_x |\dot{\theta}|$$

This azimuth extent may be due to antenna beam illumination, or spatial extent of meaningful target reflections.

A pulse-Doppler radar, to avoid aliasing in azimuth, will need to operate with a Pulse Repetition Frequency (PRF) that adequately samples this bandwidth

$$f_p \geq B_D$$

Aperture Synthesis



If the radar is moving, it does not have to maintain a constant range to the target scene. The range can always be compensated by adjusting data collection times and phases.

What is important is to traverse the necessary angle θ_{ap} to achieve the desired azimuthal (cross-range) resolution.

By employing range-rate information, azimuth resolution is now limited to

$$\rho_x = \frac{\lambda}{2\theta_{ap}} \approx \frac{\lambda}{2L} r_{c0}$$

compared to a real-beam antenna where

$$\rho_x = \theta_{az} r_{c0} = \frac{\lambda}{D} r_{c0}$$

Real aperture length

So, we have a system with azimuth resolution based on a synthetic aperture of length $2L$ instead of a real aperture of length D .

SAR Geometry Model

$\mathbf{r}_{c,n}$ = vector defining radar location for n^{th} pulse

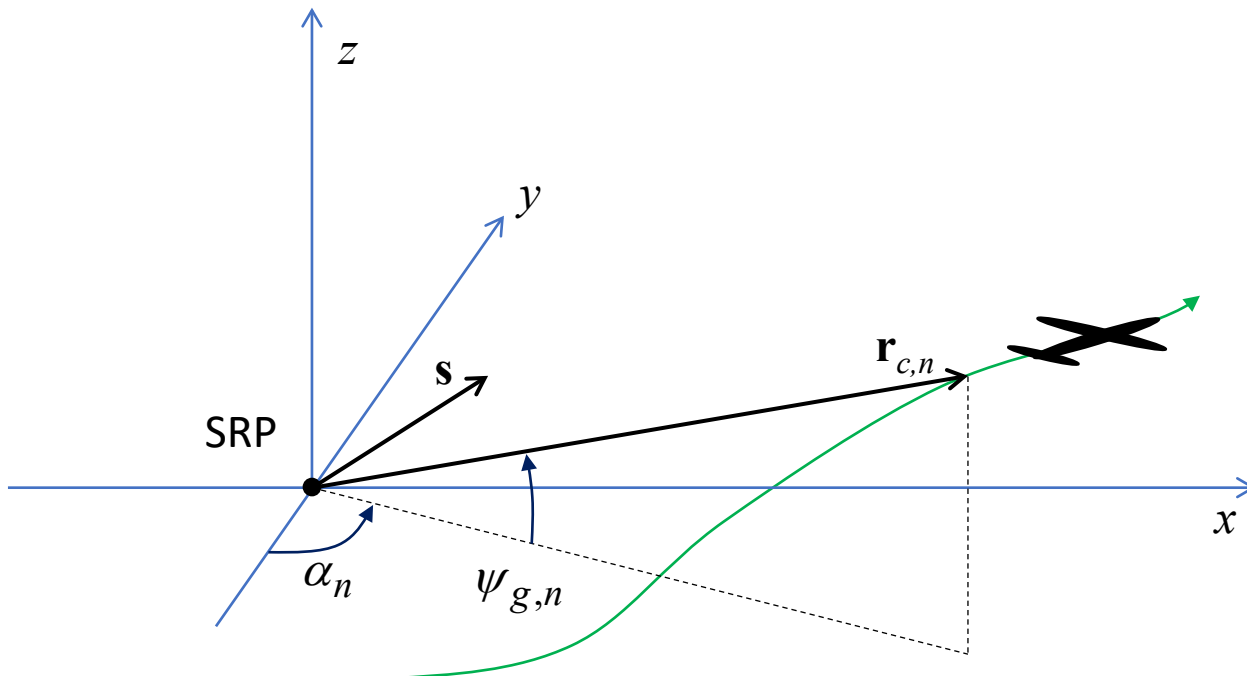
\mathbf{s} = vector defining target scatterer location

$\mathbf{r}_{s,n} = \mathbf{r}_{c,n} - \mathbf{s}$ = Vector from target scatterer to radar

SRP = Scene Reference Point
(nominal center of geometric coordinate frame)

SAR is about “space” more than “time.” Consequently, we need a good definition of the geometric relationships between radar and targets.

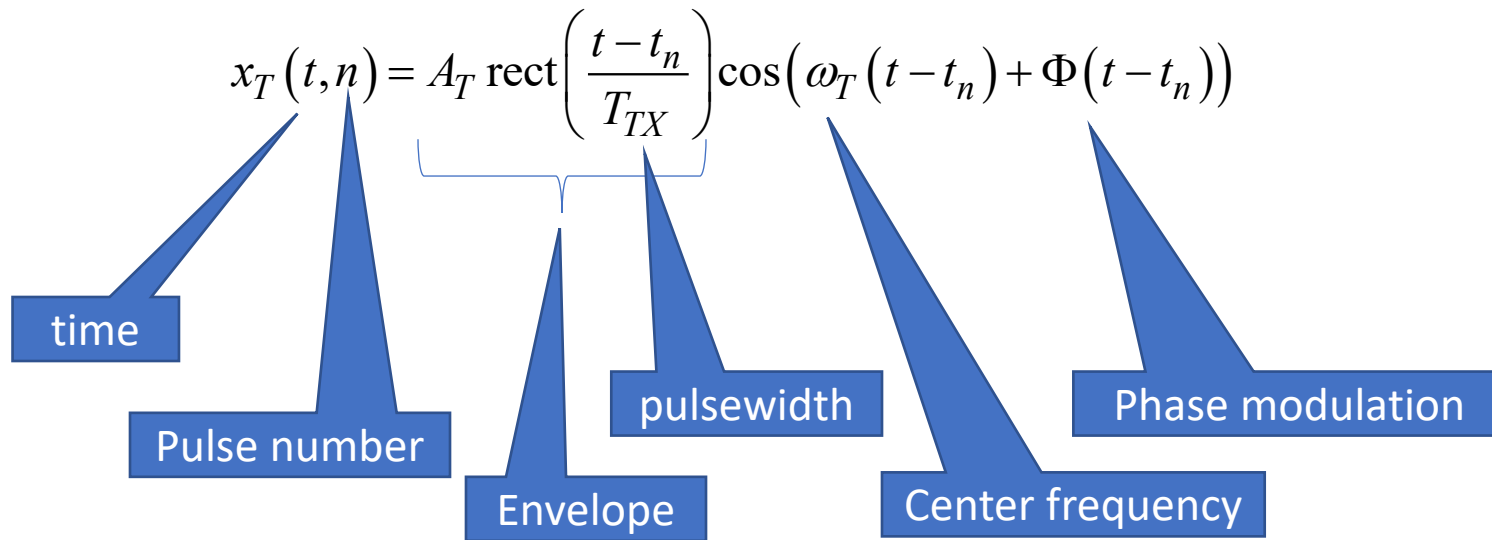
The radar will emit and collect pulses along its flight path.



Signal Model - Transmitted

We will assume a pulse-Doppler radar, with a rectangular envelope.

The Transmitted (TX) signal for pulse number n is modelled as



The phase modulation typically has bandwidth that is small compared to the center frequency. The modulation allows for range resolution via pulse compression. This could be a chirp, phase-coding, etc.

Signal Model – Received Echo

The received (RX) echo signal from a single point-target scatterer is simply an attenuated and delayed version of the transmitted signal, namely

$$x_R(t,n) = A_r \operatorname{rect}\left(\frac{t - t_n - \frac{2}{c}|\mathbf{r}_{s,n}|}{T_{TX}}\right) \cos\left(\omega_T\left(t - t_n - \frac{2}{c}|\mathbf{r}_{s,n}|\right) + \Phi\left(t - t_n - \frac{2}{c}|\mathbf{r}_{s,n}|\right)\right)$$

Received amplitude

where $\mathbf{r}_{s,n} = \mathbf{r}_{c,n} - \mathbf{s}$

known

unknown

This is one of the most fundamental presumptions in radar, and the real starting point for algorithms.

SAR Processing – Optimal Filtering

An optimal filter in the Mean-Squared sense is the “matched filter,” or “correlator.”

We implement this by creating a template for some target scene location of interest, with unity amplitude, where

$$h(t, n, \hat{s}) = x_R(t, n) \Big|_{\substack{A_r=1 \\ s=\hat{s}}}$$

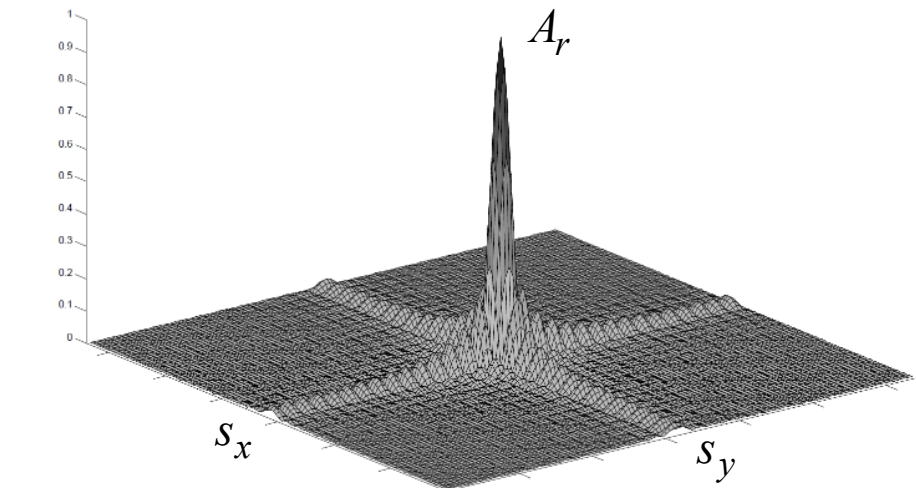
Then we correlate the received echo signal against this template, or kernel

$$y(\hat{s}) = \sum_n \int_t x_R(t, n) h^*(t, n, \hat{s}) dt$$

Very computationally expensive

where “*” denotes complex conjugate.
Note that we do this for all pulses and
over the entire pulse for each pulse.

Doing so for an array of
interesting/desired scene locations will
yield a map of radar reflectivity.



SAR Processing – Range-Doppler Processing

We can approximate the range to a specific target point as

$$|\mathbf{r}_{s,n}| \approx \frac{2}{c} \left(|\mathbf{r}_{c,n}| + s_y \cos \psi_{g,0} - s_x \cos \psi_{g,0} \right) d\alpha n$$

Impact of angular aspect variations

This uses small angle approximations with an assumed planar wavefront

After range-compressing each pulse, we arrive at a range-compressed signal model

$$x_V(\hat{s}_y, n) \approx A_r W\left(\frac{s_y - \hat{s}_y}{\rho_y}\right) \exp j\left(\frac{2\omega_T \cos \psi_{g,0}}{c} s_x d\alpha n + \begin{pmatrix} \text{inconsequential} \\ \text{error terms} \end{pmatrix}\right)$$

Range response, as projected onto the ground

Range-rate (Doppler) term; pulse-to-pulse phase change as a function of aspect angle changes

$$W(f) \approx \left(\frac{\sin(\pi f)}{\pi f} \right) = \text{sinc}(f)$$

Has peak at $f=0$, and mainlobe nominal width of 1.

The exact shape will depend on waveform characteristics, processing choices, compression filters, etc.

SAR Processing – Range-Doppler Processing

The range-rate term is linear in pulse index n , so calls for a DFT across index n , to yield

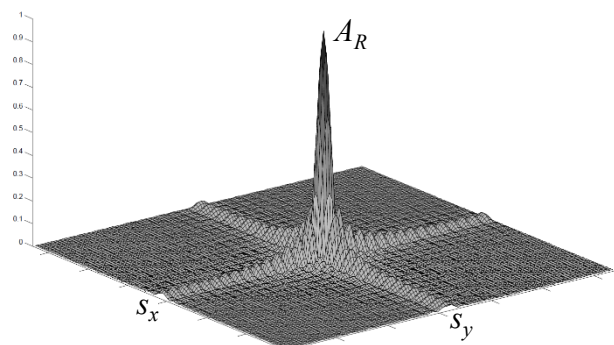
$$y(\hat{s}_y, \hat{s}_x) \approx A_R W\left(\frac{s_y - \hat{s}_y}{\rho_y}\right) W\left(\frac{s_x - \hat{s}_x}{\rho_x}\right)$$

Ground-range resolution

Ground-cross-range (azimuth) resolution

This yields a function of two parameters, (\hat{s}_x, \hat{s}_y) , where the function peaks at indices corresponding to actual target point location (s_x, s_y) .

More generally, a target scene is composed of many scatterers, and since the system and processing is linear, the echo video signal is a superposition (integration) of all of them, as is the output function (image).



SAR Processing – A Zoo of Algorithms

The previously mentioned “*inconsequential error terms*” do in fact become consequential depending on range, desired resolution, image size, etc.

There are many different SAR image formation algorithms, and usually many variations of each, to deal with these conditions, when various errors become consequential. They all have strengths and weaknesses. A partial list might include

- Doppler Beam Sharpening
- Simple Range-Doppler Processing
- Polar Format Algorithm
- Overlapped Subaperture Algorithm
- Range Migration Algorithm
- Chirp-Scaling Algorithm
- Wavenumber-Domain Processing
- Backprojection Processing

Picking one over the other is done by first examining the following:

- parameter space of the data, including frequency, bandwidth, waveform, imaging geometry, etc.
- Processing constraints, including need for real-time, image size, processing hardware, etc.

SAR Processing



Ku-band, 0.1 m resolution

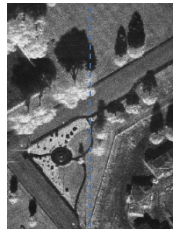
If everything works right, then we can render well-focused images that rival optical photographs.

Each pixel in a SAR image is a measure of radar energy reflected from that location in the target scene, with a resolution much finer than the real antenna's beamwidth

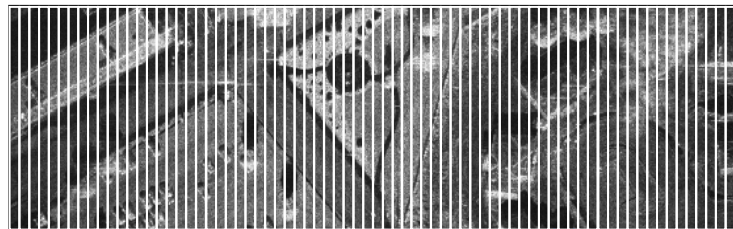
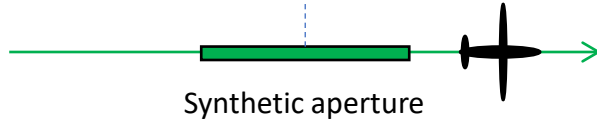
All the usual advantages of radar apply; penetration of weather, dust, smoke, etc.

Spotlight vs. Stripmap Processing

Spotlight
SAR



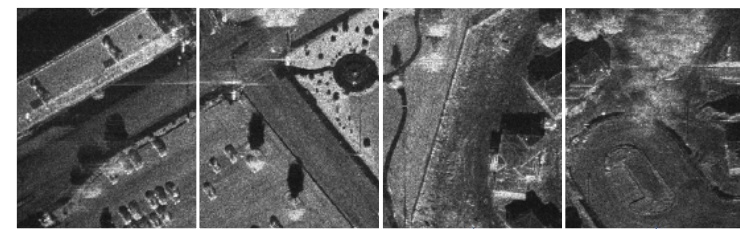
Spotlight SAR creates a single full 2-D image from a single synthetic aperture



Stripmap SAR



Classic Stripmap SAR processes a column of pixels from a single synthetic aperture, and then adds/drops data to form the next column of pixels, for an arbitrarily long composite image.



More typically today, Stripmap SAR images are formed by mosaicking individual Spotlight SAR images formed from non-overlapping distinct synthetic apertures.

A Word About Motion Measurement

SAR processing is all about compensating for range variations that occur during the data collection activity.

Ideally, we would be able to measure the radar position/motion to within a very small fraction of a wavelength; perhaps less than a degree.

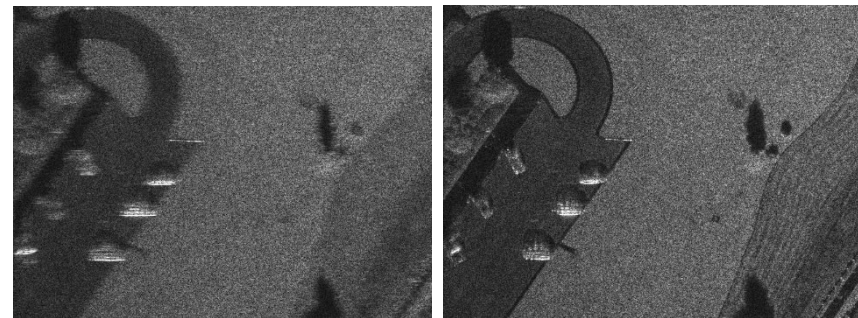
(Note that microwaves have wavelengths measured in just a few centimeters.)

A typical motion measurement system for airborne SAR uses a GPS-aided Inertial Measurement Unit (IMU).

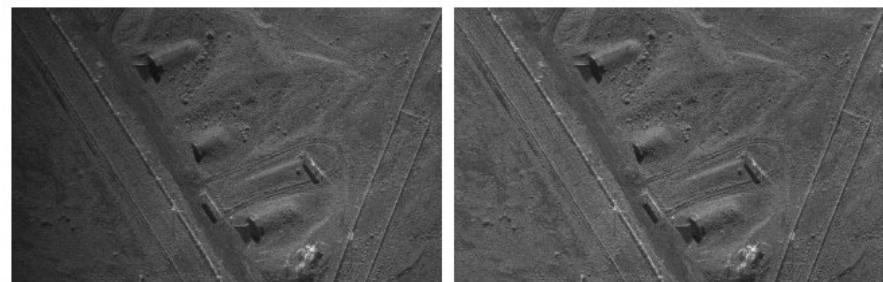
Any residual motion measurement errors, particularly in the line-of-sight direction, will cause errors in the SAR image, manifesting as phase errors.

Pulse-to-pulse phase errors

Constant errors → no appreciable effect
Linear errors → azimuth position error
Higher order errors → degraded image focus



Pointing errors due to angular attitude errors will cause improper illumination of the target scene, But not a misfocus.

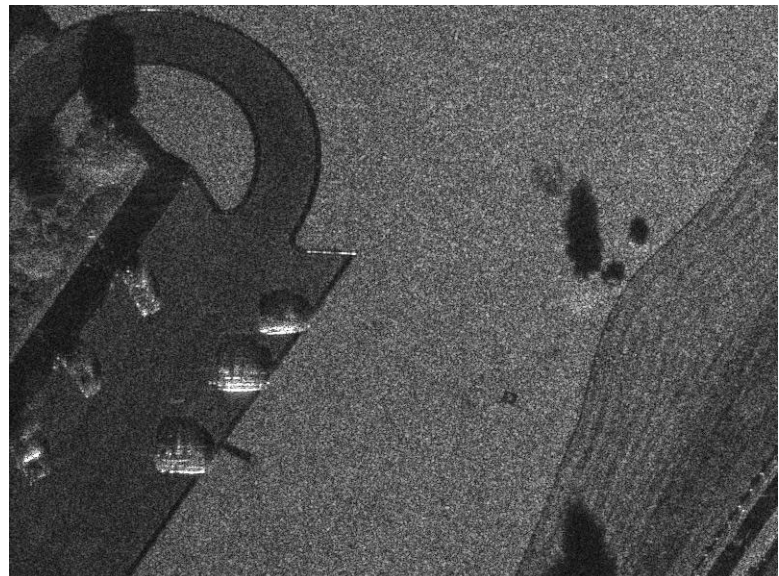
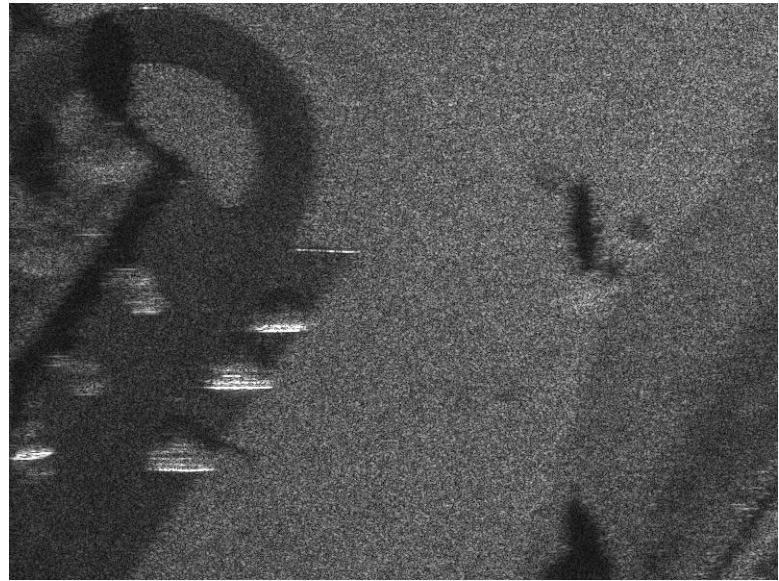


Autofocus

Autofocus is a blind deconvolution of a common phase error. These phase errors are typically due to uncompensated radar motion due to inadequate motion measurement accuracy.

Various techniques exist. All somehow measure the “blur” and attempt to de-blur the image.

- Phase-Gradient autofocus
- Map-drift autofocus
- Contrast optimization
- Prominent Point
- Entropy techniques



SAR Performance

Here we are interested in how range, power, resolution, and other factors interact with each other to allow acceptable SAR image quality.

Our measure is Signal-to-Noise Ratio (SNR)

The equation that relates these is the “radar [range] equation”

For a monostatic radar, at the RX antenna port, an instantaneous SNR measure for a single pulse can be written

$$SNR_{antenna} = \frac{P_r}{N_r} = \frac{P_T G_A^2 \lambda^2 \sigma}{(4\pi)^3 R^4 L_{radar} L_{atmos} (kTF_N) B_N}$$

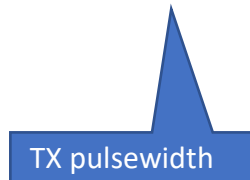
The diagram illustrates the components of the radar equation. It shows the formula for SNR_{antenna} with six callout boxes pointing to its various terms:

- Peak TX power: Points to P_T .
- Antenna gain: Points to G_A^2 .
- Radar Cross Section (RCS): Points to σ .
- Noise bandwidth: Points to B_N .
- Atmospheric propagation losses: Points to L_{atmos} .
- Radar hardware losses: Points to L_{radar} .

Signal Processing Gains in SNR

Pulse compression will increase SNR, as will Doppler processing

$$G_r \approx T_{TX} B_N$$



Doppler processing will also increase SNR by coherently combining multiple pulses

$$G_a \approx N = \frac{f_p \lambda R}{2 \rho_x v_x}$$

PRF

Number of pulses

Radar velocity

We are assuming matched filtering, and tacitly ignoring any effects due to sidelobe control measures, like window functions.

So, SAR signal processing will enhance SNR by these factors, typically by a lot, e.g. many tens of dB.

Also useful is to identify an “average” TX power as

$$P_{avg} = P_T T_{TX} f_p$$

$\underbrace{\phantom{P_T T_{TX}}}_{\text{Duty factor}}$

Radar Cross Section (RCS)

SAR usually is interested in the RCS of “distributed” clutter, which is resolution dependent.

$$\sigma = \sigma_0 \rho_x \rho_y$$

where

σ_0 = Distributed clutter reflectivity,
measured in terms of RCS per m²



Typical values at Ku-band (16.7 GHz) might be
–5 to –10 dBsm/m² for urban areas or rocky areas
–10 to –15 dBsm/m² for cropland or forest areas
–15 to –20 dBsm/m² for grasslands
–20 to –30 dBsm/m² for desert areas or road surfaces

Ground-range resolution is related
to slant-range resolution by

$$\rho_y = \left(\frac{\rho_r}{\cos \psi_g} \right)$$

Distributed clutter is usually modelled as a Gaussian-distributed random process. The characteristic reflectivity is the variance of the associated random variable.

Local grazing angle

Geometry Effects on Radar Reflectivity

Typically, the radar is specified to operate at a particular height above the ground. Consequently, grazing angle depends on this height, and the slant-range of operation. For a flat earth this is calculated as

$$\sin \psi_g = \frac{h}{R}$$

$$\cos \psi_g = \sqrt{1 - \left(\frac{h}{R}\right)^2}$$

where

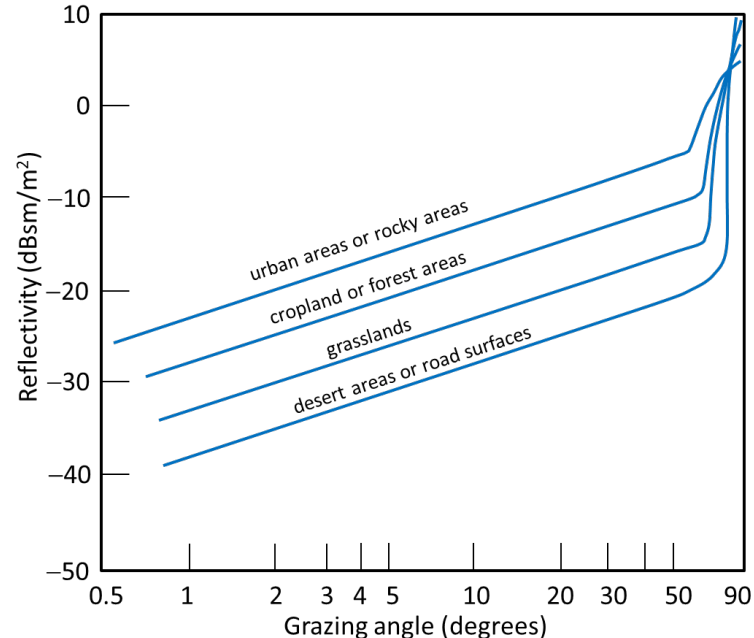
h = height of the radar above the target

Note that σ_0 also generally has a dependency on grazing angle ψ_g . This is sometimes embodied in a “constant-gamma” model for clutter. In this case the reflectivity is modelled as

$$\sigma_0 = \gamma \sin \psi_g$$

where

γ = Clutter “gamma”



Typical effects of grazing angle on clutter reflectivity

SNR and Noise Level in SAR Image

There are a number of ways to write the Radar Equation. One way is as follows.

$$SNR_{image} = \frac{P_{avg} G_A^2 \lambda^3 \left(\frac{\rho_r}{\cos \psi_g} \right) \sigma_0}{2(4\pi)^3 R^3 v_x (kTF_N) L_{radar} L_{atmos}}$$

We define an entity that answers the question
“What equivalent clutter level does the noise look like in the SAR image?”

This goes by several names

- Sigma-N
- Sigma-Noise
- Noise Equivalent Reflectivity (NER)
- Noise Equivalent Sigma 0 (NES0)

A typical maximum acceptable NER for X-band and Ku-band is -25 dBsm/m^2 , -- lower for lower frequencies.

$$\sigma_N = \frac{\sigma_0}{SNR_{image}} = \frac{2(4\pi)^3 R^3 v_x \cos \psi_g (kTF_N) L_{radar} L_{atmos}}{P_{avg} G_A^2 \lambda^3 \rho_r}$$



-30 dBsm/m²



-25



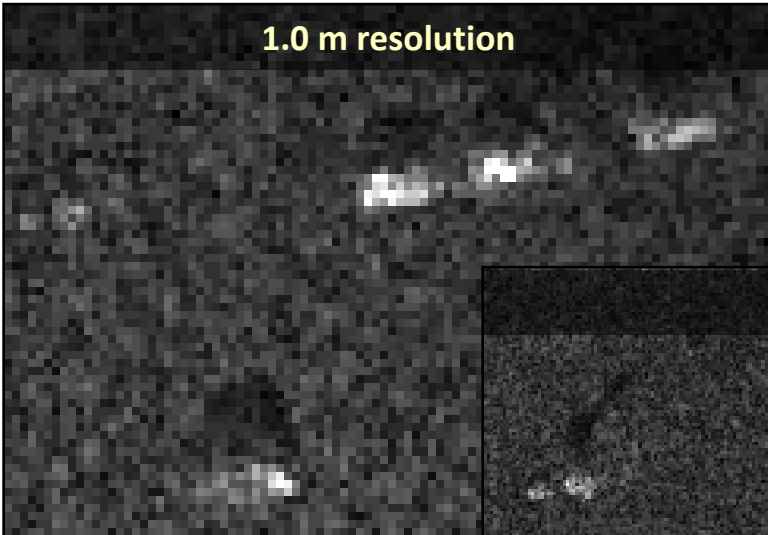
-20



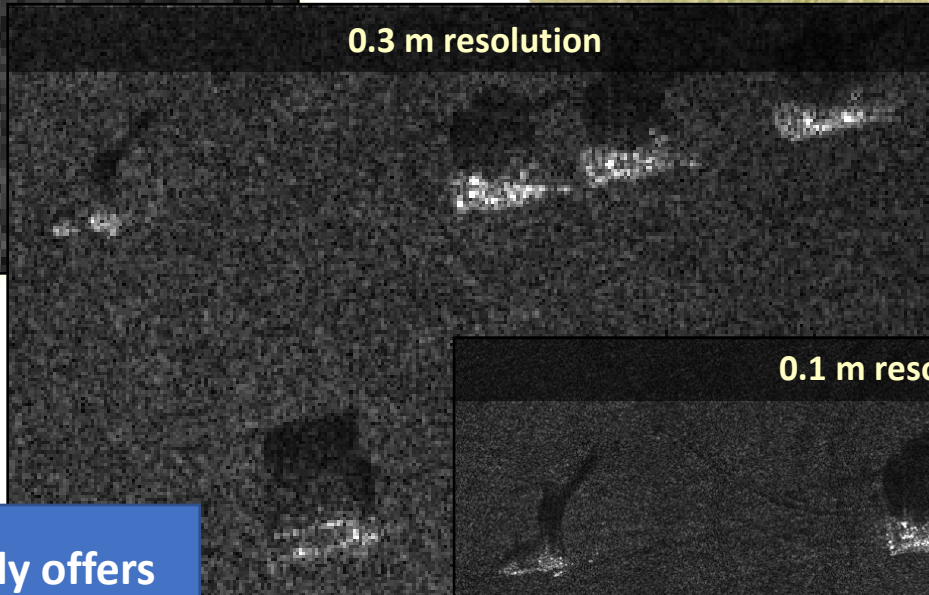
-15

SAR Image Resolution

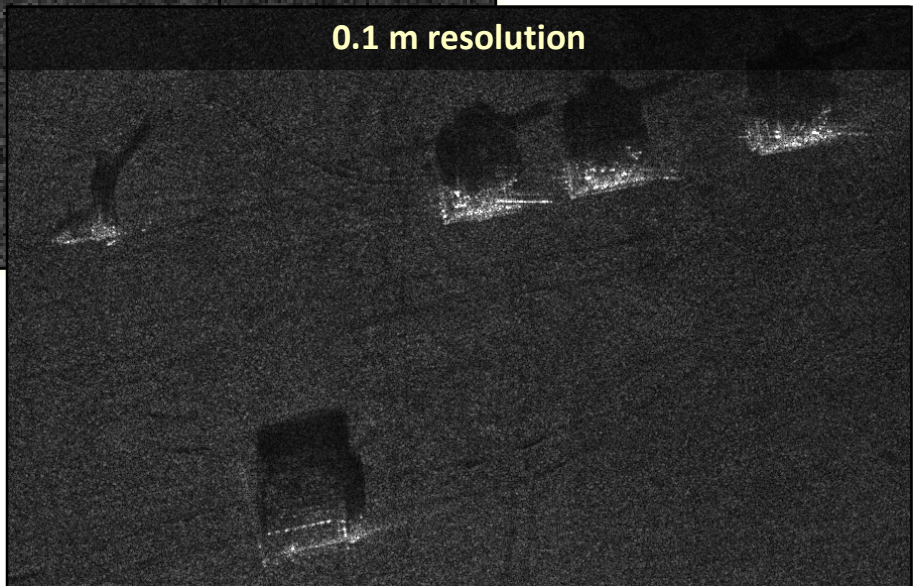
1.0 m resolution



0.3 m resolution

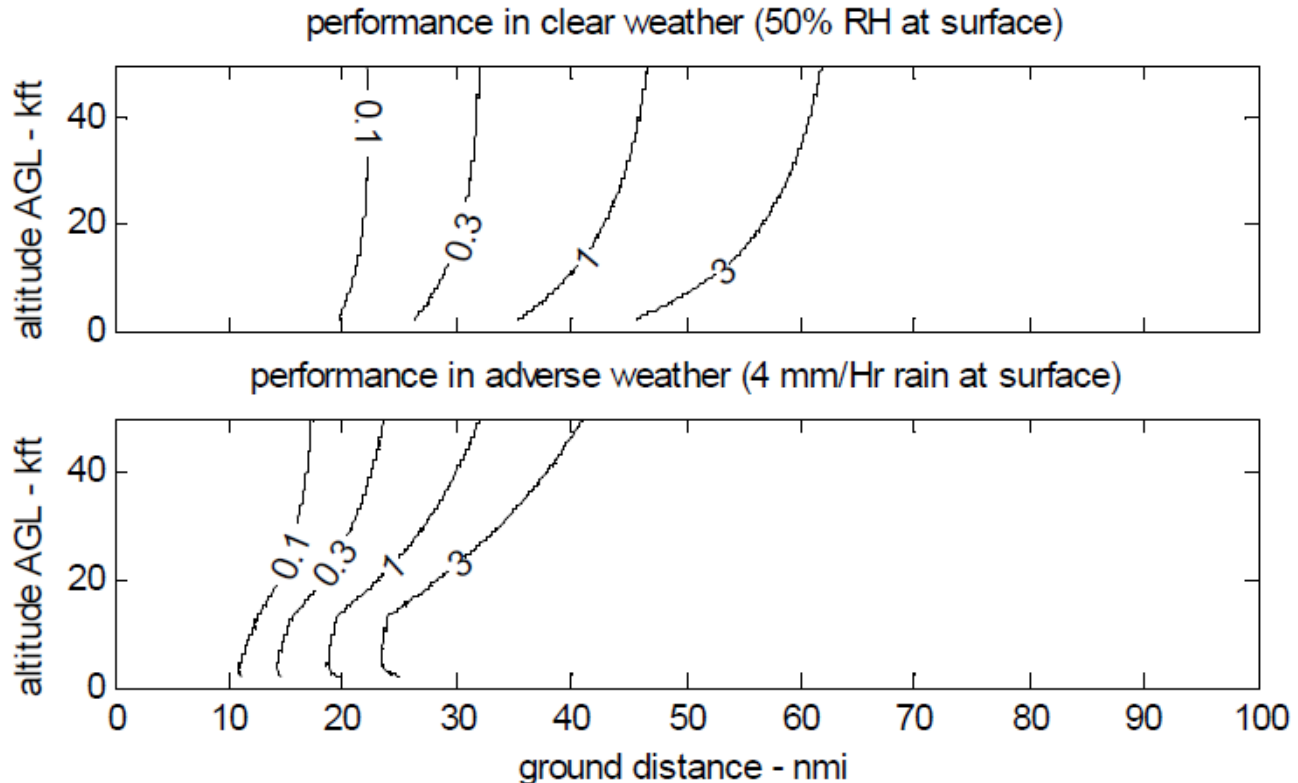


0.1 m resolution



Finer resolution clearly offers more detail – but at the expense of greater latency, more complicated processing, and shorter ranges

Geometry Limits vs. Resolution



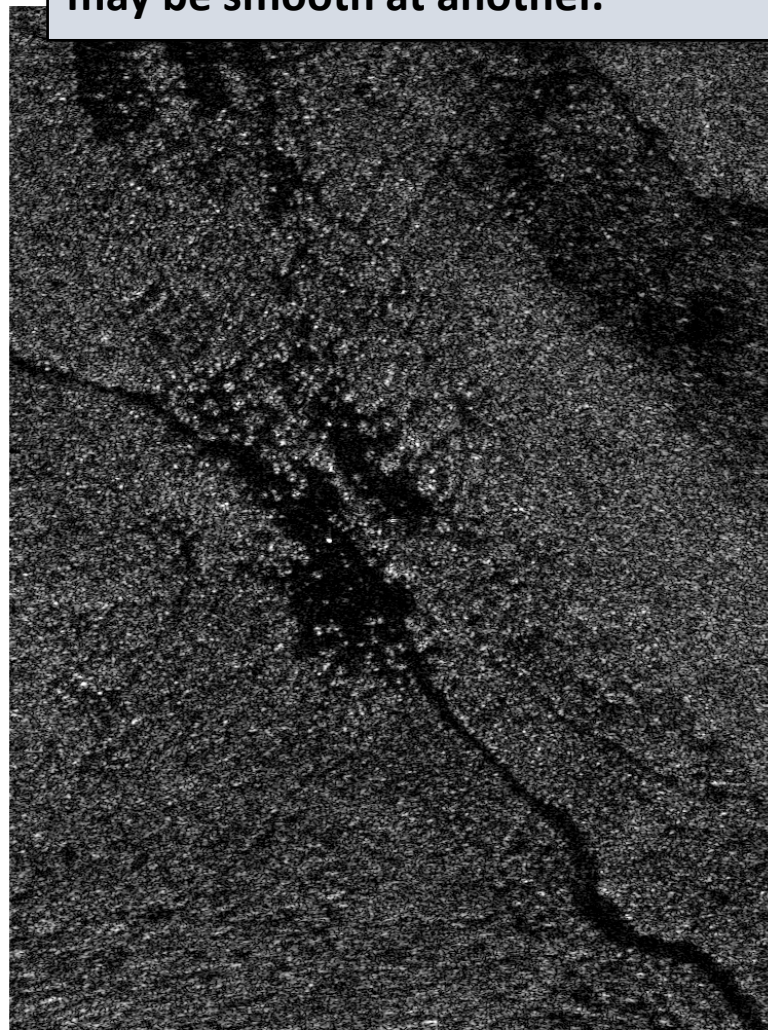
Frequency = 16.7 GHz
Power (peak) = 320 W
duty factor = 0.35
Antenna (ap area) = 93.0002 sq in
Antenna (ap aspect) = 2.7
Antenna (gain) = 30.6812 dB
Antenna (ap pwr dens) = 3.44 W/si

Velocity (ground speed) = 70 kts
Noise reflectivity = -25 dBsm/m²
Losses (signal processing) = 2 dB
Losses (radar) = 2 dB
Noise figure = 4 dB
Unambiguous range = 196 nmi
(resolution in "m")

Frequency Dependence



2 Meter Resolution / December 22, 1994
Ku-Band SAR, 15 GHz
Vertical Polarization



2 Meter Resolution / November 9, 1994
UHF SAR, 380 MHz
Vertical Polarization

Roughness is measured against wavelength. Rough at one wavelength may be smooth at another.

SAR Shadows

Some objects are more readily identified by their shadows. This is also true for otherwise stealthy targets.



Interferometric SAR (IFSAR, InSAR)

Consider two antennas offset in elevation, and a SAR image from each.

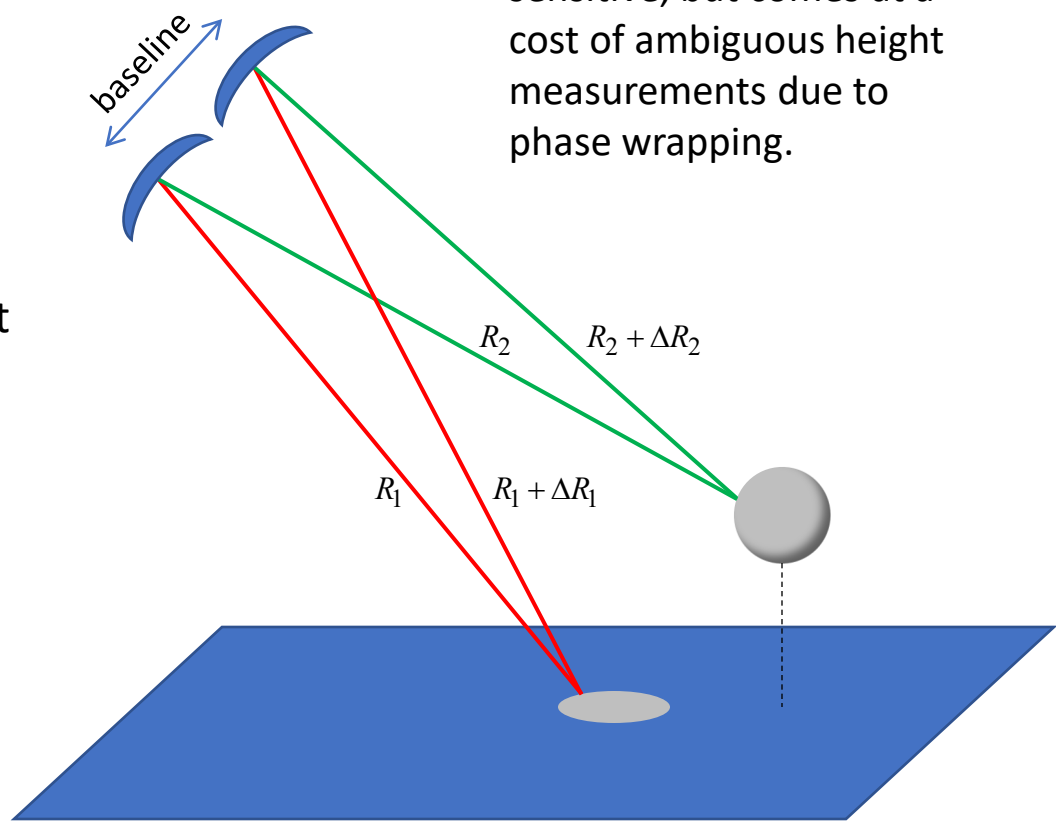
Corresponding pixels will exhibit different ranges between the two antennas, that in turn manifests as a phase difference.

This phase difference depends on elevation angle offset, due to target height.

A platform can either

1. Carry both antennas for a single-pass configuration, or
2. Carry one antenna and fly two passes, with offset collection geometries.

A bigger baseline makes the interferometer more sensitive, but comes at a cost of ambiguous height measurements due to phase wrapping.

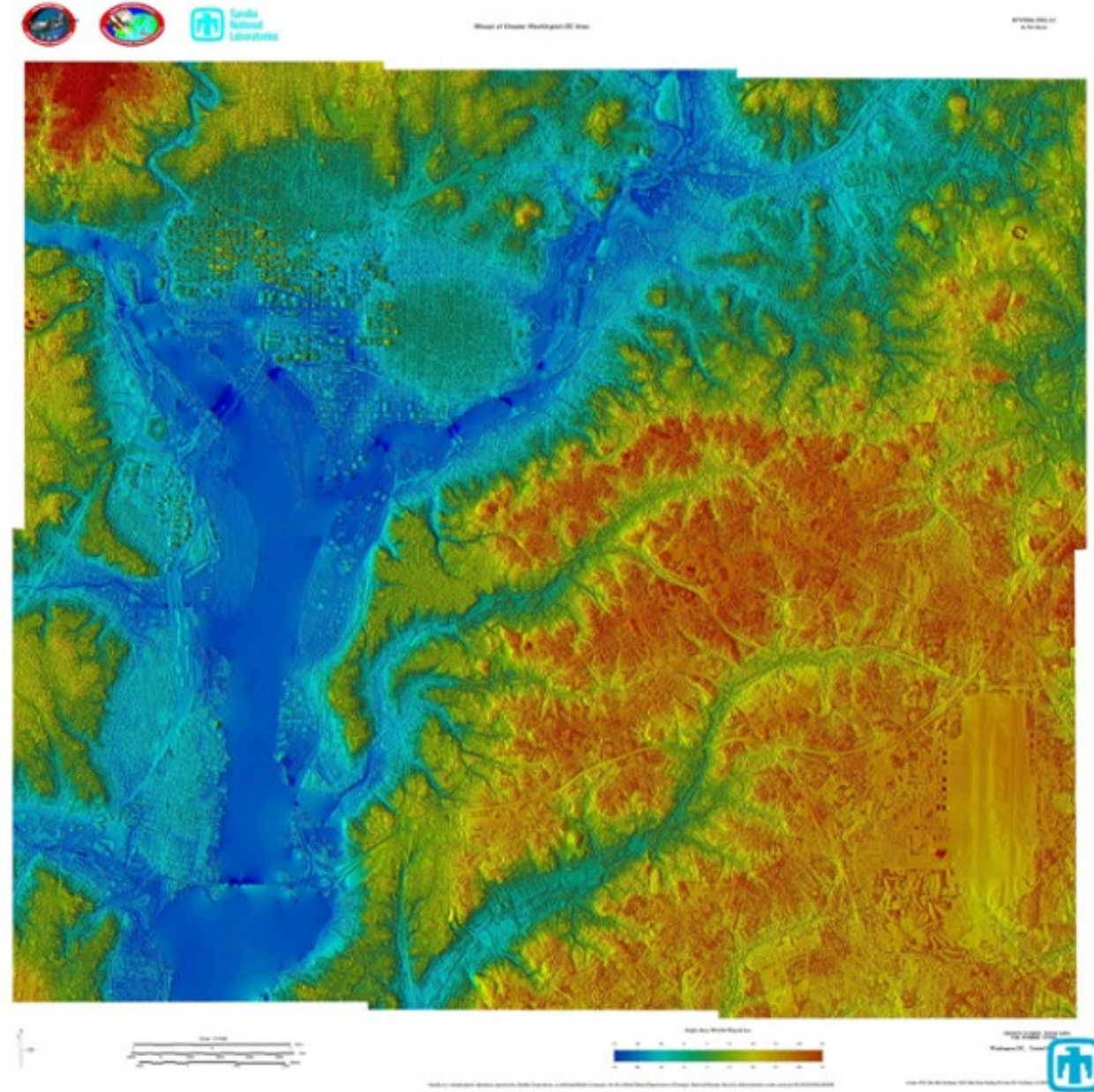


Interferometric SAR (InSAR)

This is a color coded height map of Washington, DC.

Absolute accuracy is in the 1-2 meter range for each pixel.

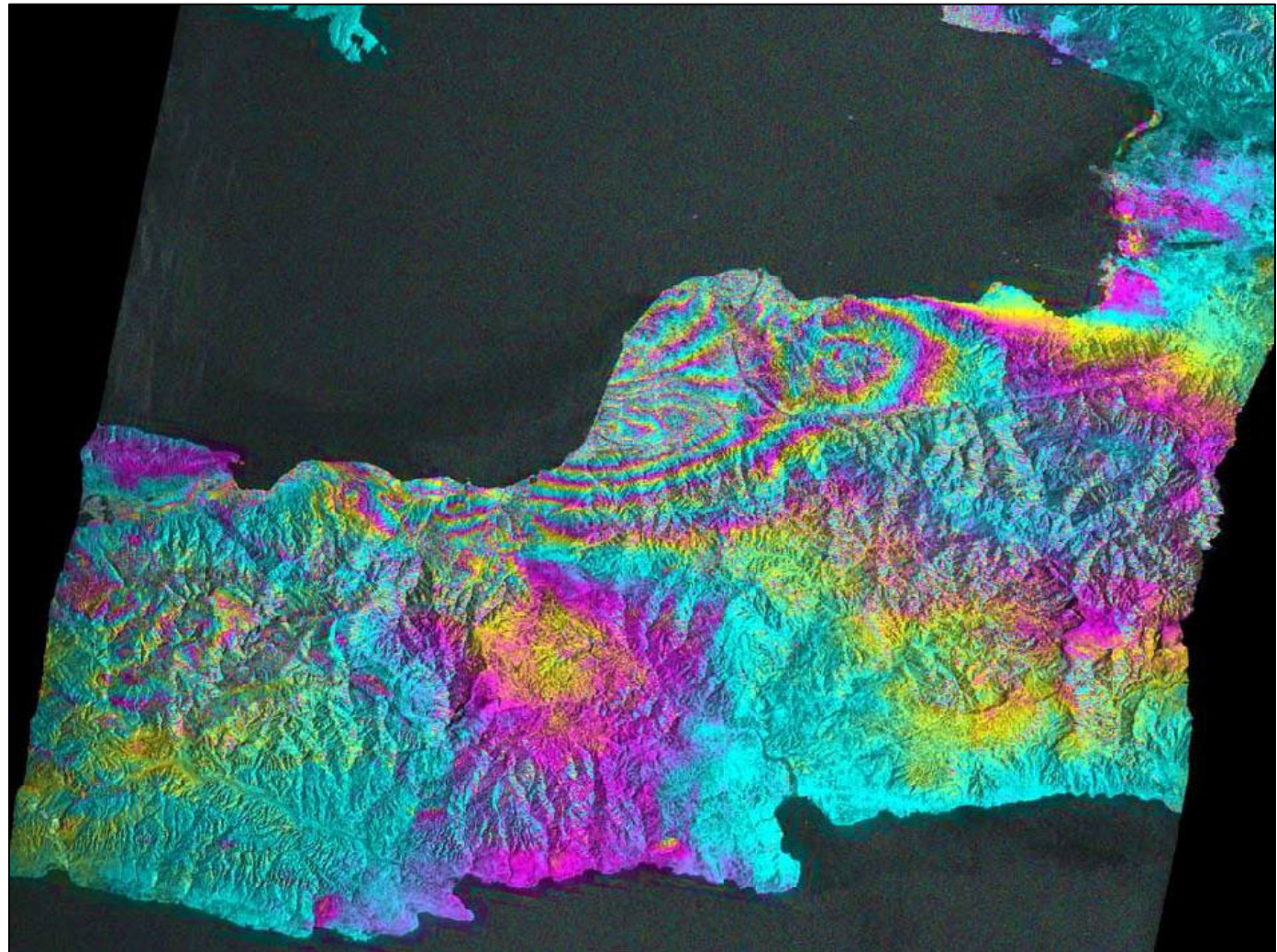
Data was collected from about 10 km standoff range.



SAR – Land Deformation

Radar interferogram
showing ground
deformation from
Haiti quake

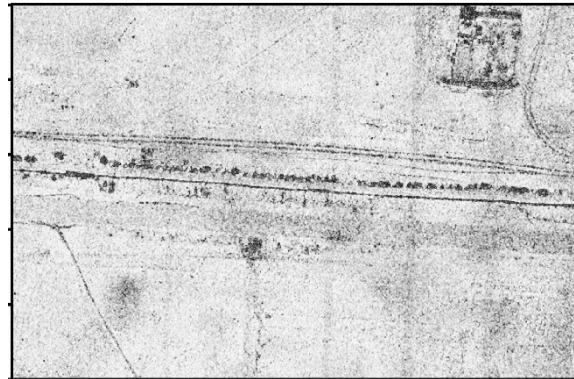
(ALOS PALSAR) The
color "fringes" show
contours of the
ground deformation
caused by the
earthquake.



Coherent Change Detection (CCD)



SAR Images



Coherence map

Coherence is essentially the normalized cross-correlation coefficient between the two images.

For images, we calculate the coherence of pixel (m,n) using a local neighborhood of K points around the pixel.

SAR assumes a stationary target scene.

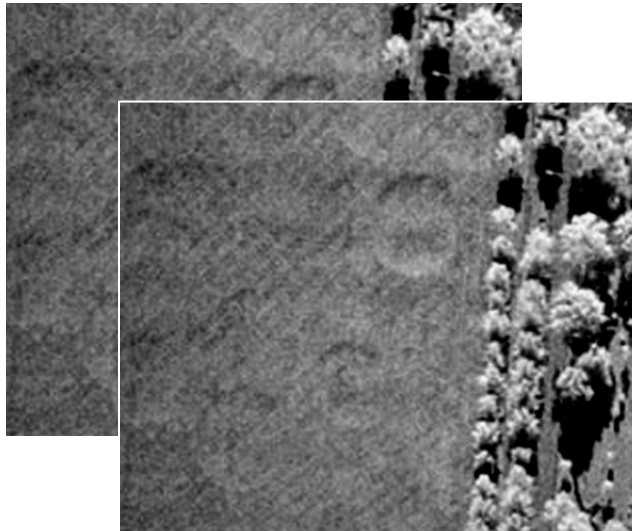
Two SAR images of the same identical scene, taken from the same geometry, but at different times, will be identical in all respects except for uncorrelated noise, i.e. they will be coherent with each other.

$$r_{xy}(\tau) = \frac{|R_{xy}(\tau)|}{\sqrt{R_{xx}(\tau)R_{yy}(\tau)}} = \frac{\left| \int_{-\infty}^{\infty} x^*(t)y(t+\tau)dt \right|}{\sqrt{\int_{-\infty}^{\infty} x^*(t)x(t+\tau)dt \int_{-\infty}^{\infty} y^*(t)y(t+\tau)dt}}$$

$$\mu(m,n) = \frac{\left| \sum_{k \in K} x_k^* y_k \right|}{\sqrt{\sum_{k \in K} x_k^* x_k \sum_{k \in K} y_k^* y_k}}$$

This is an estimate of the total coherence of pixel (m,n)

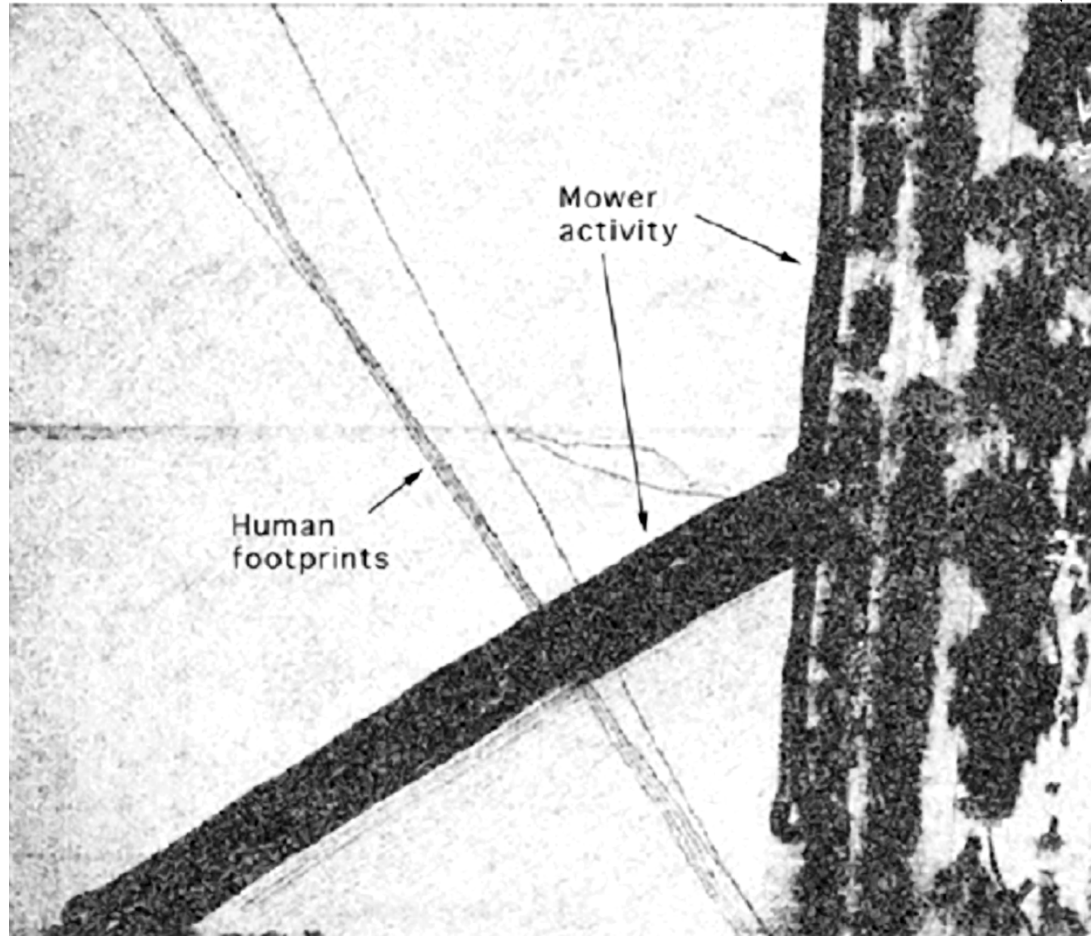
Coherent Change Detection (CCD)



Any changes in the scene that occur between the two SAR images will cause a local destruction of coherence.

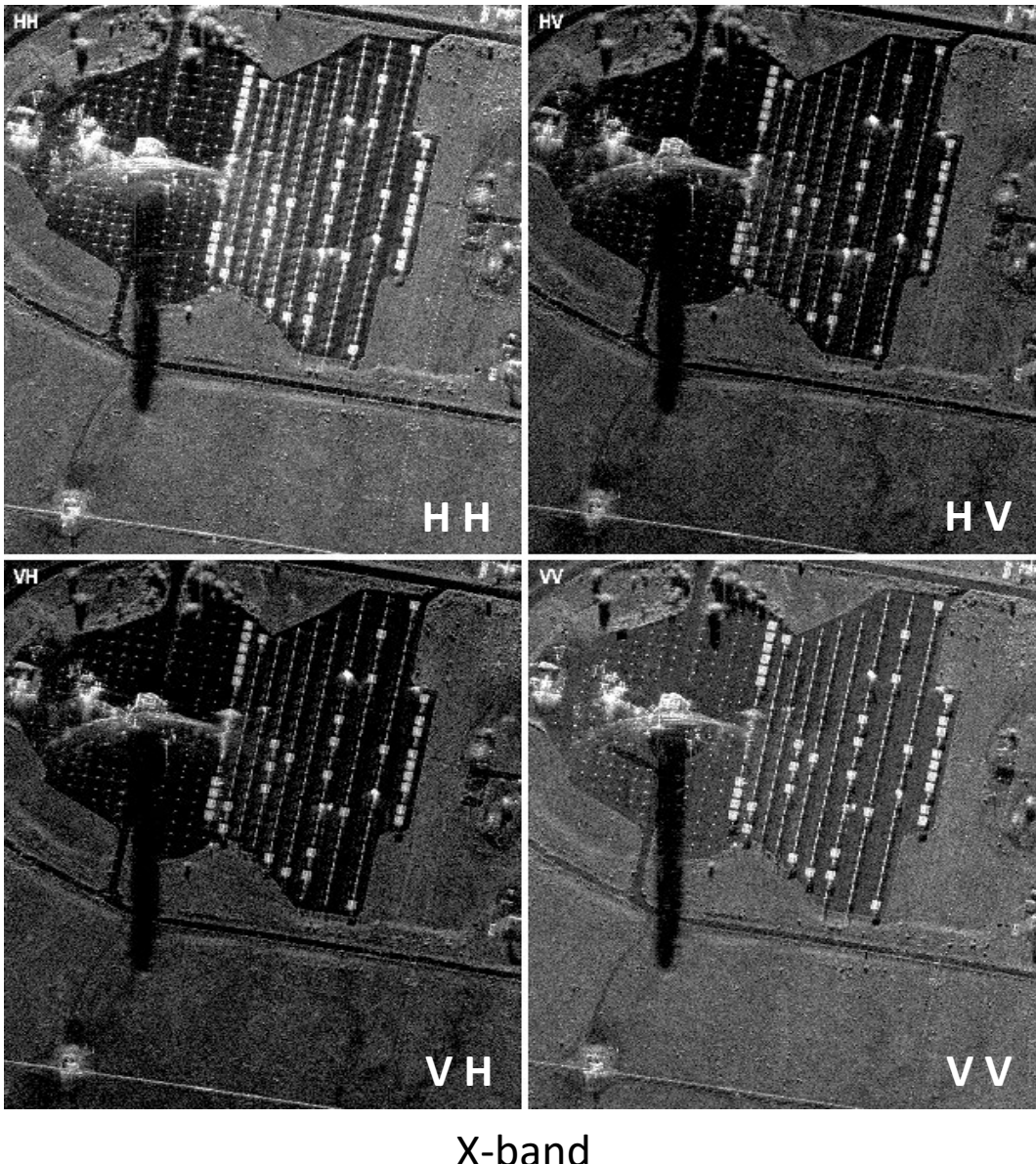
Some apparent changes are natural and unavoidable (e.g. foliage, shadows, etc.)

We are generally interested in those changes due to activities of interest, often human, but not always.



Ku-band, 4-inch resolution

Polarization Dependence



Targets are often also sensitive to polarization of the incident radiation., and re-radiate preferred polarizations.

Some features “light up” with some polarization combinations, and others “light up” with other polarization combinations.

Sometimes, target features we want to suppress can be made to “go dark” with certain polarization combinations.



Polarimetric SAR

It is often more convenient to display or otherwise render a function of the various polarimetric responses into a single image, using color as a display dimension.

These functions are often called “decompositions,” and are chosen to feature specific attributes, like even/odd bounces, and polarization rotations.



One such decomposition is the Yamaguchi decomposition which assumes all scattering in a scene can be attributed to some combination of

- 1) Bragg rough surface scattering,
- 2) even bounce from orthogonal surfaces,
- 3) canopy (i.e. volumetric scattering), and
- 4) helical scattering.



Often only display these

Even bounce
Volumetric
Bragg Surface

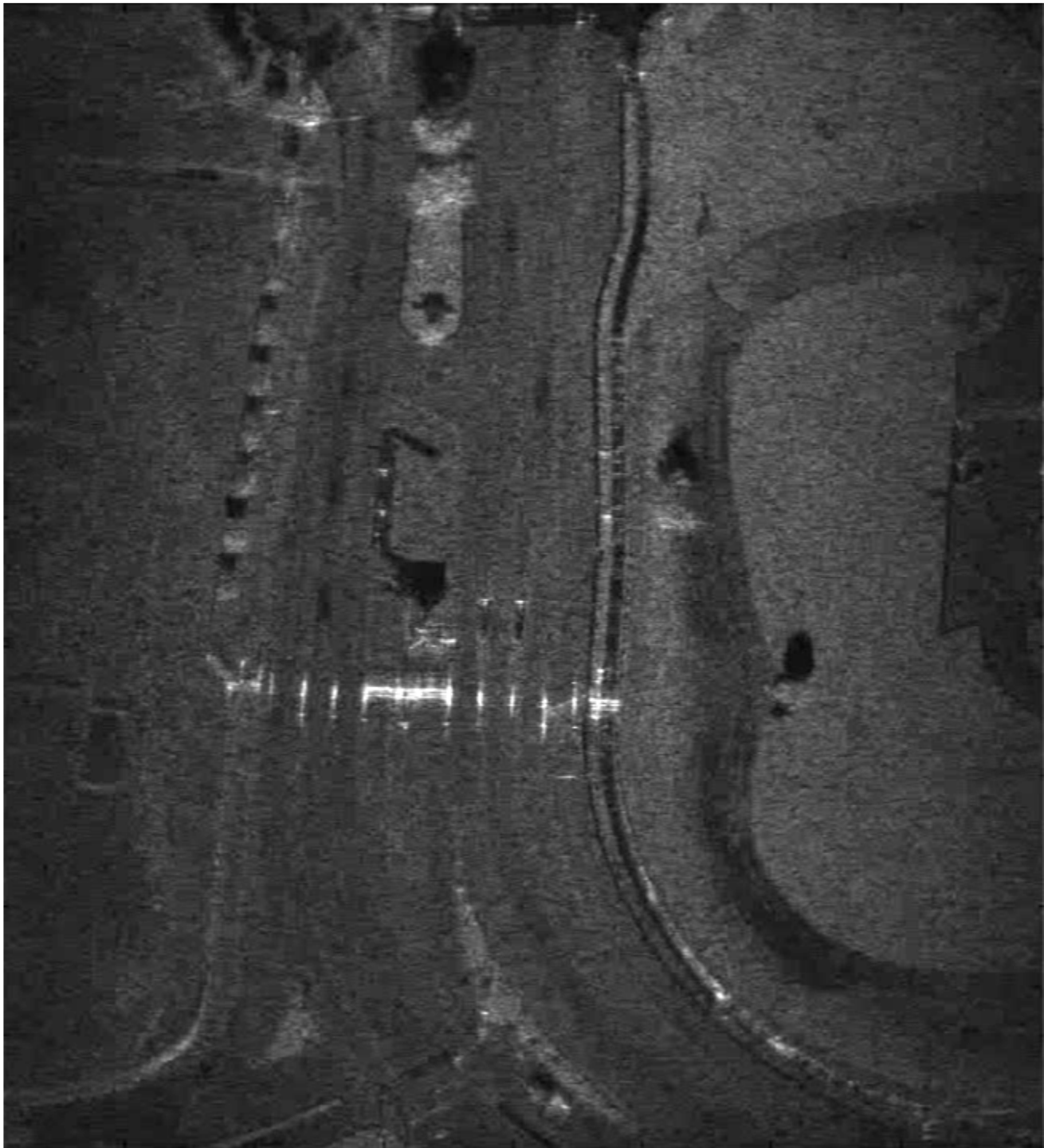
VideoSAR

Image courtesy
Google Earth



VideoSAR is particularly useful
for tracking shadows.

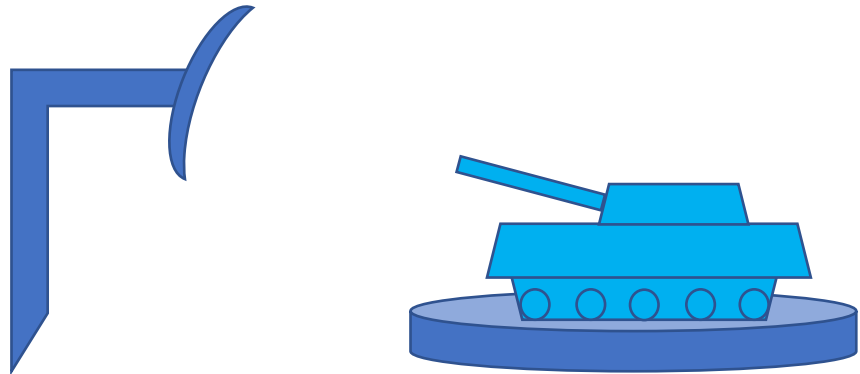
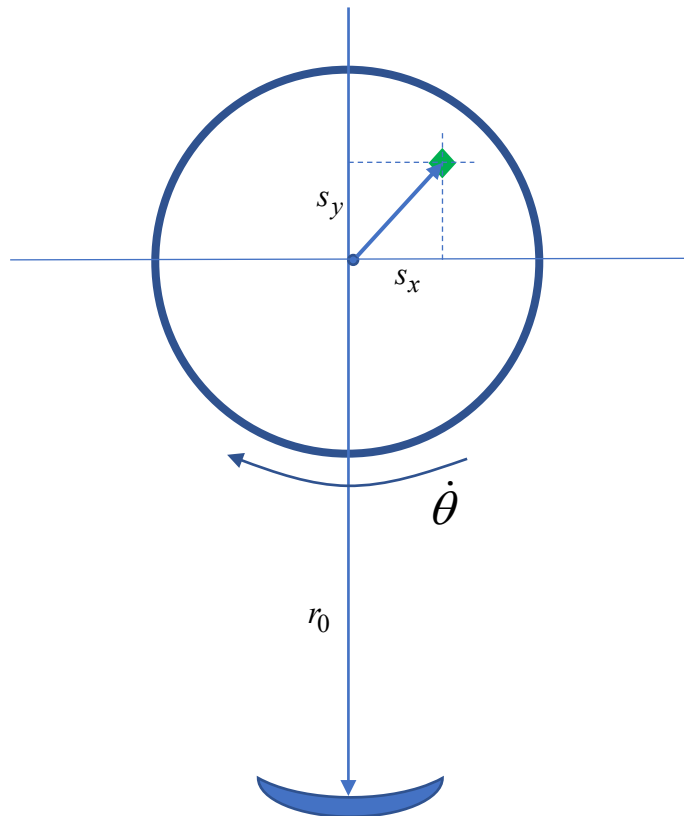
Shadows don't exhibit Doppler
shift, so there is no Minimum
Detectable Velocity.



Inverse-SAR (ISAR)

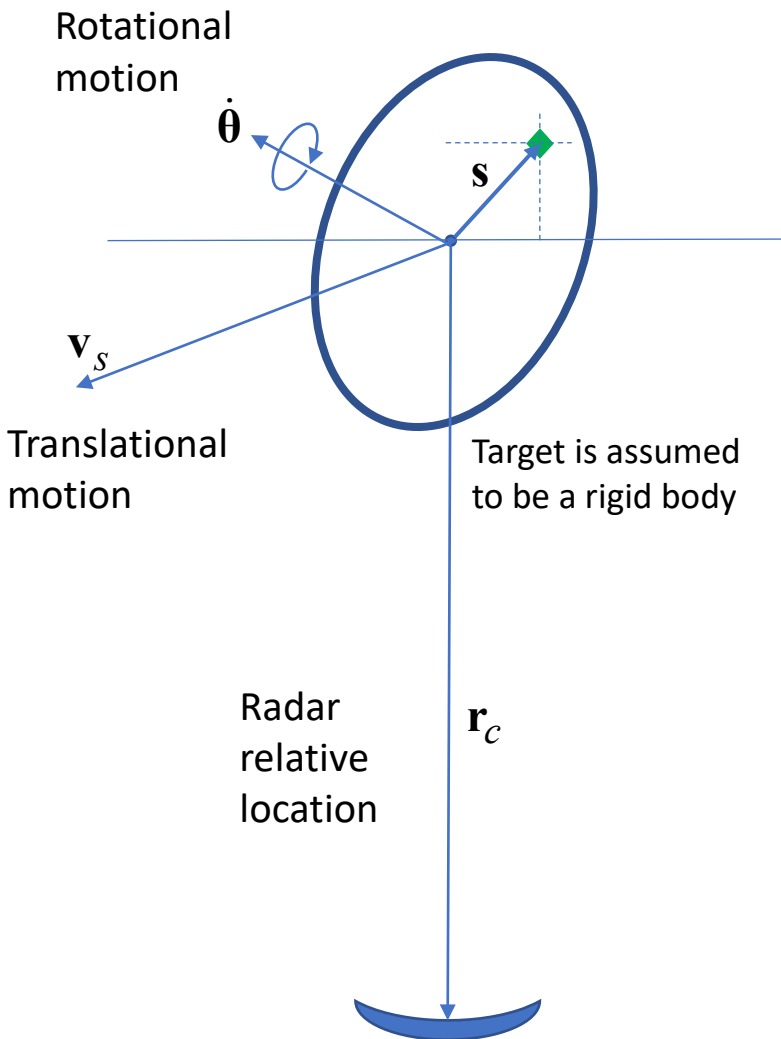
ISAR refers to coherent imaging when a principal source of relative motion is due to target motion itself.

Originally, it referred to a stationary radar with target on a turntable.



More recently, ISAR has come to mean any range-Doppler imaging where the target exhibits motion, whether known or otherwise. An example is imaging a ship moving on the open ocean.

ISAR Motions



Operationally, we generally have to contend with both unknown target translational motion, and unknown target rotational motion, with the radar itself exhibiting its own motion. Furthermore, none of these motion parameters can be presumed to be constant. For example, some might be sinusoidal, or accelerations might be involved.

Synthetic aperture imaging is about discriminating relative measures of range and range-rate.

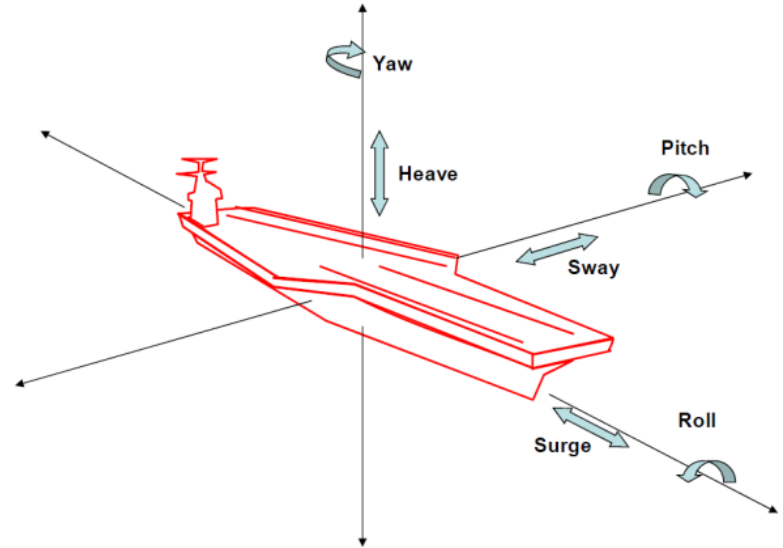
This requires measuring and compensating for some bulk ranges and range-rates, so that we can then map with respect to subtle variations around the bulk values. These variations are sometimes called “micro-Doppler.”

ISAR imaging becomes basically a sophisticated autofocus problem.

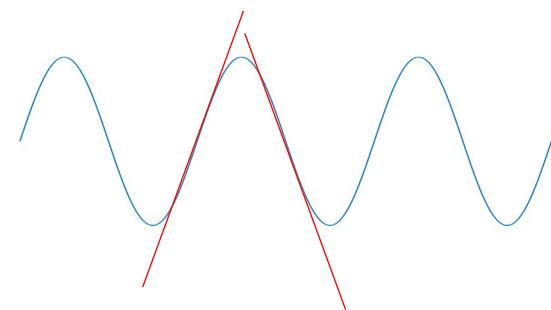
Maritime ISAR

Airborne ISAR of maritime vessels makes use of two principal motions

1. Aspect changes due to radar motion, and
2. Aspect changes due to vessel angular motions, typically sinusoidal in nature.



Even sinusoidal motion has periods of fairly linear motion.



Maritime ISAR

Relative motion will determine the target projection in a range-Doppler map.

Target
pitching
motion



Radar
transverse
flight

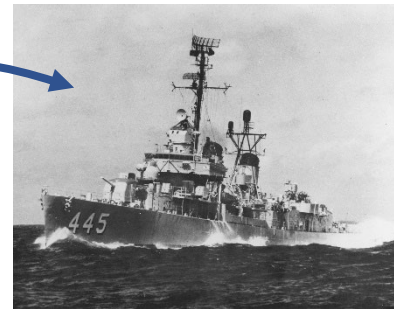
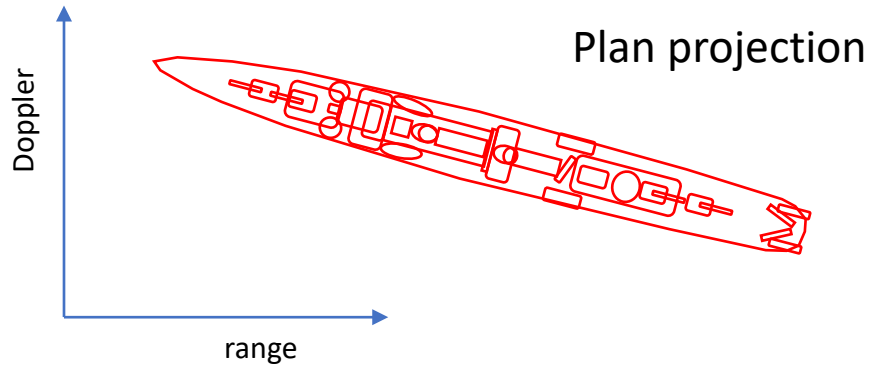
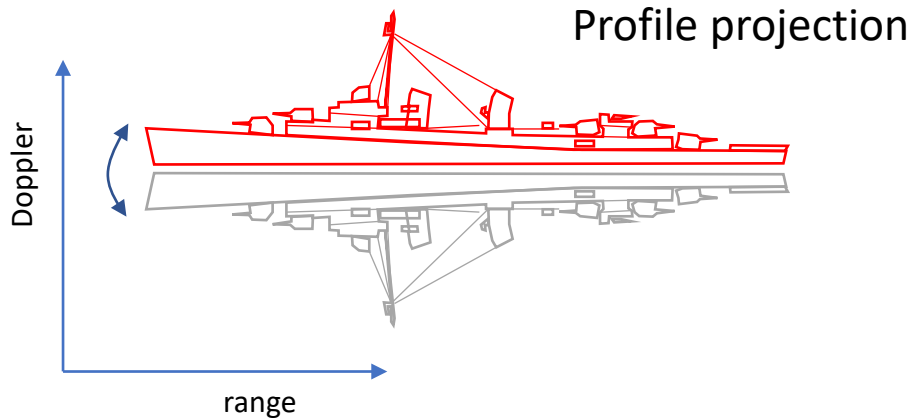
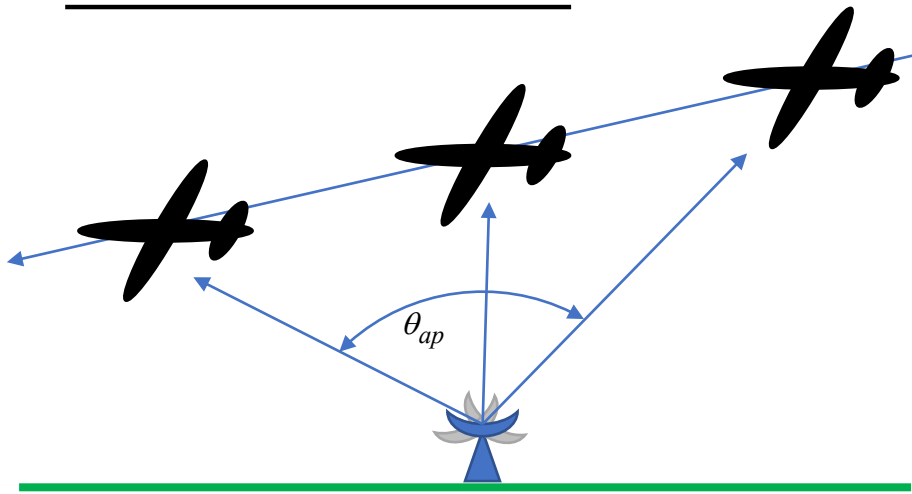


Image from Mike Moseley



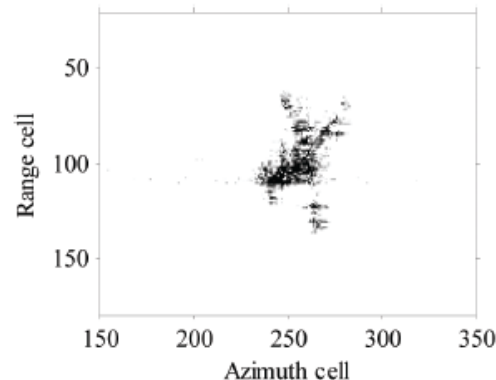
ISAR of Aircraft



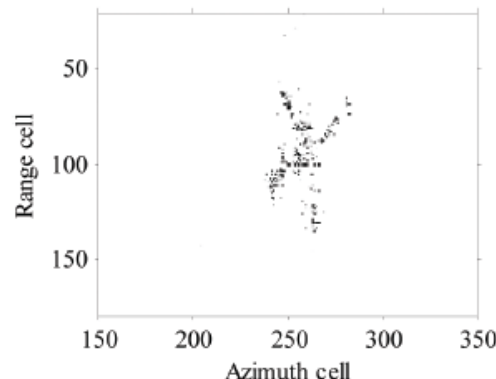
Imaging aircraft from the ground relies on the aspect change due to the aircraft's cross-range motion.



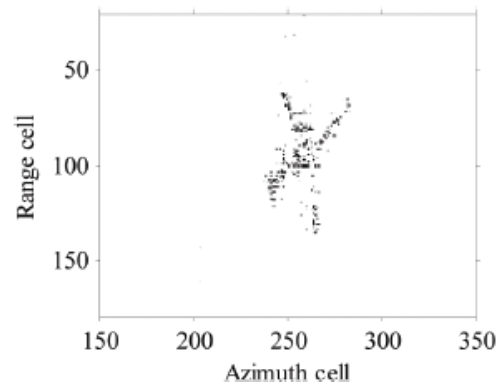
Photo: Maarten Visser: FlickrCC



ISAR image of Yak-42 via FFT



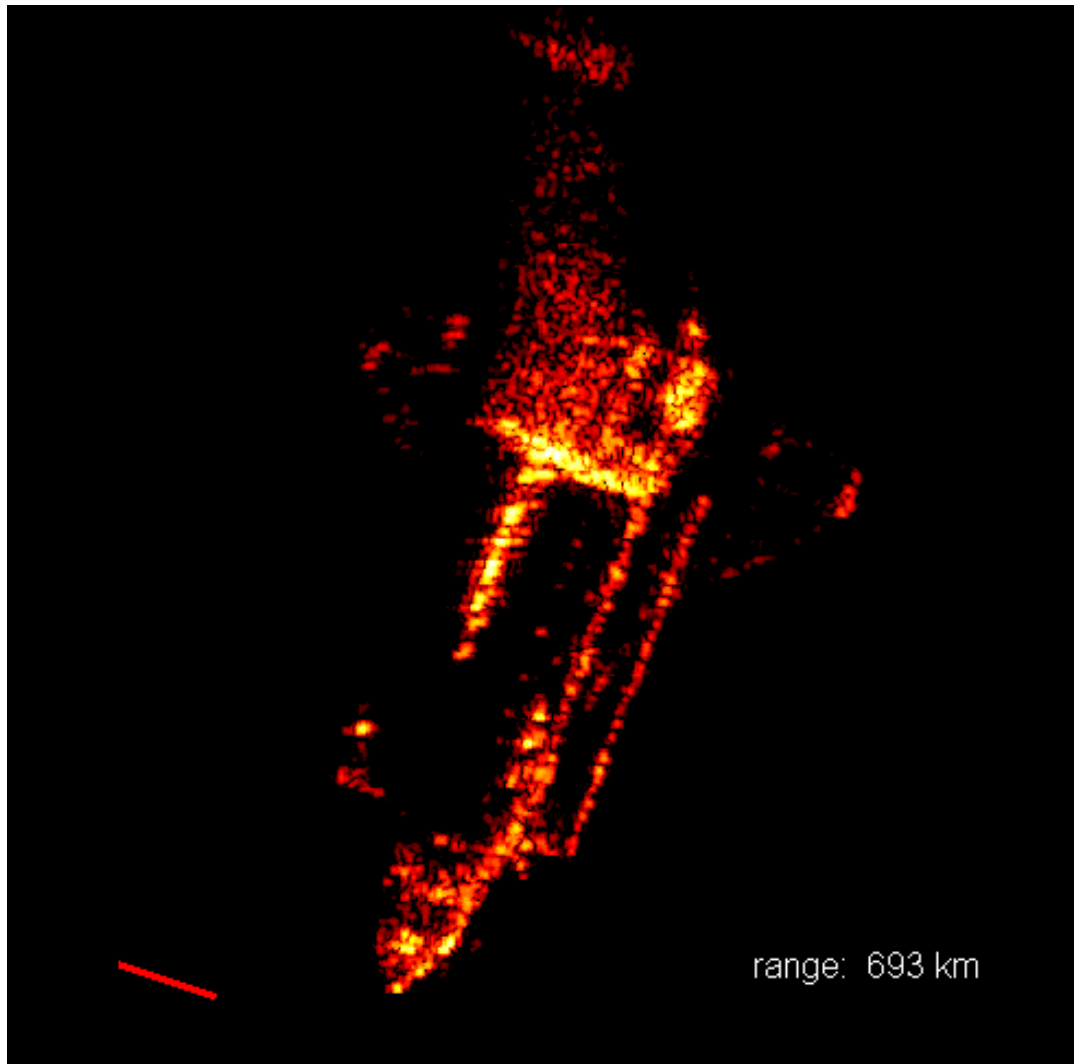
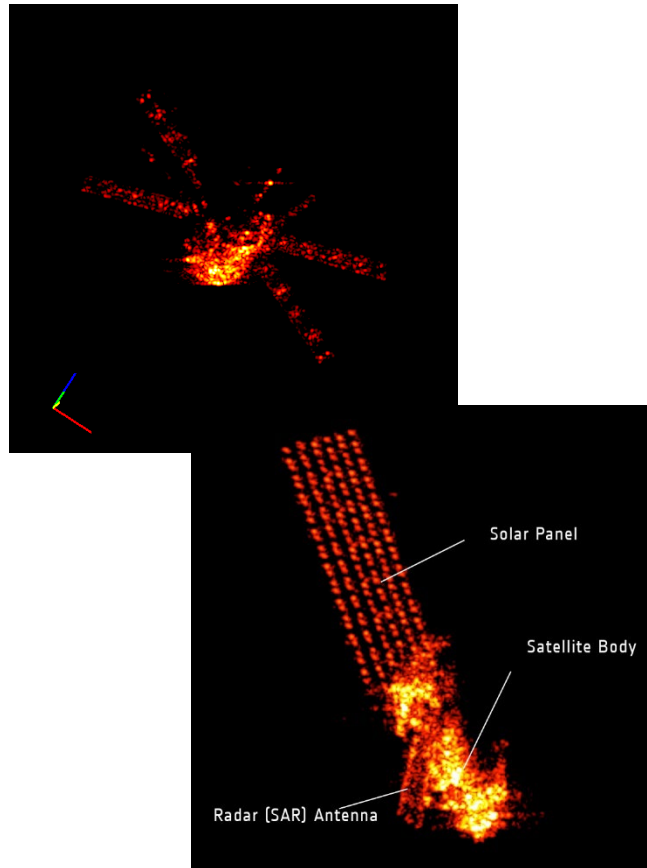
ISAR image of Yak-42 via Root-MUSIC



ISAR image of Yak-42 via SF-Root-MUSIC

ISAR of Orbital Spacecraft

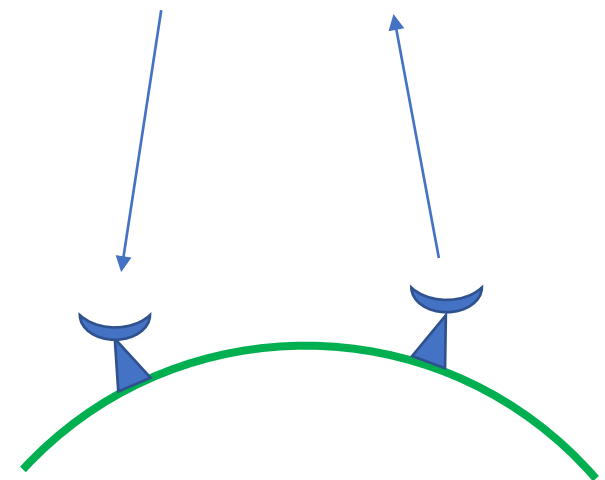
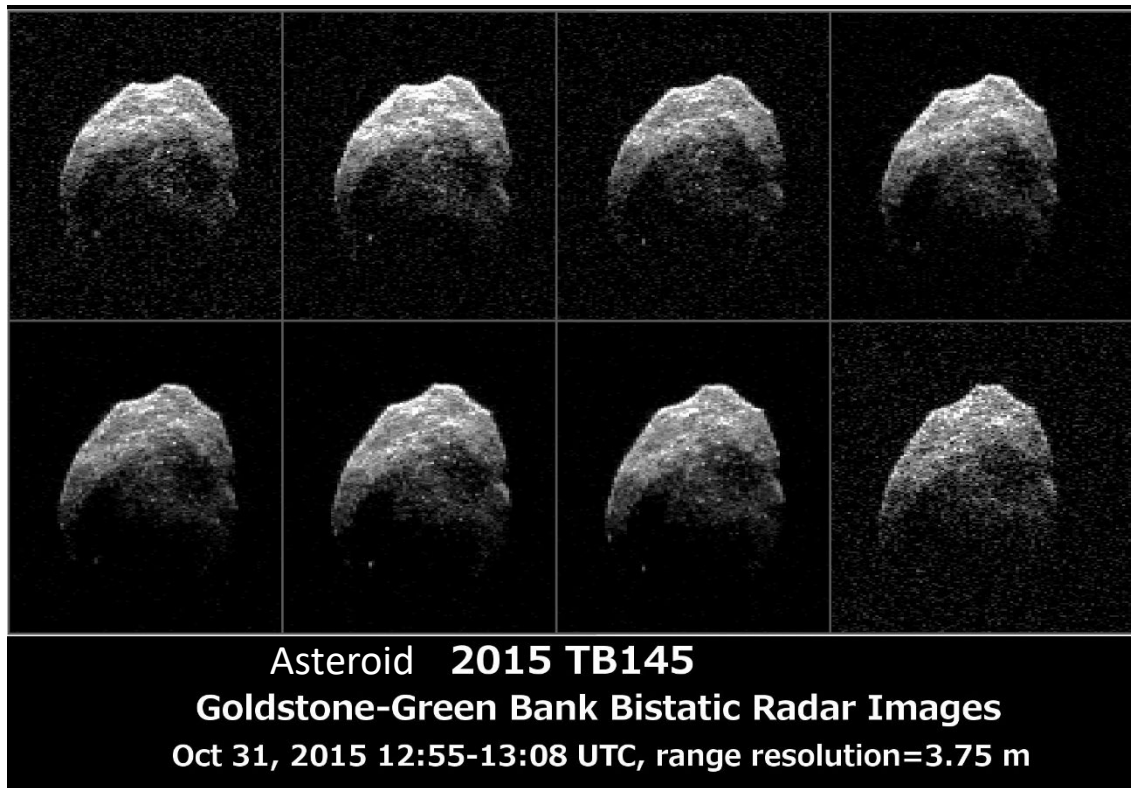
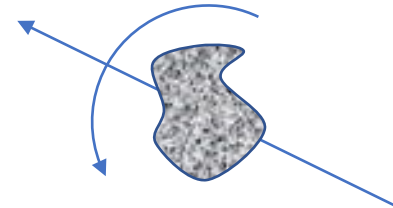
Similar to imaging aircraft, orbital spacecraft can also be imaged from the ground using ISAR.



All images courtesy Fraunhofer Institute

ISAR of Astronomical Objects

Similar to orbital spacecraft, non-earth-orbiting astronomical objects can also be so imaged by ISAR.

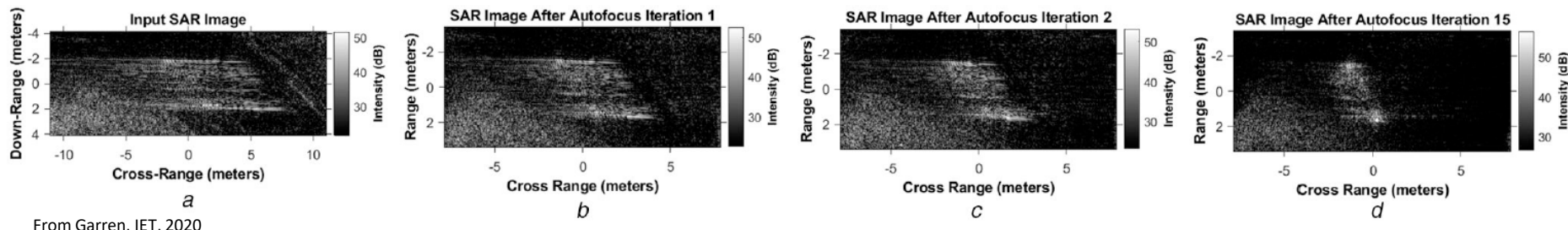


ISAR of Land Vehicles

Imaging moving land vehicles is particularly challenging for two main reasons

1. Vehicles tend to be smaller than, say, maritime vessels, so finer resolutions are required to put the same number of “pixels on target,” and
2. The surrounding clutter is generally brighter and nonhomogeneous, which interferes with focusing operations.

This remains an area of research.



From Garren, IET, 2020

Select References

1. Walter G. Carrara, Ron S. Goodman, Ronald M. Majewski, *Spotlight Synthetic Aperture Radar, Signal Processing Algorithms*, ISBN 0-89006-728-7, Artech House Publishers, 1995.
2. C. V. Jakowatz Jr., D. E. Wahl, P. H. Eichel, D. C. Ghiglia, P. A. Thompson, *Spotlight-Mode Synthetic Aperture Radar: A Signal Processing Approach*, ISBN 0-7923-9677-4, Kluwer Academic Publishers, 1996.
3. John C. Curlander, Robert N. McDonough, *Synthetic Aperture Radar, Systems & Signal Processing*, ISBN 0-471-85770-X, John Wiley & Sons, 1991.
4. Armin W. Doerry, *Performance Limits for Synthetic Aperture Radar – second edition*, Sandia National Laboratories Report SAND2006-0821, Unlimited Release, February 2006.
5. Armin W. Doerry, *Basics of Polar-Format Algorithm for Processing Synthetic Aperture Radar Images*, Sandia National Laboratories Report SAND2012-3369, Unlimited Release, May 2012.
6. Armin W. Doerry, Edward E. Bishop, John A. Miller, *Basics of Backprojection Algorithm for Processing Synthetic Aperture Radar Images*, Sandia National Laboratories Report SAND2016-1682, Unlimited Release, February 2016.
7. Victor C. Chen, Marco Martorella, *Inverse Synthetic Aperture Radar Imaging: Principles, Algorithms and Applications*, ISBN-13 : 978-1613530139, Scitech Publishing, 2014.
8. Armin W. Doerry, *Performance Limits for Maritime Inverse Synthetic Aperture Radar (ISAR)*, Sandia National Laboratories Report SAND2013-9915, Unlimited Release, November 2013.



Low-cost Radar Demonstrations

Radar Summer School

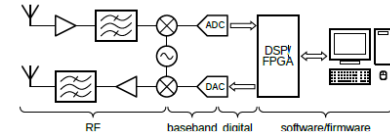
2022 IEEE Radar Conference

John P. Stralka, Ph.D., P.E.

Frank C. Robey, D.Sc.

Motivation

- ▶ When learning radar it is important to work with an actual radar and collected data as soon as possible
 - Helps solidify concepts learned in text books and papers
 - Computer simulations are valuable, but cannot completely replace real data
 - Best to validate new radar processing algorithms with real hardware
- ▶ One must play with technology to learn it
 - Learn by doing
 - Test things until they break
 - Build intuition
- ▶ Unfortunately, most radar systems are expensive and have limited access
- ▶ Fortunately, there are now options to obtain relatively low-cost components to create a radar!



SDR Hardware Platform Survey

Device	Price	Freq Range (MHz)	Duplex	ADC/DAC	Comment
RTL-SDR	\$15-40	24 to 1750	R	8b 2.4 MS/s	
Kerberos SDR	\$199	24 to 1766	4R	8b 2.4 MS/s	Synchronized
Kraken SDR	\$299	24 to 1766	5R	8b 2.4 MS/s	New model
ADALM-Pluto	\$200	325 to 3800	R T	12b 61.44 MS/s	
Lime SDR	\$323	0.1-3800	2R 2T	12b 61.44 MS/s	
HackRF One	\$340	1-6000	R T	8+8 20 MS/s	
Red Pitaya	\$241	0-62.5	2R 2T	14b 125 MS/s	Active user groups, models
KiwiSDR	\$199	0.01-30	R	14b 66.67 MS/s	Limited stock
BladeRF 2 micro	\$520	70-6000	2R 2T	12b 61.44 MS/s	
Ettus B200	\$1100	70-6000	R T	12b 61.44 MS/s	Price increase ~50%
SDRPlay Duo	\$299	0.001-2000	2R	14b 6.048 MS/s	Limited availability

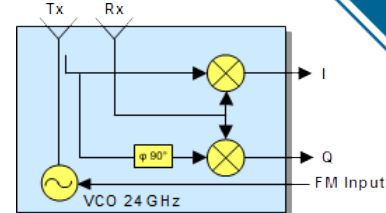
Radar Kit Survey

Device	Price	Freq Range (GHz)	Duplex (TxR)	Bandwidth	Comment
TI-AWR1642Boost Many models	\$300 + \$600?	76-81 GHz	2x4	4 GHz	Board for raw data limited availability
ADALM-Pluto	\$200	0.3 - 3.8	1x1	12b 61.44 MS/s	
Lime SDR	\$323	0.001-3.8	4x6	12b 61.44 MS/s	2x2 MIMO, kit
Ettus B200	\$1100	0.07-6	1x1	12b 61.44 MS/S	
uRAD	€199	24	1x1		Raspberry Pi shield
ADI TinyRad 24G	\$2070	24	2x4	250	
Luswave Ancortek SDR-KIT	\$2 to 5k	S, C, X, K, W	1-2x2-4	0.1-4 GHz	Very nice turn-key kits
Walabot Multiple models	\$75, 100, 160, 600	S, C, X	3, 15, 18	3.3-10 GHz, 6.3-8 GHz	Ultrawideband

Radar Modules Survey

K-LC2
RF Module

K-LC2 Figure from:
<https://www.rfbeam.ch/>



Device	Price	Freq (GHz)	Bandwidth (MHz)	Comment
RFBeam K-Lc1a	\$19	24	140	LFM ranging
RFBeam K-LC2	\$24	24	140	I/Q + ranging
MACS-007802-xx or Sage SSM-24307-xx	\$50-175	24	~100	I/Q, Vs modulate. Sometimes on ebay for <\$10
CDM324/MW2401TR11	\$3-10	24	CW	eBay
HFS DC03	\$4	5.8	CW	eBay
Rcwl-0516	\$3	2.4	CW	Short range, poor stability
Gunnplexor (several)	\$10	10.5	50	At ham flea markets
HB100	\$8	10.5	CW/50	Supply voltage modulate
Seeed BGT24LTR11	\$66	24	250	Synthesized - out of stock

Examples of Low-cost Radar Systems You can Build and/or Operate

- ▶ Audio “radar”
 - Pulse Doppler sonar using a PC speaker, microphone, and engineering software
 - Ultrasonic radar emulator
- ▶ RTL-SDR-based passive radar
 - DVB-T receiver USB dongles
 - Kerberos SDR 4-channel receiver
- ▶ Low-cost radar modules
- ▶ Cantenna radar
 - 2.4 GHz FM-CW radar with metallic coffee can antennas
- ▶ Commercial radars – short range, low power software defined FM-CW radars
 - Anterl uRAD 24 GHz radar shields for Raspberry Pi or Arduino
 - Analog Devices Demorad 24 GHz radar sensor evaluation platform
 - Texas Instruments mmWave automotive radar kits
- ▶ Ettus Research USRP with gr-radar: GNU Radio Radar Toolbox
 - Software-defined radio and free & open-source software (FOSS) toolkit
- ▶ Low-cost scientific investigations using passive bistatic radar

Realistic Expectations

- ▶ Keep in mind that many of these systems are:
 - Low power ⇒ short range
 - Low cost ⇒ limited sensitivity and stability
 - Course timing accuracy ⇒ most are FM-CW as opposed to pulsed radars
 - Small ⇒ electrically-small antennas result in limit spatial selectivity
- ▶ With that said, they still have a great deal of value for learning and practicing:
 - System design and analysis
 - Antenna fabrication and test
 - Microwave and electronic circuit analysis and fabrication
 - Signal processing
 - System test planning
 - Data collection and analysis
 - Phenomenology and environmental sensing
- ▶ Additionally, many commercial radar applications, such as automotive, have the same power, size, and cost constraints as educational systems

Audio “Radar”

Benefits of Slowing it Down

► Challenges of demonstrating pulsed radar at RF:

- Components are somewhat expensive
- Speed of propagation is fast (speed of light $\approx 3 \times 10^8$ m/s)
 - More distance needed for testing: $R = c \cdot \Delta t / 2$
- Synchronization can be less than desired with low-cost hardware

► Solution: Slow down the speed of propagation by using audio carrier frequencies!

- Speed of propagation of sound ≈ 340 m/s at sea level and 1 atmosphere
- Mechanical (i.e., sound) waves are similar to electromagnetic waves
 - Maintains wave propagation characteristics
 - Except no polarization
- Less range needed for testing
 - Sound attenuates faster than RF over distance
- Low-cost PC audio hardware: microphone, speaker, sound card

References:

W. du Plessis, "Demonstrating Radar and EW - Without Breaking the Bank," Association of Old Crows webinar, Sept. 21, 2017.

W. P. du Plessis, "Audio sonar for gaining hands-on experience of radar principles," in IEEE Radar Conference, Florence, Italy, Sept. 21-25, 2020.

Pulse Doppler Audio “Radar” Components

- ▶ “Exciter” and “Receive Processor”
 - PC (Windows, Mac, or Linux)
 - Sound card with microphone input and speaker output
 - Example: Sabrent AU-MMSA USB Audio Stereo Sound Adapter
 - Engineering software: MATLAB®, Octave, Python, etc.
 - Audio interface software
 - MATLAB®/Octave – playrec (<http://www.playrec.co.uk/>)
 - Python – python-sound device
- ▶ “Transmit Antenna”
 - Standard desktop PC speaker
- ▶ “Receive Antenna”
 - Microphone (a good one)
 - Recommendation: Genius MIC-01A
- ▶ “Moving Target Simulator (MTS)”
 - Other speaker from a stereo pair



Image by J. P. Stralka

Reference:

<https://dspillustrations.com/pages/posts/misc/using-your-soundcard-for-hands-on-digital-communication.html>

Audio “Radar” Example

- ▶ Carrier frequency = 14 kHz
 - Speed of propagation = 340 m/s
 - Sample rate = 44.1 kHz
- ▶ Pulse duration = 5.8 ms
 - Linear FM intrapulse modulation
 - Pulse bandwidth = 865 Hz
 - Time-bandwidth product = 5
 - Range resolution = 20 cm
- ▶ Pulse repetition interval = 14.58 ms
 - Pulse repetition frequency = 68.6 Hz
 - Transmit duty = 39.8%
 - Ambiguous range = 2.5 m, Ambiguous Doppler = 0.83 m/s
- ▶ Pulses per burst = 74
 - Pulse coherently integrated = 64
 - Coherent integration time = 0.93 s
 - Doppler resolution = 1.3 cm/s

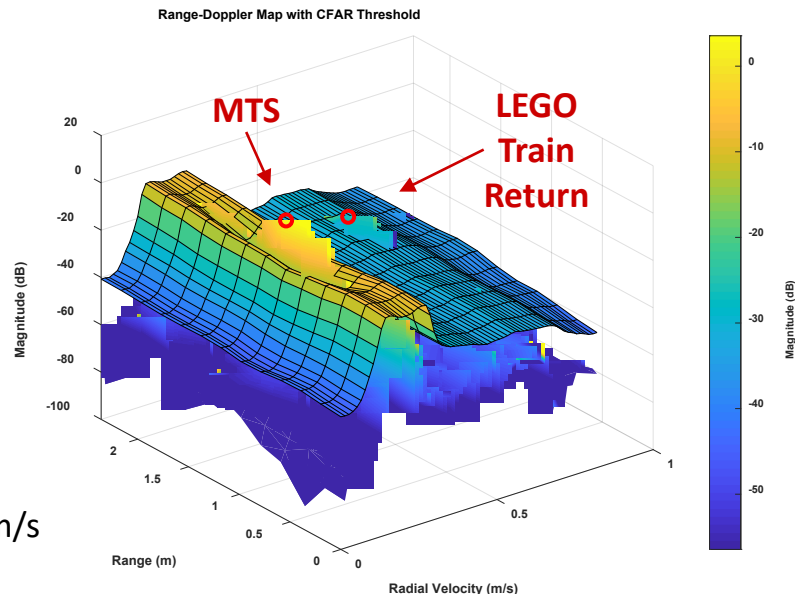
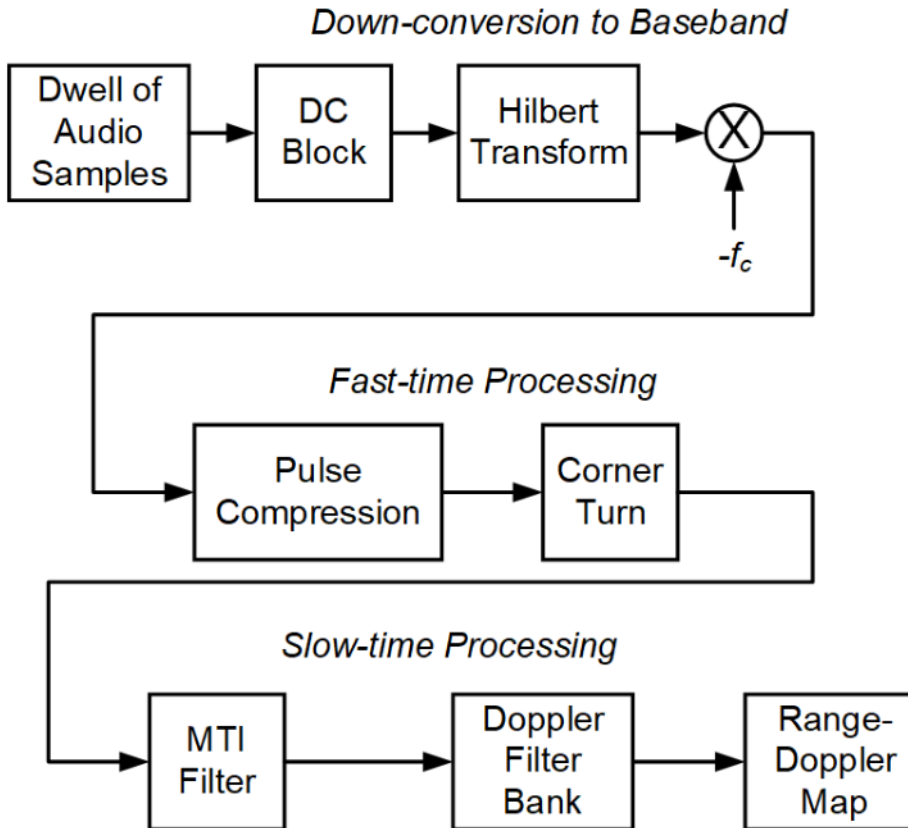


Image by J. P. Stralka

Pulse Doppler Receive Processing

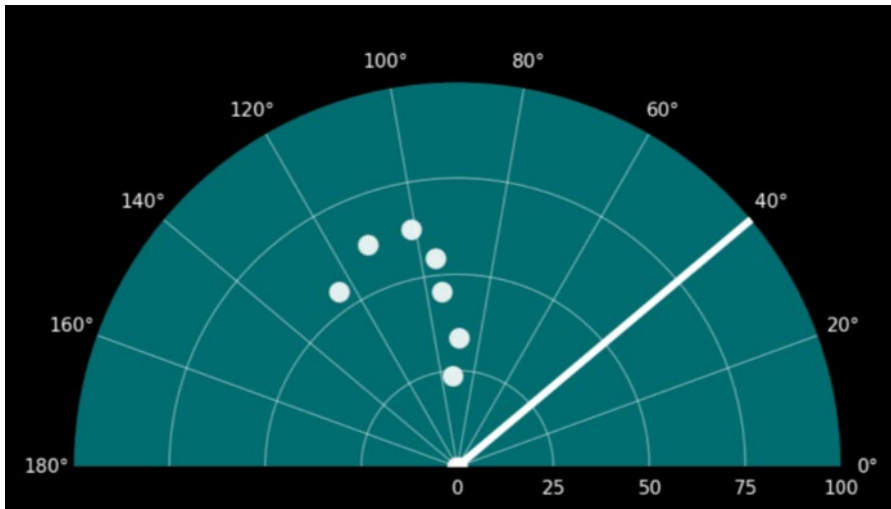


Ultrasonic Radar Emulator

<https://makersportal.com/blog/2020/3/26/arduino-raspberry-pi-radar#python-code>

► Arduino-based project

- Ultrasonic sensor (HC-SR04) used in place of an RF transceiver
 - Provides ranging data
- Servo motor angular motion recorded for azimuth measurement
- Radar plan position indicator (PPI) implemented in Python



Maker Portal HC-SR04 + MG90S Radar Kit (\$15 USD)
<https://makersportal.com/shop/hc-sr04-mg90s-radar-kit>

RTL-SDR-based Passive Radar

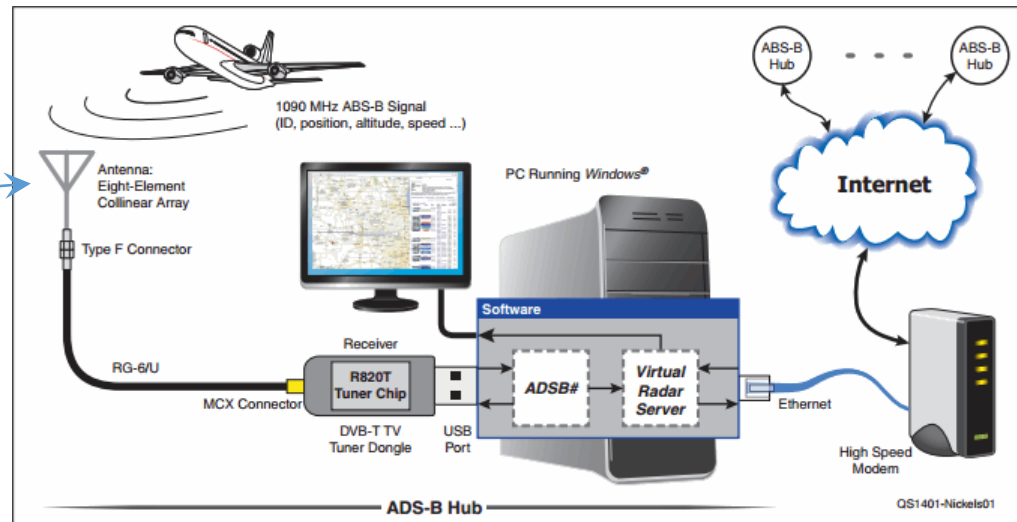
ADS-B Receiver “Virtual Radar”

- ▶ Automatic Dependent Surveillance - Broadcast (ADS-B) is a surveillance technology where aircraft use GNSS to determine its position and then periodically broadcasts it
- ▶ Air traffic control ground stations receive the broadcasts and track the reported positions
- ▶ Use DVB-T USB dongle to receive broadcasts, then decode and track in software

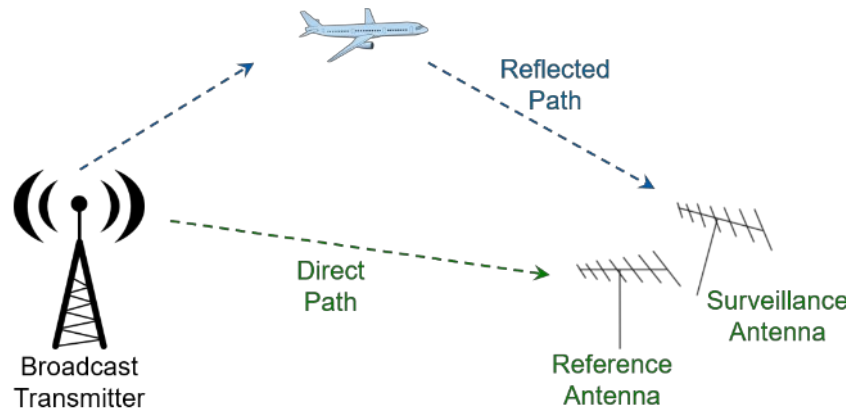
Image by J. P. Stralka



L-band
Coaxial
Collinear
Antenna



Passive Radar



- ▶ **Low-cost passive radar system**
 - Two RTL-SDR dongles
 - Two directional antennas

- ▶ **Challenges**
 - Phase cohere the clocks two dongles
 - Align data streams from both dongles

References:

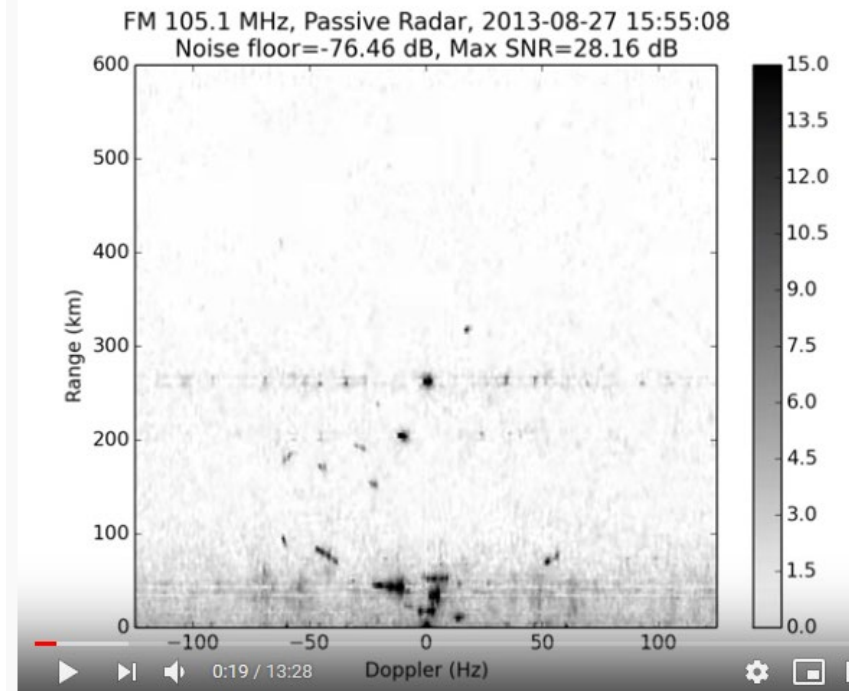
- <http://www.desktopsdr.com/>
- <http://kaira.sgo.fi/2013/09/passive-radar-with-16-dual-coherent.html>
- [W. Feng, G. Cherniak, J.-M Friedt, and M. Sato, "\(Yet another\) DVB-T based passive radar demonstration using Software Defined Radio on low-cost DVB-T receivers," in FOSDEM 18, Brussels, Belgium , February 3-4, 2018.](#)

Passive Aircraft Tracks

- ▶ Juha Vierinen provides one of the lowest cost/highest quality examples at hackaday
- ▶ Kerberos/Kraken 4/5-channel SDR alleviates much of the hardware difficulty



Juha Vierinen's cross-wiring Kraken SDR



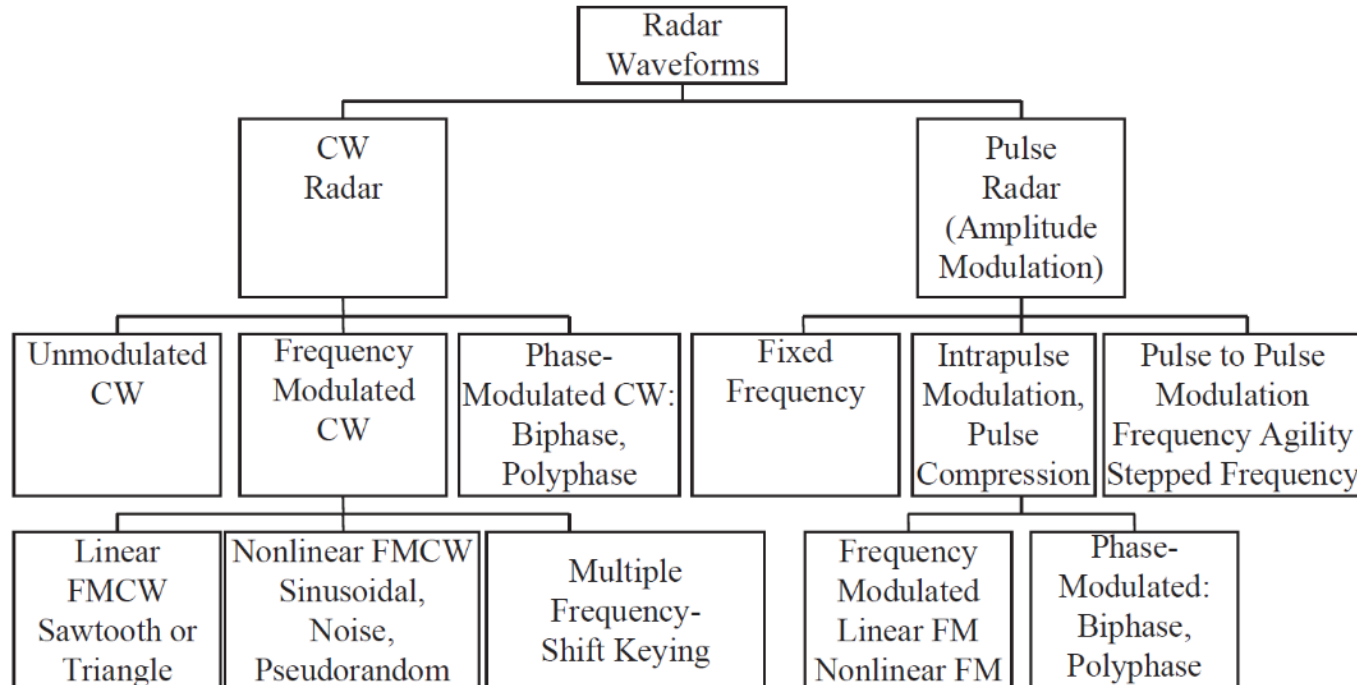
<https://www.youtube.com/watch?v=-k2ZuhAzOac>

References: https://www.gnuradio.org/grcon/grcon18/presentations/software_defined_radar_remote_sensing_and_space_physics/juha_grcon_keynote.pdf

<https://hackaday.com/2015/06/05/building-your-own-sdr-based-passive-radar-on-a-shoestring/>

FM-CW Radar Fundamentals

Radar Waveform Taxonomy

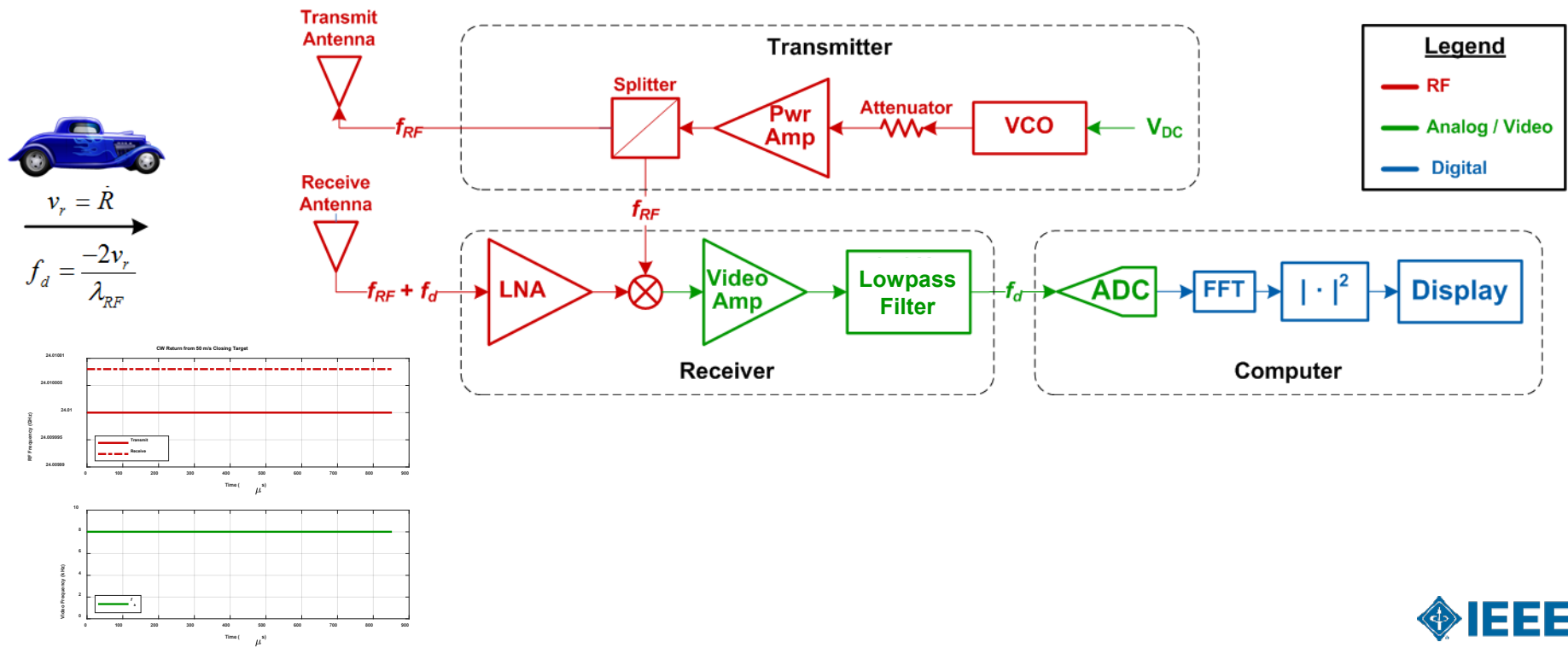


Reference:

C. J. Baker and S. O. Piper, "Continuous wave radar," in *Principles of Modern Radar, Vol. III: Radar Applications*, W. L. Melvin and J. A. Scheer, Eds.. Edison, NJ, SciTech Publishing, 2014, ch. 2, sec. 2.2, p. 23.

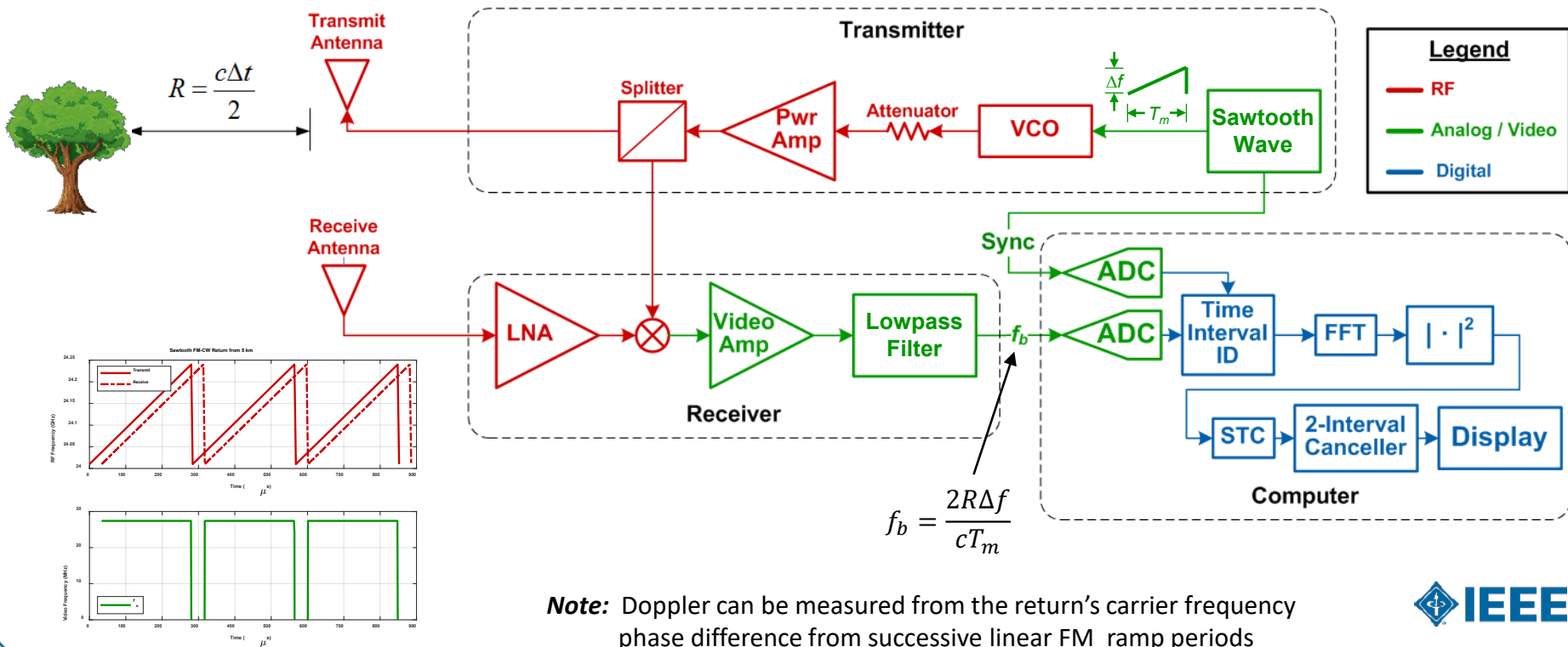
Unmodulated CW Radar

Allows Doppler Measurements



Sawtooth FM-CW Radar

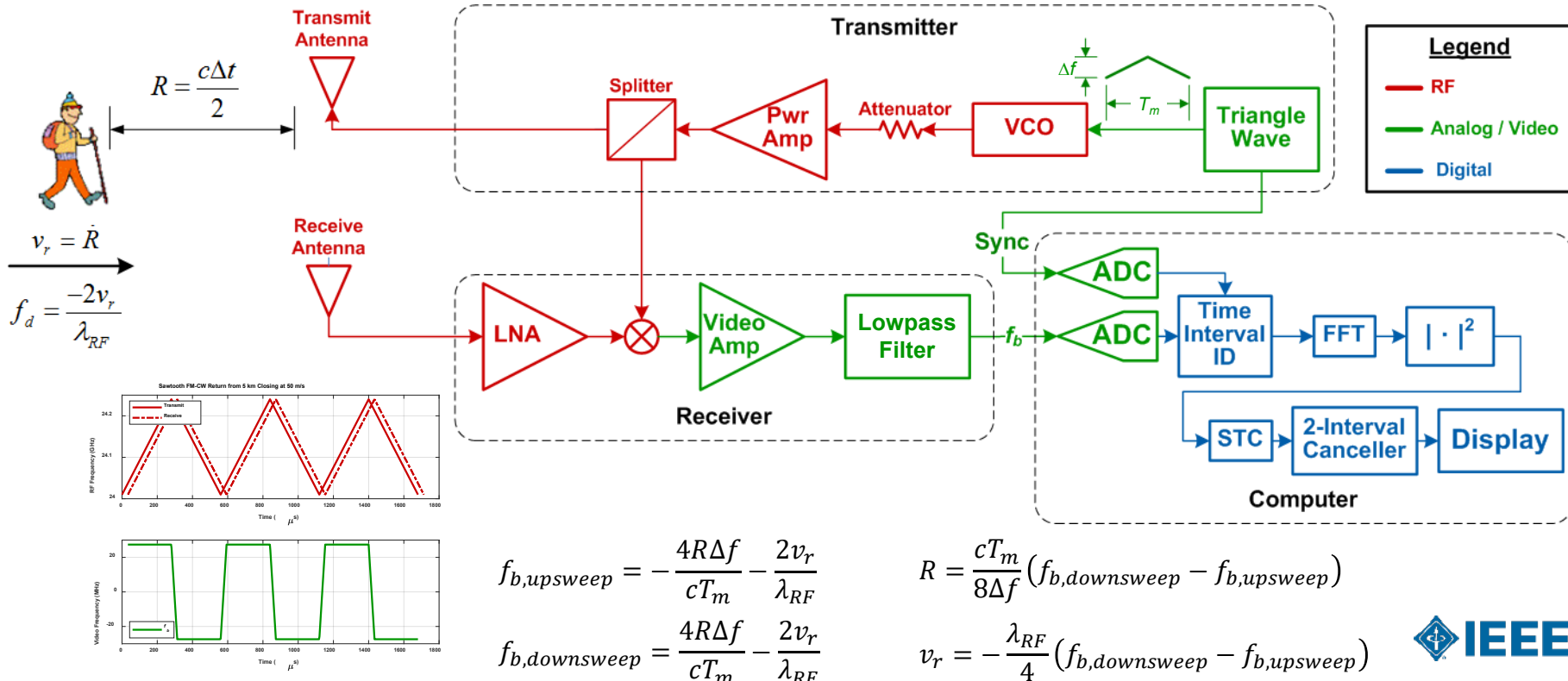
Allows Range Measurements



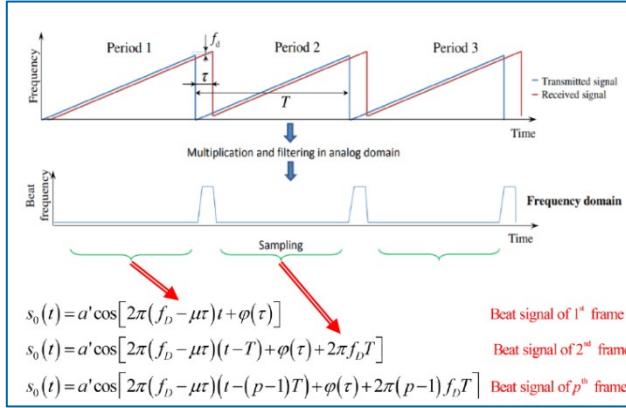
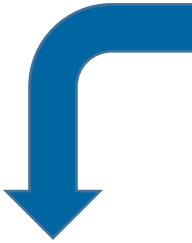
Note: Doppler can be measured from the return's carrier frequency phase difference from successive linear FM ramp periods

Triangle FM-CW Radar

Allows for Range and Doppler Measurements



Coherent Range-Doppler Processing of FM-CW

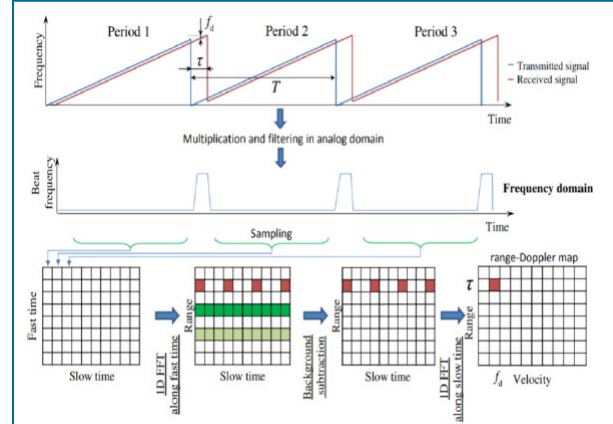
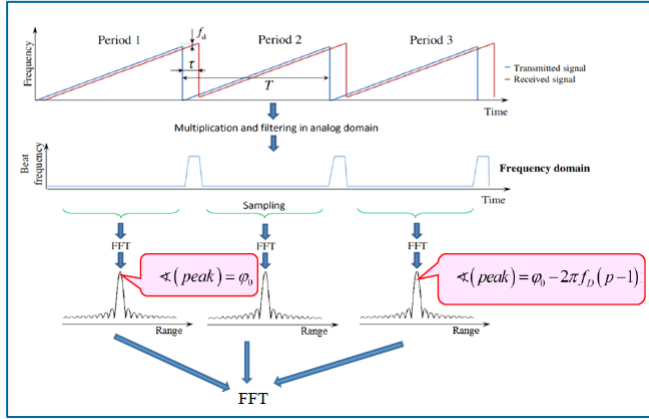


Reference:

N. Levanon, "Continuous wave (CW) radar," in *Radar - Concise Course*. Tel Aviv, Israel: Tel Aviv University, 2021, ch. 15, sec. 15.2, pp. 15.5-15.6, https://www.eng.tau.ac.il/~nadav/levanon_radar_course_vo_2.pdf

Signal Acquisition

Fast-Time (Range) Processing



Slow-Time (Doppler) Processing



Low-cost Radar Modules

Low-cost Radar Modules

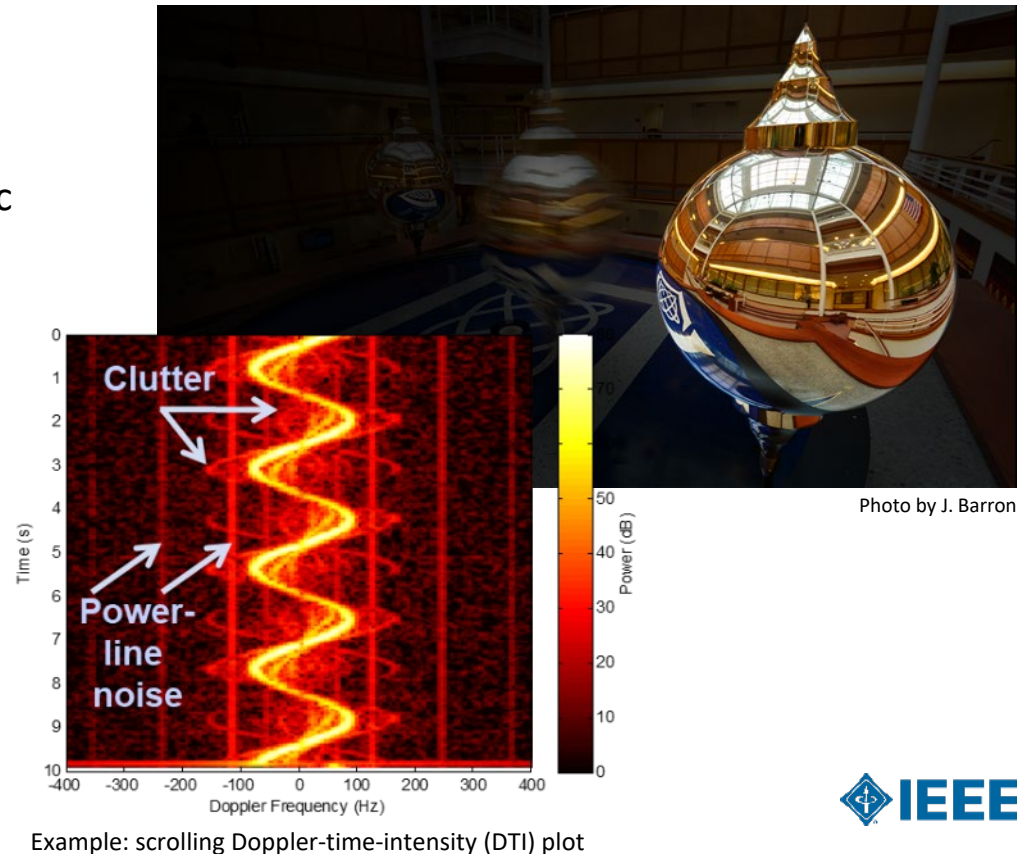
- ▶ Motion sensors can be used as basis of very low cost radar
- ▶ Many of these components found on eBay, Amazon.com, DX at low cost
- ▶ “Stereo” Doppler modules provide relative velocity, not just speed
- ▶ Many provide ranging using linear FM waveforms



Image by F. C. Robey

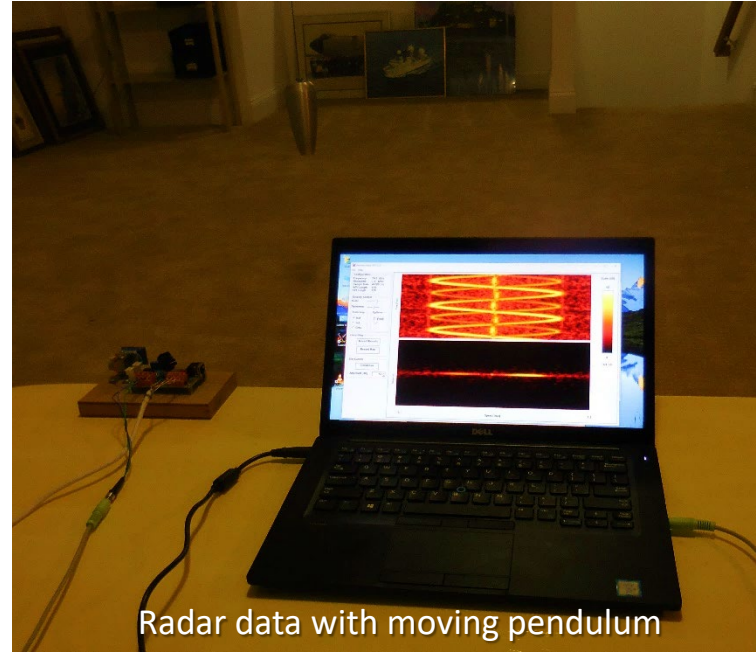
Foucault Pendulum Radar in MIT-LL Atrium

- ▶ Museum quality display
 - Kiosk with explanations
 - Real time display of pendulum harmonic motion
- ▶ Radars based on Sage SSM-24307
- ▶ Real-time software in C with many features of larger radars



Small Radar Example

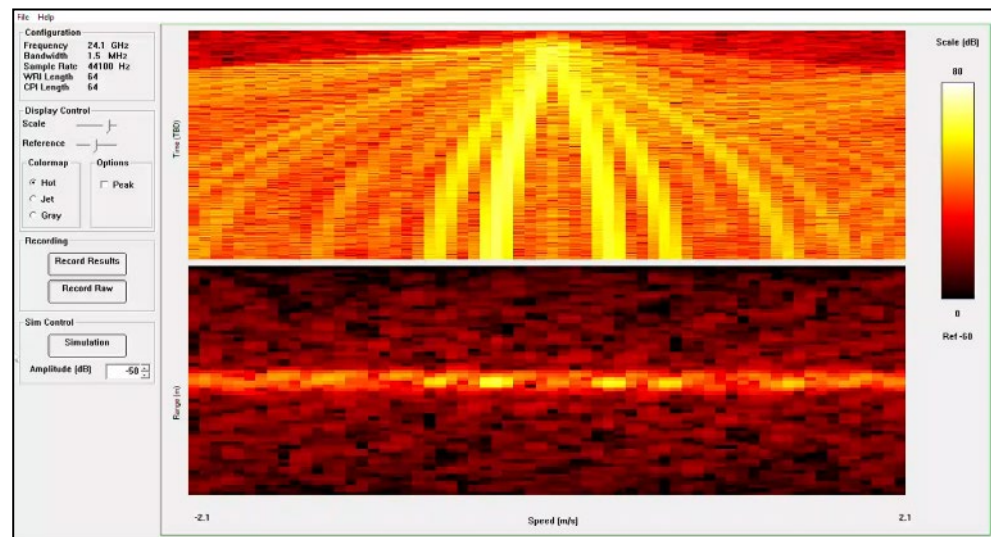
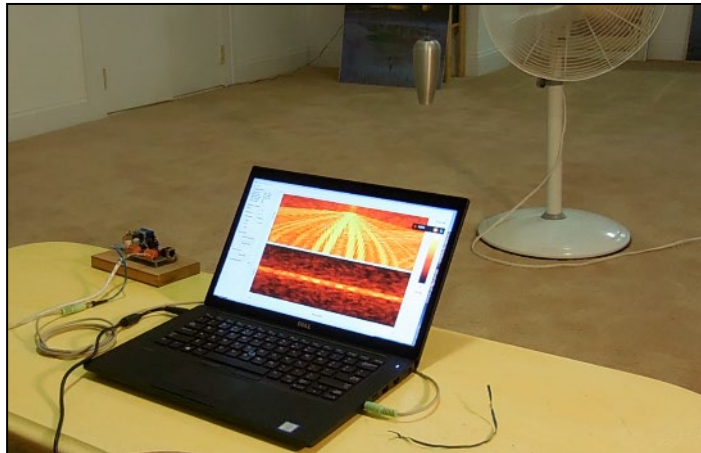
{play pendulum demonstration video}



Videos by F. C. Robey

Small Radar Example

{play fan demonstration video}



Videos by F. C. Robey

Cantenna Radar

Cantenna Radar Project

- ▶ In 2011, MIT began offering a short course to build and test a low-cost radar system
 - Measure range and Doppler
 - Form synthetic aperture radar (SAR) images
- ▶ Simple radar focused on RF aspects
 - Moderate-cost ($\approx \$500$)
 - ISM band (2.4-2.5 GHz)
 - CW and FM-CW modes
 - Independent transmit and receive antennas for isolation
 - Returns sampled by PC sound card or microcontroller
 - Processing can be done in MATLAB[®], Octave, or Python
- ▶ Course materials available on MIT's OpenCourseWare (OCW) web site
- ▶ Based upon a design by Gregory L. Charvat, Ph.D.

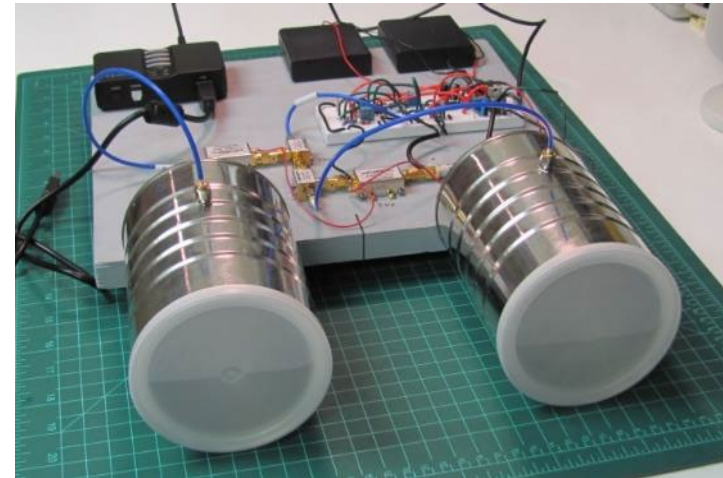


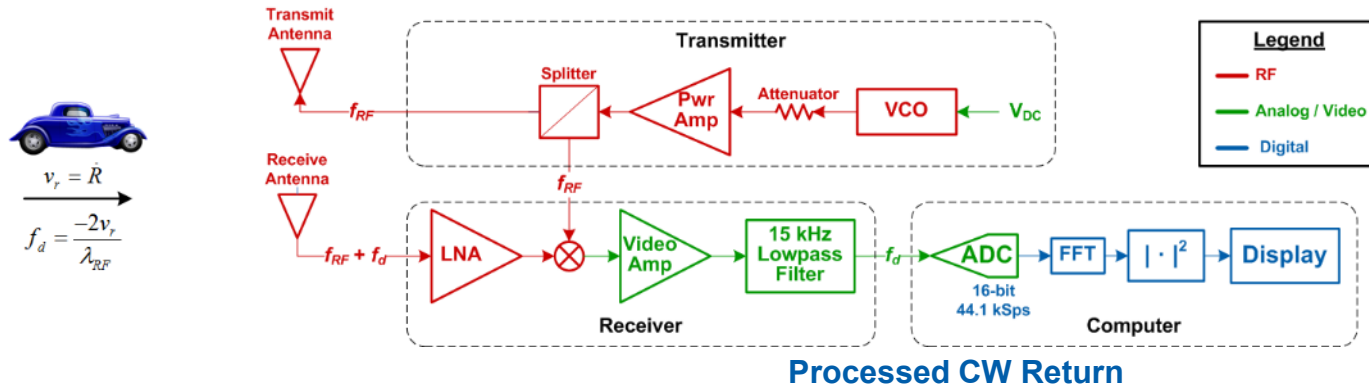
Image by J. P. Stralka

References:

- <http://ocw.mit.edu/resources/res-l1-003-build-a-small-radar-system-capable-of-sensing-range-doppler-and-synthetic-aperture-radar-imaging-january-iap-2011/>
- G. L. Charvat, *Small and Short-Range Radar Systems*. Boca Raton, FL: CRC Press, 2014.
- https://llx.mit.edu/courses/course-v1:MITLL+MITLLx01+Q2_2019/info
- https://llx.mit.edu/courses/course-v1:MITLL+MITLLx06+Summer_2020/about

Cantenna Radar CW Mode

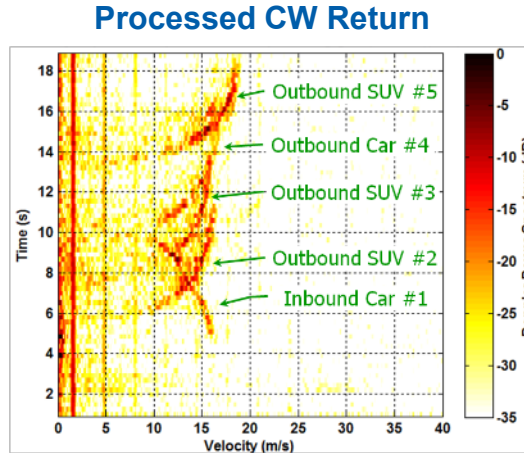
Range Rate (Doppler) Measurement



Truth Data

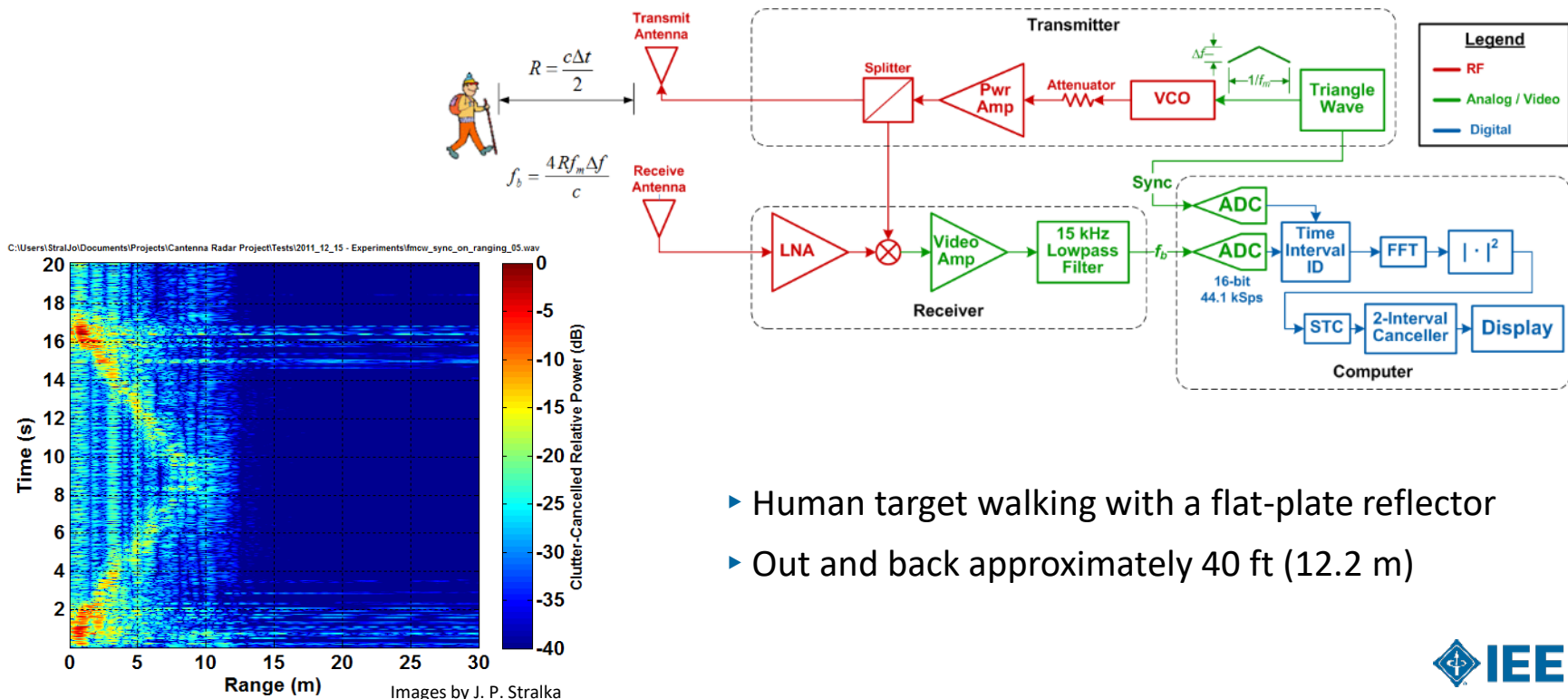


Images by J. P. Stralka



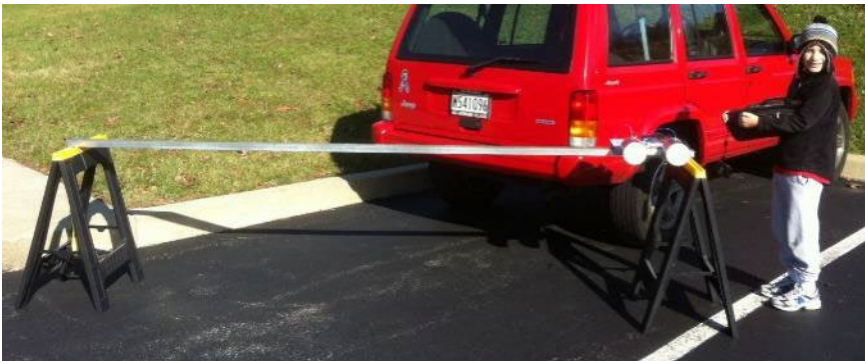
Cantenna Radar FM-CW Mode

Range Measurement

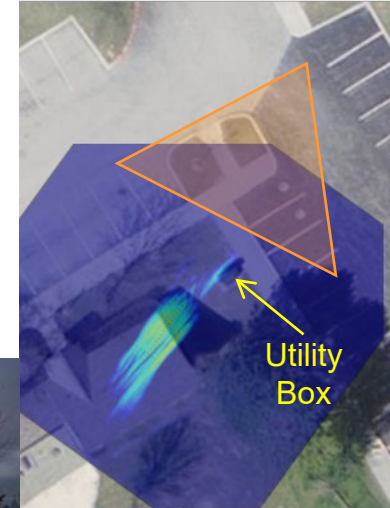


Cantenna Radar SAR Mode

Imaging with FM-CW



- ▶ Range profiles collected every 2 inches over 8 feet
- ▶ Range Migration Algorithm (RMA) used to form image

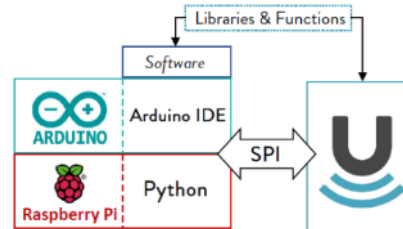
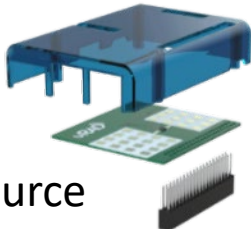


Images by J. P. Stralka

uRAD Software-Defined FM-CW Radar

Anterel's uRAD FM-CW Radar Shield

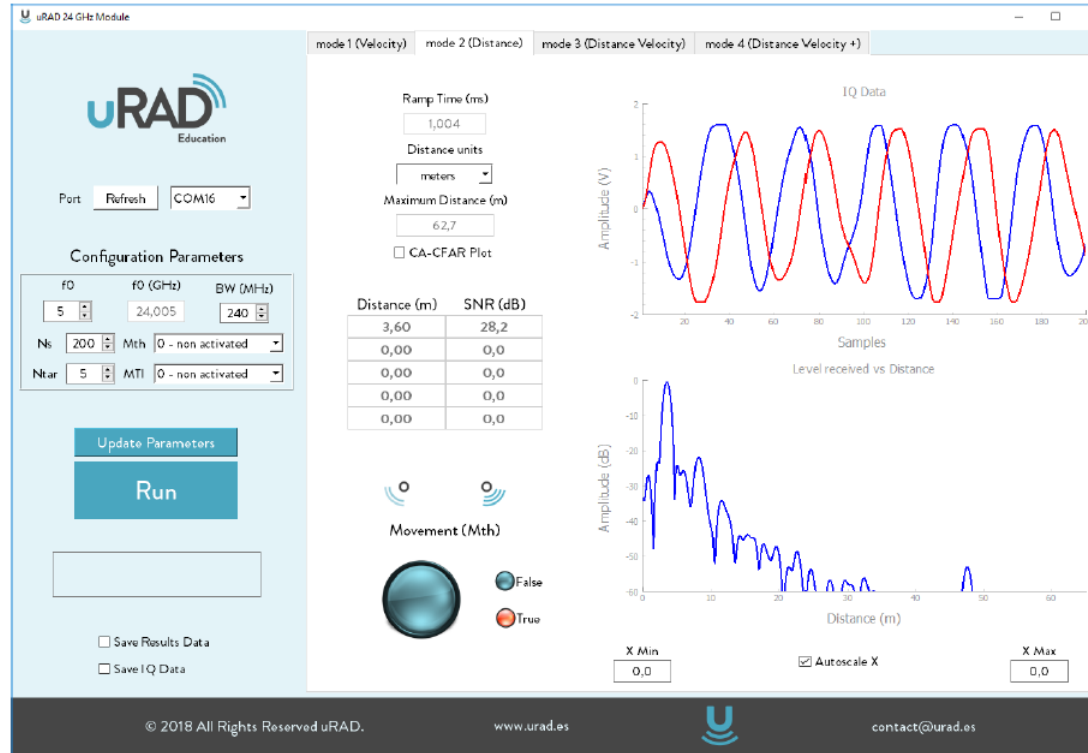
- ▶ Raspberry Pi or Arduino shield
 - Currently €199 ($\cong \$240$)
- ▶ Graphical user interface and Python source code provided
- ▶ K-band (24 GHz)
- ▶ FM-CW waveforms/modes
 - Continuous wave (CW) – Doppler measurements
 - Frequency-modulated continuous wave (FM-CW)
 - Sawtooth – range measurements
 - Triangular – range & Doppler measurements
 - Synthesized signal generator



Images by Anterel

Features	Doppler	Sawtooth	Triangular
Velocity measurement	Yes	No	Yes
Distance measurement	No	Yes	Yes
Accuracy	Best	High	Best
Complexity	Low	Medium	High
Update rate	Best	Very High	High

uRAD GUI



The graphical user interface also allows saving results and IQ signals in real time in order to process the results later.

Image by Anterel



Analog Device's Demorad

ADI's Demorad Radar Evaluation Platform

- ▶ Enables rapid product prototyping ($\approx \$2,400$)
- ▶ Can measure real-time information, such as:
 - Target / object presence
 - Its movement, angular position, velocity, and range
- ▶ 24 GHz ISM band operation
- ▶ FM-CW
- ▶ Range-Doppler processing
- ▶ Digital beamforming
 - 2 transmit antennas
 - 4 receive antennas
 - 2x4 TDMA MIMO



Images by Analog Devices



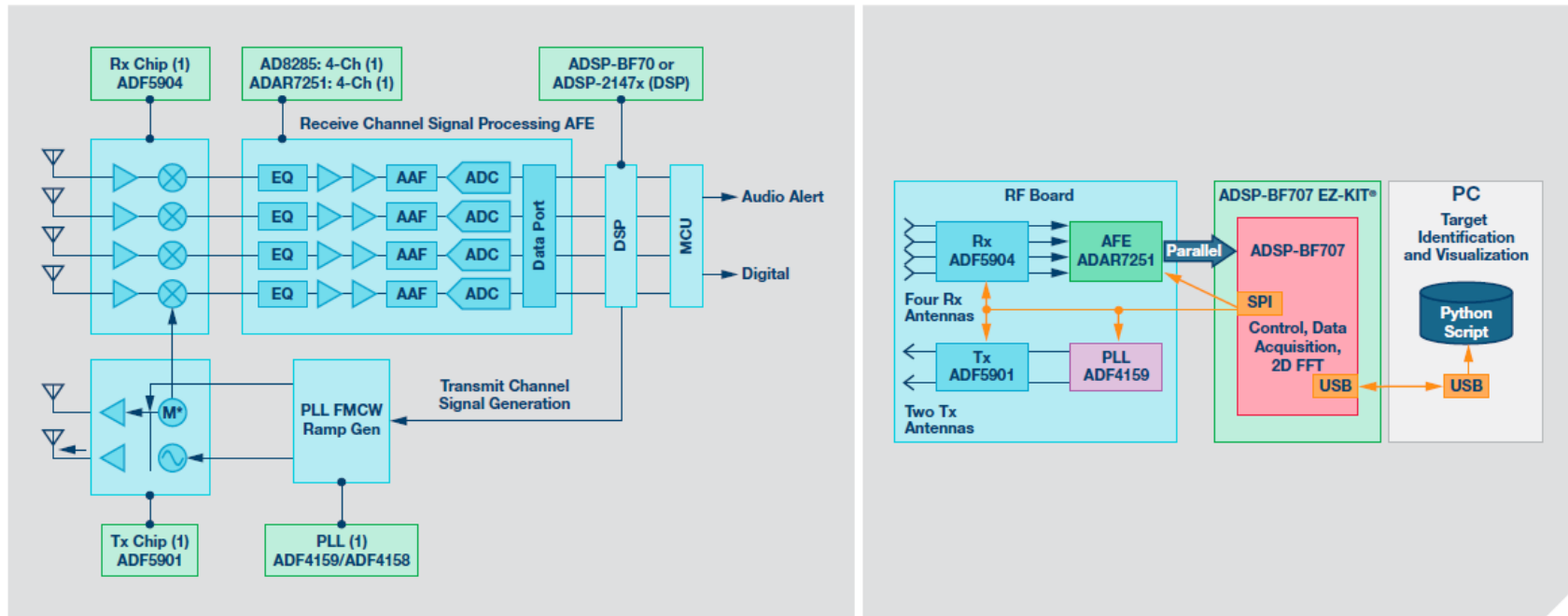
- MathWorks support for integration with MATLAB & Simulink

Reference: <http://www.analog.com/media/en/news-marketing-collateral/product-highlight/Demorad-24-GHz-Radar-Sensor-Platform.pdf>

NOTE: Demorad has been superseded by TinyRad ($=\$2,100$)

<https://www.analog.com/en/design-center/evaluation-hardware-and-software/evaluation-boards-kits/EVAL-TinyRad.html>

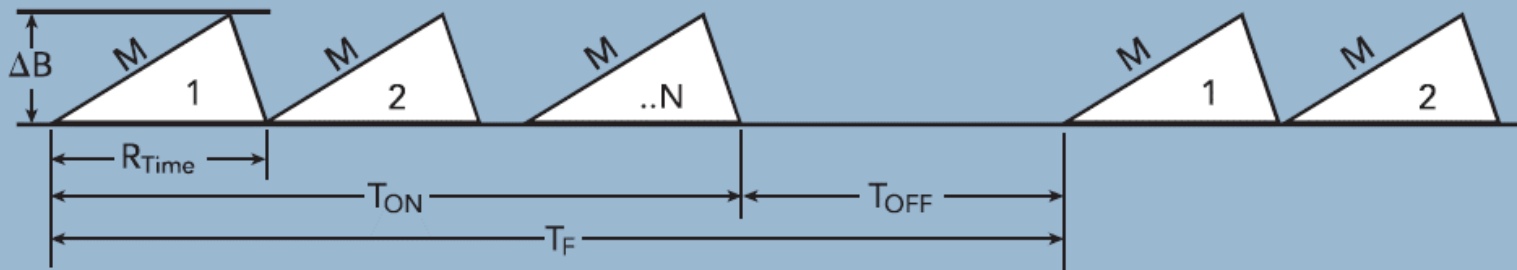
Demorad Architecture



Reference:

A. Kapoor, "Using 24 GHz radar to speed commercial UAV adoption," *Microwave Journal*, vol. 61, no. 1, pp. 44-50, Jan. 2018.

Demorad's FM-CW Waveform



- Range Resolution $\Delta R = \frac{C}{2*\Delta B}$
- Velocity Resolution $\Delta V = \frac{\lambda}{2*N*R_{Time}}$
- Angle Resolution $\Delta \theta = \frac{\lambda}{D}$

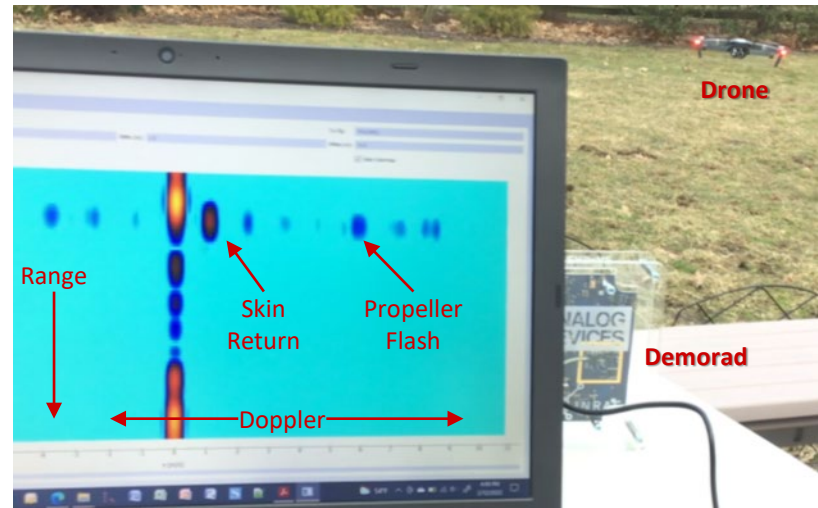
M: FFT Points for Range Determination
N: FFT Points for Velocity Determination
 T_{on} (Dwell Time): Time Transmit Antenna Is Working
 T_{OFF} : Time Transmit Antenna Is Not Transmitting
 R_{Time} : Total (Up + Down) Time For Each Ramp
D: Width Of Antenna Receive Array
 λ : Transmitted Wavelength

Reference:

Demorad's FM-CW Operation

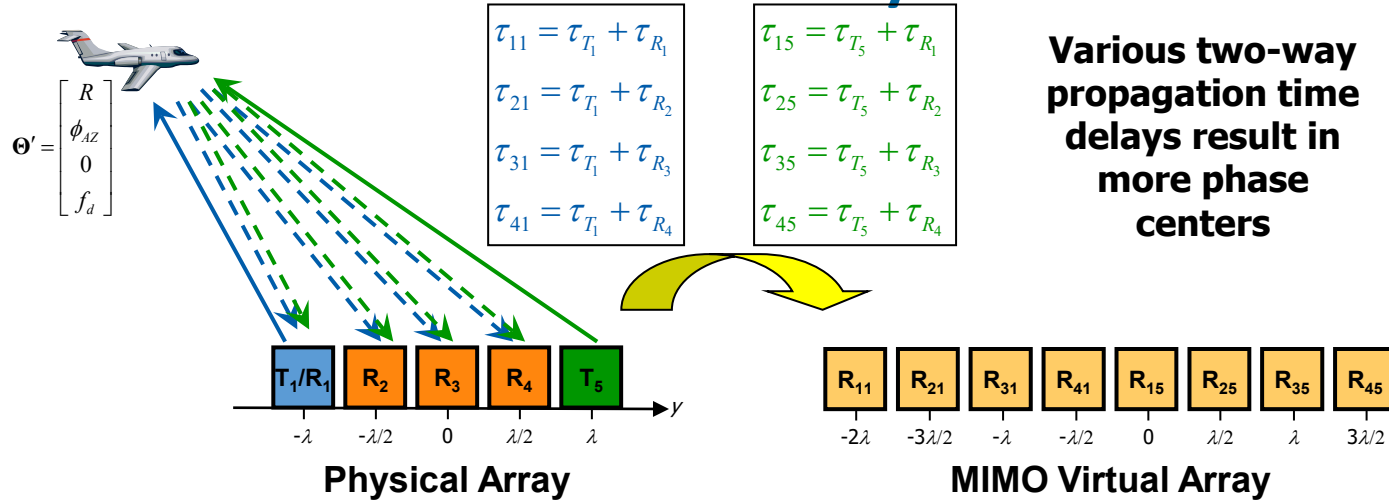
{play drone demonstration video}

Parameter	Symbol	Value	Unit
Chirp Start Frequency	f_{start}	24,010	MHz
Chirp Stop Frequency	f_{stop}	24,240	MHz
Bandwidth	B	230	MHz
Range Resolution	ρ_r	65	cm
Up-chirp Duration	T_{up}	280	μs
Down-chirp Duration	T_{down}	4	μs
Chirp Repitition Interval	T_p	284	μs
Sampling Rate	f_s	1	Msps
Number of Samples per Up-chirp	N	256	samples
Number of Chirps per Frame	N_p	128	pulses



Video by J. P. Stralka

Collocated Antennas – Virtual Array



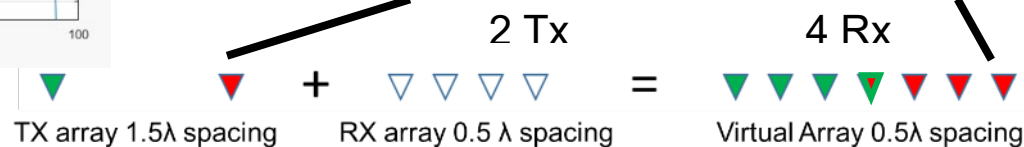
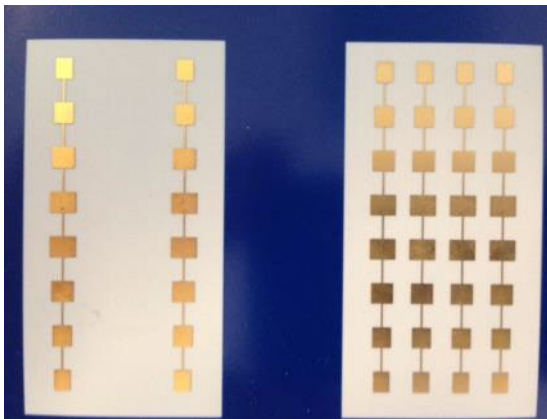
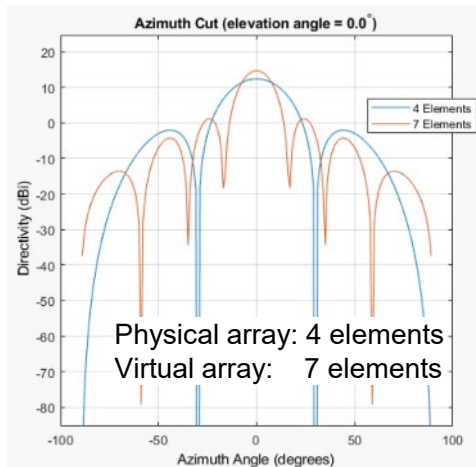
channel matrix $[\mathbf{H}]_{ki} = h_{ki} = e^{-j\frac{2\pi}{\lambda}(\mathbf{x}_{k,R} + \mathbf{x}_{i,T})^T \mathbf{u}(\phi_{AZ}, \theta_{EL})} = e^{-j\frac{2\pi}{\lambda}(y_{k,R} + y_{i,T}) \sin(\phi_{AZ})}$

$$\mathbf{H} = \begin{bmatrix} e^{j4\pi \sin(\phi_{AZ})} & 1 \\ e^{j3\pi \sin(\phi_{AZ})} & e^{-j\pi \sin(\phi_{AZ})} \\ e^{j2\pi \sin(\phi_{AZ})} & e^{-j2\pi \sin(\phi_{AZ})} \\ e^{j1\pi \sin(\phi_{AZ})} & e^{-j3\pi \sin(\phi_{AZ})} \end{bmatrix}$$

- MIMO virtual array is constructed by convolving the transmit element positions and receive sensor positions
- Effective array length increase leads to reduction in angle estimation errors

MIMO Radar Virtual Array to Improve Angular Resolution

Demorad



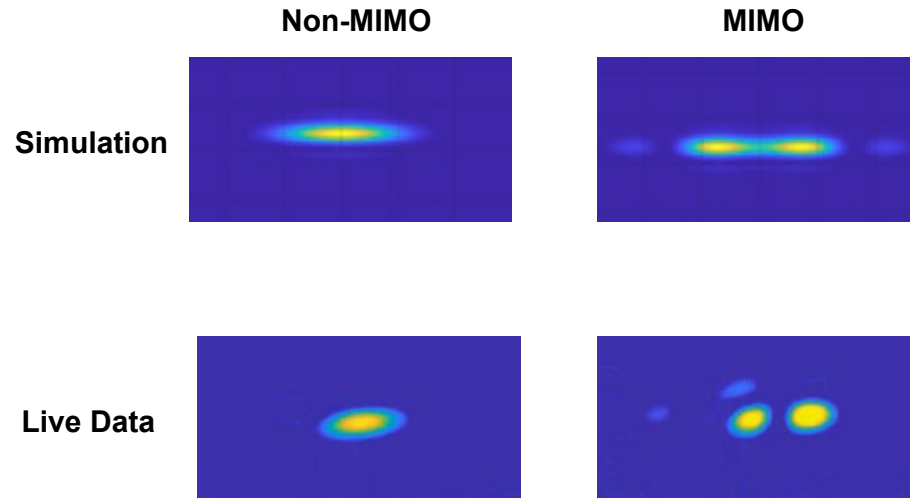
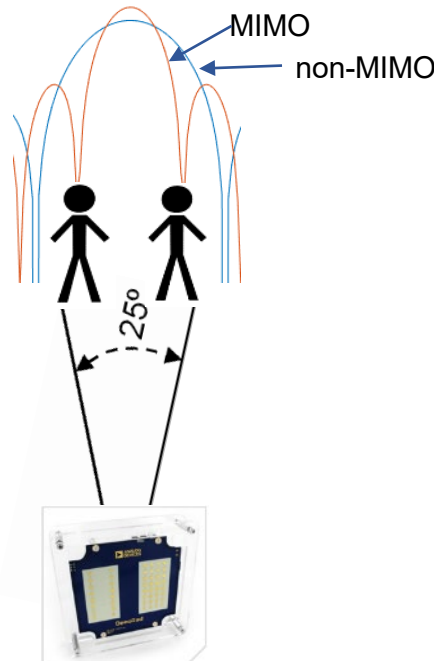
$$\text{Spatial convolution: } [1\ 0\ 0\ 1] * [1\ 1\ 1\ 1] = [1\ 1\ 1\ 2\ 1\ 1\ 1]$$

Virtual Array Elements (1:3) = Rx elements (1:3) for Tx pulse 1

Virtual Array Element (4) = 0.5*(Rx element 4 for Tx pulse 1) + (Rx element 1 for Tx pulse 2)

Virtual Array Elements (5:7) = Rx elements (2:4) for Tx pulse 2

MathWorks' MIMO Radar Demonstration with Demorad

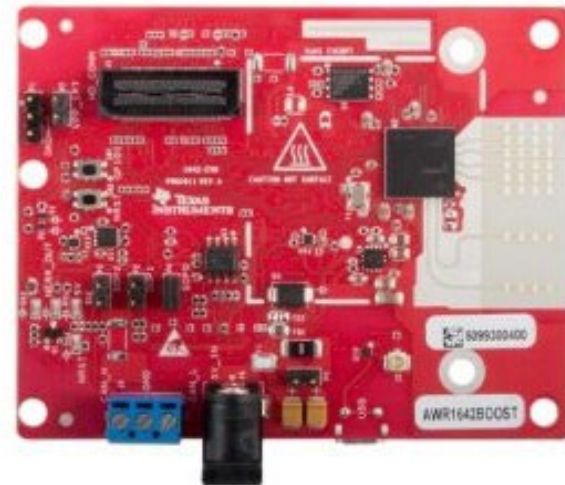


Graphics courtesy of Rick Gentile (MathWorks).

Texas Instruments mmWave Radars

Texas Instruments Development Kits

- ▶ TI produces a number of development kits for their 60-81 GHz radars
 - Very wide 4 GHz bandwidth using stretch – 4 cm resolution!
 - Precise locked LFM waveform generator for low phase noise
 - All use multiple-input/multiple-output (MIMO)
- ▶ The stand-alone radar development kit produces detection point clouds. Data capture board required for capture of IQ data.
 - Development board: AWR1642BOOST, \$299
 - Data capture: DCA1000EVM, \$499
- ▶ Very steep learning curve / not easy to use
- ▶ However, quite rewarding if you are interested in wideband or automotive applications



AWR1642 2x4 MIMO radar



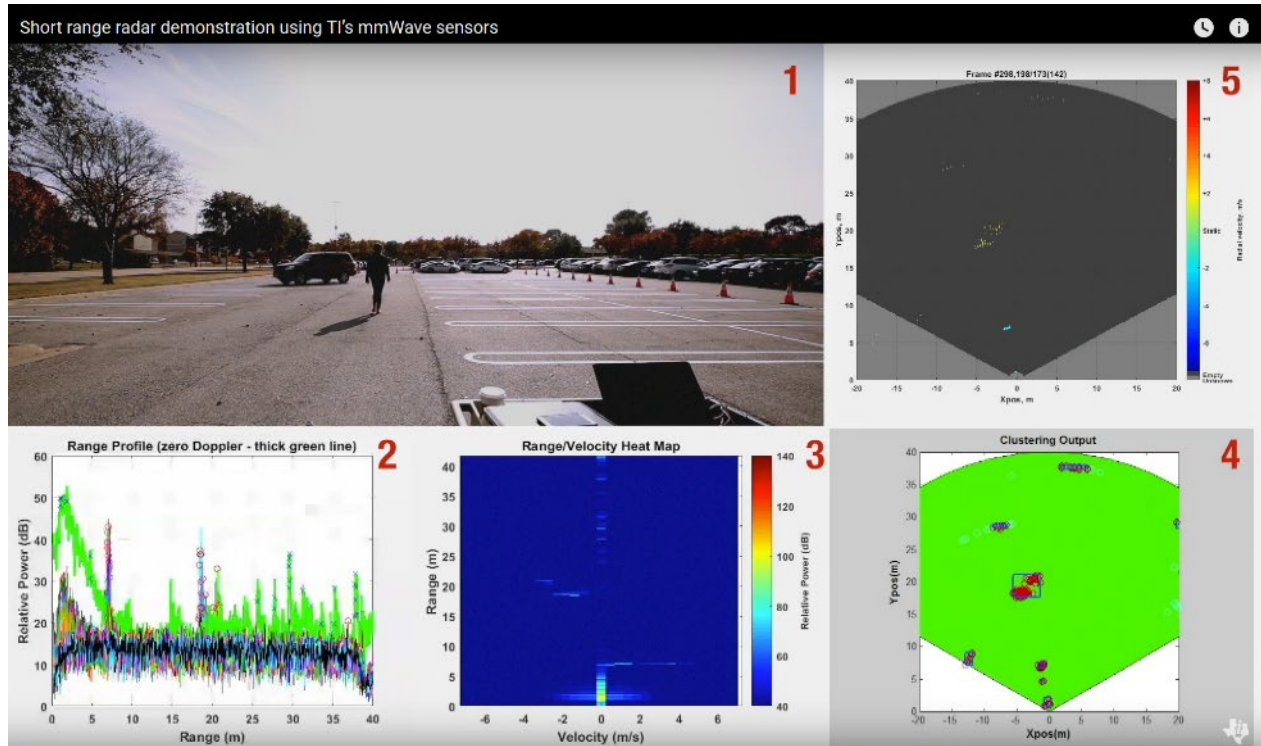
References:

<https://www.ti.com/sensors/mmwave-radar/automotive/overview.html>

<https://www.ti.com/tool/AWR1642BOOST>

TI Radar Demonstration

- ▶ 77 GHz automotive radar
 - 4 cm resolution
 - 40 m range



Reference:

<https://www.youtube.com/watch?v=ziQjbVXcSts>

Ettus Research USRP with gr-radar: GNU Radio Radar Toolbox

GNU Radio and gr-radar

- ▶ GNU Radio
 - Free & open-source software development toolkit
 - Provides signal processing blocks to implement software radios
 - Used with readily-available low-cost external RF hardware to create software-defined radios, or without hardware in a simulation-like environment
 - ▶ gr-radar: GNU Radio Radar Toolbox
 - GNU Radio out-of-tree (OOT) module
 - Toolbox of commonly used radar algorithms
 - Developed by Stefan Wunsch (Karlsruhe Institute of Technology) as part of Google Summer of Code 2014 (GSoc14)
 - Currently not compatible with GNU Radio 3.8
 - Use GNU Radio 3.7
 - Included as part of the 64-bit Windows binaries for GNU Radio 3.7
 - <http://www.gcndevelopment.com/gnuradio/index.htm>
 - ▶ Implemented radar types with example flowgraph:
 - CW (tested on hardware and simulation)
 - FSK (tested on hardware and simulation)
 - Dual CW (tested on hardware and simulation)
 - FM-CW (only simulation)
 - OFDM (only simulation)
 - ▶ References:
 - <https://grradar.wordpress.com/>
 - <https://github.com/kit-cel/gr-radar>
 - <https://github.com/analogdevicesinc/gr-ofdmradar>
 - ▶ Peak detection algorithms:
 - Max power detection (single peak detection)
 - OS-CFAR (multi peak detection)
 - OS-CFAR 2D (multi peak detection, e. g. for OFDM matrices)
 - ▶ Hardware interface and simulator:
 - Echotimer (UHD interface) for two or one USRP (multi USRP support is in work)
 - Sync setup for measuring hardware delay
 - Simulator with multi target capability and range, velocity, RCS, and azimuth as target property
 - ▶ Processing blocks:
 - Crop matrix
 - Transpose matrix
 - OFDM cyclic prefix remover
 - ▶ OFDM matrix division with zero-padding and discarding carriers
 - Split packages for FM-CW and FSK
 - FFT for tagged streams
 - Message manipulator and gate for target property message
- R. Seal and J. Urbina, "GnuRadar: an open-source software-defined radio receiver platform for radar applications," *IEEE Aerosp. Electron. Syst. Mag.*, vol. 35, no. 2, pp. 30-36, Feb., 2020.

FSK Radar Demonstration Flowgraph

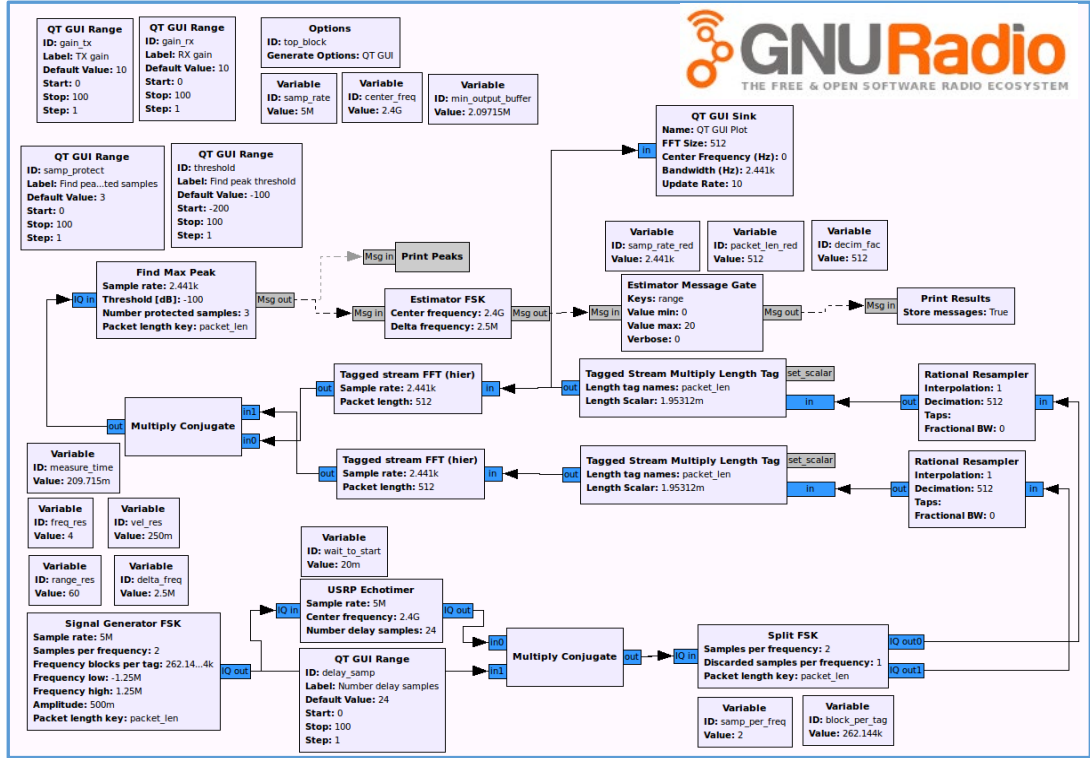


Image by S. Wunsch



Image by Ettus Research

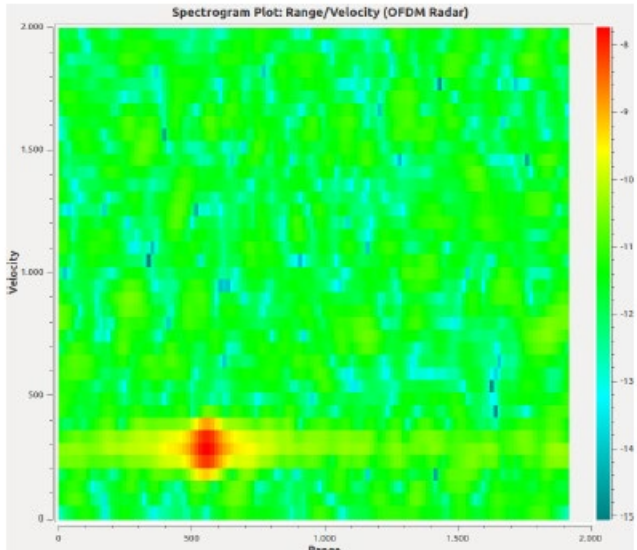


Image by S. Wunsch



Low-cost Scientific Investigations using Passive Bistatic Radar

Atmospheric Sciences and Radar

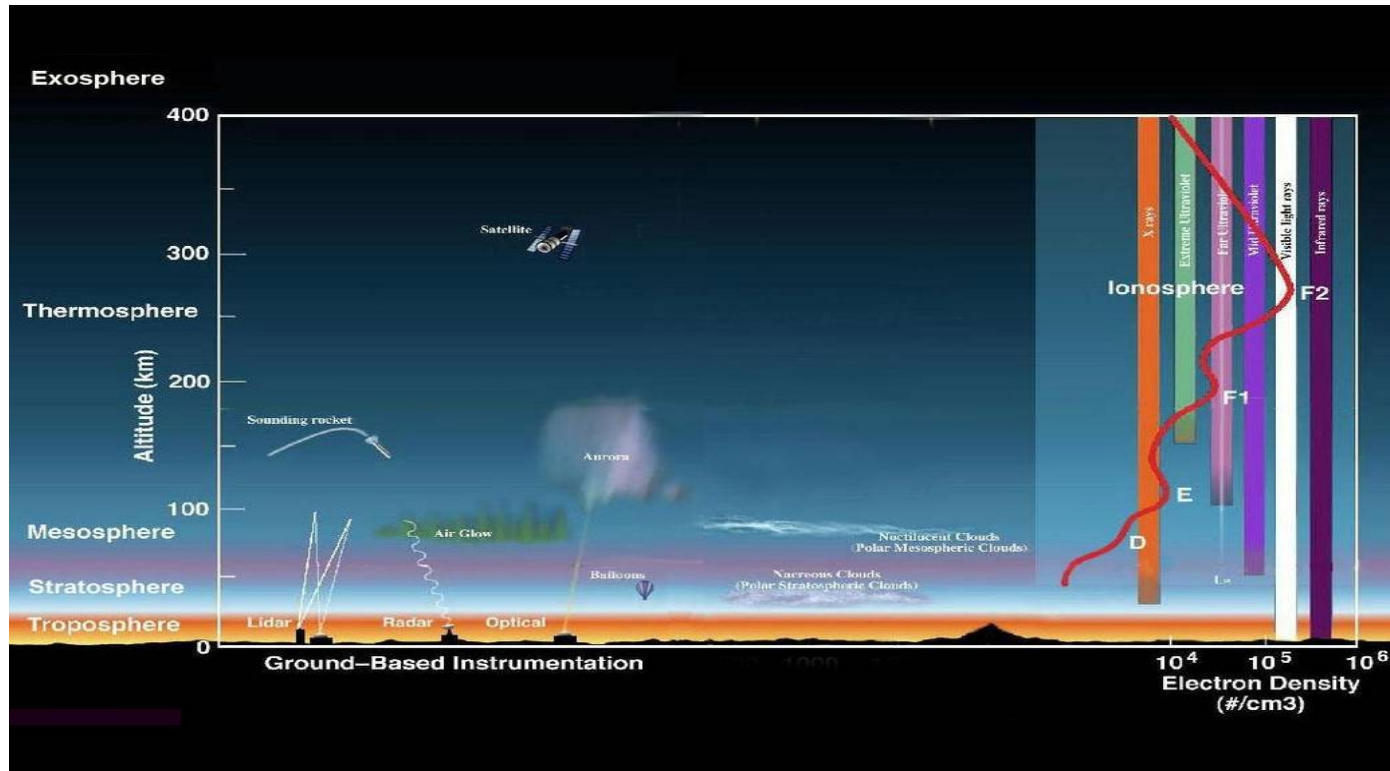
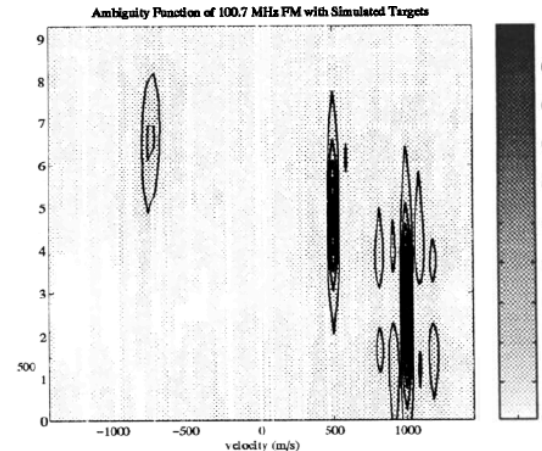


Image from: https://www.nasa.gov/mission_pages/sunearth/science/atmosphere-layers2.html

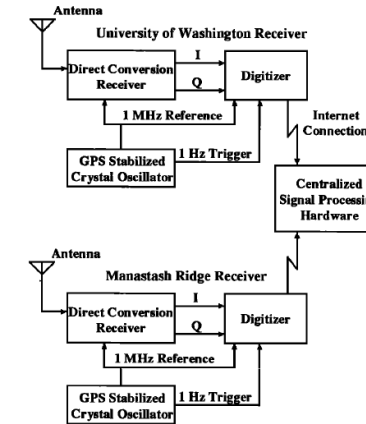
Atmospheric Remote Sensing

- ▶ Passive bistatic radar has been used for decades to better understand geophysical phenomena
 - Meteor characterization, upper atmospheric ionization, atmospheric turbulence
- ▶ Low-cost SDR make similar experiments accessible for students and hobbyists
- ▶ Measurements no longer require large budget and facilities



References:

- J. D. Sahr and F. D. Lind, "The Manastash Ridge radar: A passive bistatic radar for upper atmospheric radio science," *Radio Science*, vol. 32, no. 6, Nov-Dec 1997.
- F. D. Lind, J.D. Sahr, and D. M. Gidner, "First passive radar observations of auroral E-region irregularities," *Geophysical Res Ltrs*, vol. 26, no. 14, July 15, 1999.



1998 custom hardware

Example Low -cost Passive Radar Measurements For Ionospheric and Meteor Research

- ▶ Coastal Ocean Dynamics Applications Radar (CODAR) Transmitter is typically used for ocean surface current monitoring
- ▶ CODAR transmissions can be repurposed for investigation of ionospheric scattering phenomena
- ▶ Many systems have been built using Ettus Research USRP software-defined radios with good results
 - RFSPACE and KiwiSDR receivers also being used

References:

http://www.ibelings.com/N4IP_Labs/N4IP_Labs/CODAR-WERA.html

<https://destevez.net/2017/12/using-codar-for-ionospheric-sounding/>

[https://icerm.brown.edu/materials/Slides/sp-f17-w4/Radar_Problem_2_Presentation \] Frank Robey, MIT Lincoln Laboratory.pdf](https://icerm.brown.edu/materials/Slides/sp-f17-w4/Radar_Problem_2_Presentation] Frank Robey, MIT Lincoln Laboratory.pdf)

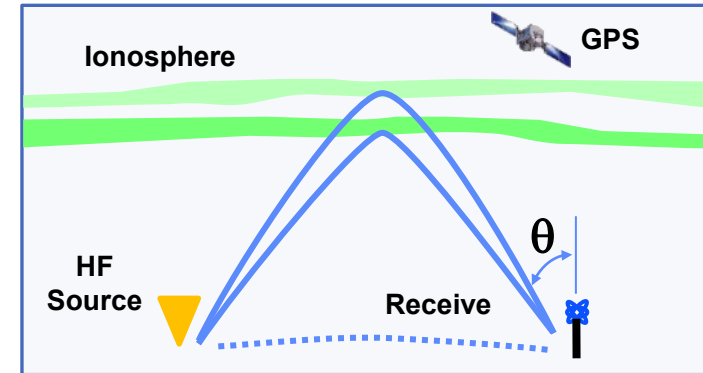
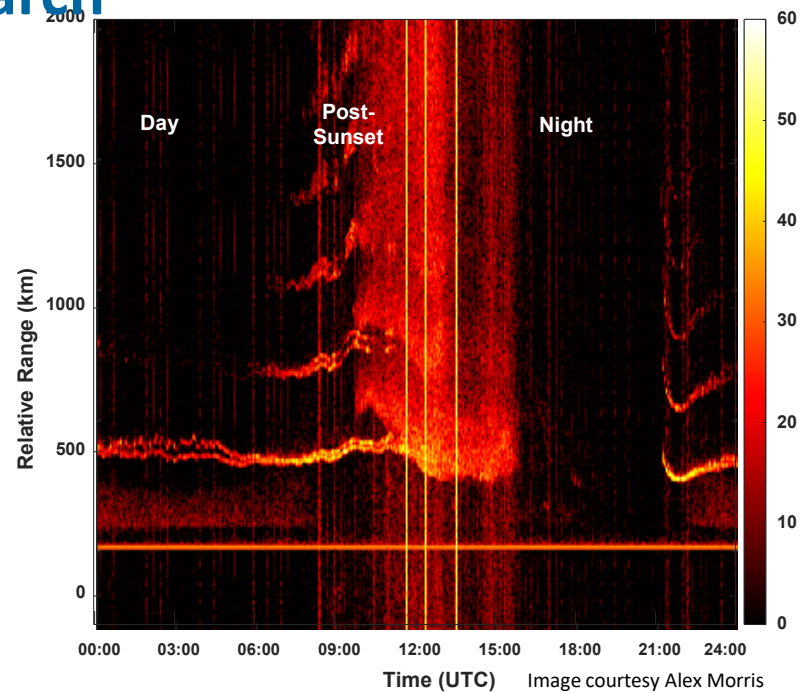
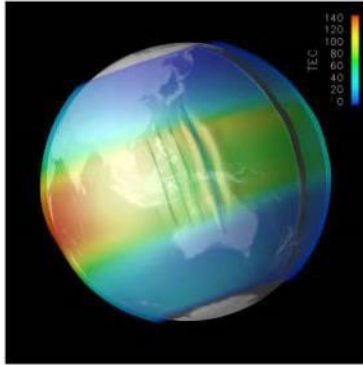


Image by F. C. Robey

Example Low Cost Passive Radar Measurements For Ionospheric and Meteor Research

- ▶ Image on right shows multiple propagation modes, returns from multiple ionospheric layers, cavity resonance, ionospheric motion, impact of D-layer
 - Software based on Ettus example programs, processing in MATLAB® or Octave
- ▶ A global network of passive radar receivers would complement network of ionospheric measurement GPS receivers to better understand dynamics and global energy transport



Appendix A

Data Sets

Publicly-available Radar Data Sets

- ▶ IEEE Data Port: <https://ieee-dataport.org/>
 - DARPA KASSPER Radar Data Set
 - Synthetic high-fidelity site-specific radar data set for multi-channel space-time adaptive processing (STAP)
 - Drone RCS measurements (26-40 GHz)
 - RCS measurements of consumer drones performed with the transmitter and receiver spatially co-located in the anechoic chamber
 - HH, HV/VH, and VV polarizations
- ▶ NASA Alaska Satellite Facility (ACF) Distributed Active Archive Center (DAAC)
 - Synthetic aperture radar (SAR) data from spaceborne and airborne platforms
 - <https://ASF.alaska.edu/about-asf-daac/>
- ▶ NIST RF Dataset of Incumbent Radar Systems in the 3.5 GHz Citizens Broadband Radio Service (CBRS) Band
 - 3.55 – 3.7 GHz RF dataset is suitable for development and testing of machine/deep learning detection algorithms for spectrum sharing research
 - Synthetically generated radar waveforms with added white Gaussian noise
 - <https://data.nist.gov/od/id/mds2-2116>
- ▶ McMaster University IPIX Radar Sea Clutter Database
 - High-quality, well-documented sea clutter data
 - Obtained with a coherent X-band radar, with advanced features such as dual transmit/receive polarization, frequency agility, and stare/surveillance mode
 - <http://soma.mcmaster.ca/ipix/>

It is also instructive to process data sets

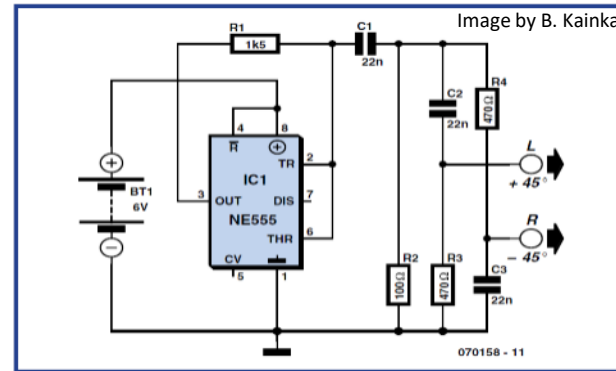


Appendix B

Tips for PC Audio Devices

PC Soundcard Testing

- ▶ PC soundcard characteristics crucial for systems that use them as analog-to-digital converters (ADCs) on receive
 - must have a stereo line-level input
 - must be equipped with an input anti-aliasing filter
 - sample rate must be at least 48 kHz
 - must be able to cope with signals up to 24 kHz
- ▶ Performance should be tested prior to using in a system
- ▶ A 15-kHz square wave generator can be built to provide a test stimulus
- ▶ SDRadio software displays purity of the spectrum
 - <http://digilander.libero.it/i2phd/sdradio/>



Kainka's Test Circuit to Generate I and Q Signals

Reference:

B. Kainka, "SDR soundcard tester", *Elektor Electronics Magazine*, p. 75, June, 2007.

NOTE: Consider using an inexpensive USB-based microcontroller development board for your ADC as an alternative to a PC soundcard

SDR Soundcard Test Example

Dell Dimension 8400 – **Good!**

Creative SoundBlaster Audigy 2 ZS (Line In)

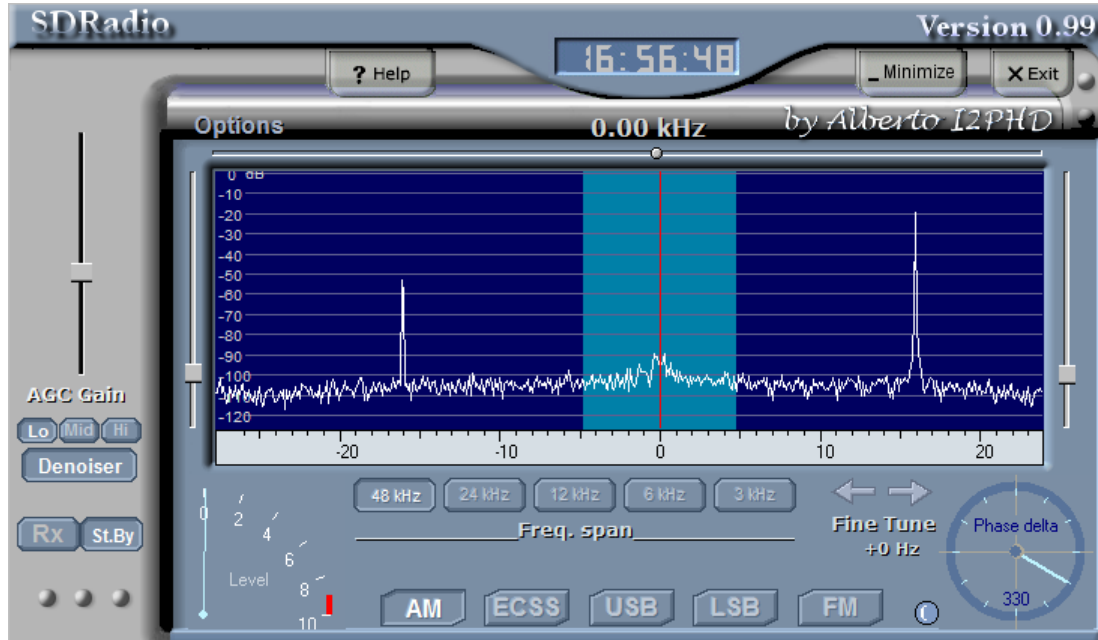


Image by J. P. Stralka

SDR Soundcard Test Example

HP Compaq 8510w Mobile Workstation – **Bad!**

SoundMAX Integrated Digital HD Audio (Microphone – w/out Voice Enhancements)

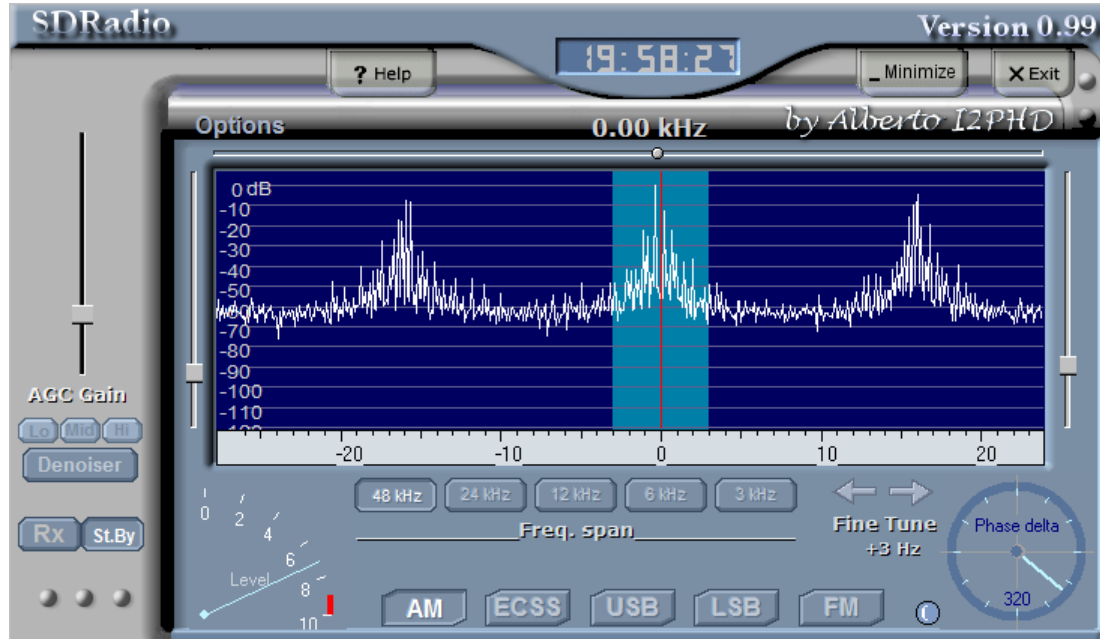


Image by J. P. Stralka

SDR Soundcard Test Example

Asus Eee PC 1000HE – **Good!**

Sewell 7.1 Channel USB Sound Box (Line In)

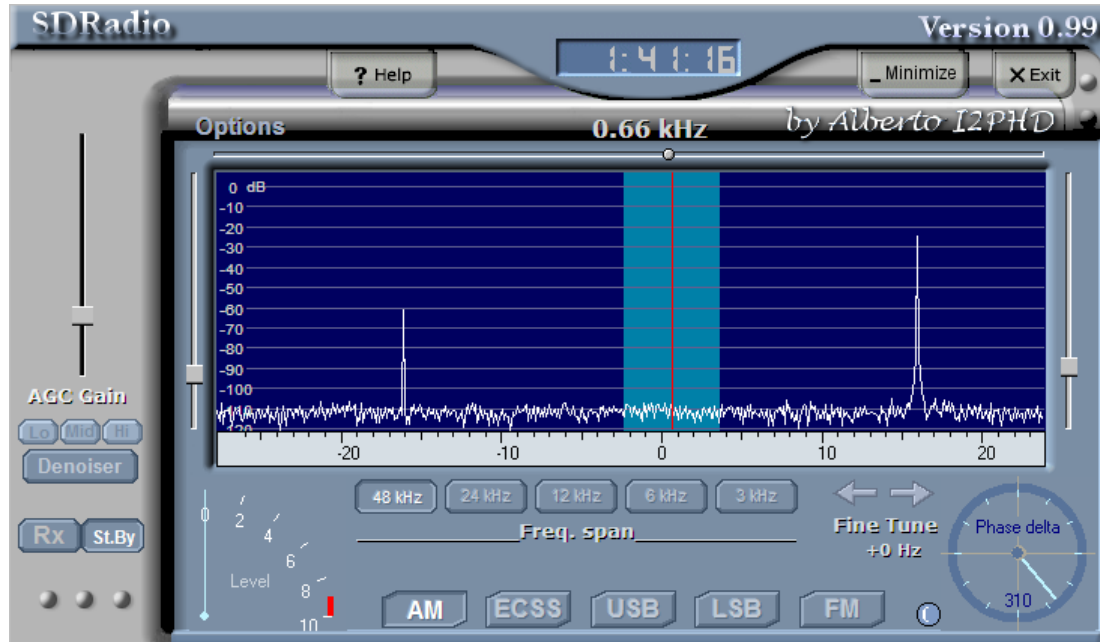


Image by J. P. Stralka

SDR Soundcard Test Example

Lenovo ThinkPad T540P – **Good!**

Sabrent AU-MMSA USB Audio Stereo Sound Adapter (Microphone In)

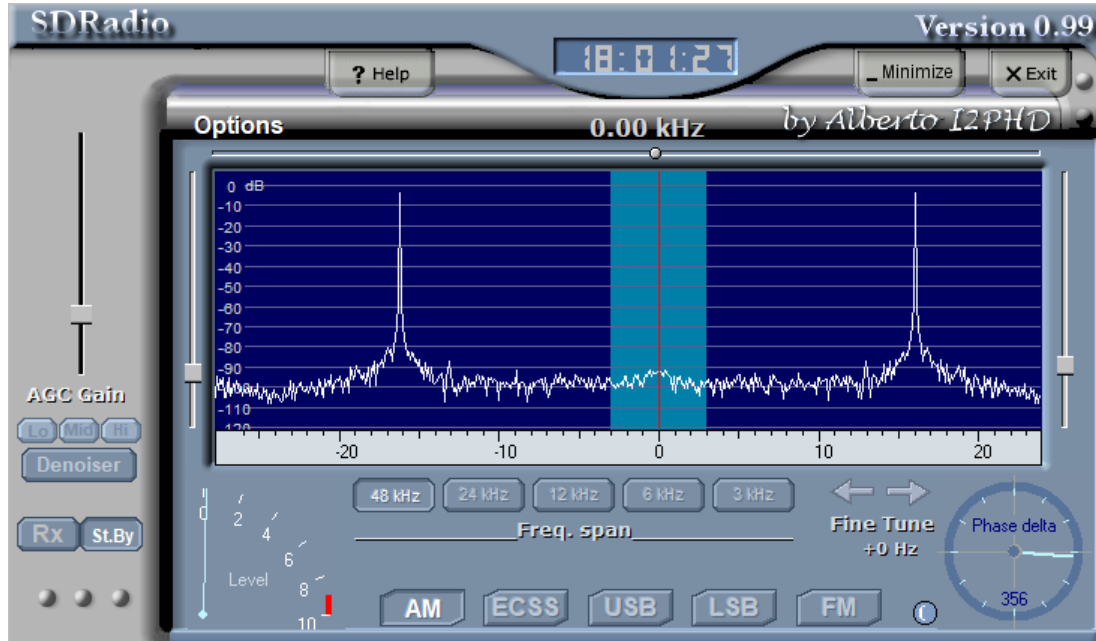


Image by J. P. Stralka

Capturing Audio Samples for Analysis

- ▶ Record audio using an audio application to save as a WAV-file
 - Audacity is a free open source digital audio editor and recording computer software application
 - <https://www.audacityteam.org/>
 - Read WAV-file into preferred engineering software MATLAB, Octave, Python, etc.
- ▶ Use a utility to play and record within MATLAB®, Octave, or Python itself
 - MATLAB®/Octave: playrec (<http://www.playrec.co.uk/>)
 - Python:
 - Soundcard
 - sounddevice
 - Paddio
- ▶ Radar RTP
 - In process of being open-sourced
 - Uses PortAudio for recording of raw radar data

Appendix C

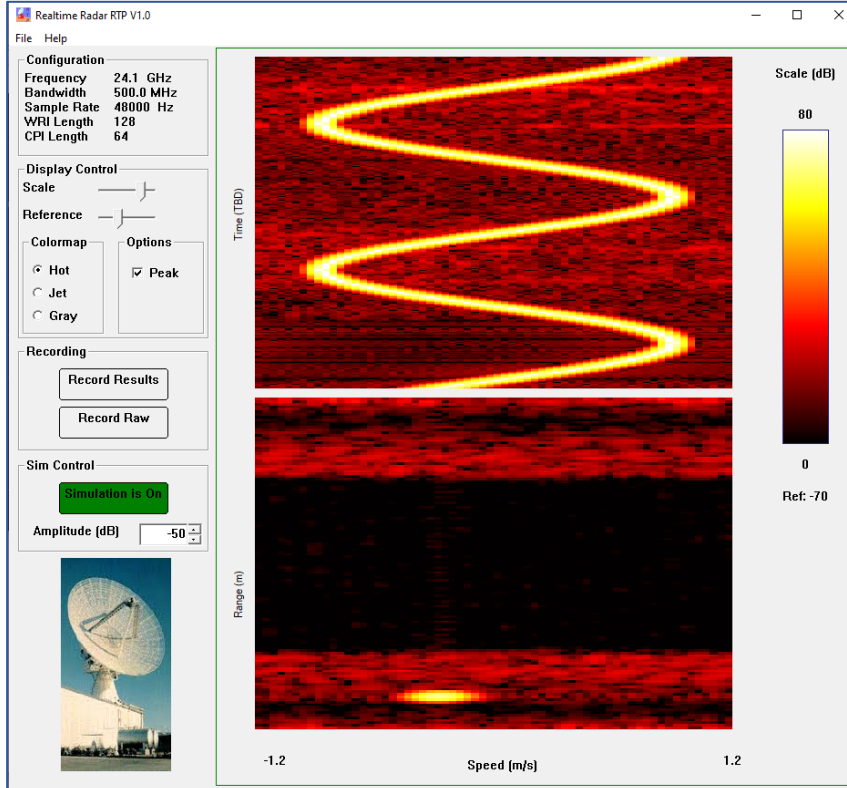
Low-cost Radar Software

Low-cost Radar Software

- A stumbling block to do-it-yourself can be the software to collect and process the data.
The following are some examples of software resources:

- gr-radar: GNU Radio Radar Toolbox: <https://github.com/kit-cel/gr-radar>
- Anterl uRAD: <https://urad.es/en/>
- SAR - Pyradar: <https://pyradar-tools.readthedocs.io/en/latest/>
- Maritime SAR ship detection: SUMO: <https://github.com/ec-europa/sumo>
- Weather radar: <https://openradarscience.org/projects/>
- Surveillance radar software for biological applications- RadR: <https://radr-project.org/radr-project.org/index.html>
- Amateur radar software with recording can provide foundation and spectral awareness for radar:
 - SDR#: <https://airspy.com/download/>
 - SpectraVue: <http://www.rfspace.com/RFSPACE/SpectraVue.html>
 - SdrDx: <https://fyngyrz.com/?p=915>
 - GrOsmoSDR: <https://osmocom.org/projects/gr-osmosdr/wiki>
 - RTL-SDR: <https://www rtl-sdr.com/big-list-rtl-sdr-supported-software/>
 - KerberosSDR: <https://github.com/rtlsdrblog/kerberossdr>

Radar Realtime Program (RTP)



- ▶ Performs real-time data capture, processing and display
 - Pulse compression
 - Doppler processing
- ▶ Uses default audio interface for input
 - 1 to 8 audio ADC channels
 - Up to 4 separate radars
- ▶ Provides synchronized sawtooth for modulation
- ▶ Operation configurable through .ini file
- ▶ Executable will be provided to participants of summer school
- ▶ Source will be available at IEEE or via GitHub at (TBD)

Appendix D

Become a Ham!

Benefits of Being a Ham

- ▶ Ham radio (aka amateur radio) for communications is a great hobby to pursue in parallel with radar
- ▶ Benefits include:
 - Working with RF from LF through mm-waves
 - Designing practical antennas
 - Studying propagation phenomena
 - Joining an international community of enthusiasts
 - Understanding allocations and usage rules of the RF spectrum
- ▶ For more information:
 - International Amateur Radio Union (IARU)
 - <https://www.iaru.org/>
 - American Radio Relay League (ARRL)
 - <http://www.arrl.org/>

▶ This has been KC3BMQ and N1PKT... 73!





This material is based upon work supported in part by the Department of the Navy and Department of the Air Force under Air Force Contract No. FA8702-15-D-0001. Any opinions, findings, conclusions or recommendations expressed in this material are those of the author(s) and do not necessarily reflect the views of the Department of the Navy or Department of the Air Force.

Target Tracking

James Nesteroff, PhD

Introduction and Expectations

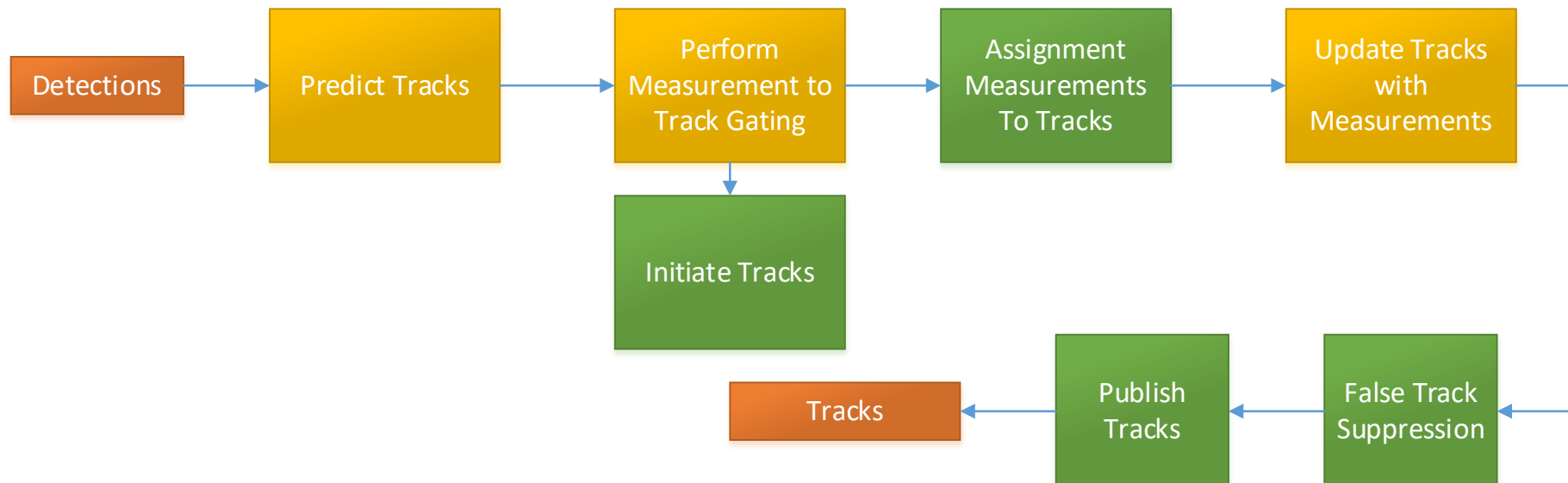
- This section of the course is intended to be a gentle introduction to target tracking
 - This is also not intended to be too heavy on the math
- Touch on the highlights of target tracking by a step-by-step walkthrough of a simple multi-target tracking architecture
- One important point to make: Understanding the algorithms used in tracking is just as important as understanding how to analyze data
- Making a simple tracker is not hard and there are plenty of good (and free) frameworks to work with:
 - Stone Soup¹ - Python
 - NRL Tracking Component Library² - MATLAB

1. <https://stonesoup.readthedocs.io/en/v0.1b8/index.html>

2. <https://github.com/USNavalResearchLaboratory/TrackerComponentLibrary>

High Level Tracking Architecture

Detections go in and tracks come out...



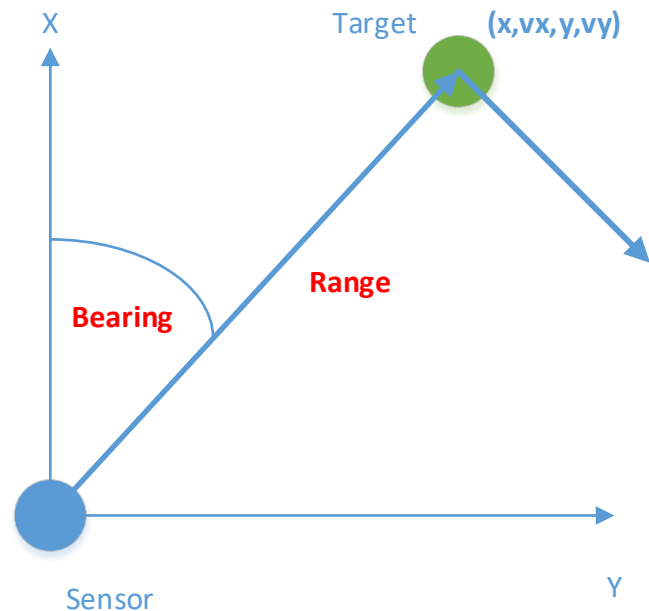
Function that uses a part of the state estimator

Agenda

- Start with the basics of state estimation
- Work through several different types of estimators
- Non-linear estimator extensions
- Extend the state estimation discussion to measurement to track gating
- Compile the associations together and perform data association
- Discuss different types of data association techniques
- Track score and confirming / deleting tracks

State Estimation^{1,2,3}

- One of the central functions in a tracking system
- What is a **state** of a target?
 - Can be position, velocity, acceleration, ...
- The process of state estimation involves taking in sensor measurements and using them to estimate the state of a target over time
- The state estimator (or filter) also provides, under certain assumptions, the uncertainty of the **state** estimate
- Types of sensor **measurements** (for example)
 - Range, angle, Doppler
- Types of Estimators
 - Least Squares
 - Recursive (e.g. Kalman Filter)



-
1. Blackman, Samuel, and Robert Popoli. "Design and analysis of modern tracking systems" Norwood, MA: Artech House, 1999. (1999). Chapter 3
 2. Simon, Dan. *Optimal state estimation: Kalman, H infinity, and nonlinear approaches*. John Wiley & Sons, 2006.
 3. Bar-Shalom, Yaakov, X. Rong Li, and Thiagalingam Kirubarajan. *Estimation with applications to tracking and navigation: theory algorithms and software*. John Wiley & Sons, 2004.

Least Squares Estimator

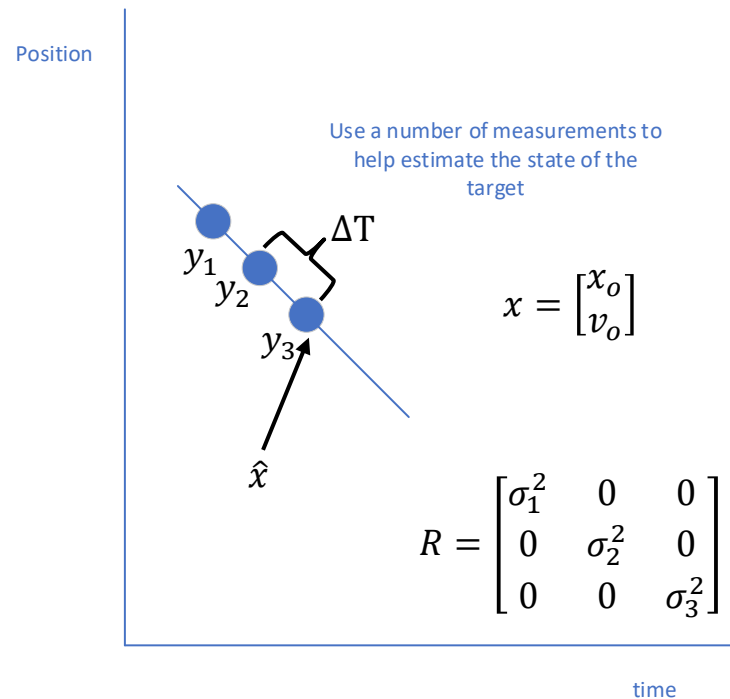
- For simplicity, think of finding the velocity of a target moving in 1D knowing only the position at each time t_k
- Let \vec{y}_k be a vector of measurements from time 0 to time t_k and assume there are n measurements
- Let \vec{x} be a vector that consists of the number of states to be estimated (perhaps position and velocity) and there maybe m of states.
- R is a matrix of measurement uncertainties
- Let H be an $n \times m$ matrix that projects the state into measurement space (*measurement matrix*). In our case, this is

$$H_k = [1 \quad k\Delta T] \quad k = 1 \dots n$$

- So that the estimated state is given by

$$\hat{x} = (H^T R^{-1} H)^{-1} H^T R^{-1} y$$

- But ...
 - That's a lot of measurements to store and...
 - What if the target changes direction during the estimate?



See pp. 79-97 in Simon, Dan. *Optimal state estimation: Kalman, H infinity, and nonlinear approaches*. John Wiley & Sons, 2006 for a nice discussion of this topic

Enter Recursion

- Now, as opposed to storing measurements we update the state as measurements come in

$$\hat{x}_k = \hat{x}_{k-1} + K_k(y_k - H_k\hat{x}_{k-1})$$

New state estimate

Gain

Error between the current measurement and what the previous state estimate looks like in measurement space (residual)

- This assumes we can describe the measurements in terms of the state as

$$y_k = H_k x + v_k \quad \leftarrow \text{Measurement Noise (assumed zero mean and independent)}$$

- Continuing the example from the previous slide this means,

$$y_k = x_o + v_o k \Delta T$$

- The gain is given by: $K_k = P_{k-1} H_k^T (H_k P_{k-1} H_k^T + R_k)^{-1}$

- Where the state covariance is P_k

$$P_k = (I - K_k H_k) P_{k-1} (I - K_k H_k)^T + K_k R_k K_k^T$$

Recursion: The recipe

- Step 1: Initialize your state and covariance (take a guess)¹
- Step 2: For each time step (and new measurement)
 - Calculate the gain $K_k = P_{k-1}H_k^T(H_kP_{k-1}H_k^T + R_k)^{-1}$
 - Update the state estimate: $\hat{x}_k = \hat{x}_{k-1} + K_k(y_k - H_k\hat{x}_{k-1})$
 - Find the current state covariance: $P_k = (I - K_kH_k)P_{k-1}(I - K_kH_k)^T + K_kR_kK_k^T$
- So, by giving up storing measurements at each time step we now need to assume an initial state and covariance
- Great, but ... if the target doesn't exactly fit the motion model I assumed ... then what?

1. This is an interesting topic see Bar-Shalom, Yaakov, X. Rong Li, and Thiagalingam Kirubarajan. *Estimation with applications to tracking and navigation: theory algorithms and software*. John Wiley & Sons, 2004. Chapter 5.5

Enter the (Linear) Kalman Filter

- Assume the linear dynamical system:

Propagates the state forward in time

$$x_k = F_{k-1}x_{k-1} + w_{k-1}$$

Process Noise $\langle w_k w_j \rangle = Q_k \delta_{j,k}$

For example, $F = \begin{bmatrix} 1 & \Delta T \\ 0 & 1 \end{bmatrix}$ for our previous example of estimating position and velocity

- Process Noise
 - Accounts for a lack of knowledge in the maneuverability of the target
- How do you figure out what process noise to use?
 - There are many different types of models¹
 - For a position and velocity state estimate one possibility is *Piecewise Constant White Noise Acceleration Model*

$$Q = \begin{pmatrix} T^4/4 & T^3/2 \\ T^3/2 & T^2 \end{pmatrix} \sigma_v^2$$

- Which has the nice property that²

$$0.5a_{max} \leq \sigma_v \leq a_{max}$$

1. Blackman, Samuel, and Robert Popoli. "Design and analysis of modern tracking systems" Norwood, MA: Artech House, 1999. (1999). Chapter 4 for an in-depth introduction to the subject

2. Bar-Shalom, Yaakov, X. Rong Li, and Thiagalingam Kirubarajan. *Estimation with applications to tracking and navigation: theory algorithms and software*. John Wiley & Sons, 2004.

Putting it all together: The Kalman recipe

- Step 1: Initialize your state and covariance (take a guess)
- Step 2: For each time step (and new measurement)
 - Propagate (predict) your state and covariance to the time of measurement

$$\begin{aligned}x_{k|k-1} &= F_{k-1}x_{k-1|k-1} \\P_{k|k-1} &= F_{k-1}P_{k|k}F_{k-1}^T + Q\end{aligned}$$

- Find the gain: $K_k = P_{k|k-1}H_k^T(H_kP_{k|k-1}H_k^T + R_k)^{-1}$
- Update the state estimate:
$$x_{k|k} = x_{k|k-1} + K_k(y_k - H_kx_{k|k-1})$$
- Find the current state covariance: $P_{k|k} = (I - K_kH_k)P_{k|k-1}(I - K_kH_k)^T + K_kR_kK_k^T$



time

Summary on State Estimation

- For tracking it is important to get it right
- There are different types of state estimators for different situations: *Least squares and recursive*
- If you *really* know your state motion model, then least squares estimation will work
- If you somewhat know your motion model, then use a recursive estimator like the Kalman filter and choose your process noise
- Problem: Everything we talked about assumed a linear problem
 - Measurements are related to the state by $y = Hx$.
 - Motion model can be described by $x(T) = \begin{bmatrix} 1 & T \\ 0 & 1 \end{bmatrix} x(0)$, for example

Non-Linear extensions

- Non-linear relation between state and measurement:

$$x = R \sin(B)$$

$$y = R \cos(B)$$

- Non-Linear motion model: Motion in constant gravity with *drag*¹

$$a_D = -\frac{1}{2} \alpha \rho(h) \|v\| \vec{v}$$

- Filter options (in order of computational complexity):

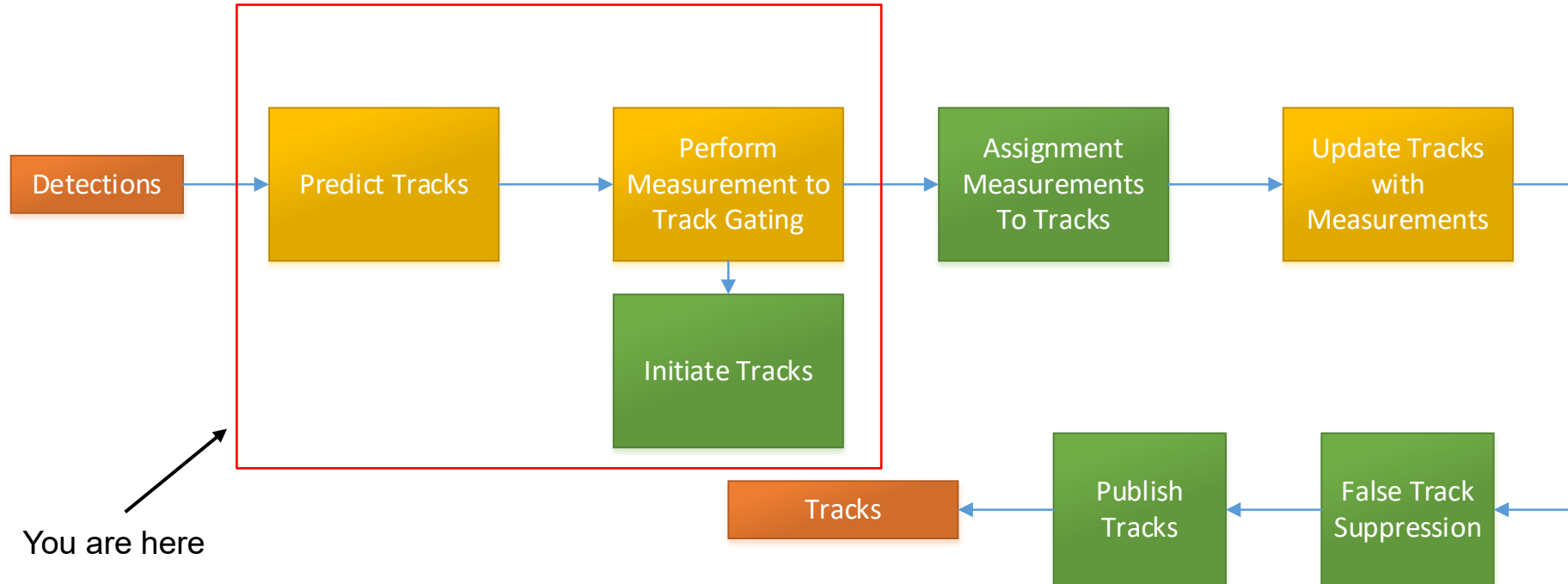
- Extended Kalman Filter (EKF): *Use a first order Taylor expansion to “linearize” either the F matrix or H matrix or both*
- Unscented Kalman Filter: *Approximate the mean and covariance of a non-linear distribution by a set of sample (sigma) points*
- Particle Filter: *Monte Carlo estimation of non-linear distribution*
- Recursive Bayesian Filter²: *Numerically integrate the Chapman Kolmogorov equations and apply Bayes rule*

1. X. Rong Li and V. P. Jilkov. “Survey of Maneuvering Target Tracking II: Motion Models of Ballistic and Space Targets”, *IEEE Transactions on Aerospace and Electronic Systems*, 46 (1), 2010.

2. Note: The Kalman filter is an exact solution to the Bayes Filter under the conditions of IID process and measurement noise as well as Gaussian, and linearity assumptions. See Simon (2006), Chapter 15.1

High Level Tracking Architecture

Detections go in and tracks come out...

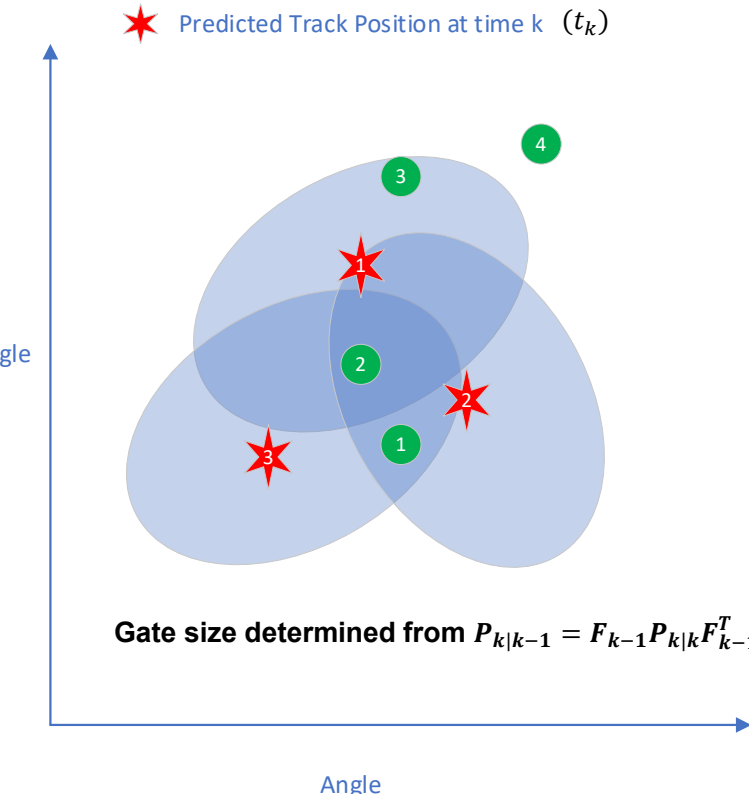
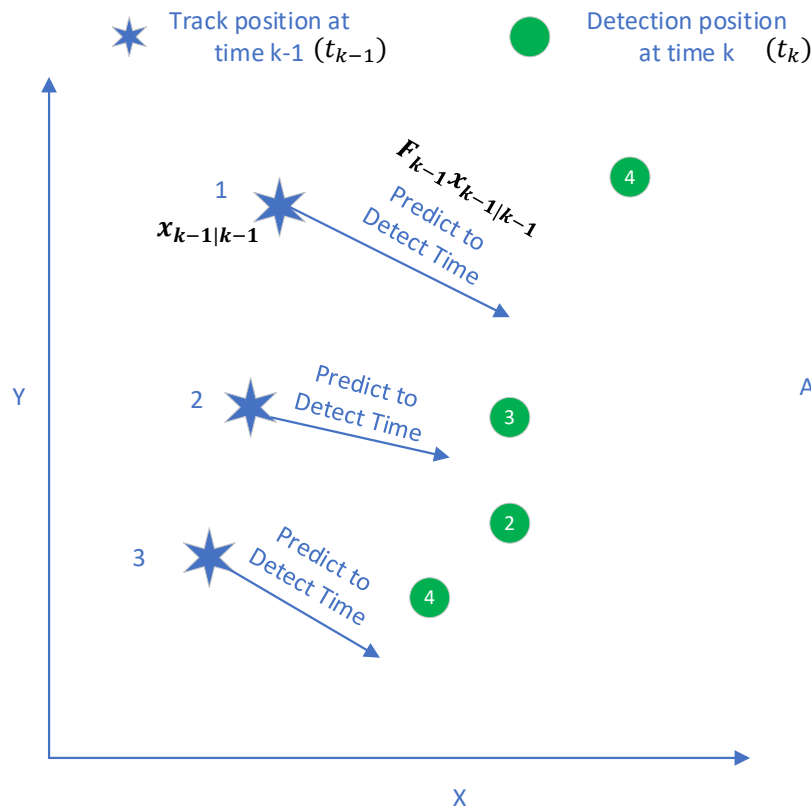


 Function that uses a part of the state estimator

Agenda

- Start with the basics of state estimation
- Work through several different types of estimators
- Non-linear estimator extensions
- **Extend the state estimation discussion to measurement to track gating**
- Compile the associations together and perform data association
- Discuss different types of data association techniques
- Track score and confirming / deleting tracks

Prediction and Gating

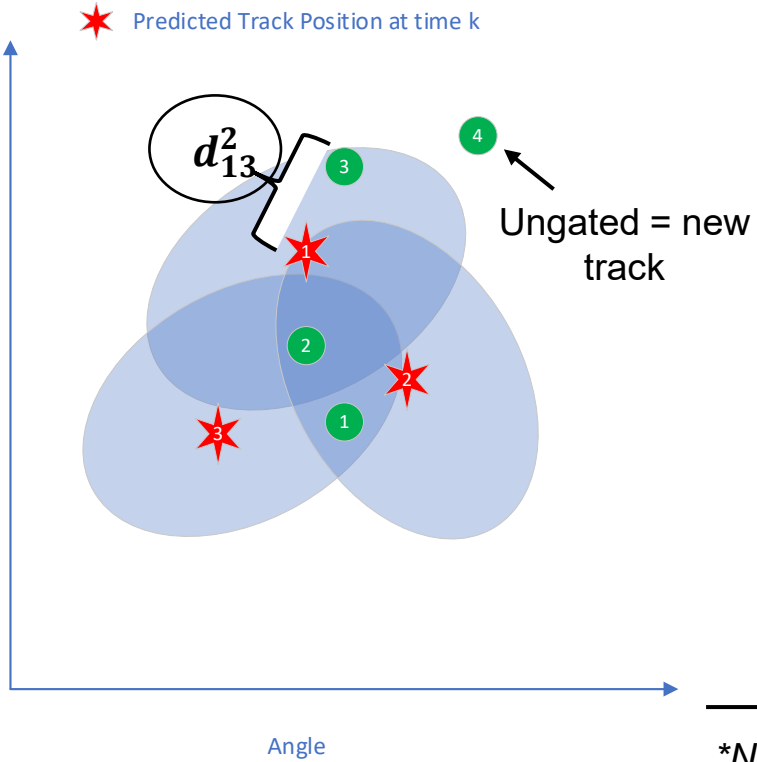


The Why and How of Gating¹

- The purpose of gating detections to track is to remove unlikely associations (like 4 in the previous example) from being used to update the filter
- Usually consists of two stages coarse and fine
- Focus on fine gating
- Fine gating is done with measurements (usually) and thus we need to project the predicted state and covariance into measurement space:
 - $y_{k|k-1} = Hx_{k|k-1}$ and $S = HP_{k|k-1}H^T + R$
- Form,
 - $d^2 = (y_k - y_{k|k-1})^T S^{-1} (y_k - y_{k|k-1})$
- This can be thought of as a *chi-squared distribution* (χ^2)²: the sum of squares of standard “normal” distributed random variables
- The more general name for this is Mahalanobis Distance
- If $d^2 >$ Threshold then the detection is not gated

1. See section 6.3 and references therein of Blackman, Samuel, and Robert Popoli. "Design and analysis of modern tracking systems" Norwood, MA: Artech House, 1999. (1999).
2. There are other metrics that can be used besides chi-squared, see the above reference

Gating: An example



“Cost” Matrix

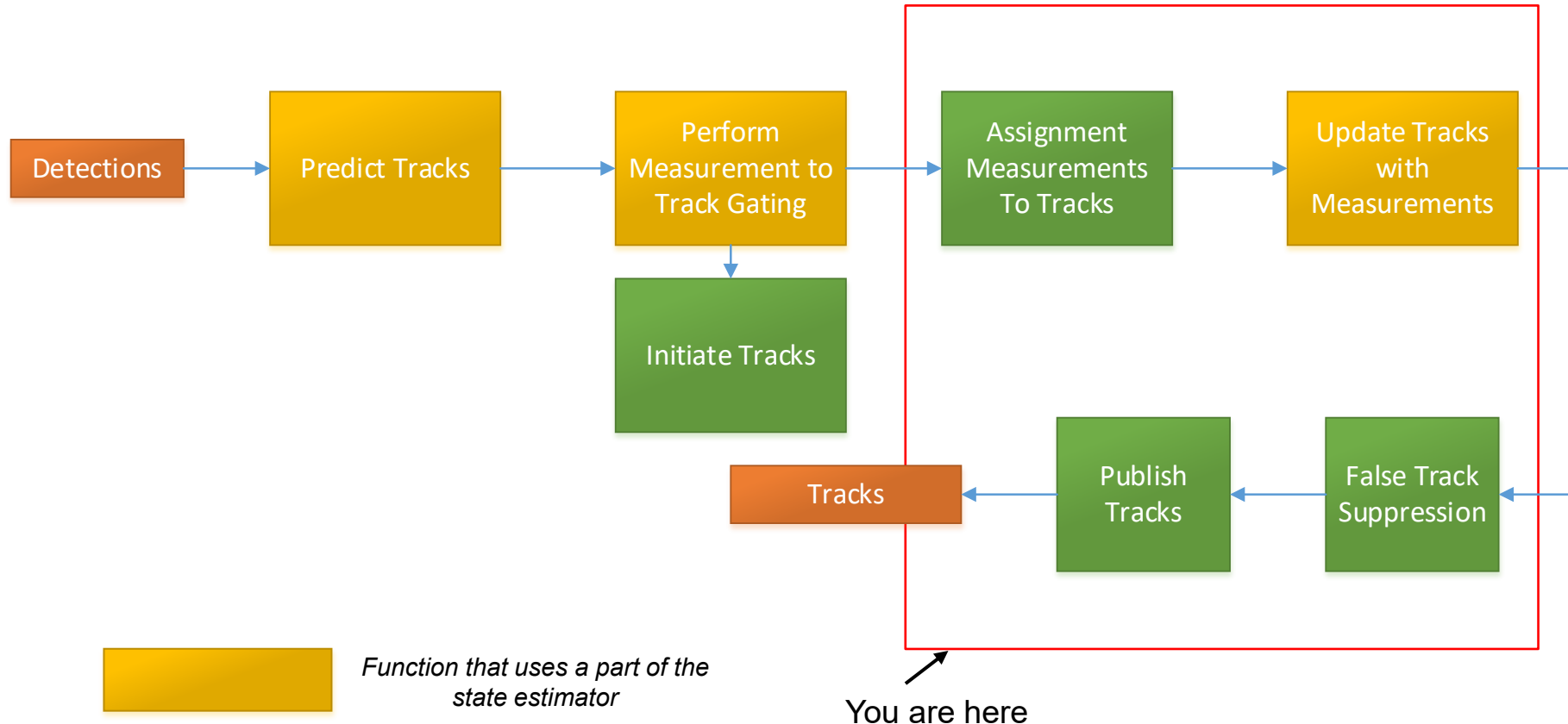
	T_1	T_2	T_3
D_1		9	8
D_2	3*	6	4
D_3	10		

How do you pick the best measurement to track assignment?

*Numbers based on previous reference's example on p.340

High Level Tracking Architecture

Detections go in and tracks come out...



Agenda

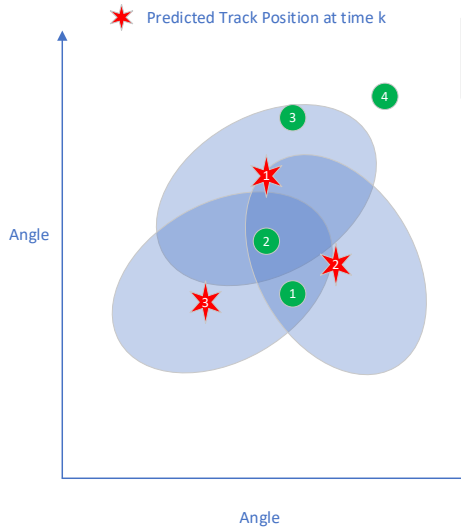
- Start with the basics of state estimation
- Work through several different types of estimators
- Non-linear estimator extensions
- Extend the state estimation discussion to measurement to track gating
- **Compile the associations together and perform data association**
- **Discuss different types of data association techniques**
- **Track score and confirming / deleting tracks**

Data Association, Assignment, and Update

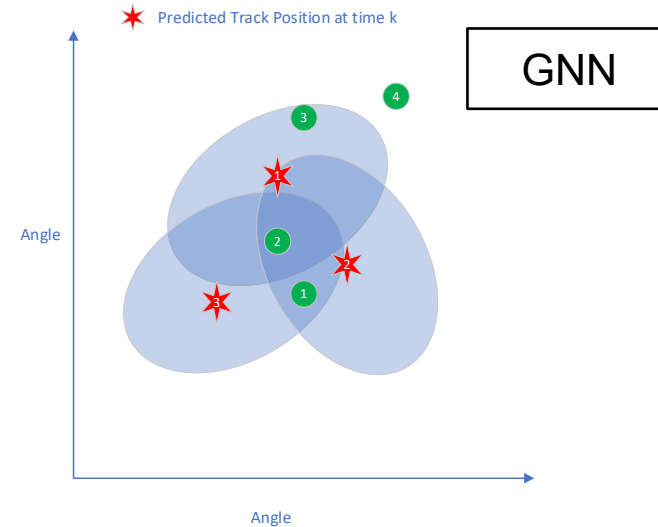
- How to choose the “best” combination of measurements to update the tracks is at the heart of multiple target tracking
- There are many different techniques all with pros and cons
- Examples (in order of computational complexity)
 - Nearest Neighbor : Choose the closest detection to a track
 - Global nearest neighbor: Choose the set of measurements which minimizes the total cost of measurement to track assignment
 - Requires the use of assignment algorithms such as Munkres, Auction, or JVC
 - Joint Probabilistic Data Association (JPDA)¹: Uses all observations in a track gate with probability-weighting
 - Multiple Hypothesis Tracking: Form “hypotheses” for track to measurement association that are evaluated at a later time
 - Multi-frame Assignment

1. There is a nice tutorial of this here: https://stonesoup.readthedocs.io/en/latest/auto_tutorials/08_JPDATutorial.html

Nearest Neighbor (NN) versus Global Nearest Neighbor (GNN)



These assigned measurements are passed to the Kalman filter for update



A naïve implementation of NN would potentially assign two detections to track 1

	T_1	T_2	T_3
D_1		9	(8)
D_2	(3)	6	4
D_3	10		

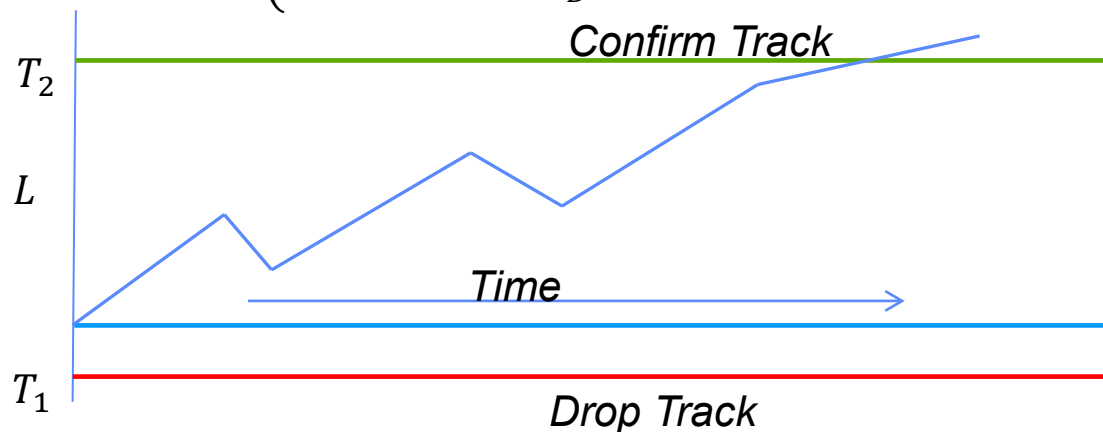
	T_1	T_2	T_3
D_1		(9)	8
D_2	3	6	(4)
D_3	10		

False Track Suppression and the Sequential Probability Ratio Test (SPRT): Is it real or not?

SPRT $L = \frac{\text{Probability of Received Data Being From a True Target}}{\text{Probability of Received Data Being From a False Target}}$

$$L = \begin{cases} \ln \left[\frac{P_D}{(2\pi)^{M/2} \beta_{FT} |S|^{1/2}} \right] - \frac{d^2}{2} & \text{Hit} \\ 1 - P_D & \text{Miss} \end{cases}$$

P_D = Probability of Detection
 β_{FT} = False Alarm Density



S = Covariance Matrix in Measurement Space

d = Statistical Distance

M = Number of Measurement Dimensions

This is a relatively simple model for declaring a track confirmed or dropping a track. Note that the track score L is accumulated over time

Summary

- Target tracking was explained by way of a walkthrough of a simple tracking architecture
- We discussed:
 - The different types of state estimation (linear and non-linear)
 - How prediction and gating works with state estimation
 - Types of algorithms used for data association
 - A simple form of track confirmation
- There is a lot more to cover which can be found in the references cited. This includes:
 - Choice of tracking coordinate systems
 - Effect of measurement non-linearities on filter performance
 - Filter Initialization
- Additional References
 - Stone, Lawrence D., et al. *Bayesian multiple target tracking*. Artech House, 2013.
 - https://icerm.brown.edu/materials/Slides/sp-f17-w2/Intro_to_Single-Scan_Target_Tracking_1_David_Crouse_Naval_Research_Laboratory.pdf

March 2022

AESS Radar Summer School Space-Time Adaptive Processing (STAP)

William L. Melvin, Ph.D.
Georgia Institute of Technology
(404)-407-8274, bill.melvin@gtri.gatech.edu

Outline

- **Preliminaries – notation and operations**
- Role of STAP in modern radar systems
- Spatial, temporal, and space-time sampling
- Space-time signal models
- Space-time signal processing and figures of merit
- STAP formulation
- Practical STAP implementation
- Summary

Common Notation

- The following is some commonly used notation
- Context is important and will generally clarify notation

\mathbf{x} = generic data snapshot

\mathbf{s} = generic signal response

\mathbf{w} = generic weight vector

$\hat{\mathbf{w}}$ = generic estimated/implemented weight vector

\mathbf{R} = generic covariance matrix

$\hat{\mathbf{R}}$ = estimated covariance matrix

y = scalar filter output

- Subscripts generally mean...
- “ k ” → range-bin
- “ s ” → spatial dimension
- “ t ” → temporal dimension
- “ $s-t$ ” → space-time dimension

For example...

y_k = k-th range bin output

$\mathbf{x}_{k/s-t}$ = range bin k , space-time snapshot

$\mathbf{x}_t \in C^{N \times 1}$ → length- N temporal snapshot

Inner and Outer Products

- Inner Product: Multiplying two vectors to get a scalar

$$\mathbf{W}^H \mathbf{X} = y$$

Superscript “H” means conjugate transpose
(1xM) (Mx1) (1x1)

- If the inner product of 2 vectors equals zero, the vectors are called **orthogonal** (perpendicular)

- Outer Product: Multiplying two vectors to get a matrix

$$\mathbf{X} \mathbf{X}^H = \mathbf{R}$$

(Mx1) (1xM) (MxM)

Hadamard (Schur) Product

- Element by element multiplication of two vectors or matrices

$$\mathbf{x} \odot \mathbf{y} = \begin{bmatrix} x_1 \\ x_2 \\ \vdots \\ x_M \end{bmatrix} \odot \begin{bmatrix} y_1 \\ y_2 \\ \vdots \\ y_M \end{bmatrix} = \begin{bmatrix} x_1 y_1 \\ x_2 y_2 \\ \vdots \\ x_M y_M \end{bmatrix}$$

- Standard multiplication
- Vectors or matrices must have the exact same dimensions
- STAP Application: Add a windowing function (Hanning, Taylor, etc.) to the conventional beamformer to suppress sidelobes

Kronecker Product

- Get all combinations of elements of two vectors or matrices

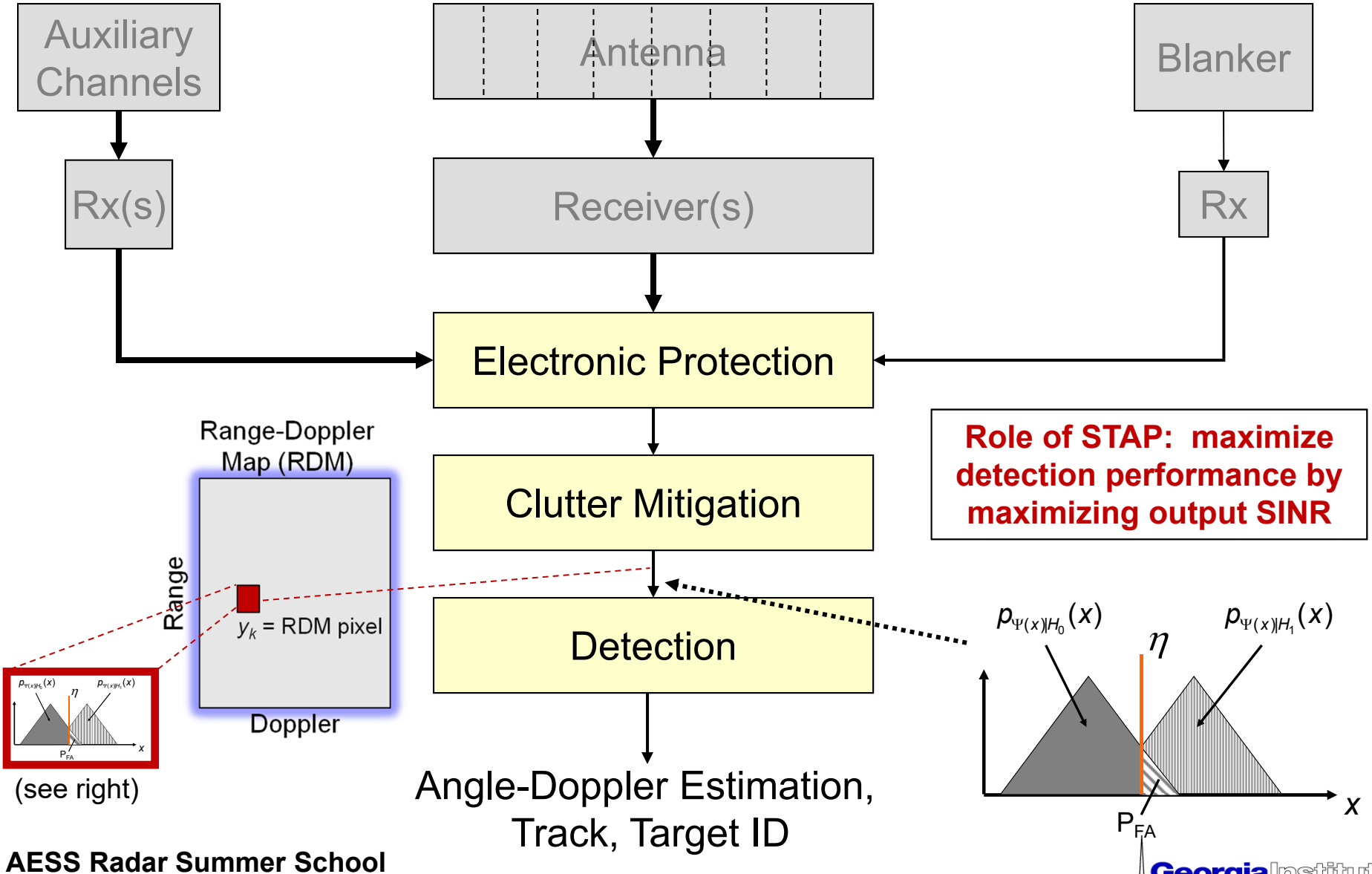
$$\begin{matrix} \mathbf{x}_{(M \times 1)} \otimes \mathbf{y}_{(N \times 1)} = \begin{bmatrix} x_1 \\ x_2 \\ \vdots \\ x_M \end{bmatrix} \otimes \begin{bmatrix} y_1 \\ y_2 \\ \vdots \\ y_N \end{bmatrix} = \end{matrix} \begin{matrix} x_1 \begin{bmatrix} y_1 \\ \vdots \\ y_N \end{bmatrix} \\ x_2 \begin{bmatrix} y_1 \\ \vdots \\ y_N \end{bmatrix} \\ \vdots \\ x_M \begin{bmatrix} y_1 \\ \vdots \\ y_N \end{bmatrix} \end{matrix} = \mathbf{z}_{(NM \times 1)}$$

- STAP Application: Combine temporal and spatial steering vectors into the space-time steering vector, $\mathbf{s}_{s-t} = \mathbf{s}_t \otimes \mathbf{s}_s$

Outline

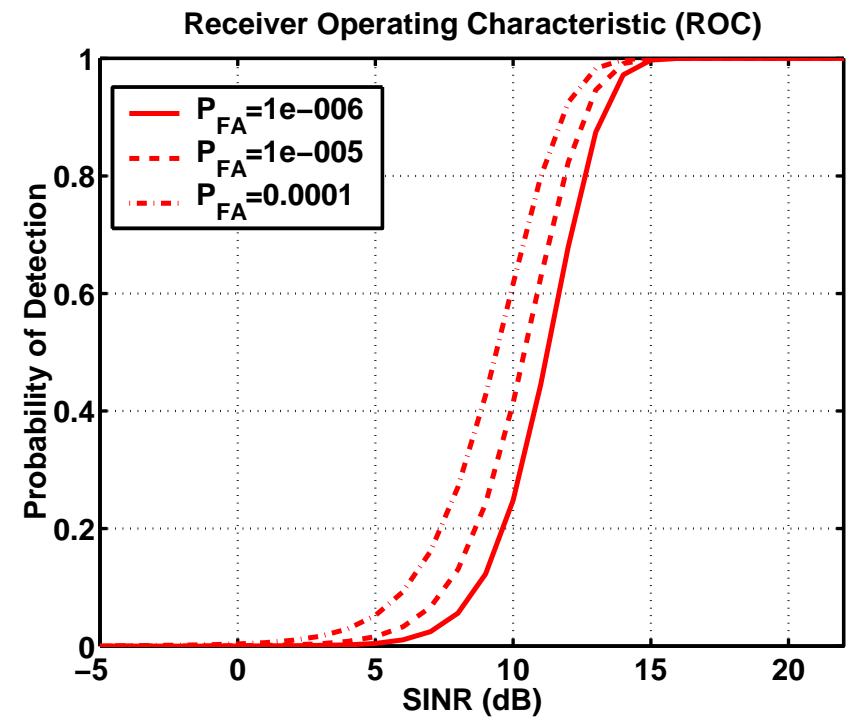
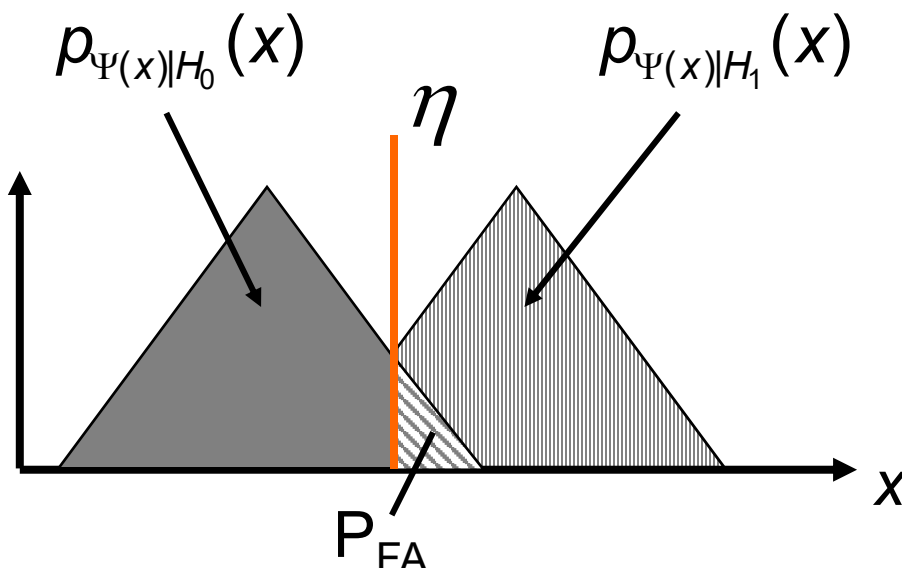
- Preliminaries – notation and operations
- **Role of STAP in modern radar systems**
- Spatial, temporal, and space-time sampling
- Space-time signal models
- Space-time signal processing and figures of merit
- STAP formulation
- Practical STAP implementation
- Summary

Multidimensional Radar Signal Processing



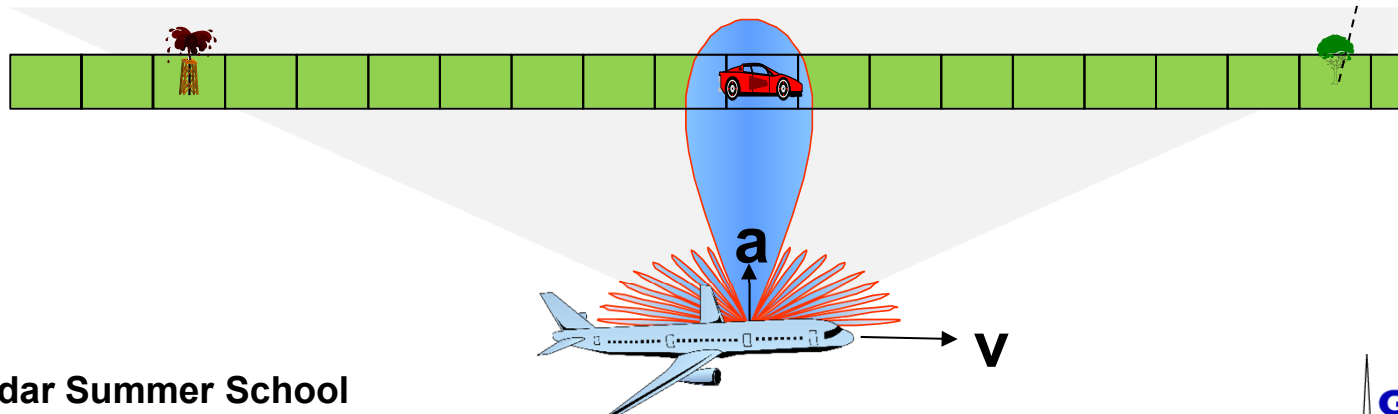
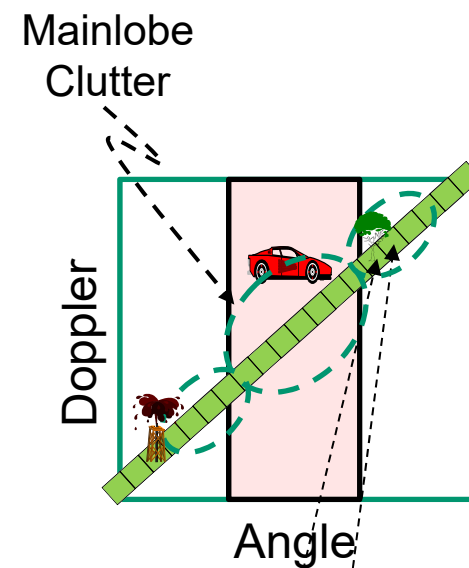
Radar Detection: Common Observances [1-2]

- P_D and P_{FA} move together
 - E.g., As the threshold decreases, P_D and P_{FA} both increase
- Decision rule operates in regions of conditional density overlap in an “optimal” fashion
- **STAP maximizes P_D for a fixed P_{FA} (multivariate Gaussian disturbance case) by maximizing output SINR!**



Key Radar Detection Challenges [2-10]

- Doppler-spread mainlobe clutter masks slow moving targets
- Stationary clutter response is coupled in angle and Doppler
 - Specifying angle uniquely specifies Doppler and viceversa
- STAP objective: discriminate the target's angle-Doppler response from that of the stationary clutter background



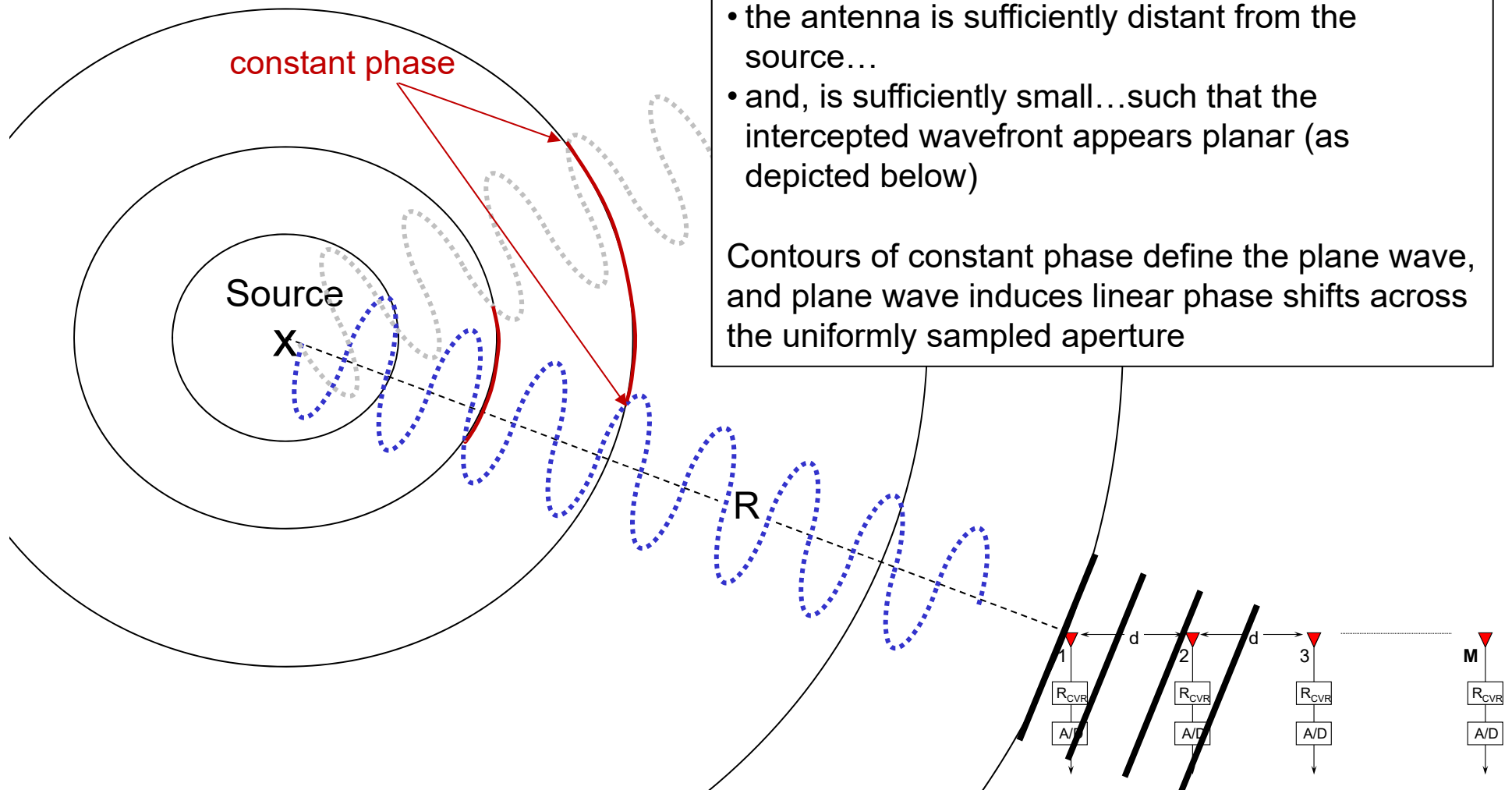
Outline

- Preliminaries – notation and operations
- Role of STAP in modern radar systems
- **Spatial, temporal, and space-time sampling**
- Space-time signal models
- Space-time signal processing and figures of merit
- STAP formulation
- Practical STAP implementation
- Summary

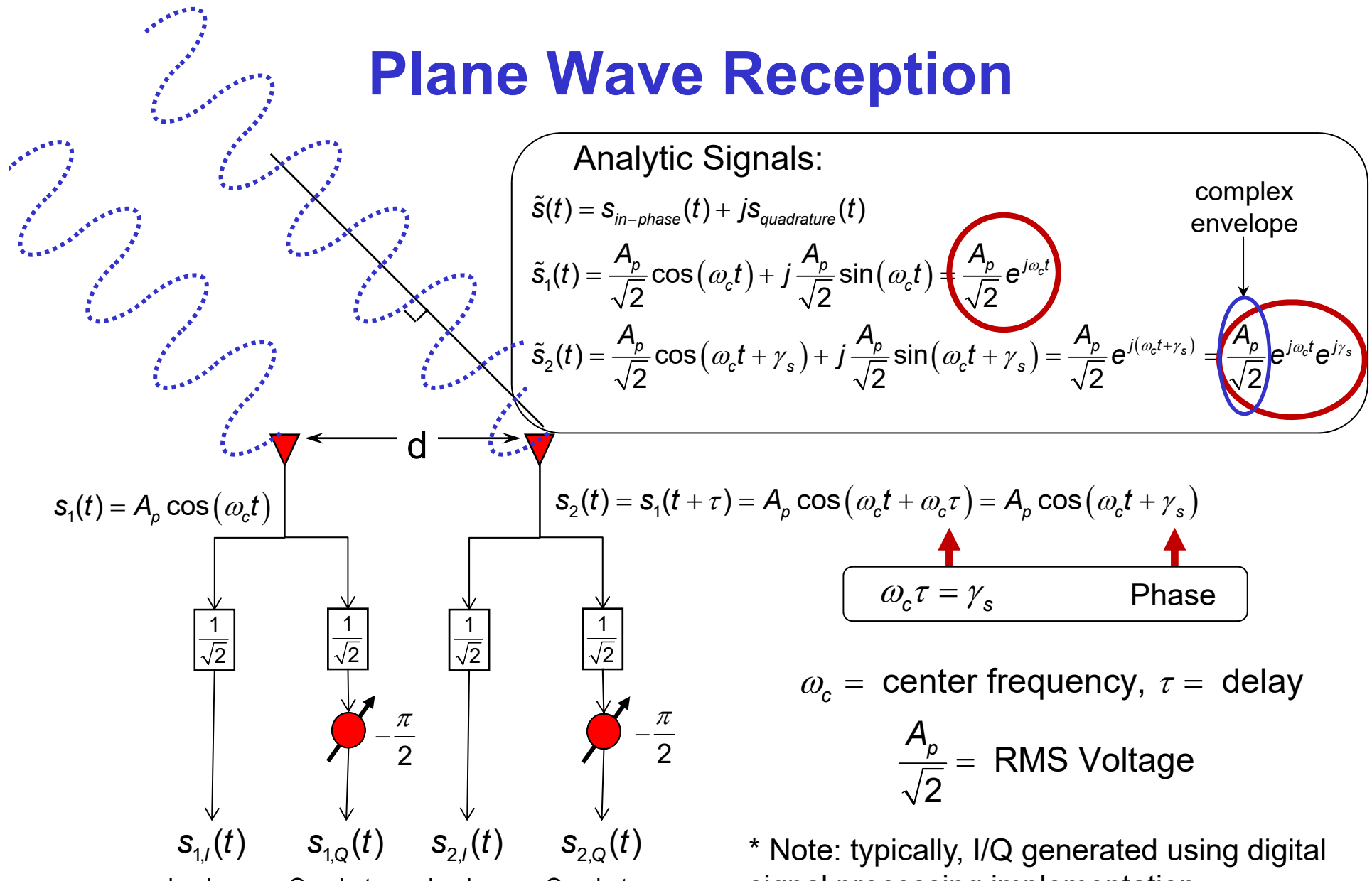
Beamforming [1]

- A beamformer is a spatial filter
 - Signal from specified direction coherently “stacks,” while beamformer mitigates signals from other directions
 - Non-adaptive beamformer essentially a bandpass filter
 - Adaptive filter tailors response to colored-noise environment
- Beamforming generally requires both amplitude and phase weighting of measured signals
 - Either in analog, digital or hybrid hardware
- Resolution typically limited to beamwidth
 - $\phi_{B,null} = \lambda / L_{azimuth}$ (Rayleigh Criterion)
 - Super-resolution “beamformers” overcome this limit (e.g., 10:1 beamsplit)

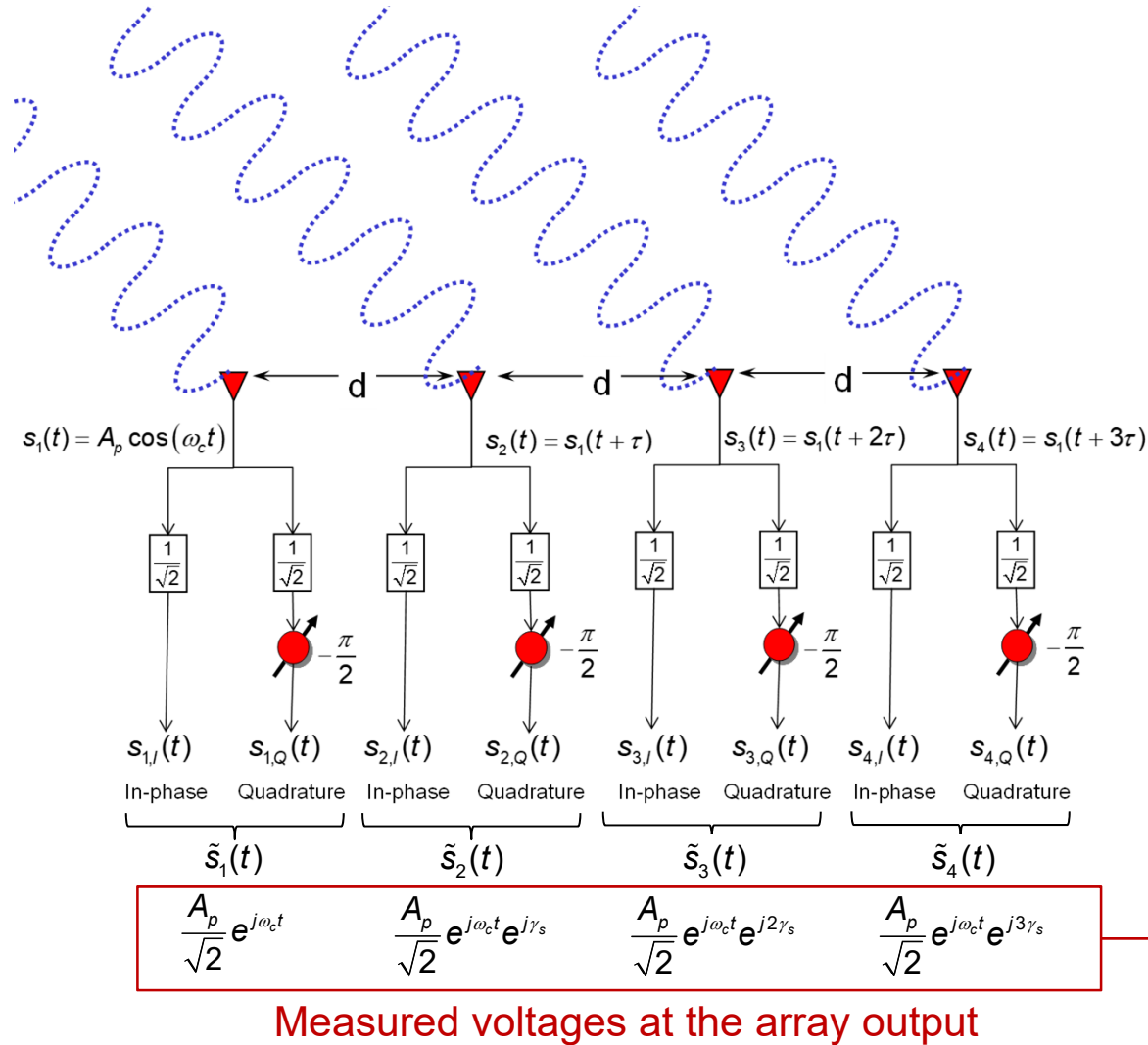
Plane Wave Propagation



Plane Wave Reception



Array Sampling and the Signal Vector



(Receive signal vector, with channel 1 as the origin)

$$\mathbf{s} = \frac{A_p}{\sqrt{2}} \begin{bmatrix} 1 \\ e^{j\omega_c \tau_{s/2}} \\ e^{j\omega_c \tau_{s/3}} \\ e^{j\omega_c \tau_{s/4}} \end{bmatrix} = \frac{A_p}{\sqrt{2}} \begin{bmatrix} 1 \\ e^{j\gamma_s} \\ e^{j2\gamma_s} \\ e^{j3\gamma_s} \end{bmatrix}$$

$\mathbf{s} = \mathbf{a}_s \mathbf{s}_s$

$a_s = \frac{A_p}{\sqrt{2}}$

Demodulate:
complex baseband

$$\mathbf{s}_s = \begin{bmatrix} 1 \\ e^{j\gamma_s} \\ e^{j2\gamma_s} \\ e^{j3\gamma_s} \end{bmatrix}$$

complex envelope

Maximum Signal-to-Noise Ratio (SNR) Filter (a.k.a. Matched Filter)

Signal and noise snapshots: $\mathbf{s}, \mathbf{n} \in \mathbb{C}^{M \times 1}$

Uncorrelated noise signal: $\mathbf{n} \sim \mathcal{CN}(\mathbf{0}, \mathbf{R}_n)$; $\mathbf{R}_n = \sigma_n^2 \mathbf{I}_M$

$$SNR = \frac{P_s}{P_n} = \frac{E[y_s y_s^*]}{E[y_n y_n^*]} = \frac{E[(\mathbf{w}^H \mathbf{s})(\mathbf{s}^H \mathbf{w})]}{E[(\mathbf{w}^H \mathbf{n})(\mathbf{n}^H \mathbf{w})]} = \frac{\mathbf{w}^H \mathbf{R}_s \mathbf{w}}{\mathbf{w}^H \mathbf{R}_n \mathbf{w}}$$

$$= \frac{\sigma_s^2}{\sigma_n^2} \frac{|\mathbf{w}^H \mathbf{s}_s|^2}{\mathbf{w}^H \mathbf{w}} \leq \frac{\sigma_s^2}{\sigma_n^2} \frac{(\mathbf{w}^H \mathbf{w})(\mathbf{s}_s^H \mathbf{s}_s)}{\mathbf{w}^H \mathbf{w}}$$

$\mathbf{R}_s = \sigma_s^2 \mathbf{s}_s \mathbf{s}_s^H$
 $y_s = \mathbf{w}^H \mathbf{s}$
 $y_n = \mathbf{w}^H \mathbf{n}$

Achieves the upper bound when $\mathbf{w} = \mu \mathbf{s}_s \dots$

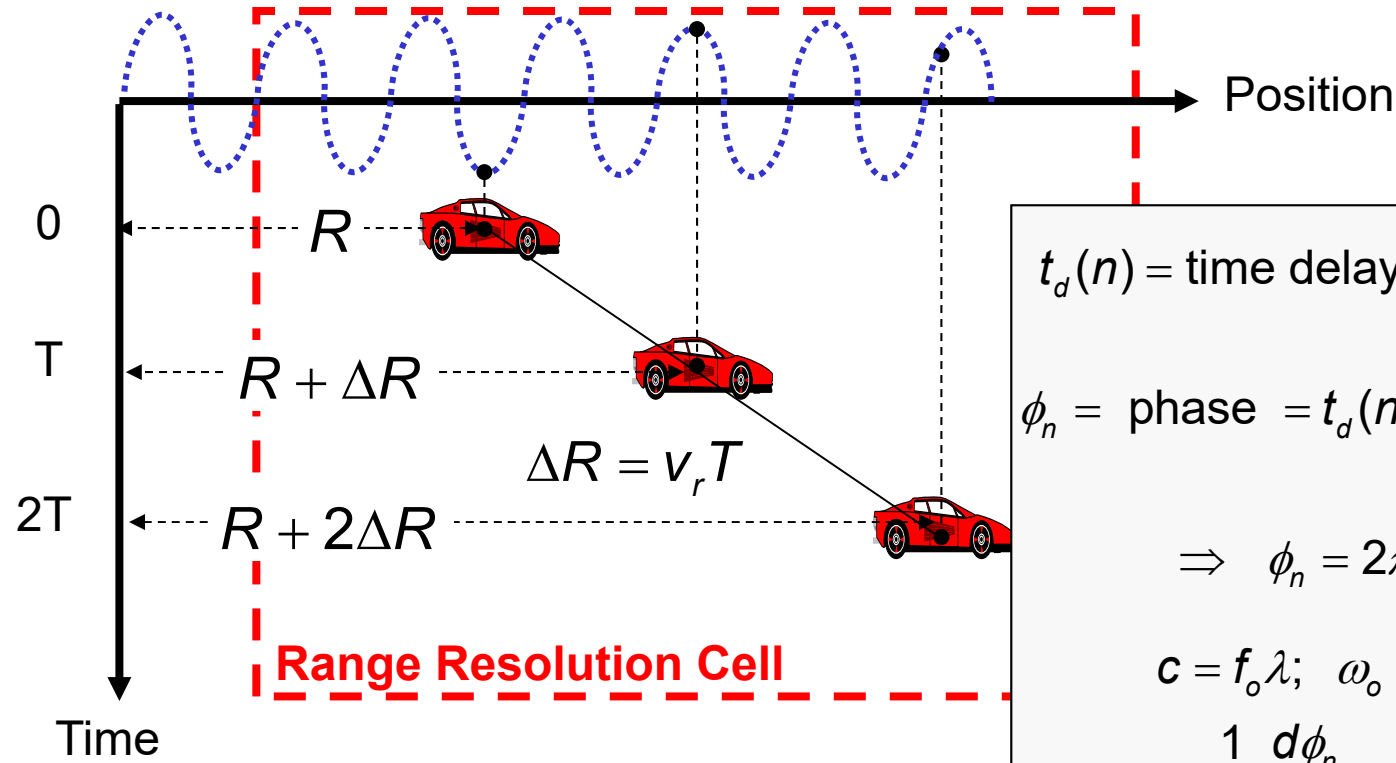
$$SNR = \left(\frac{\sigma_s^2}{\sigma_n^2} \right) M$$

Single Channel
SNR

Integration Gain

Arbitrary scalar

Temporal Sampling



$$t_d(n) = \text{time delay} = \frac{\text{dist.}}{c} = \frac{2R + n2\Delta R}{c}$$

$$\phi_n = \text{phase} = t_d(n)\omega_o = \left[\frac{2R + n2\Delta R}{f_o\lambda} \right] 2\pi f_o$$

$$\Rightarrow \phi_n = 2\pi \left(\frac{2R}{\lambda} \right) + 2\pi n \left(\frac{2\Delta R}{\lambda} \right);$$

$$c = f_o\lambda; \quad \omega_o = 2\pi f_o; \quad \Delta R = v_r T$$

$$\frac{1}{2\pi} \frac{d\phi_n}{dt} = f_d = \frac{2\Delta R}{\lambda \Delta t} = \frac{2v_r}{\lambda}$$

Receive temporal data: $\mathbf{x}_t = [a_s e^{-j\phi_0} \quad a_s e^{-j\phi_1} \quad \dots \quad a_s e^{-j\phi_{N-1}}]^T + \mathbf{n} = \mathbf{a}' \mathbf{s}_t(f_d) + \mathbf{n}$

Doppler steering vector: $\mathbf{s}_t = \begin{bmatrix} 1 & e^{j2\pi\left(\frac{2v_r}{\lambda}\right)T} & e^{j2\pi\left(\frac{2v_r}{\lambda}\right)2T} \end{bmatrix}^T = \begin{bmatrix} 1 & e^{j2\pi f_d T} & e^{j2\pi f_d 2T} \end{bmatrix}^T$

Steering Vectors

- Originally used to describe the spatial response of the array to signal with a specific direction of arrival (DOA)
 - The conjugate “steers” the beam
 - Terminology also used to describe temporal response
 - Matched filter

1-D Spatial Steering Vector (uniformly-spaced linear array, or ULA)

$$\mathbf{s}_s(\gamma_s) = [1 \quad e^{j\gamma_s} \quad e^{j2\gamma_s} \quad \dots \quad e^{j(M-1)\gamma_s}]^T \quad (= \mathbf{v}_s(\gamma_s))$$

Temporal Steering Vector

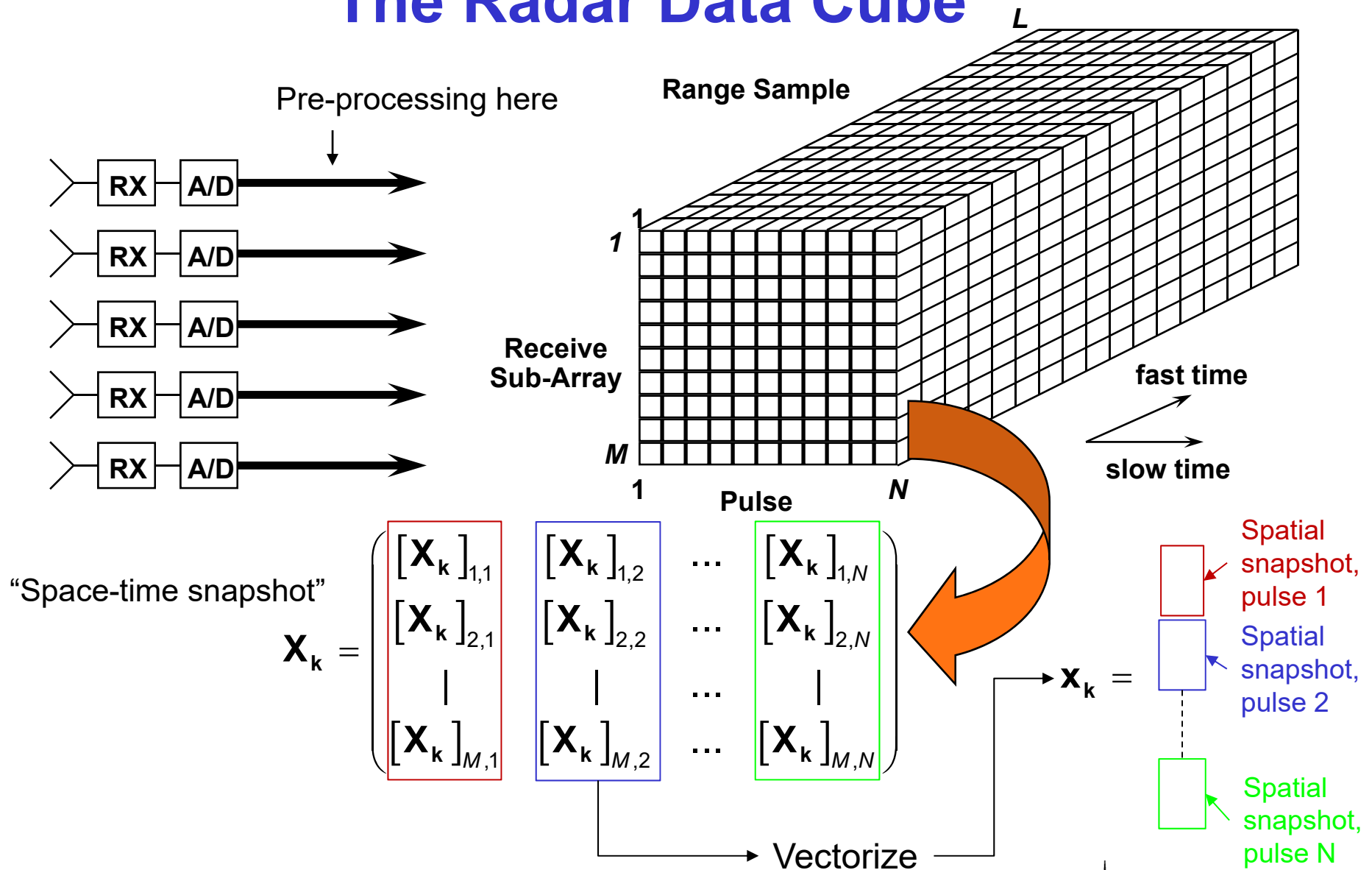
$$\mathbf{s}_t(\tilde{f}_d) = [1 \quad e^{j\tilde{f}_d} \quad e^{j2\tilde{f}_d} \quad \dots \quad e^{j(N-1)\tilde{f}_d}]^T \quad (= \mathbf{v}_t(\tilde{f}_d))$$

(Normalized Doppler)

$$\tilde{f}_d = 2\pi f_d T = 2\pi \left(\frac{2v_r}{\lambda} \right) T$$

Hypothesized
steering vectors

The Radar Data Cube



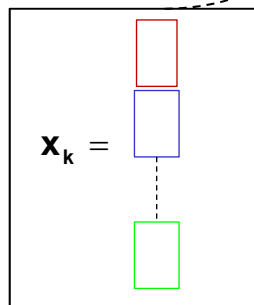
Space-Time Signal Vector

Response of pulse-Doppler array to a unity amplitude signal from a specific DOA with a specific Doppler frequency

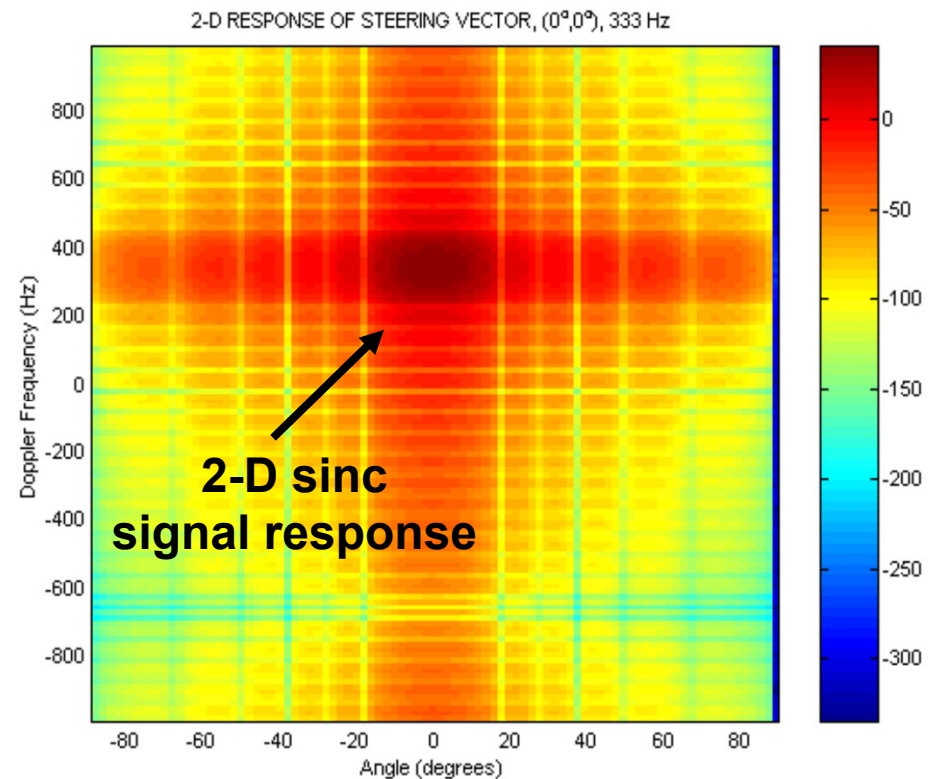
$$\mathbf{s}_{\text{s-t}}(\gamma_s, \tilde{f}_d) = \mathbf{s}_t(\tilde{f}_d) \otimes \mathbf{s}_s(\gamma_s)$$

Note utility of Kronecker product:

$$\mathbf{s}_{\text{s-t}}(\gamma_s, \tilde{f}_d) = \begin{bmatrix} 1 \cdot \mathbf{s}_s(\gamma_s) \\ e^{j\tilde{f}_d} \cdot \mathbf{s}_s(\gamma_s) \\ \vdots \\ e^{j(N-1)\tilde{f}_d} \cdot \mathbf{s}_s(\gamma_s) \end{bmatrix}$$



Kronecker product replicates data formatting



Covariance Matrix for Single Scatterer in Receiver Noise

$$\mathbf{x} = a_s \mathbf{s}_{s-t} + \mathbf{n} \quad (\text{Received space-time data vector})$$

$$\mathbf{n} \sim \mathcal{CN}(\mathbf{0}, \sigma_n^2 \mathbf{I}_{NM}), \text{ where } \sigma_n^2 \text{ is noise power} \quad (\text{Uncorrelated Rx noise})$$

$$E[a_s a_s^*] = E[|a_s|^2] = \sigma_s^2 \quad (\text{Signal power})$$

Hypothesized steering vector,
a guess at \mathbf{s}_{s-t}

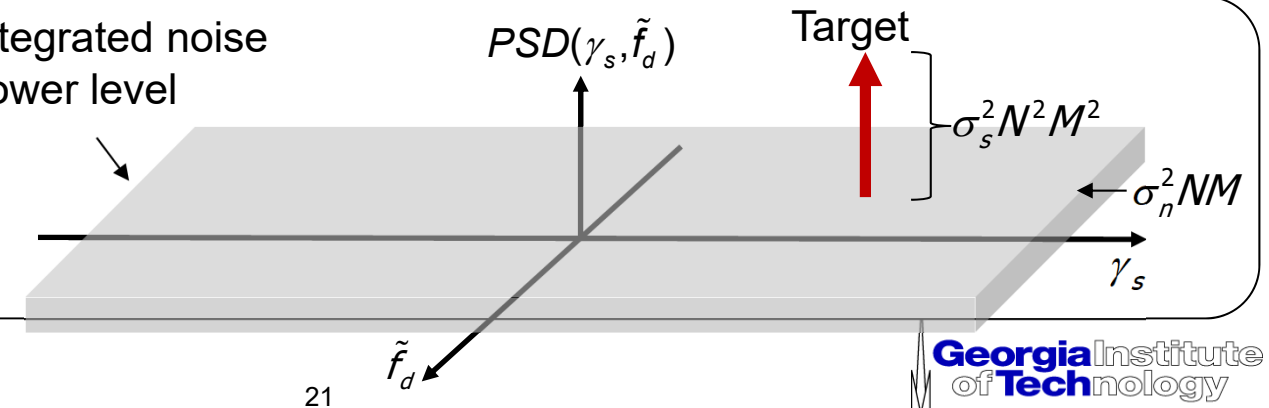
$$\mathbf{R}_x = E[\mathbf{x}\mathbf{x}^H] - \mu\mu^H = \underbrace{\sigma_s^2 \mathbf{s}_{s-t} \mathbf{s}_{s-t}^H}_{\text{mean vector}} + \underbrace{\sigma_n^2 \mathbf{I}_{NM}}_{(b)}$$

(a) Covariance matrix of sinusoid $a_s \mathbf{s}_{s-t}$
 (b) Covariance matrix of Rx noise, \mathbf{n}

Fourier transform of the covariance matrix is the PSD:

$$PSD(\gamma_s, \tilde{f}_d) = E\left[\left|\mathbf{v}_{s-t}^H(\gamma_s, \tilde{f}_d) \mathbf{x}\right|^2\right] = \mathbf{v}_{s-t}^H(\gamma_s, \tilde{f}_d) \mathbf{R}_x \mathbf{v}_{s-t}(\gamma_s, \tilde{f}_d) = \sigma_s^2 \left|\mathbf{v}_{s-t}^H(\gamma_s, \tilde{f}_d) \mathbf{s}_{s-t}\right|^2 + \sigma_n^2 NM$$

The covariance matrix encodes the characteristics of the signal environment



Outline

- Preliminaries – notation and operations
- Role of STAP in modern radar systems
- Spatial, temporal, and space-time sampling
- **Space-time signal models**
- Space-time signal processing and figures of merit
- STAP formulation
- Practical STAP implementation
- Summary

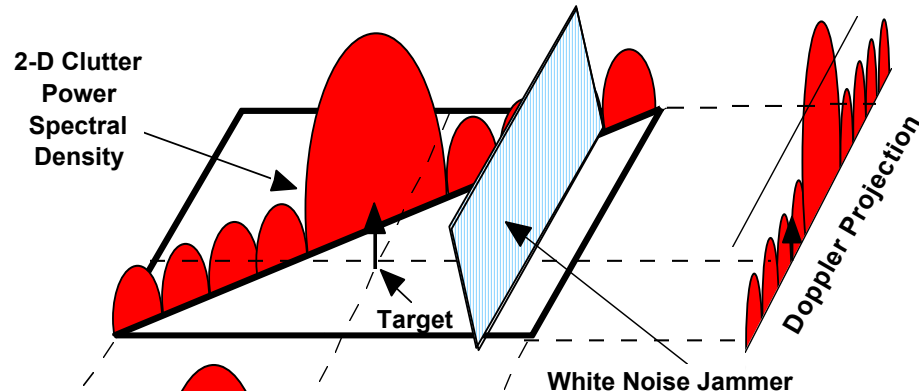
Target Model Description [12]

Model	PDF	Fluctuation Rate
Swerling 1	Rayleigh	Scan-to-scan (read “coherent over CPI”)
Swerling 2	Rayleigh	Pulse-to-pulse (read “noncoherent among CPIs”)
Swerling 3	Dominant + Rayleigh	Scan-to-scan (read “coherent over CPI”)
Swerling 4	Dominant + Rayleigh	Pulse-to-pulse (read “noncoherent among CPIs”)
Swerling 0 or 5	Delta Function	Non-fluctuating, fixed amplitude
Partially correlated	Rayleigh	Partially decorrelates pulse-to-pulse

$$\mathbf{t}_k = \alpha_T \mathbf{s}_t(\tilde{f}_d) \otimes \mathbf{s}_s(\gamma_s) = \alpha_T \mathbf{s}_{s-t}(\gamma_s, \tilde{f}_d)$$

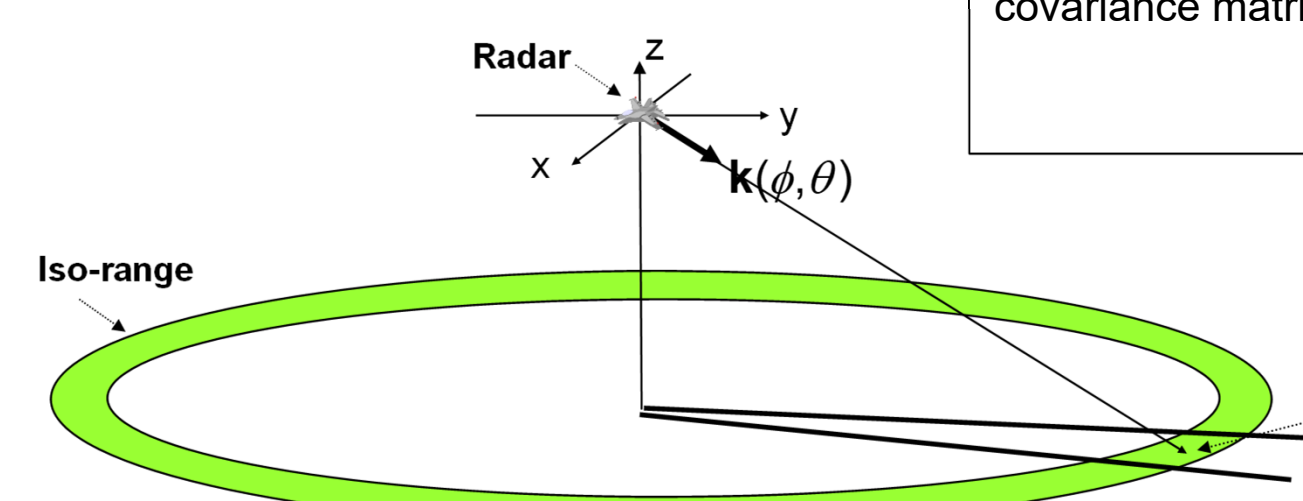
Complex voltage tied to target scattering phenomenology

Basic Ground Clutter Model [6-9]



$$\mathbf{R}_{c/k} = \sum_{m=1}^{N_c} \sum_{n=1}^{N_a} \sigma_{m,n}^2 \mathbf{s}_{s-t}(\gamma_{s/m,n}, \tilde{f}_{d/m,n}) \mathbf{s}_{s-t}^H(\gamma_{s/m,n}, \tilde{f}_{d/m,n})$$

Azimuth Projection



Voltage due to m^{th} patch,
 n^{th} range ambiguity

$$\mathbf{c}_k = \sum_{m=1}^{N_c} \sum_{n=1}^{N_a} \underbrace{\alpha_{m,n}}_{\text{Space-time steering vector}} \mathbf{s}_{s-t}(\gamma_{s/m,n}, \tilde{f}_{d/m,n})$$

Clutter space-time covariance matrix

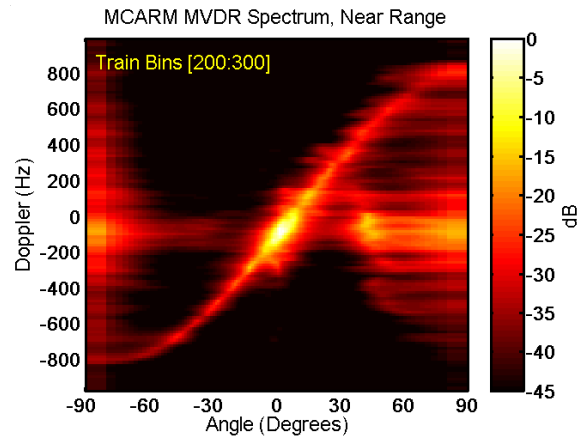
Clutter patch power

$$\sigma_{m,n}^2 = E[|\alpha_{m,n}|^2]$$

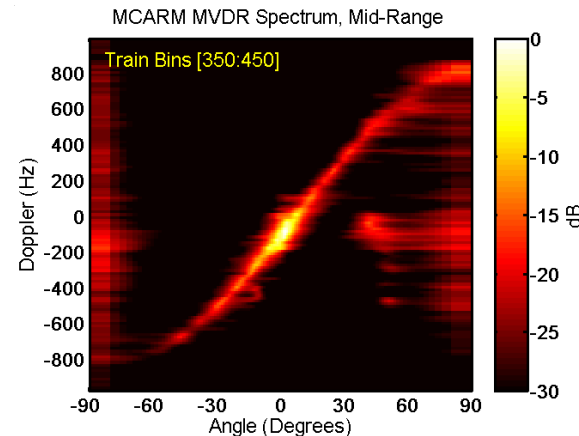
N_c = azimuthal granularity
 N_a = # of range ambiguities
 Narrowband Case

Multi-Channel Airborne Radar Measurements (MCARM) [13]

Measured MCARM MVDR spectrum estimate, training bins 200 to 300

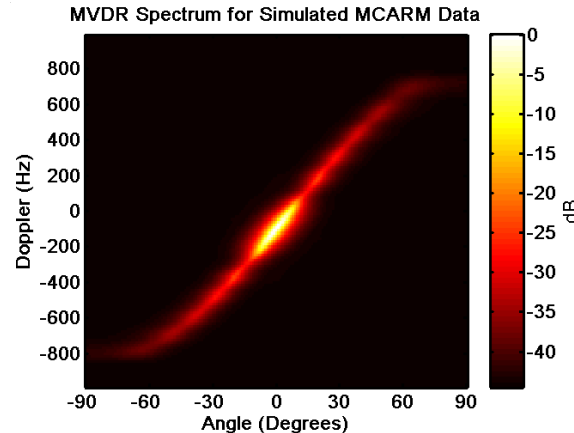


Measured MCARM MVDR spectrum estimate, training bins 350 to 450



24 Channel, L-Band Radar
Mounted on BAC 1-11

MVDR spectrum for MCARM simulation



Narrowband Radio Frequency Interference (RFI)

- Corrupts reflected signals with noise-like waveform occupying at least part of the radar receive bandwidth
 - Spatially correlated, generally white in slow-time

$n = \text{pulse number}$
 $T = \text{PRI}$

Interference waveform Spatial steering vector

$$\mathbf{j}_{s/k}(nT) = w(nT) \mathbf{s}_s(\gamma_s) \quad (\text{RFI spatial snapshot})$$

$$E[w(nT)w^*(mT)] = \sigma_j^2 \delta((n-m)T) \quad (\text{waveform correlation})$$

$$\mathbf{R}_J = \sigma_j^2 \mathbf{s}_s(\gamma_s) \mathbf{s}_s^H(\gamma_s) \in \mathbb{C}^{M \times M} \quad (\text{RFI } \mathbf{spatial} \text{ covariance matrix})$$

Single channel/single pulse interference power

$$\mathbf{R}_{\text{RFI}} = E \left[\begin{bmatrix} \mathbf{x}_J(0) \\ \vdots \\ \mathbf{x}_J((N-1)T) \end{bmatrix} \begin{bmatrix} \mathbf{x}_J^H(0) & \cdots & \mathbf{x}_J^H((N-1)T) \end{bmatrix} \right] = \mathbf{I}_N \otimes \mathbf{R}_J \in \mathbb{C}^{NM \times NM}$$

(interference **spatio-temporal** covariance matrix)

Space-Time Data Under Two Hypotheses

Signal Components

\mathbf{c}_k = clutter snapshot, k^{th} range bin; $\mathbf{c}_k \sim \mathcal{CN}(\mathbf{0}, \mathbf{R}_{c/k})$

\mathbf{n}_k = receiver noise snapshot, k^{th} range bin; $\mathbf{n}_k \sim \mathcal{CN}(\mathbf{0}, \sigma_n^2 \mathbf{I}_{NM})$

\mathbf{j}_k = interference snapshot, k^{th} range bin; $\mathbf{j}_k \sim \mathcal{CN}(\mathbf{0}, \mathbf{R}_{RFI})$

\mathbf{t}_k = target snapshot, k^{th} range bin

Hypotheses

$H_0 : \mathbf{x}_k = \mathbf{c}_k + \mathbf{j}_k + \mathbf{n}_k$ Null Hypothesis (Target Absent)

$H_1 : \mathbf{x}_k = \mathbf{t}_k + \mathbf{c}_k + \mathbf{j}_k + \mathbf{n}_k$ Alternative Hypothesis (Target Present)

Null Hypothesis Covariance Matrix

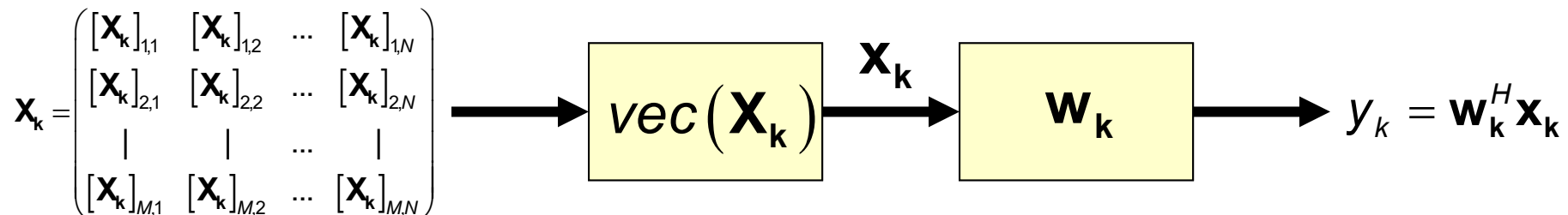
$$\mathbf{R}_{H_0} = \mathbf{R}_k = \mathbf{R}_{c/k} + \mathbf{R}_{RFI} + \sigma_n^2 \mathbf{I}_{NM}$$

Outline

- Preliminaries – notation and operations
- Role of STAP in modern radar systems
- Spatial, temporal, and space-time sampling
- Space-time signal models
- **Space-time signal processing and figures of merit**
- STAP formulation
- Practical STAP implementation
- Summary

Merging Detection Theory & Array Processing

- Detector form on previous slides valid for arbitrary \mathbf{w}_k
 - E.g., Non-adaptive beamforming and Doppler processing
 - E.g., Dispaced Phase Center Antenna (DPCA) processing
 - Other
- The prior result shows that maximizing SINR equivalently maximizes P_D for a fixed P_{FA}



$$SINR = \frac{\text{Signal Power}}{\text{Interference + Noise Power}} = \frac{E[y_{k/s}y_{k/s}^*]}{E[y_{k/H_0}y_{k/H_0}^*]} = \frac{\mathbf{w}_k^H \mathbf{R}_{k/s} \mathbf{w}_k}{\mathbf{w}_k^H \mathbf{R}_{k/H_0} \mathbf{w}_k};$$

$\mathbf{R}_{k/H_0} = E[\mathbf{x}_{k/H_0} \mathbf{x}_{k/H_0}^*]$ = Clairvoyant Interference+Noise Covariance Matrix;

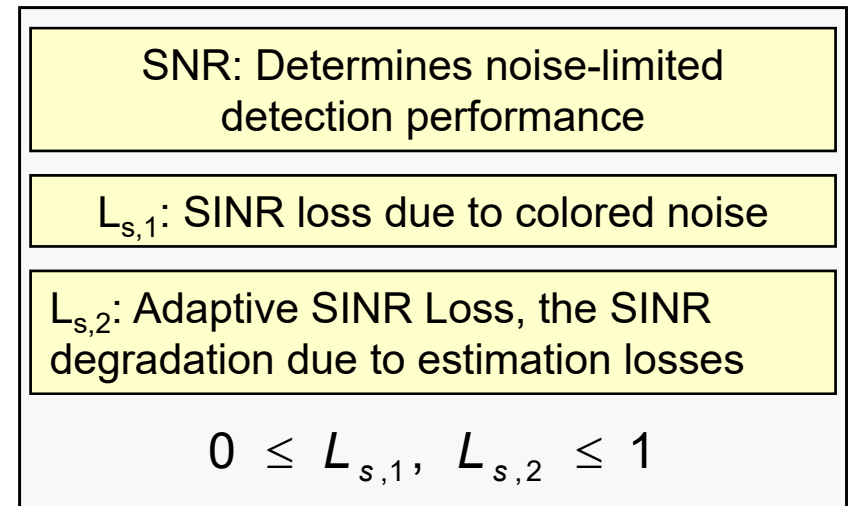
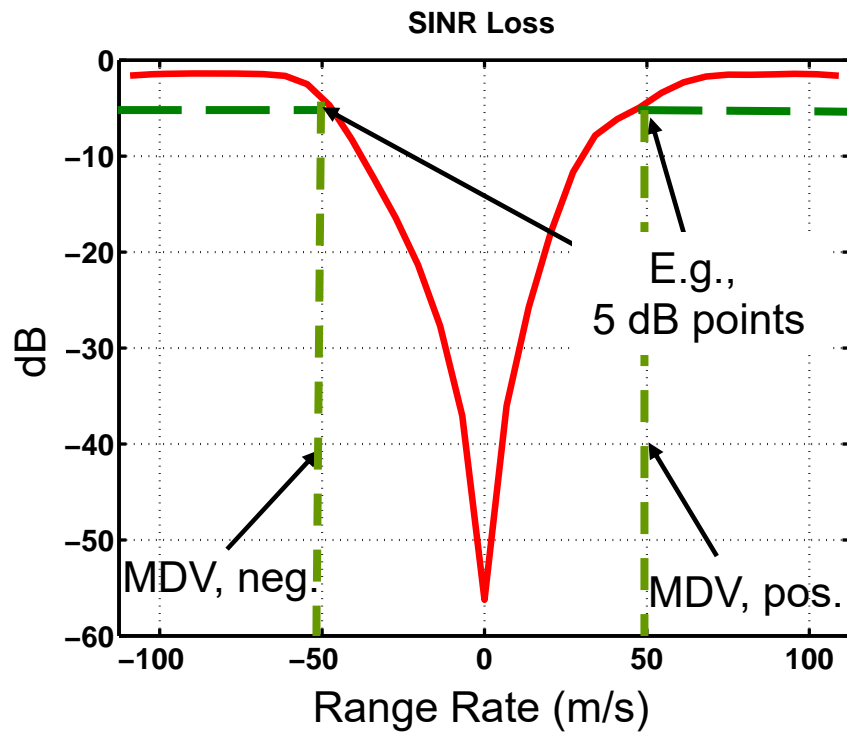
$\mathbf{R}_{k/s} = E[\mathbf{x}_{k/s} \mathbf{x}_{k/s}^*]$ = Signal Covariance Matrix.

SINR Loss [6-8]

- In the Gaussian case, SINR relates directly to P_D and P_{FA}
 - Convenient and instructive to consider SINR Loss as a key metric

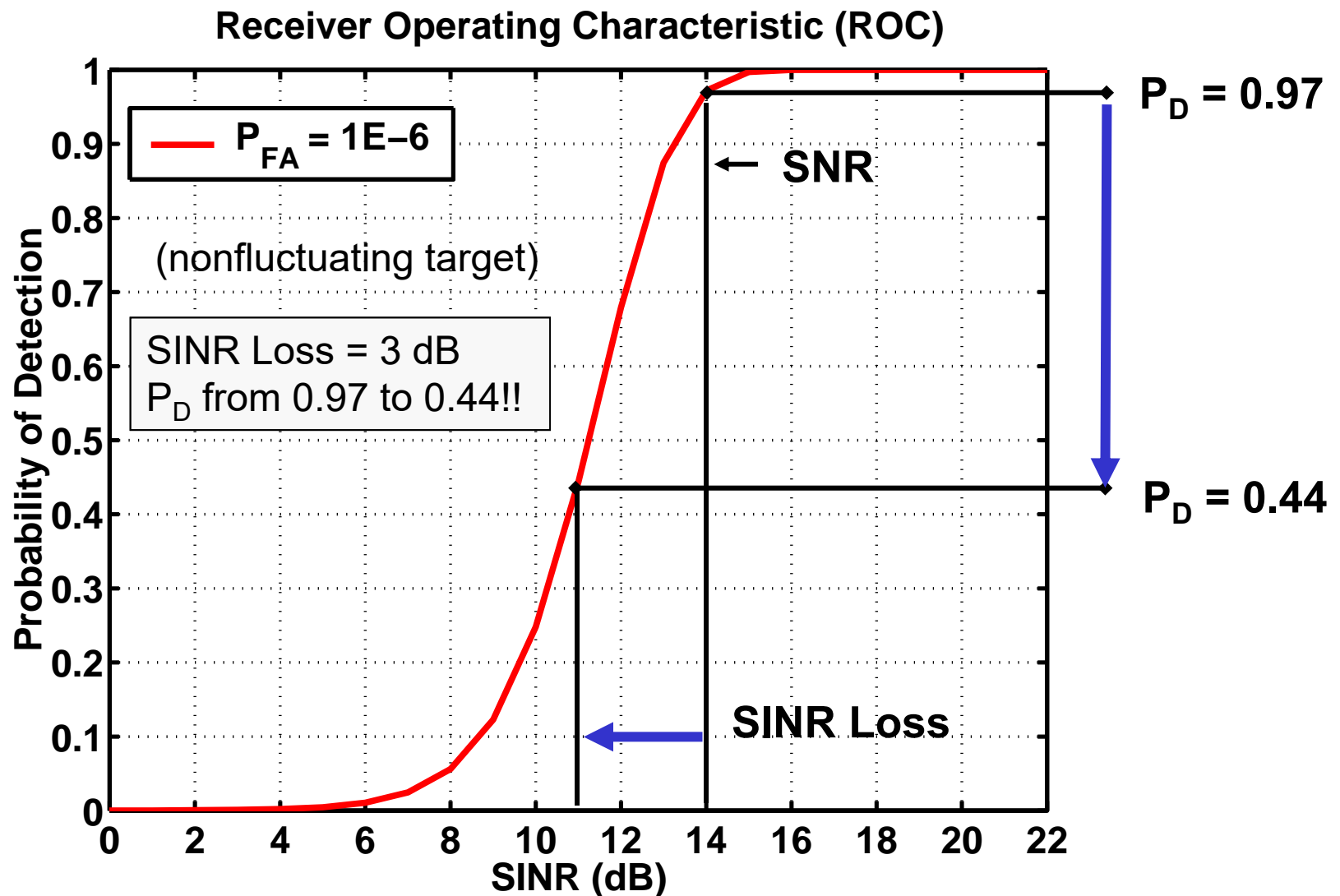
$$SINR(\gamma_s, \tilde{f}_d) = \underbrace{SNR(\gamma_s)}_{\text{Noise-Limited, RRE}} \cdot \left(\frac{SINR_{optimal}(\gamma_s, \tilde{f}_d)}{SNR(\gamma_s)} \right) \cdot \left(\frac{SINR_{adaptive}(\gamma_s, \tilde{f}_d)}{SINR_{optimal}(\gamma_s, \tilde{f}_d)} \right)$$

$$L_{s,1}(\gamma_s, \tilde{f}_d) \quad L_{s,2}(\gamma_s, \tilde{f}_d)$$



RRE = radar range equation
MDV = minimum detectable velocity

Relationship Between SNR, SINR Loss and P_D



Outline

- Preliminaries – notation and operations
- Role of STAP in modern radar systems
- Spatial, temporal, and space-time sampling
- Space-time signal models
- Space-time signal processing and figures of merit
- **STAP formulation**
- Practical STAP implementation
- Summary

The Maximum SINR Weight Vector [2-9]

Signal and I+N snapshots: $\mathbf{s}, \mathbf{x}_n \in \mathbb{C}^{NM \times 1}$

Target signal: $\mathbf{s} = \alpha_T \mathbf{s}_{s-t}(\gamma_s, \tilde{f}_d)$; $\sigma_s^2 = E\left[\left|\alpha_T / \sqrt{2}\right|^2\right]$

Interference-plus-noise signal: $\mathbf{x}_n \sim \mathcal{CN}(\mathbf{0}, \mathbf{R}_n = \mathbf{R}_{H_0} = \mathbf{R}_k)$

$$\begin{aligned}
 SINR &= \frac{P_s}{P_n} = \frac{E[y_s y_s^*]}{E[y_n y_n^*]} = \frac{E[(\mathbf{w}^H \mathbf{s})(\mathbf{s}^H \mathbf{w})]}{E[(\mathbf{w}^H \mathbf{x}_n)(\mathbf{x}_n^H \mathbf{w})]} = \frac{\mathbf{w}^H \mathbf{R}_s \mathbf{w}}{\mathbf{w}^H \mathbf{R}_n \mathbf{w}} \\
 &= \sigma_s^2 \frac{|\tilde{\mathbf{w}}^H \tilde{\mathbf{s}}|^2}{\tilde{\mathbf{w}}^H \tilde{\mathbf{w}}} \leq \sigma_s^2 \frac{(\tilde{\mathbf{w}}^H \tilde{\mathbf{w}})(\tilde{\mathbf{s}}^H \tilde{\mathbf{s}})}{\tilde{\mathbf{w}}^H \tilde{\mathbf{w}}}
 \end{aligned}$$

\$\mathbf{R}_s = \sigma_s^2 \mathbf{s}_{s-t} \mathbf{s}_{s-t}^H\$
\$y_s = \mathbf{w}^H \mathbf{s}\$
\$y_n = \mathbf{w}^H \mathbf{x}_n\$

$\tilde{\mathbf{w}} = \mathbf{R}_n^{1/2} \mathbf{w}; \quad \tilde{\mathbf{s}} = \mathbf{R}_n^{-1/2} \mathbf{s}_{s-t}(\gamma_s, \tilde{f}_d)$

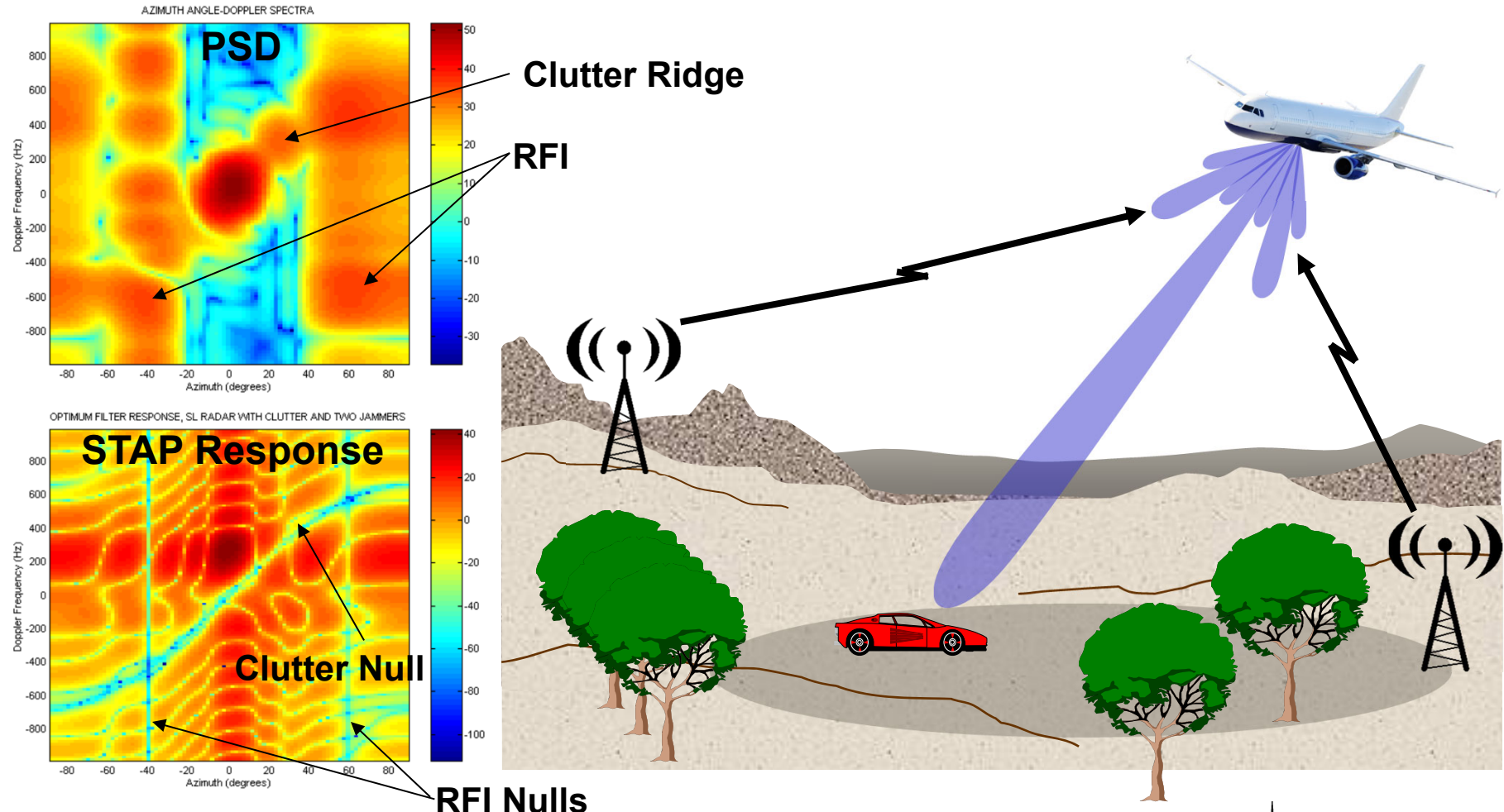
Achieves the upper bound when $\tilde{\mathbf{w}} = \tilde{\mathbf{s}}$, or $\mathbf{w} = \mu \mathbf{R}_n^{-1} \mathbf{s}_{s-t}(\gamma_s, \tilde{f}_d) \dots$

$$SINR_{\max} = \sigma_s^2 \mathbf{s}_{s-t}^H \mathbf{R}_n^{-1} \mathbf{s}_{s-t}$$

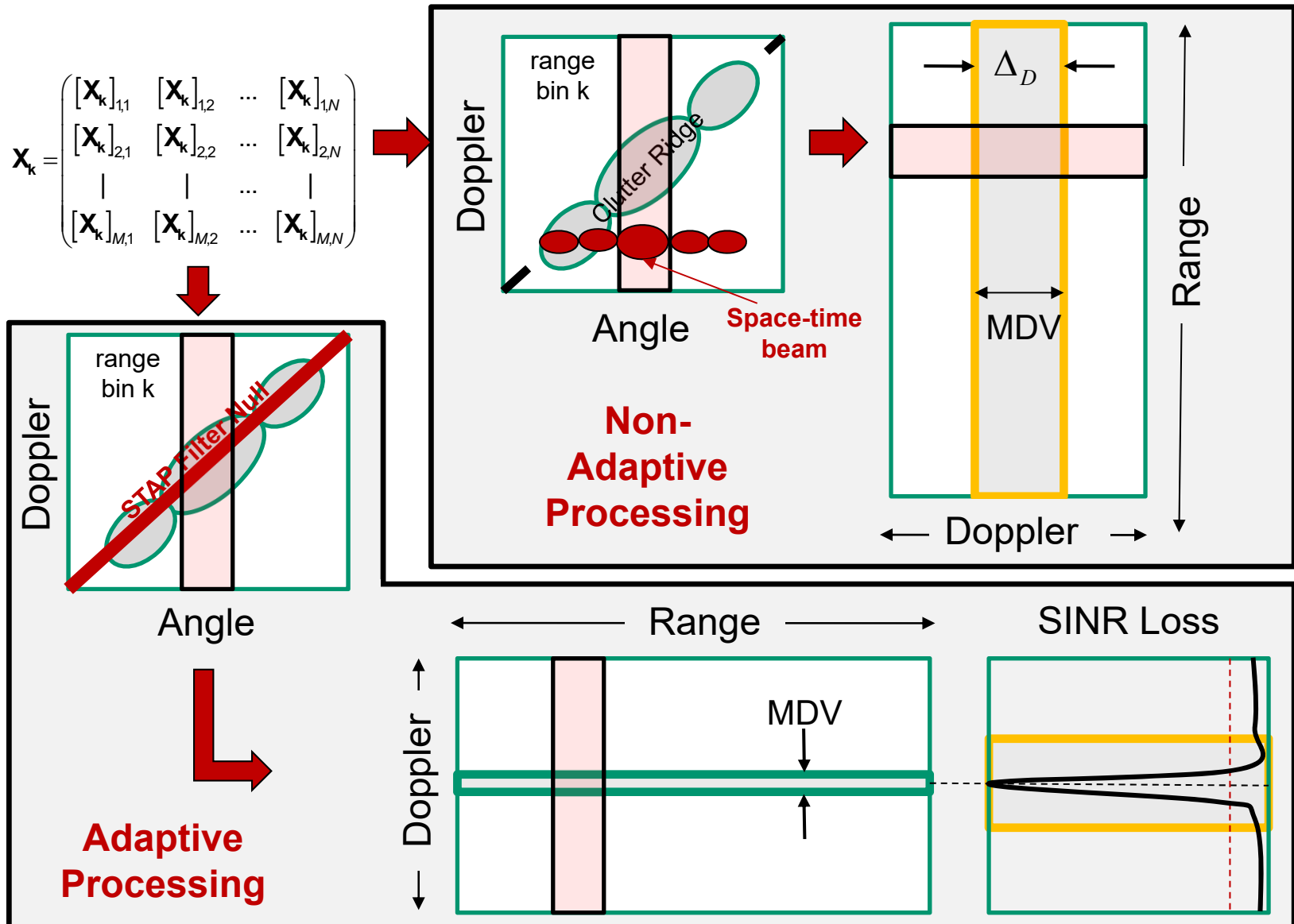
Arbitrary scalar

Space-Time Adaptive Processing (STAP)

Space-time adaptivity enables simultaneous clutter and RFI suppression (**Detection of interference-limited, moving targets**)



STAP Range-Doppler Map (RDM) [10]



Maximum Likelihood Estimate (MLE) [11]

(Reed, Mallett and Brennan (RMB) Rule)

$$\hat{\mathbf{R}}_k = \frac{1}{K} \sum_{\substack{m=1 \\ m \neq k}}^K \mathbf{x}_m \mathbf{x}_m^H$$

Assuming \mathbf{x}_m are independent and identically distributed (*iid*) interference plus noise samples only:

$$\rho(\hat{\mathbf{R}}_k) = (\text{SINR} | \hat{\mathbf{w}}_k) / (\text{SINR}_{\text{Optimum}}) = L_{s,2}$$

$$E[\rho(\hat{\mathbf{R}}_k)] = (K + 2 - M_d) / (K + 1)$$

$$M_d = \dim(\mathbf{x}_m) \quad (= NM)$$

To be, on average,
within 3dB of optimum:

$$K = 2NM - 3$$

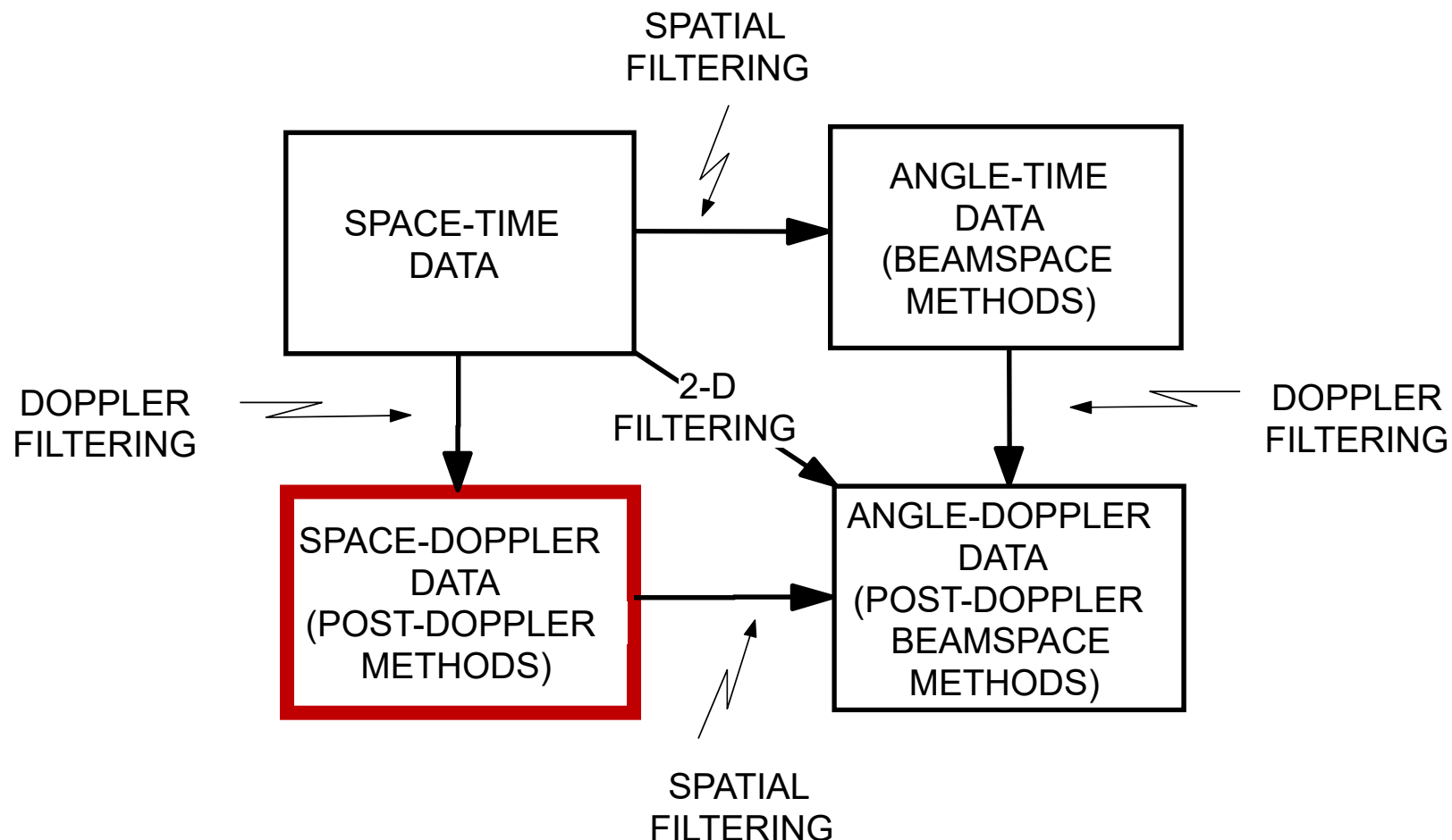
Issues

- Finite Sample Support
- Nonstationary Clutter
- Heterogeneous Clutter [13]

Outline

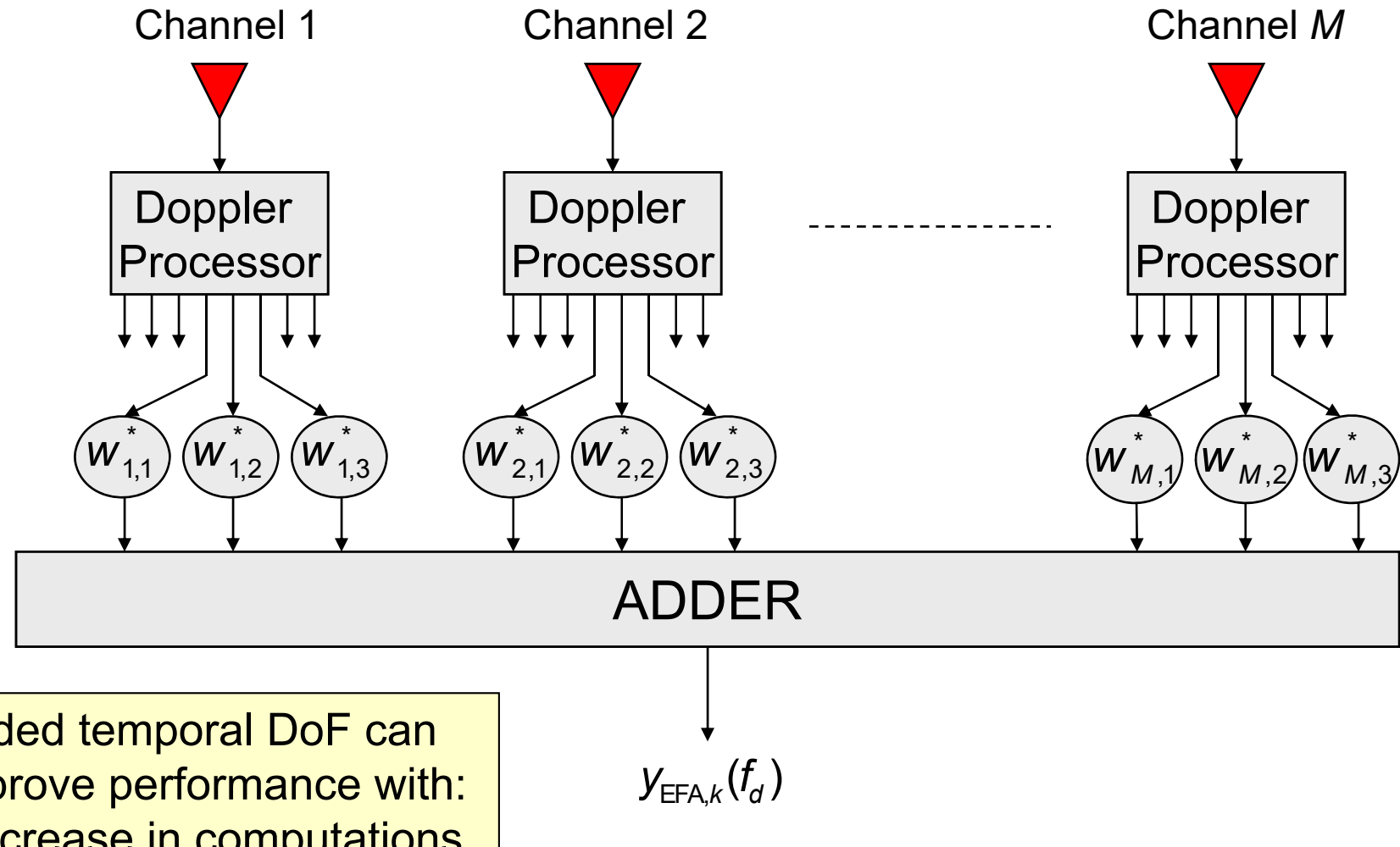
- Preliminaries – notation and operations
- Role of STAP in modern radar systems
- Spatial, temporal, and space-time sampling
- Space-time signal models
- Space-time signal processing and figures of merit
- STAP formulation
- **Practical STAP implementation**
- Summary

Reduced-Dimension STAP Processing [6]

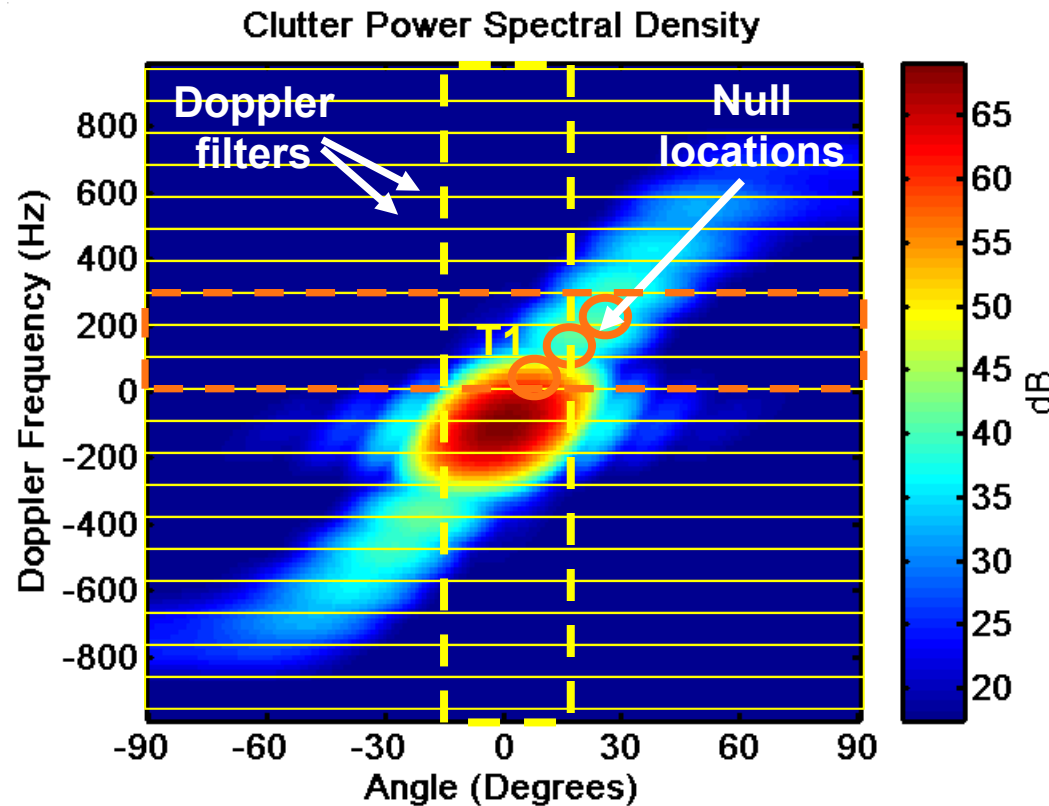


Advantages: (1) Reduced computational burden;
(2) Reduced training sample requirements

Extended Factored Approach (EFA) [14]



EFA Operation



- Can place $N_t M - 1$ nulls along a diagonal line
 - N_t is temporal DoF
- Provides good performance in endo-clutter region

Mathematical Description of RD-STAP Methods

$$\tilde{\mathbf{x}}_k = \mathbf{T}_{RD}^H \mathbf{x}_k \in \mathbb{C}^{Px1}; \quad P \ll NM \quad \tilde{\mathbf{s}} = \mathbf{T}_{RD}^H \mathbf{s}_{s-t} \in \mathbb{C}^{Px1}$$

$$\tilde{\mathbf{R}}_k = E\left[\mathbf{T}_{RD}^H \mathbf{x}_k \mathbf{x}_k^H \mathbf{T}_{RD}\right] \in \mathbb{C}^{PxP} \Rightarrow \tilde{\mathbf{R}}_k = \mathbf{T}_{RD}^H \mathbf{R}_k \mathbf{T}_{RD}$$

$$\tilde{\mathbf{w}}_k = \tilde{\mu}_{RD} \tilde{\mathbf{R}}_k^{-1} \tilde{\mathbf{s}} \Rightarrow \hat{\tilde{\mathbf{w}}}_k = \hat{\tilde{\mu}}_{RD} \hat{\tilde{\mathbf{R}}}_k^{-1} \tilde{\mathbf{v}}$$

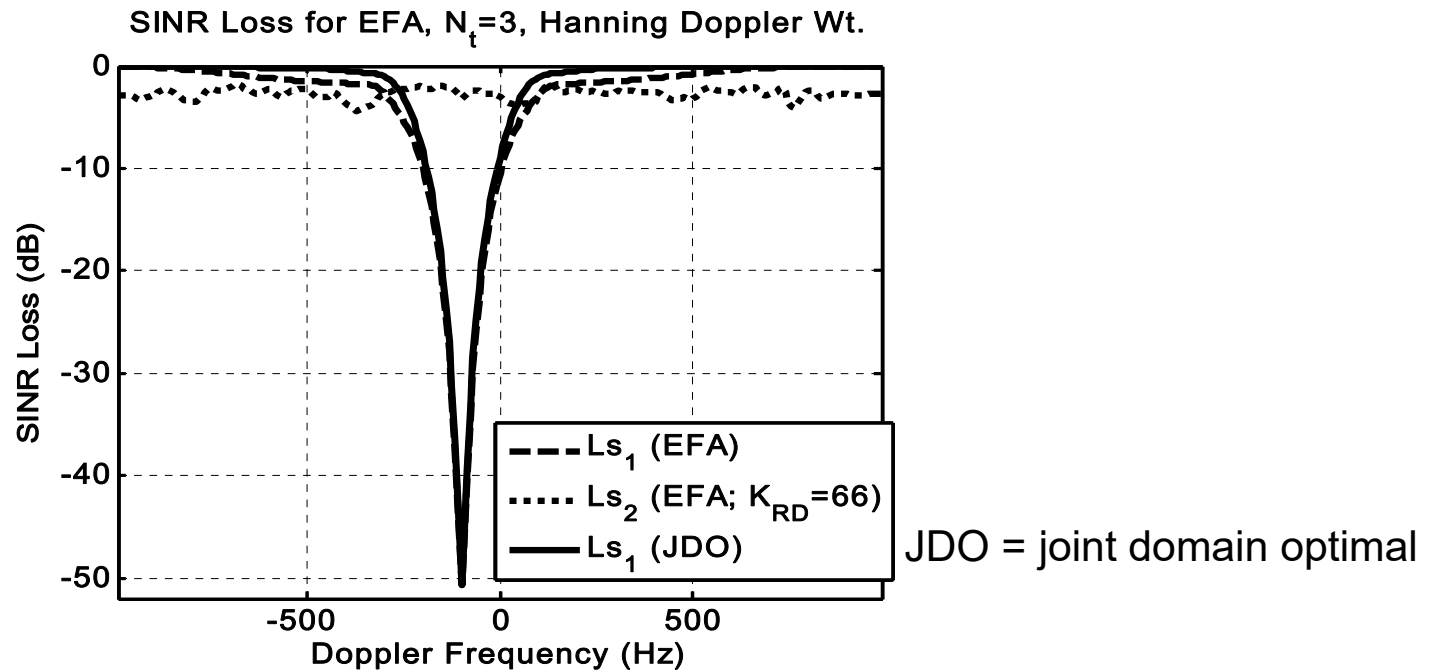
clairvoyantadaptive

$$\hat{\tilde{\mathbf{R}}}_k = \frac{1}{K_{RD}} \sum_{m=1}^{K_{RD}} \tilde{\mathbf{x}}_m \tilde{\mathbf{x}}_m^H$$

(see [6-8])

- SINR and SINR loss calculated in usual manner
 - Ratio of quadratics or ratio of quadratic forms
 - \mathbf{T}_{RD} needed to benchmark algorithms
 - In some cases, \mathbf{T}_{RD} needed for implementation

Performance Comparison of EFA to Full-Dimension STAP



- Performance bound for the optimal space-time processor and EFA with a training window size equal to twice the processor's adaptive DoFs
- Doppler offset a result of a yaw angle of approximately six degrees
- CNR is on the order of 50-55 dB

Outline

- Preliminaries – notation and operations
- Role of STAP in modern radar systems
- Spatial, temporal, and space-time sampling
- Space-time signal models
- Space-time signal processing and figures of merit
- STAP formulation
- Practical STAP implementation
- **Summary**

Summary

- Provided a high-level overview on STAP...see the references for more information!
- STAP is a data-adaptive approach to mitigate clutter and RFI
 - Narrowband RFI → spatial nulling
 - Ground clutter → spatial and slow-time nulling (angle-Doppler)
 - Wideband RFI → spatial and fast-time nulling (angle-RF frequency)
- The covariance matrix “models” the interference environment
 - STAP is a super-resolution technique...separates target and interference to within a fraction of a beamwidth
- Practical STAP issues: reduced-dimension STAP, covariance matrix estimation

References

- [1] D.H. Johnson and D.E. Dudgeon, Array Signal Processing: Concepts and Techniques, Prentice-Hall, Englewood Cliffs, NJ, 1993.
- [2] L.E. Brennan and I.S. Reed, "Theory of adaptive radar," *IEEE Trans. AES*, Vol. 9, No. 2, March 1973, pp. 237-252.
- [3] R. Klemm, Space-Time Adaptive Processing: Principles and Applications, IEE Radar, Sonar, Navigation and Avionics 9, IEE Press, 1998.
- [4] R. Klemm, Principles of Space-Time Adaptive Processing, 2nd Ed., IEE Radar, Sonar, Navigation and Avionics 12, IEE Press, UK, 2002.
- [5] J.R. Guerci, Space-Time Adaptive Processing for Radar, Artech House, Norwood, MA, 2003.
- [6] J. Ward, Space-Time Adaptive Processing for Airborne Radar, Lincoln Laboratory Tech. Rept., ESC-TR-94-109, December 1994.
- [7] W.L. Melvin, "STAP overview," *IEEE AES Systems Magazine – Special Tutorials Issue*, Vol. 19, No. 1, January 2004, pp. 19-35.
- [8] W.L. Melvin, "Space-time adaptive processing for radar," Academic Press Library in Signal Processing. Vol. 2, Communications and Radar Signal Processing, Eds. Rama Chellappa, Sergios Theodoridis, Academic Press, ISBN 978-0-12-396500-4, 2014, pp. 595-665.
- [9] W.L. Melvin, "Clutter suppression using space-time adaptive processing," in Principles of Modern Radar: Advanced Techniques, ed. W. Melvin and J. Scheer, Sci-Tech Publishing, 2011.
- [10] William Melvin, "Surface moving target indication," in Principles of Modern Radar: Radar Applications, Chapter 9, Eds. W.L. Melvin and J.A. Scheer, SciTech Publishing, 2013.
- [11] I.S. Reed, J.D. Mallett, and L.E. Brennan, "Rapid convergence rate in adaptive arrays," *IEEE Trans. AES*, Vol. 10, No. 6, November 1974, pp. 853-863.
- [12] M.I. Skolnik, Introduction to Radar Systems, 2nd Ed., McGraw Hill, New York, NY, 1980.
- [13] W.L. Melvin and G.A. Showman, "Knowledge-aided parametric covariance estimation," *IEEE Trans. AES*, July 2006, pp. 1021-1042.
- [14] R.C. DiPietro, "Extended factored space-time processing for airborne radar," in *Proc. 26th Asilomar Conf.*, Pacific Grove, CA, Oct. 1992, pp. 425-430.

Meteorological Radars

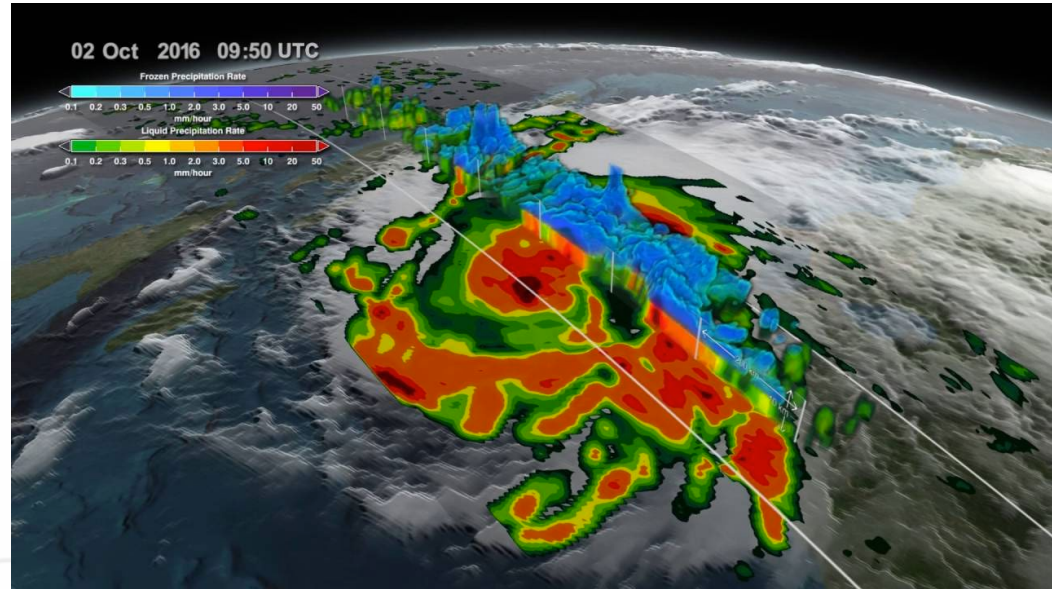
Pavlos Kollias

Stony Brook University
Brookhaven National Laboratory

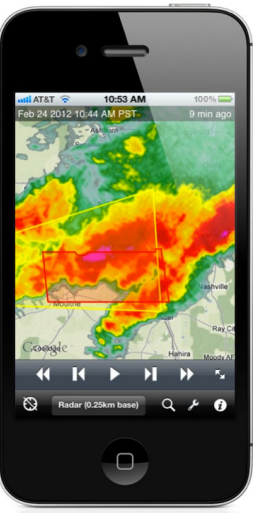
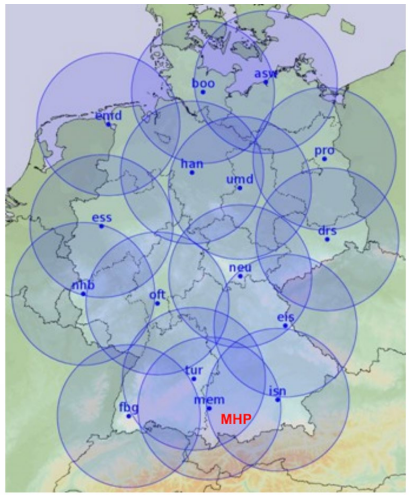


Radar Applications in Meteorology

- Precipitation measurements
- Cloud measurements
- Wind measurements
- Turbulence detection
- Severe storm nowcasting
- Hail detection
- Hurricane structure



Use of Radars in Meteorology



Agriculture

Aviation

Energy & Utilities

Ground Transportation

Insurance

Hydrology

Flash Flooding



SCIENCE

University

haven™ National Laboratory

Meteorological Radar Primer I

Radars transmit their own microwave energy and measure the properties of the return signal:

Amplitude (~size of particles)

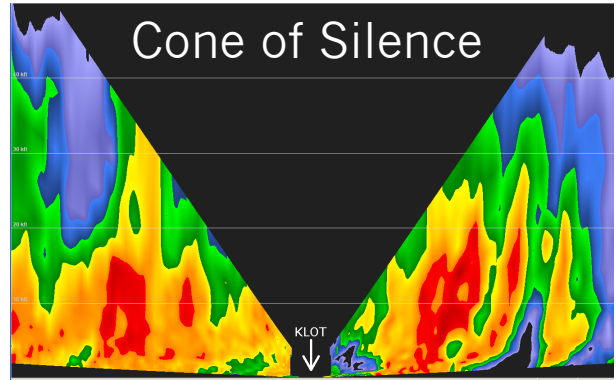
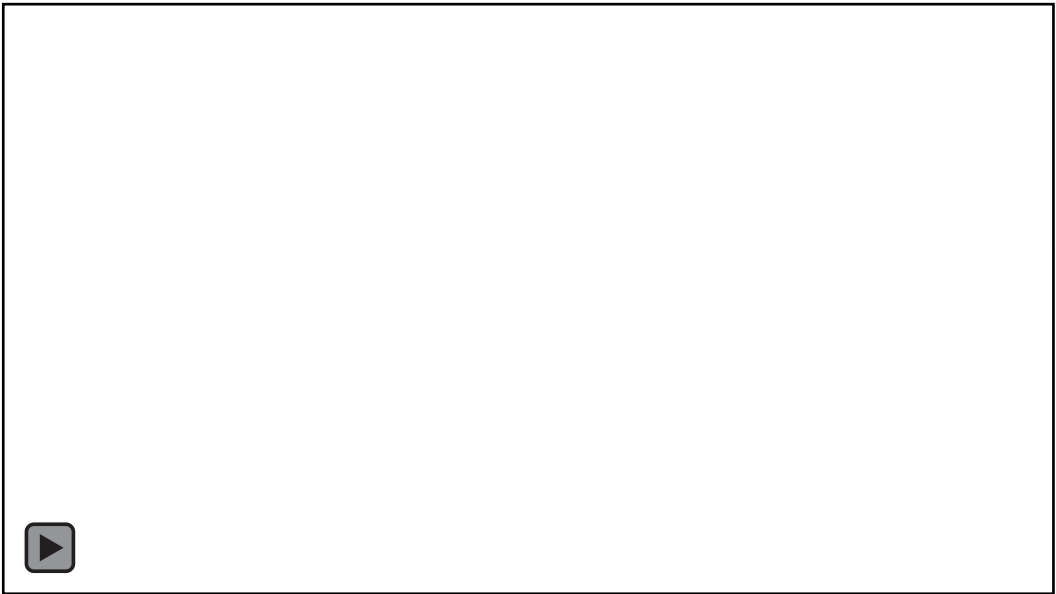
Phase (~motion)

Polarization (~mass, particle shape)

During the last 2 decades considerable progress in signal processing, transmitted waveform, data quality and multi-parametric inversions has been achieved.



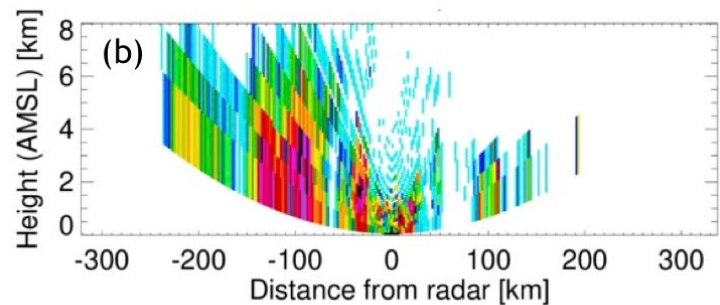
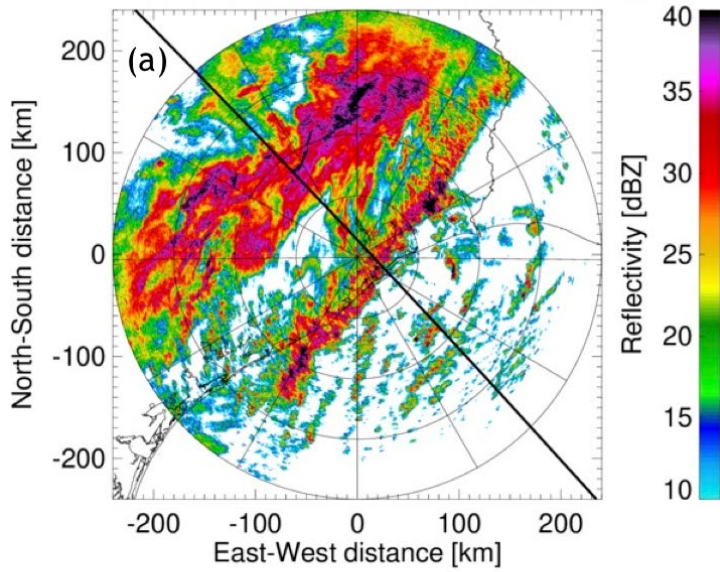
Meteorological Radar Primer II



Sit and spin scan strategy

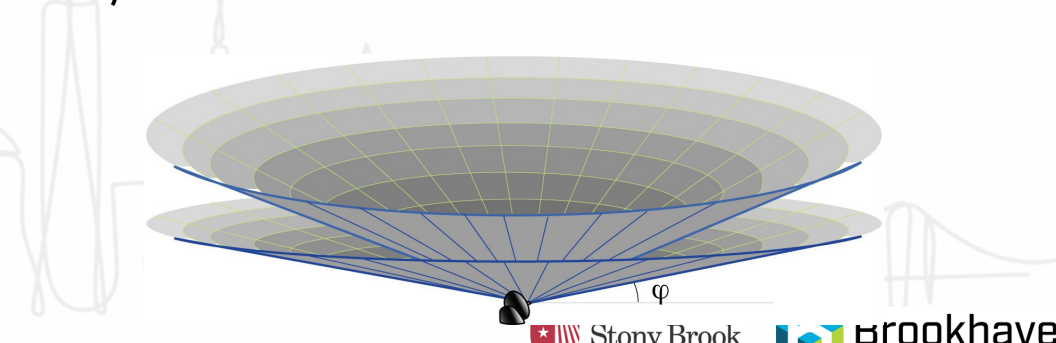


23/01/2019 08:12:07 / Elevation 0.483°

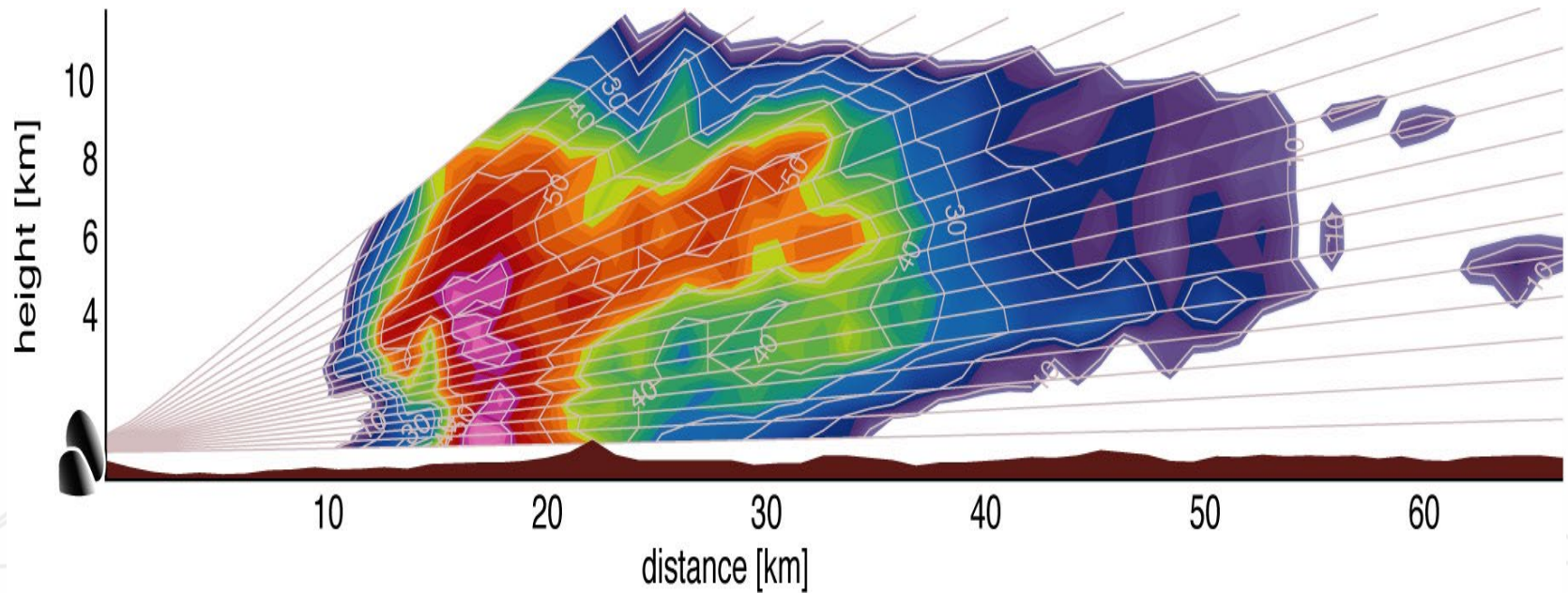


Meteorologists are interested not only in 2-D (horizontal) maps of precipitation but also in the 3-D structure of storms. Scanning radars can provide the data for it by first using an appropriate scanning strategy to sample the atmosphere.

Operational radars will typically sample the atmosphere by performing scans at several elevation angles every few minutes (typically 5 to 10) called *volume scans*.



RHI (Range-Height indicator): A vertical cross-section of radar parameters for a given azimuthal direction.



Radar bands

Radar Band	Frequency (f)*	Wavelength (λ)*
L	1 – 2 GHz	15 – 30 cm
S	2 – 4 GHz	8 – 15 cm
C	4 – 8 GHz	4 – 8 cm
X	8 – 12 GHz	2.5 – 4 cm
K _u	12 – 18 GHz	1.7 – 2.5 cm
K	18 – 27 GHz	1.2 – 1.7 cm
K _a	27 – 40 GHz	0.75 – 1.2 cm
W	40 – 300 GHz	1 – 7.5 mm



Wind Profilers



Operational Weather Radars



Short-range Weather Radars



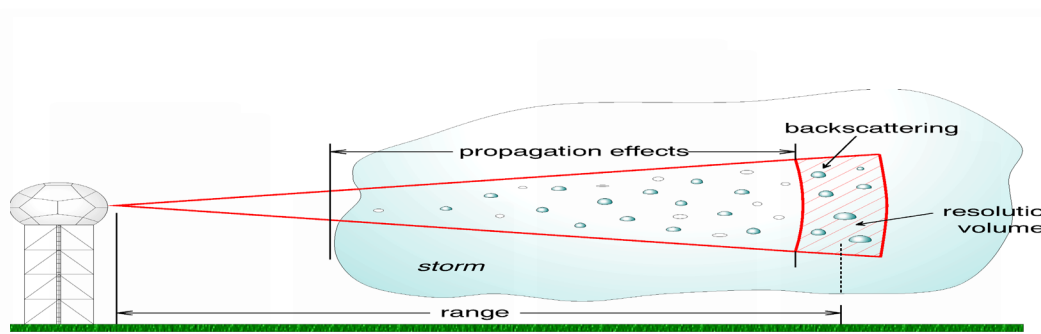
Cloud Radars

* Note: $\lambda f = c$

Adapted from Rinehart (2004)

Propagation of Radar Waves in the Atmosphere

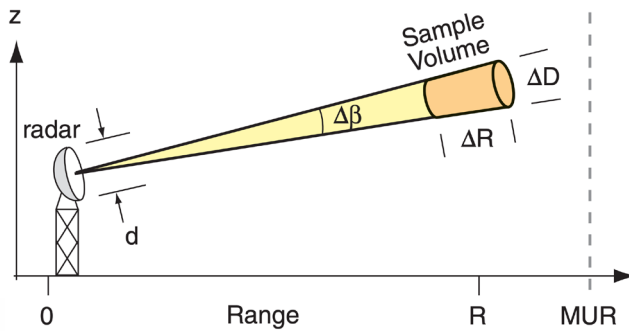
The radio wave frequency used by weather radars is specifically chosen for its ability to "interact" with cloud and precipitation particles.



Propagation effect refers to the process whereby cloud and precipitation particles, as a whole, work to modify the power and phase of the transmitted signal. These changes gradually accumulate as the wave propagates through the atmosphere, clouds, and precipitation (and, after being reflected, back through the precipitation, clouds, and atmosphere to the radar again).

The meteorological radar volume

$$Volume = \frac{\pi}{4} R^2 \Delta\beta^2 dR$$



In contrast to single-target applications (e.g., military or air-traffic control), the targets in meteorology are distributed over large volumes. Thus, it is more practical to use the backscattering cross section per sampling volume, also called radar reflectivity η (m^2 per m^3)

Radar cross-section of volume

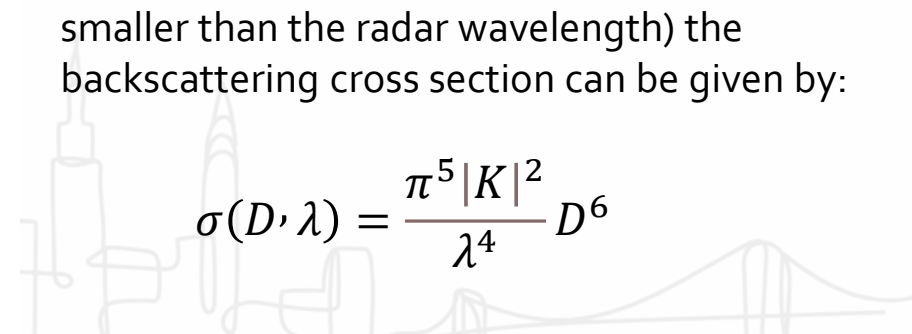
$$\sigma_{vol} = \sum_k^{N_{tot}} \sigma_k = \sum_i^{N_{m3}} \sigma_i \cdot Volume$$

$$\sigma_{vol} = \eta \cdot Volume$$

reflectivity

In case of Rayleigh scattering (particles much smaller than the radar wavelength) the backscattering cross section can be given by:

$$\sigma(D, \lambda) = \frac{\pi^5 |K|^2}{\lambda^4} D^6$$



Doviak and Zrnic, 1993

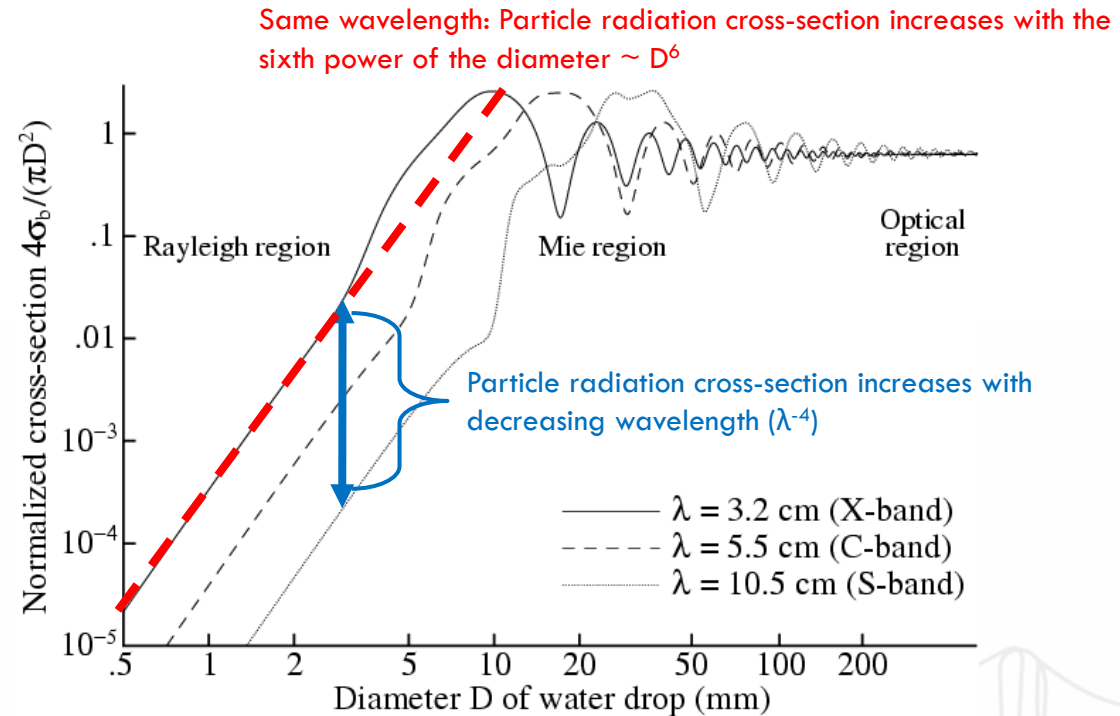
Hydrometeors (rain, snow, hail...). For most radars, they are Rayleigh scatterers for which scattering is proportional to $D^6\lambda^{-4}$

Double the particle size, 64 times more backscattering

Ten times larger particle, 10^6 times more backscattering

Shorten the radar wavelength by a factor of 10, and the particle backscattering increases by 10^4

Kollias et al., 2007 BAMS



Weather Radar Equation

Assuming Rayleigh scattering spheres of diameter D

Received
Power (mW)

$$\bar{P}_r = \frac{\pi^3 c}{1024 \ln 2} \left[\frac{P_t \tau G^2 \theta^2}{\lambda^2} \right] \left[|\kappa|^2 \frac{Z}{r^2} \right]$$

const



radar

target

$$10 \log \bar{P}_r = 10 \log Z - 20 \log r + C$$

C is a constant determined by radar parameters and the dielectric character of the target

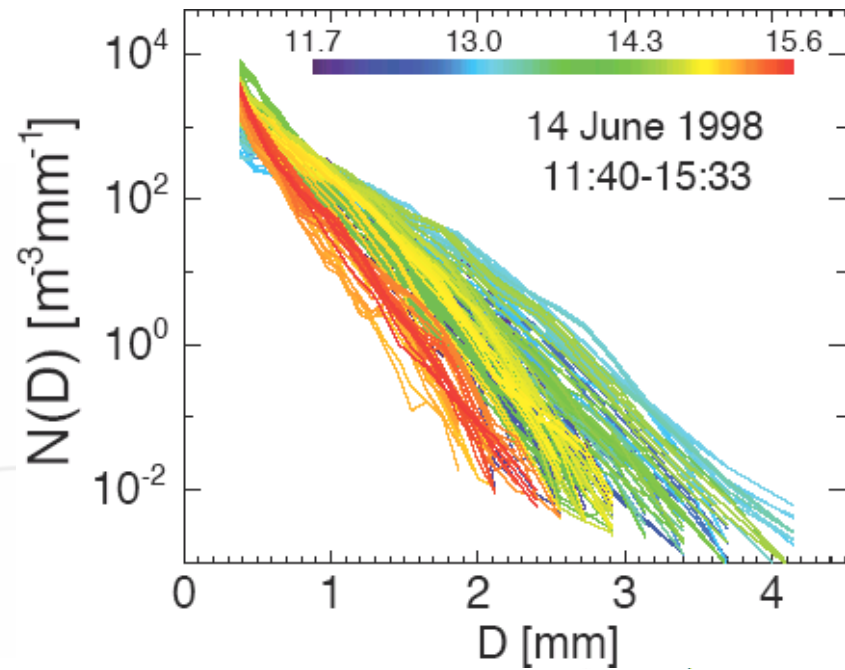


Introduce the radar reflectivity factor Z, where

$$Z \left[\text{mm}^6 \text{m}^{-3} \right] \equiv \frac{1}{\Delta V} \sum_{\Delta V} D^6 = \int_{D_{\min}}^{D_{\max}} D^6 N(D) dD$$

where $N(D)dD$ is the number of drops of a given diameter per unit volume.

$$Z[\text{dBZ}] = 10 \log(Z[\text{mm}^6 \text{m}^{-3}])$$



Radar Reflectivity factor

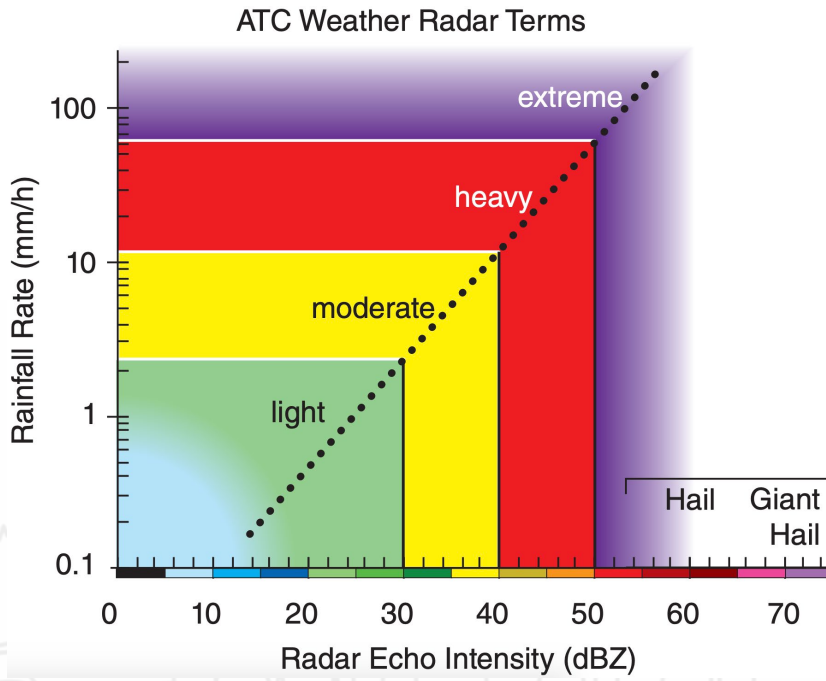
Because the reflectivity factor spans several orders of magnitude, it is generally expressed in "dBZ":

$$dBZ = 10 \log_{10}(Z);$$

Example:

$$Z = 200 \text{ mm}^6/\text{m}^3 \rightarrow$$

$$dBZ = 10 \log_{10}(200) \\ = 23 \text{ dBZ}$$



Reflectivity – Rainfall/Cloud Relations

reflectivity ($\text{mm}^6 \text{m}^{-3}$)

$$z = \int_D D^6 N(D) dD$$

liquid water content (gm^{-3})

$$\text{LWC} = \frac{\pi}{6} \int_D D^3 N(D) dD$$

raindrop volume

rainfall rate (mm h^{-1})

$$R = \frac{\pi}{6} \int_D D^3 v(D) N(D) dD$$

terminal fall velocity

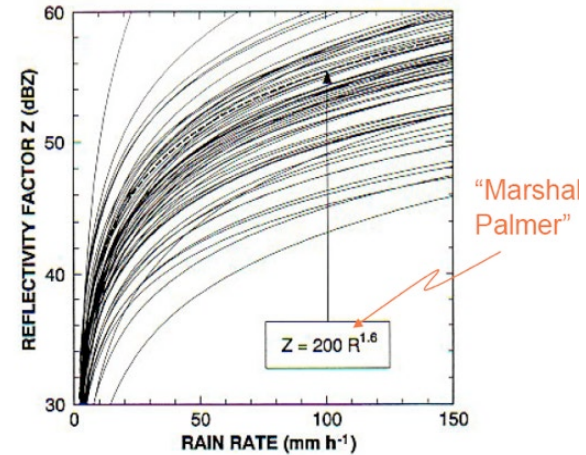


Fig. 8.6 Sixty-nine R , Z relationships from Battan (1973).

The radar “bright” band and melting snow

For rain, $|K|^2 \sim 0.9$,
For snow, $|K|^2 \sim 0.2$

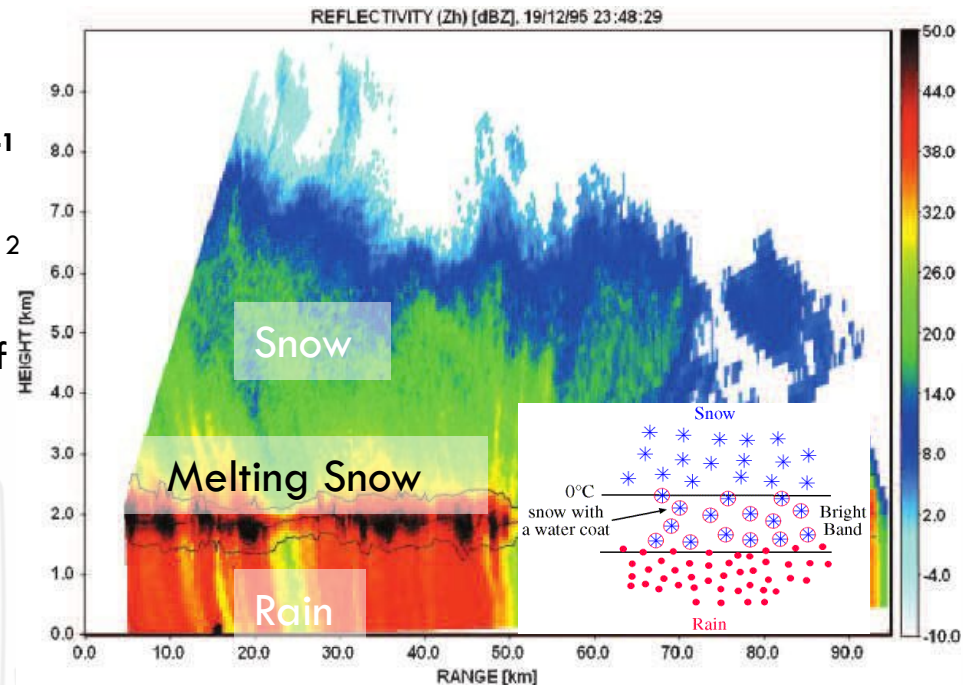
$$V_{\text{rain}} \sim 6 \text{ ms}^{-1}$$
$$V_{\text{snow}} \sim 1.5 \text{ ms}^{-1}$$

When a snowflake melts, it gets water covered ($|K|^2$ increases rapidly towards 0.9) but its density and fall speed only increase slowly; hence the number of hydrometeors per unit volume remains high.

--> $|K|^2 Z$ (or received power) increases.

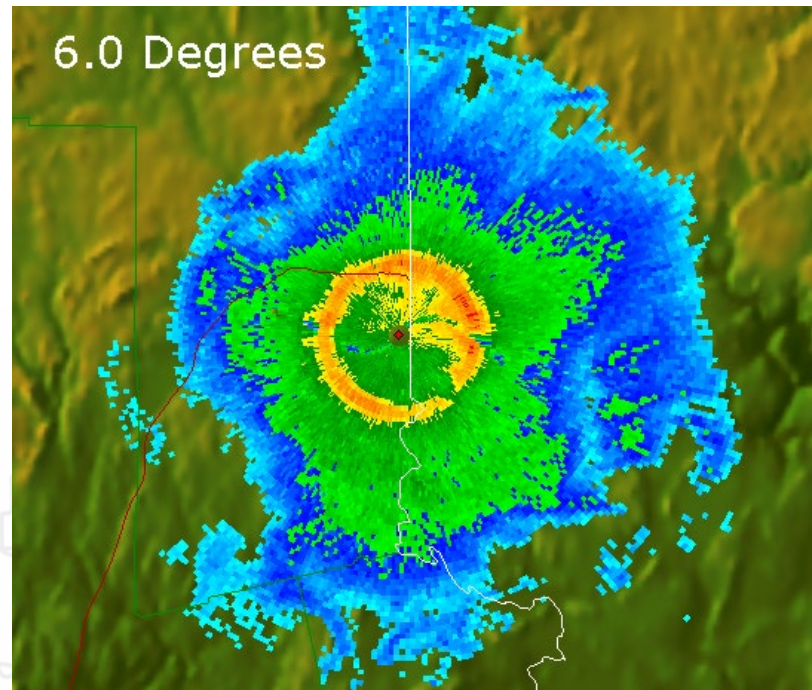
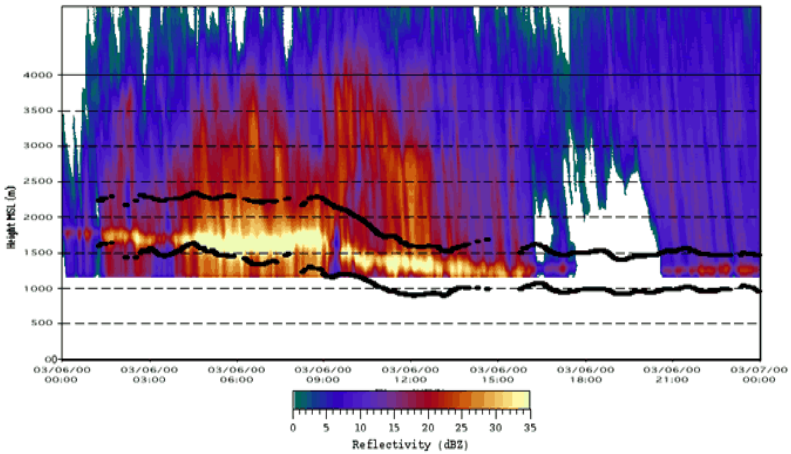
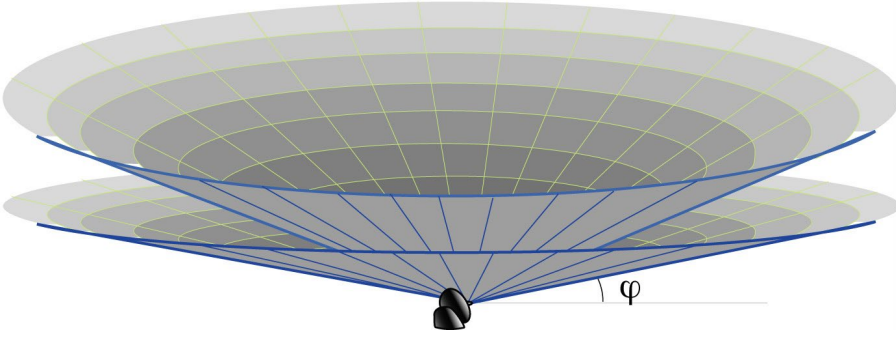
At the final stages of melting, the ice structure collapses, and the melted snowflakes speed up and spread apart.

--> $|K|^2 Z$ (or received power) decreases.

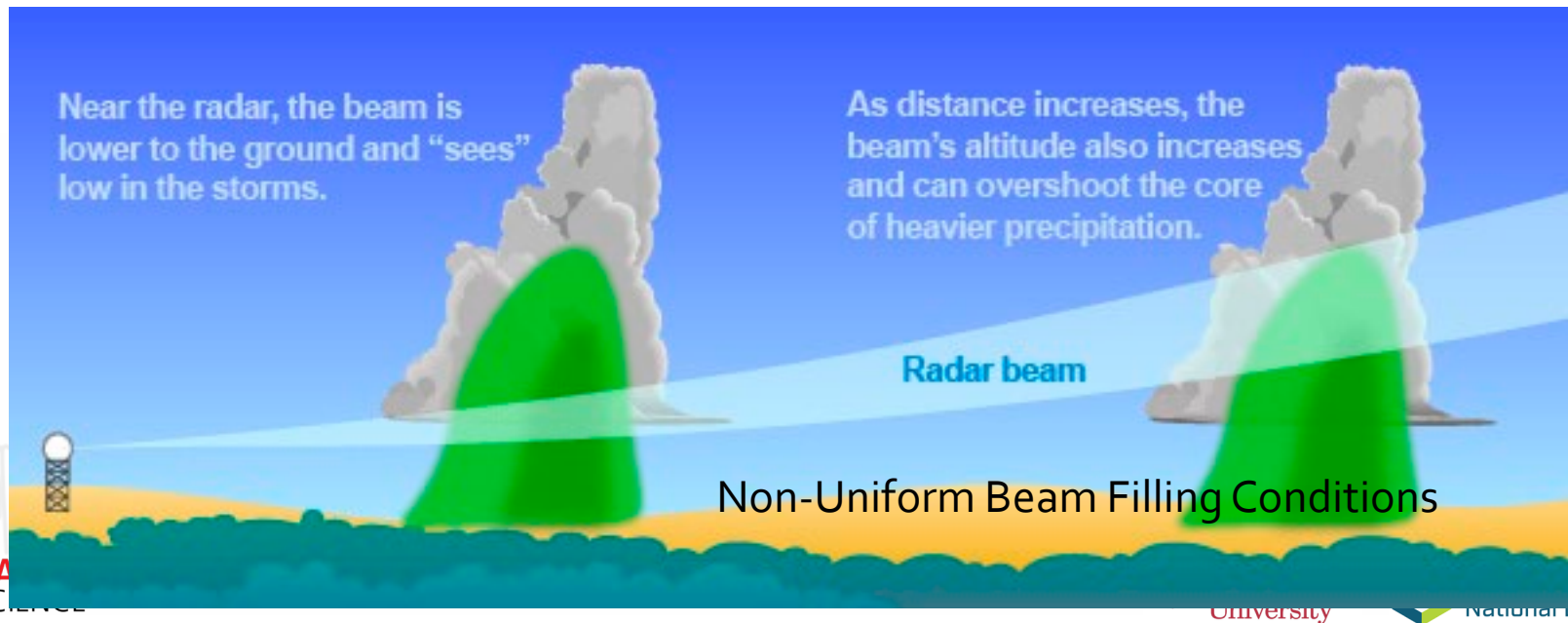


Rico-Ramirex and Cluckie, 2007

The radar “bright” band and melting snow



Big implication of radar beam height increasing with range (under normal propagation conditions) combined with broadening of the radar beam: *The radar cannot “see” the low level structures of storms, nor resolve their spatial structure as well as at close ranges. Thus, for purposes of radar applications such as rainfall estimation, the uncertainty of the measurements increases markedly with range.*



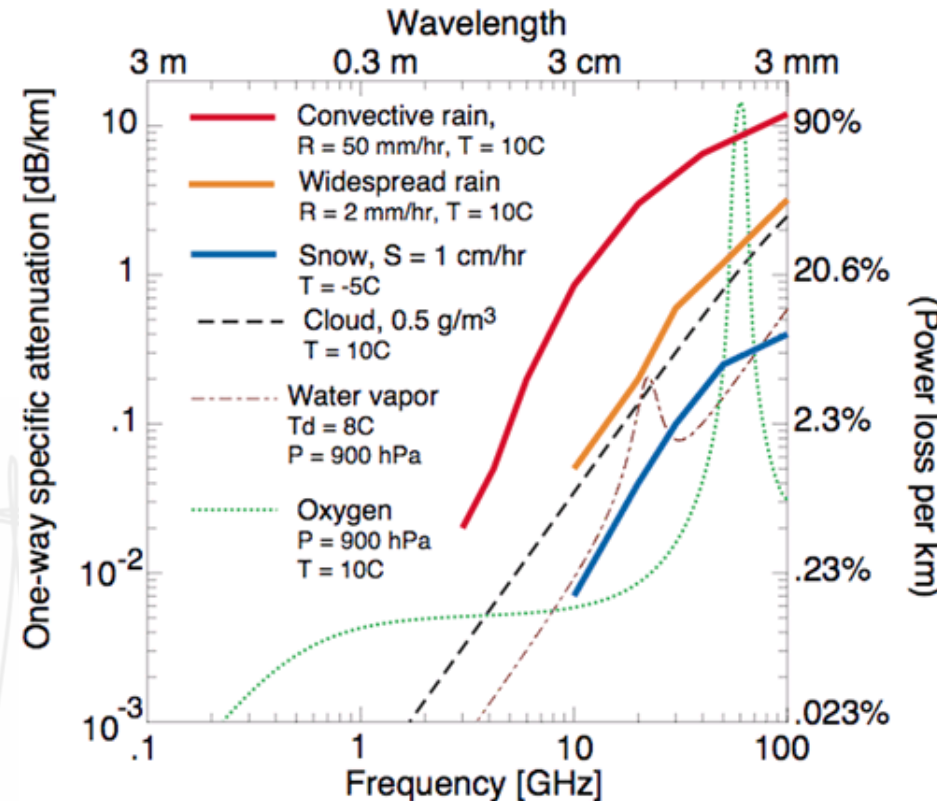
Attenuation due to Hydrometeors, water vapor and oxygen

Attenuation can be caused by gases (oxygen, water vapor) and hydrometeors (cloud, rain, snow, hail...).

Attenuation (except for oxygen) increases rapidly with increasing frequency (or decreasing wavelengths).

At S-Band, attenuation can be easily corrected for.

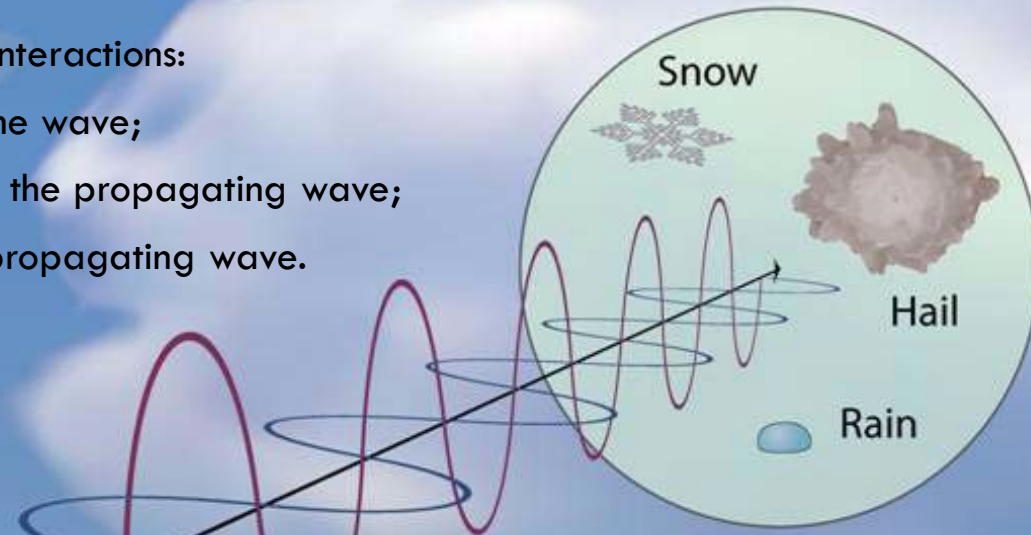
Attenuation at C-band is more pronounced, and sometimes not properly corrected for.



Dual Polarization Meteorological Radar

Three types of wave-target interactions:

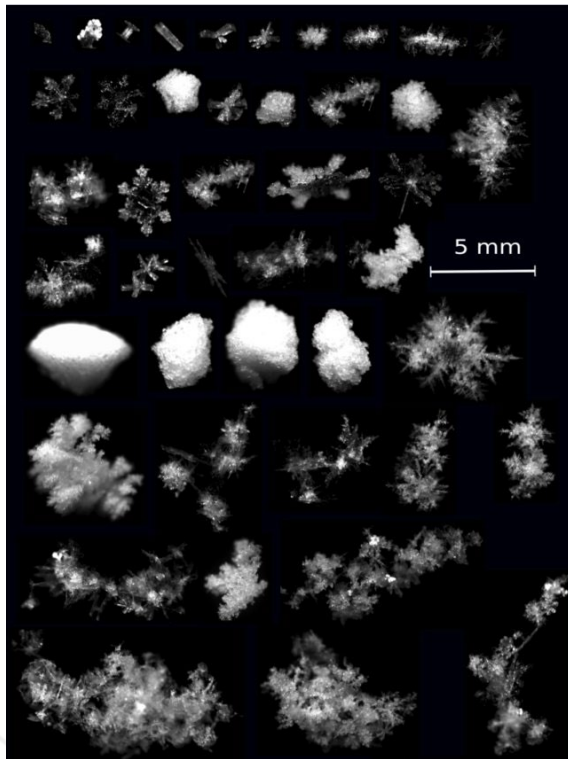
- 1) Partial reflection of the wave;
- 2) Partial attenuation of the propagating wave;
- 3) Partial delay of the propagating wave.



Wave-target interaction done via electric field;
If the target is not-symmetric, the magnitude of
the wave-target interaction will be
different at both polarizations →
Shape information.

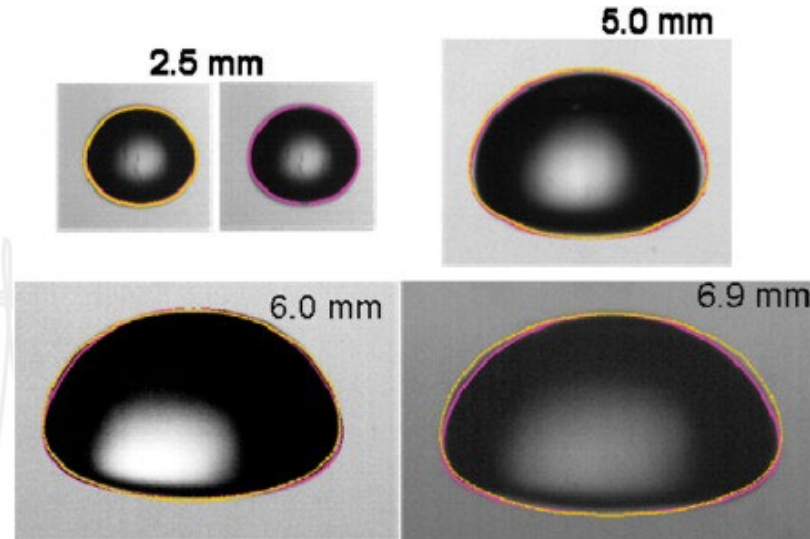


Can Polarimetry add meteorological Information?



Garrett et al., 2012

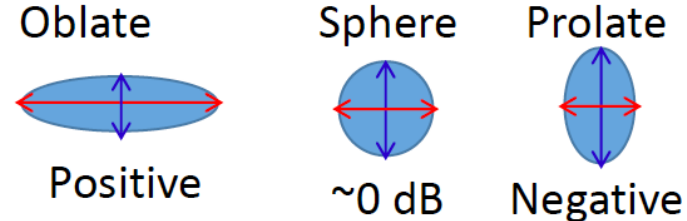
→ yes, because hydrometeors are
not spheres



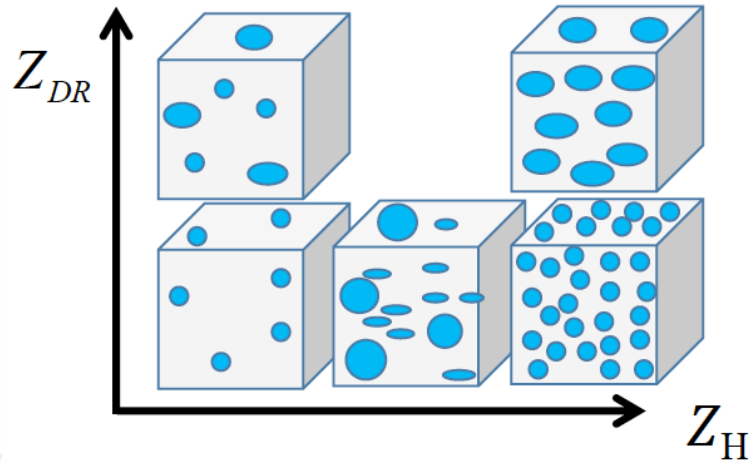
Beard et al., 2010

Z_{DR}: Differential reflectivity (dB)

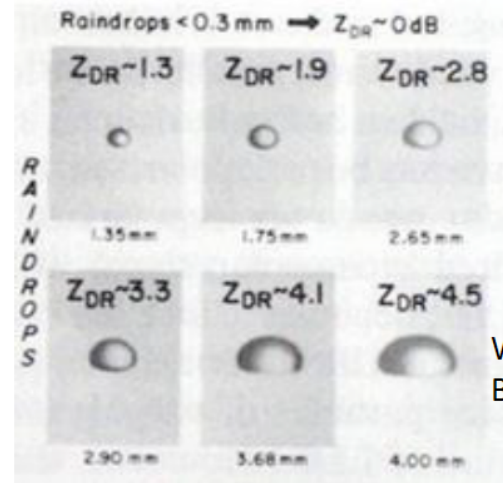
$$Z_{DR} = 10 \log_{10} \frac{Z_h}{Z_v} [\text{dB}]$$



Aspect ratio and bulk density of larger particles



Falling raindrops become oblate due to air resistance.



Wakimoto and Bringi (1988)

→ Useful to detect large raindrops and oriented ice (e.g., dendrites)

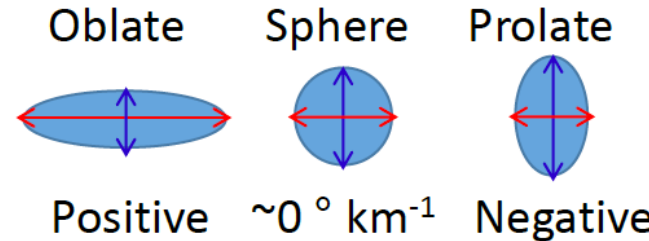
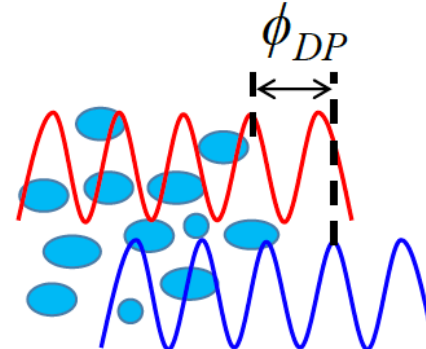
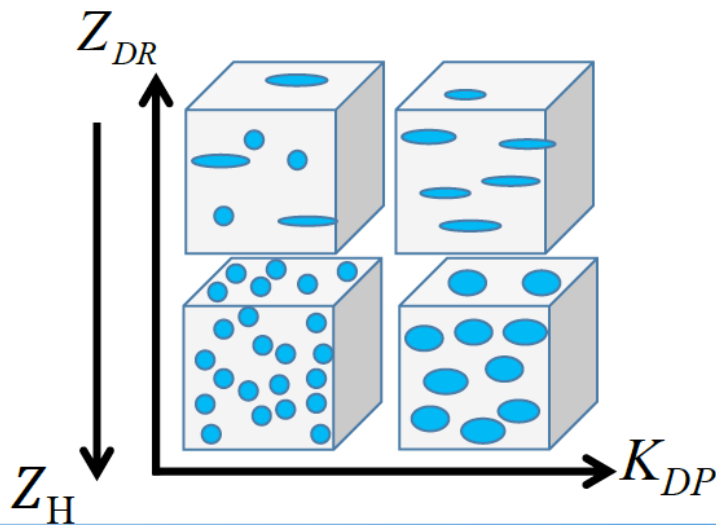
K_{DP} : Specific differential phase shift ($^{\circ} \text{ km}^{-1}$)

$$K_{DP} = \frac{\varphi_{DP}(r_2) - \varphi_{DP}(r_1)}{2(r_2 - r_1)}$$

r : Distance from radar

$$K_{DP} = \left(\frac{180}{\lambda} \right) 10^{-3} CW \left(1 - \overline{r_m} \right)$$

r_m : Mean aspect ratio W : Water content

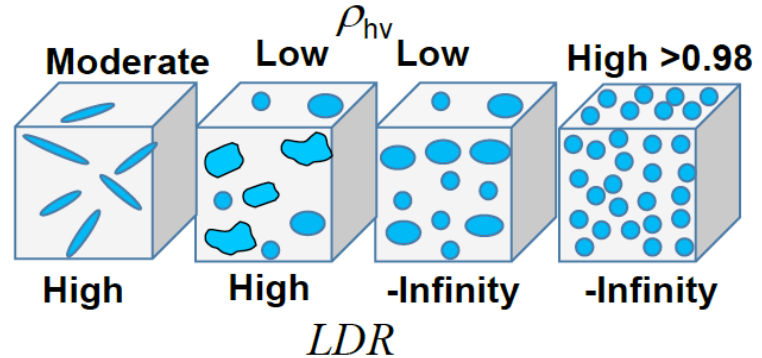


Aspect ratio, bulk density, mass;
sensitive to oriented particles and
mass

ρ_{hv} : Correlation coefficient between horizontally- and vertically-polarized waves

$$\rho_{hv} = \frac{\langle \langle n s_v s_h \rangle \rangle}{\langle n |s_h|^2 \rangle^{1/2} \langle n |s_v|^2 \rangle^{1/2}}$$

S_h : Backscatter signal for horizontal polarization
 S_v : Backscatter signal for vertical polarization
 n : Number density



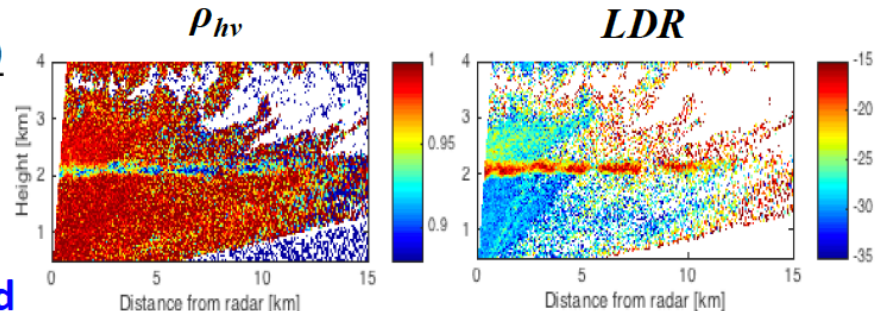
Decrease when irregular-shape particles dominate or different shapes mix

LDR: Linear depolarization ratio

$$LDR = 10 \log_{10} \frac{Z_{vh}}{Z_{hh}}$$

Z_{vh} : V return of H transmission

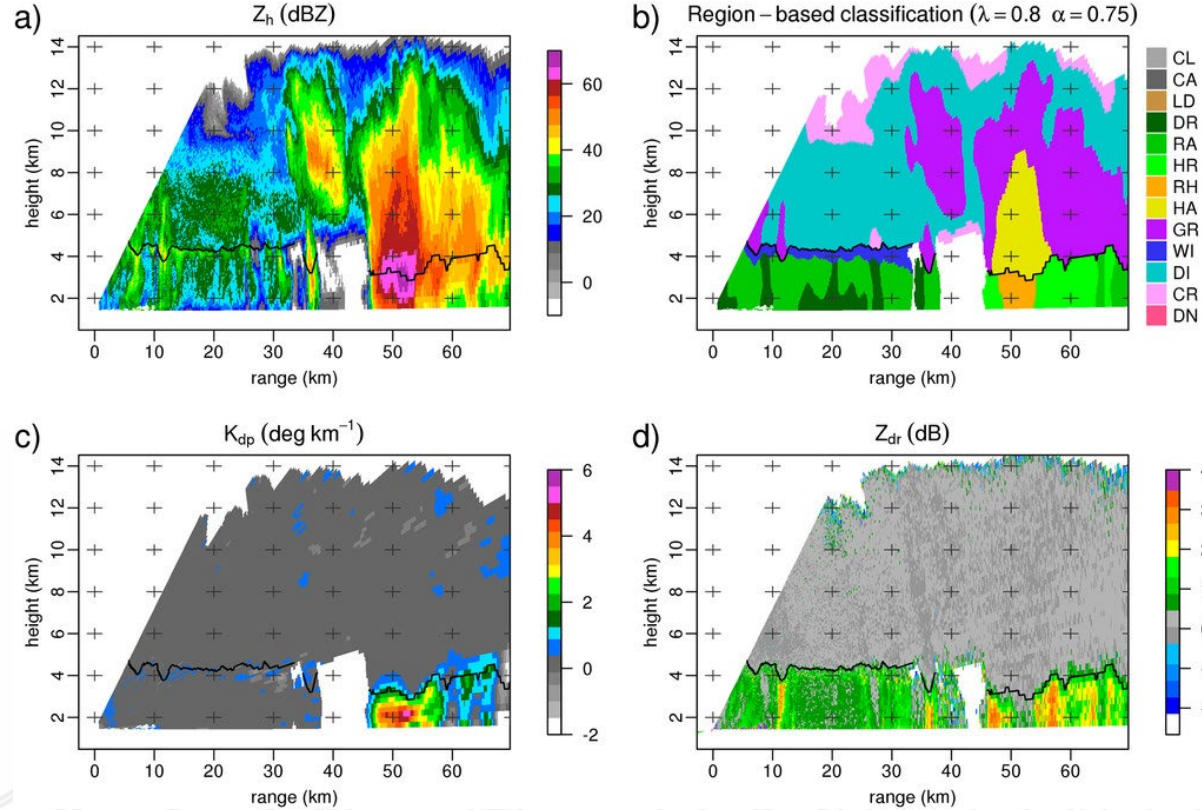
Sensitive to asymmetric particles and randomly oriented prolate particles



Dual-Polarization Parameters

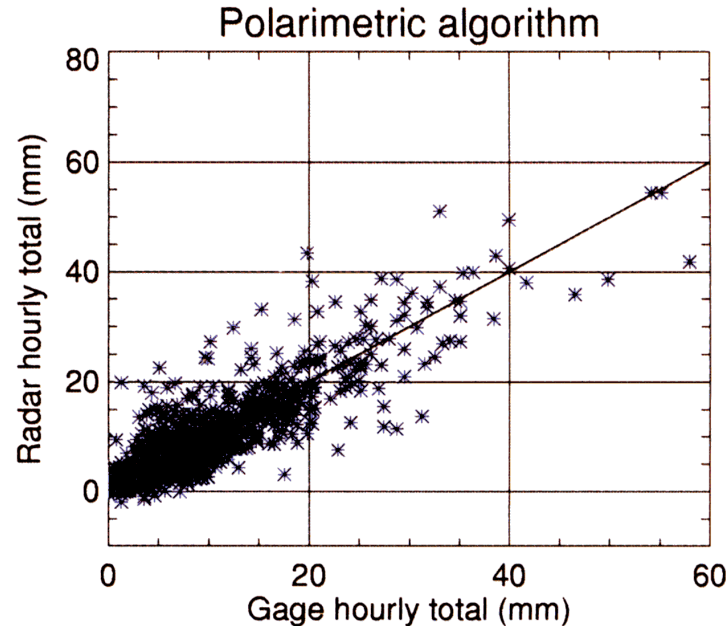
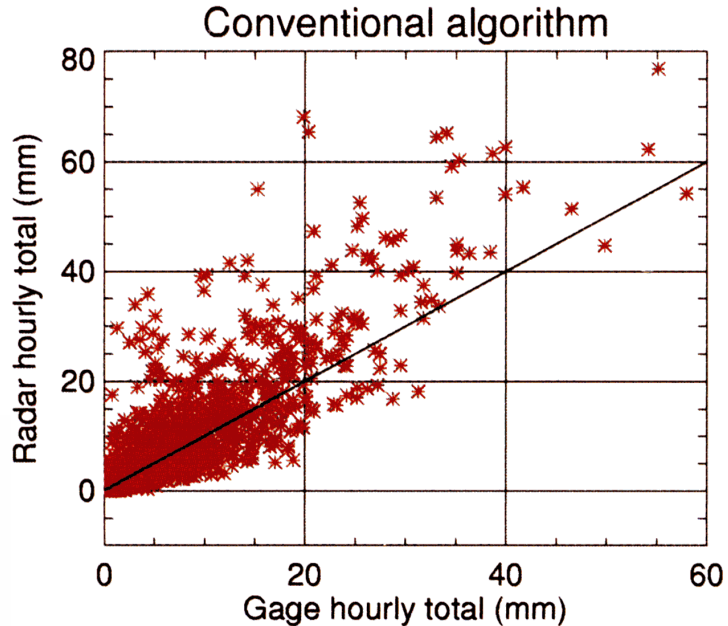
- Z_{DR} : A measure of the average horizontal to vertical axis ratio of targets.
- ρ_{co} : A measure of the uniformity in the shapes and orientations of targets in the sampling volume.
- ϕ_{DP} : A measure of the total path-integrated "mass \times deformation (or H/V ratio – 1)". Its range derivative, K_{DP} , is used to estimate rain.
- L_{DR} : When defined as P_{HV} / P_{HH} , it is a function of the average lack of symmetry of individual targets with respect to the horizontal plane.

Hydrometeor Classification from dual-polarization radar



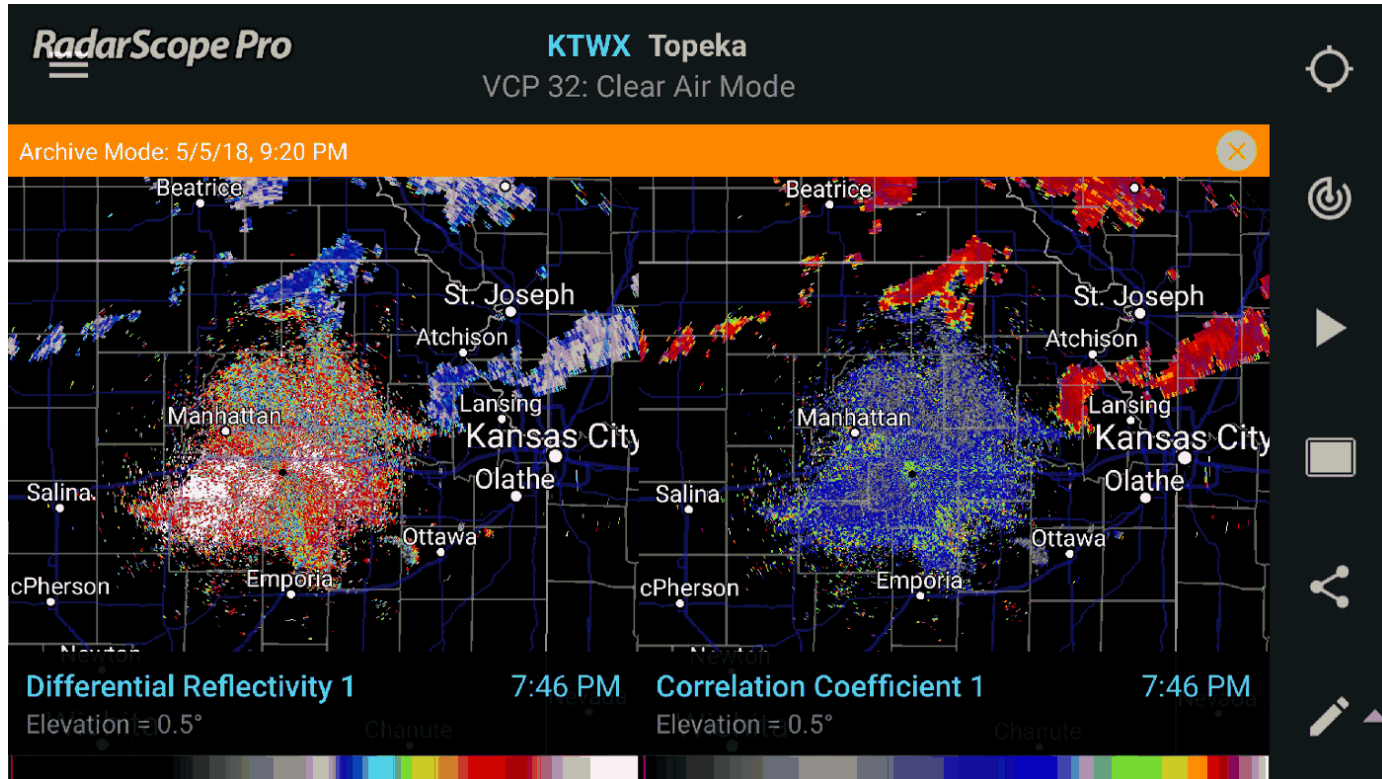
The RHI along the 45° azimuth at 2257 UTC 2 Jul 2008, from CHILL radar: (a) reflectivity, (b) region-based hydrometeor classification, (c) K_{dp} , and (d) Z_{dr} .

Improved Precipitation Estimation



- Z_{DR} → Drop shape info → “Mean” drop size info
- Target type information
- Φ_{DP} providing $\int [\text{target elongation} * \text{amount}] dr$
- More possibilities to obtain precipitation rate.

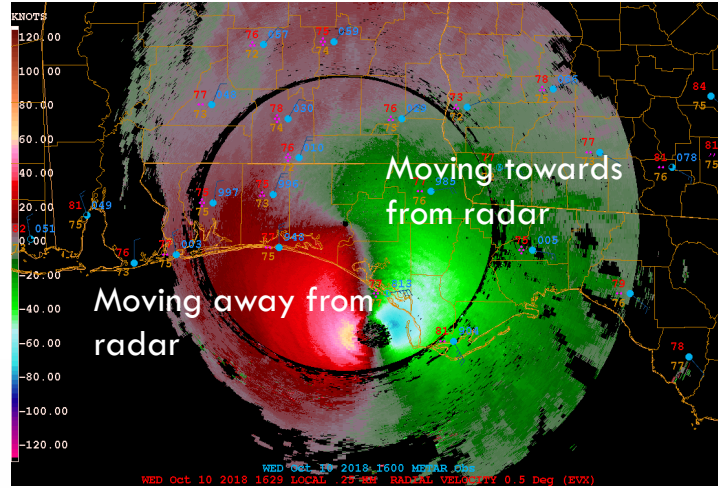
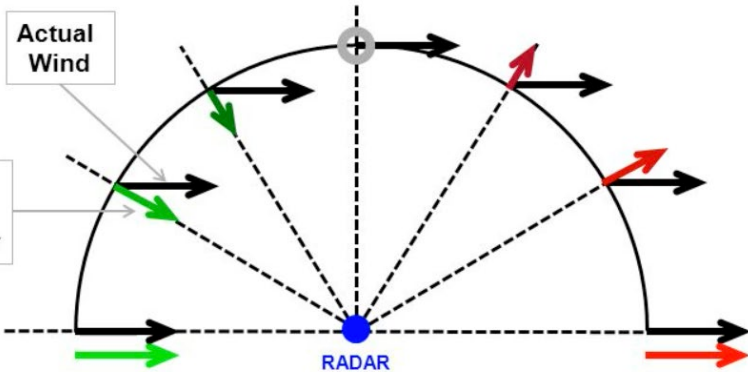
Identification of Biological Scatterers



<https://medium.com/@WeatherDecTech/radarscope-birds-bats-and-bugs-f3d796946e46>

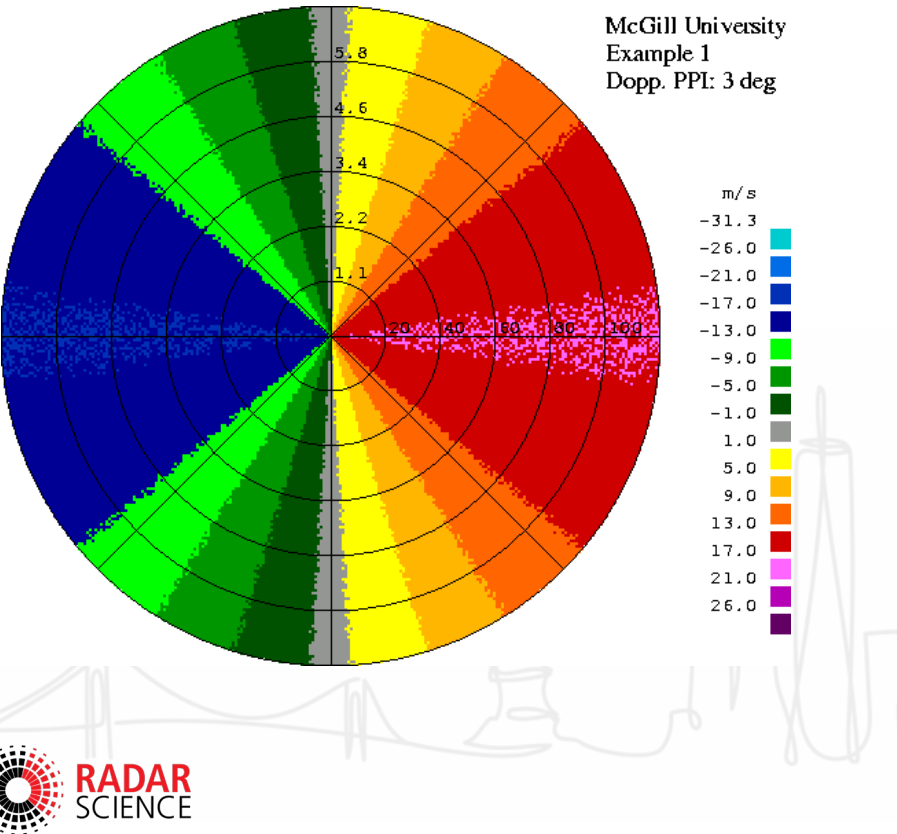
Doppler velocity

The measured radial velocity is the projection of the 3-D wind vector along the radar radial direction

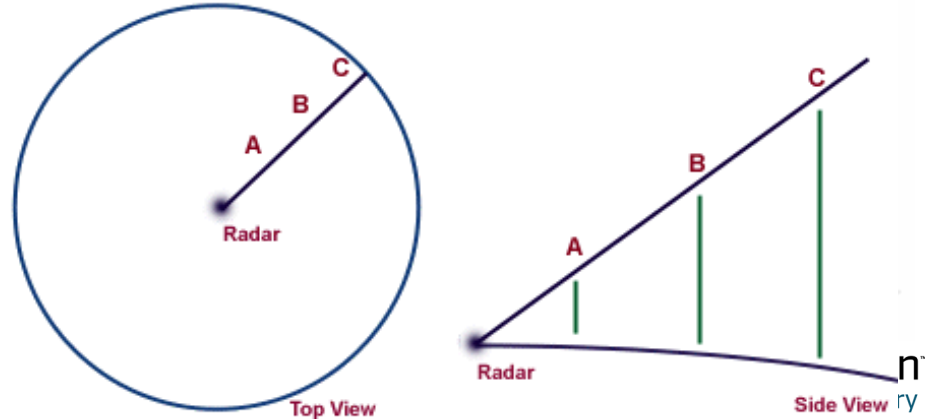


A negative shift ("red shift") is caused by targets moving away from the radar (positive radial Doppler velocity)

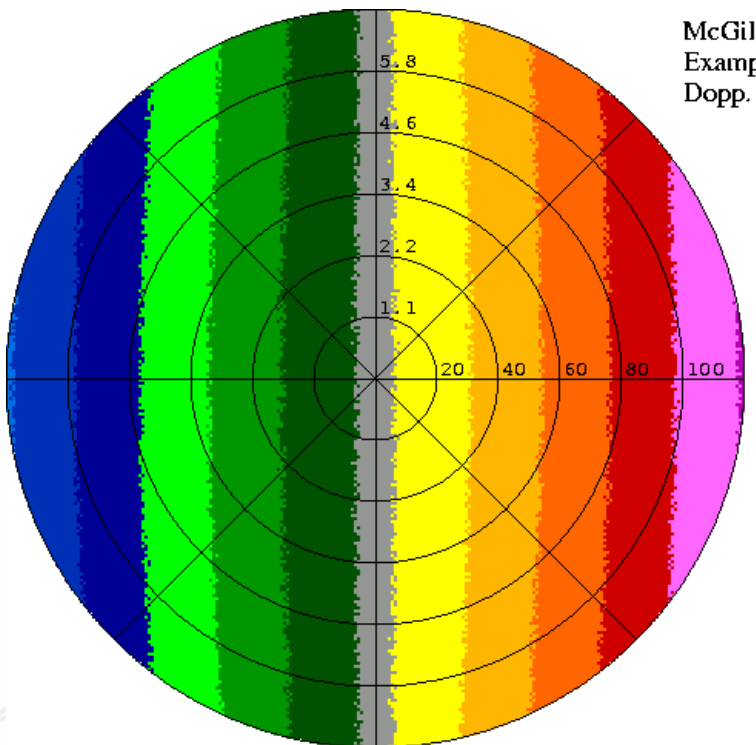
PPI Doppler velocity: Wind changes with height and with distance



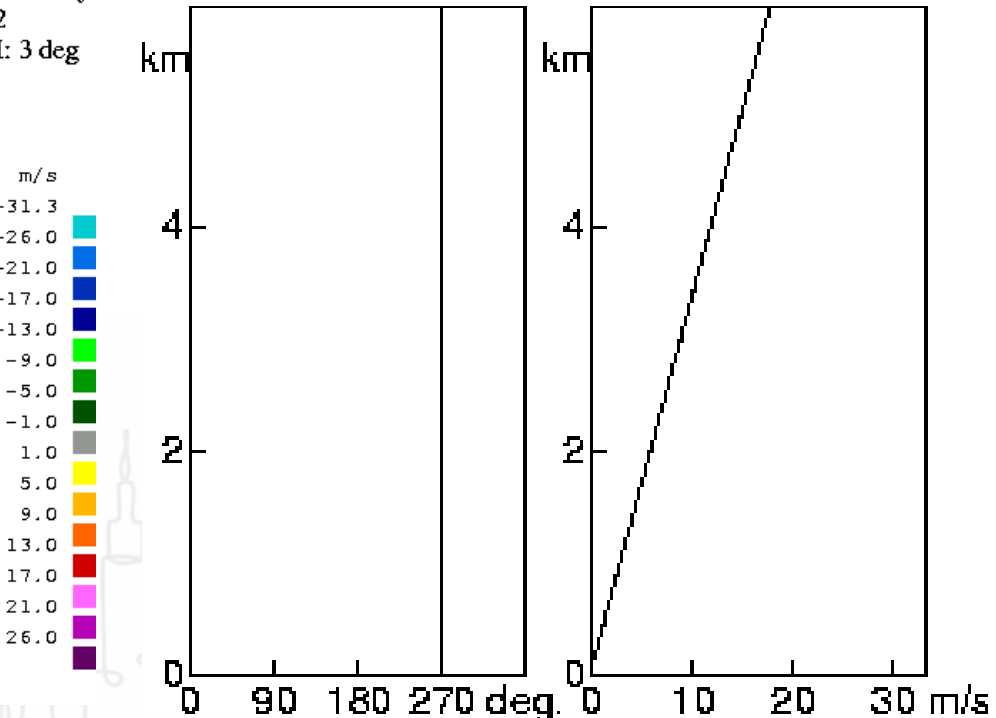
In general, radar "horizontal" scans (known as PPIs) are made at a given elevation angle. As a result, as range increases, so does the height sampled by the radar beam. Measurements made at close range will be representative of winds at low levels, while measurements at far ranges will be representative of winds at high levels.



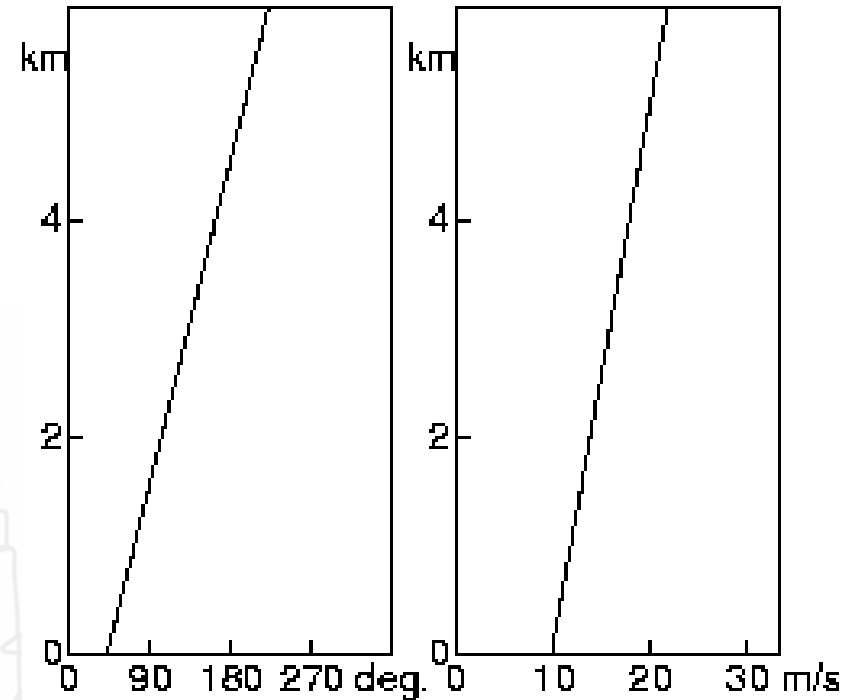
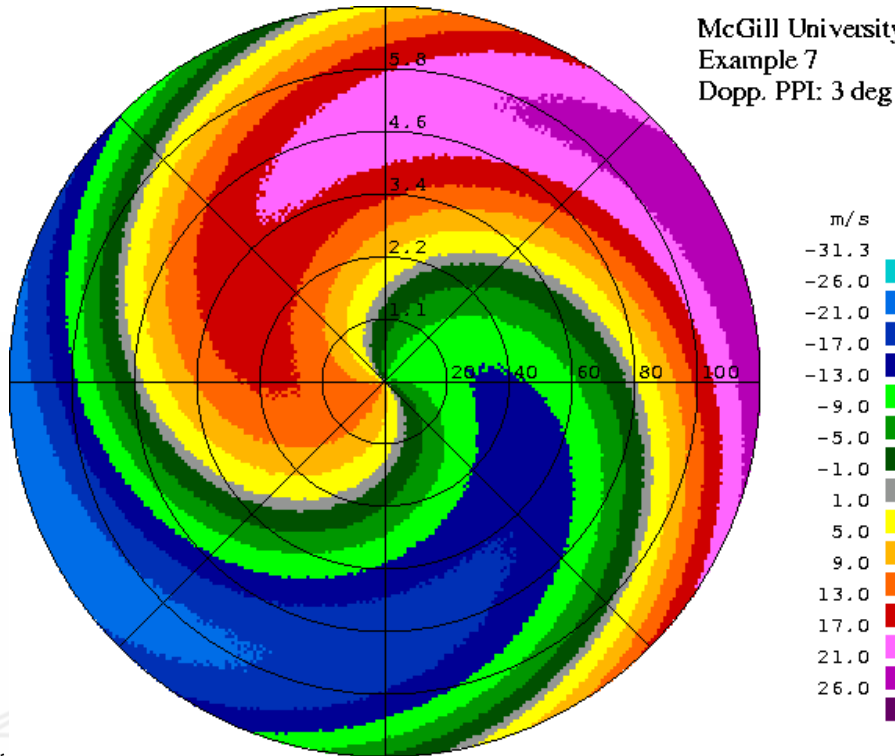
Velocity shear example I



McGill University
Example 2
Dopp. PPI: 3 deg



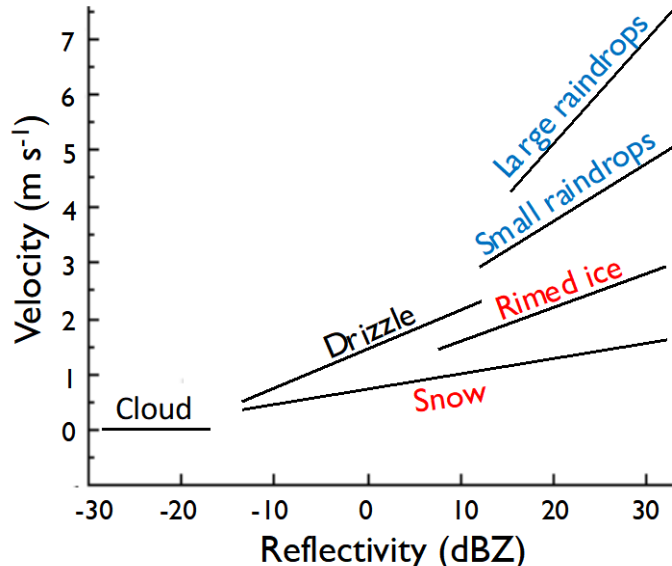
Velocity shear example II



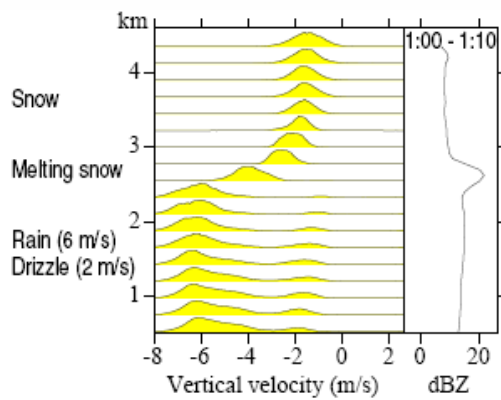
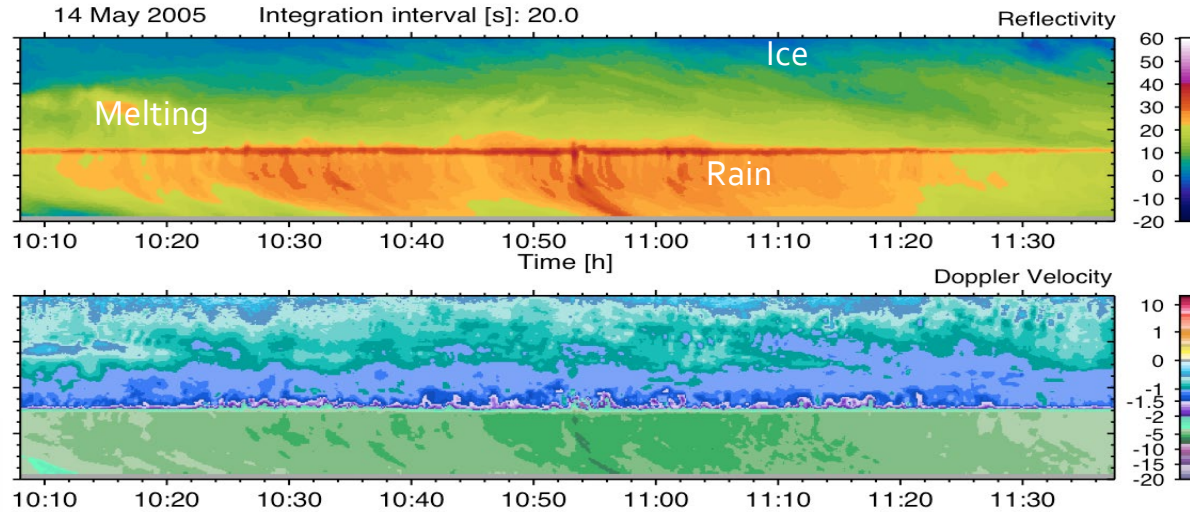
Advantages of vertically pointing radars (VPR)

High resolution measurements of the profile of the radar reflectivity

Measures the vertical motion of hydrometeors (terminal velocity and vertical air motion)

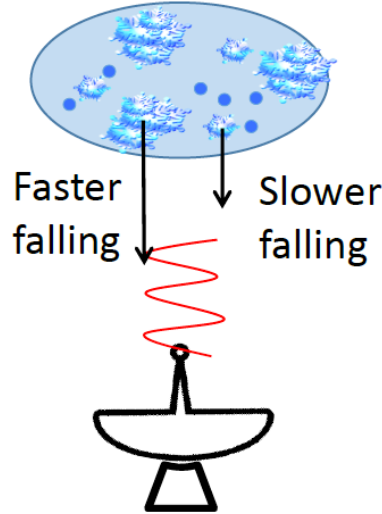


Advantages of vertically pointing radars (VPR)



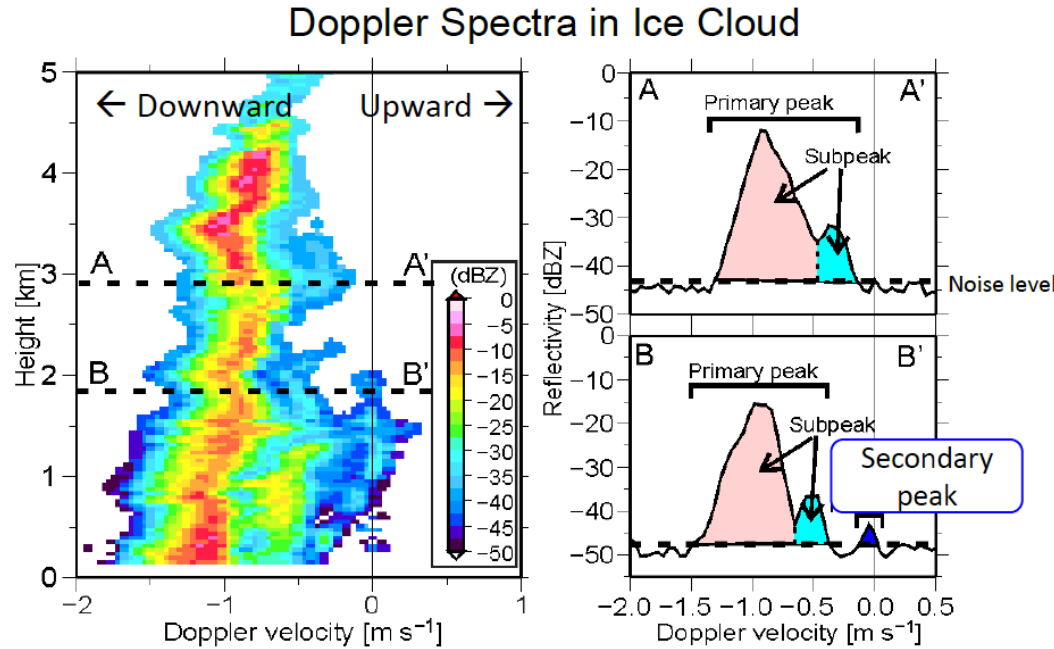
Why do we need to record the radar Doppler spectrum?

Utility of Radar Doppler Spectra



Vertically-pointing radar (KAZR):

- Observe Doppler velocity attributed to fall velocity
- Capable to decompose different particles



- Fast-falling subpeak DV << 0 m/s : Large ice particles
- Slow-falling subpeak DV < 0 m/s : Small ice particles
- Secondary peak DV =~0 m/s : Supercooled liquid

Role of Military in Radar Meteorology



US Air Force @ McGill



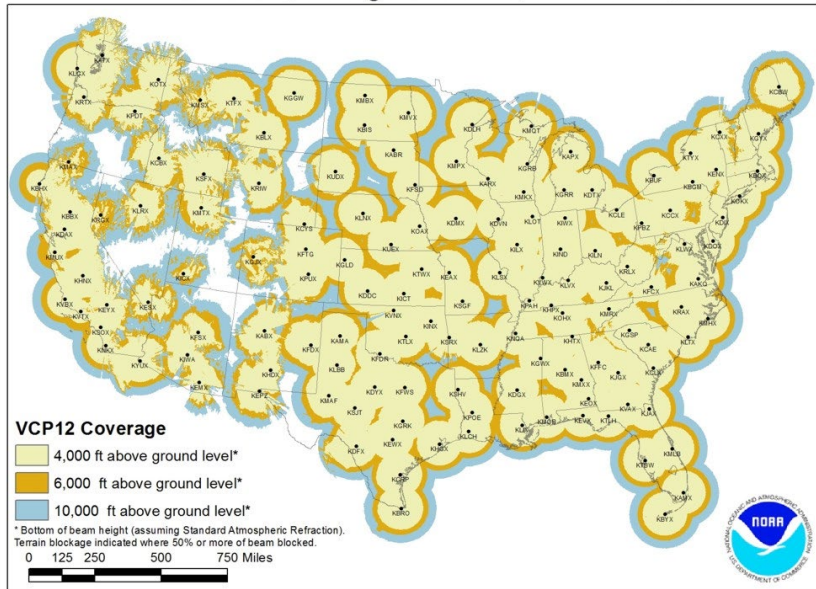
US Navy @ NSSL/OU



US Air Force @ CSU-CHILL

NEXRAD Weather Network

NEXRAD Coverage Below 10,000 Feet AGL



160 Doppler radars
230 km average distance



An Introduction to Digital Arrays

Architectural Considerations and Commercial Technologies

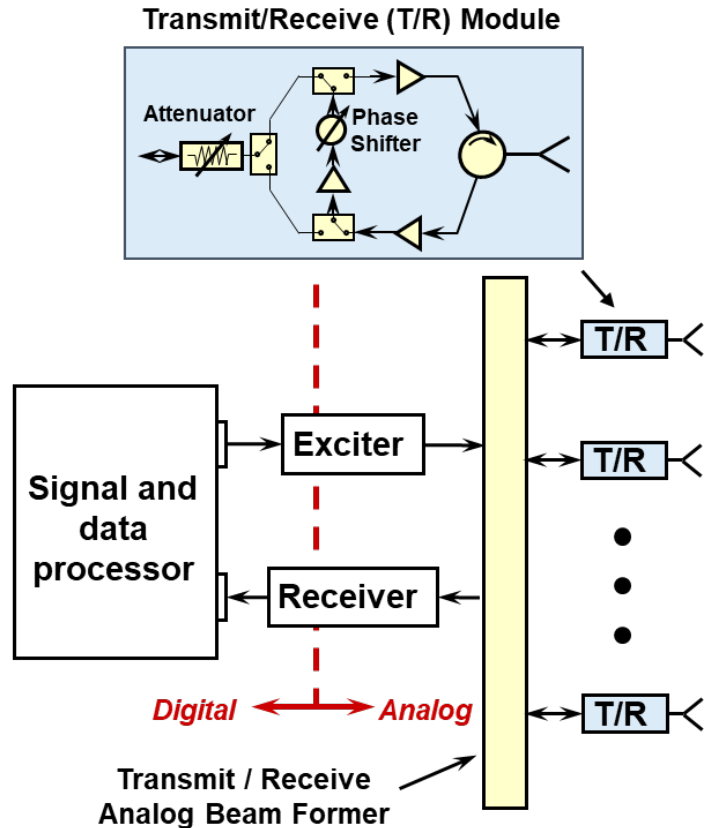
Kenneth W. O'Haver
Johns Hopkins Applied Physics Laboratory
Laurel, MD 20723

Introduction

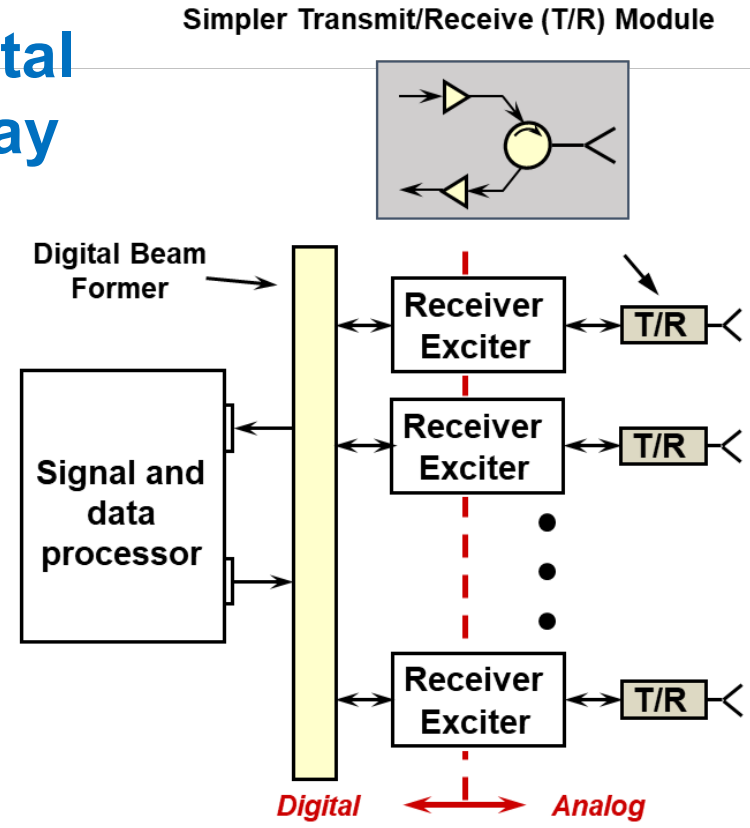
- Objective
 - Provide an introduction to digital arrays, including the fundamental elements, architectural trades, and enabling technologies with commercial examples.
- Outline
 - Digital array basics.
 - Architectural trades:
 - Centralized vs distributed beamforming.
 - Digital beamforming implementation.
 - Frequency generation and distribution.
 - General digital transmit/receive module
 - Contrast with analog arrays.
 - Enabling semiconductor technologies and examples of commercial components.

Analog and Digital Arrays

Analog Active Array



Digital Array

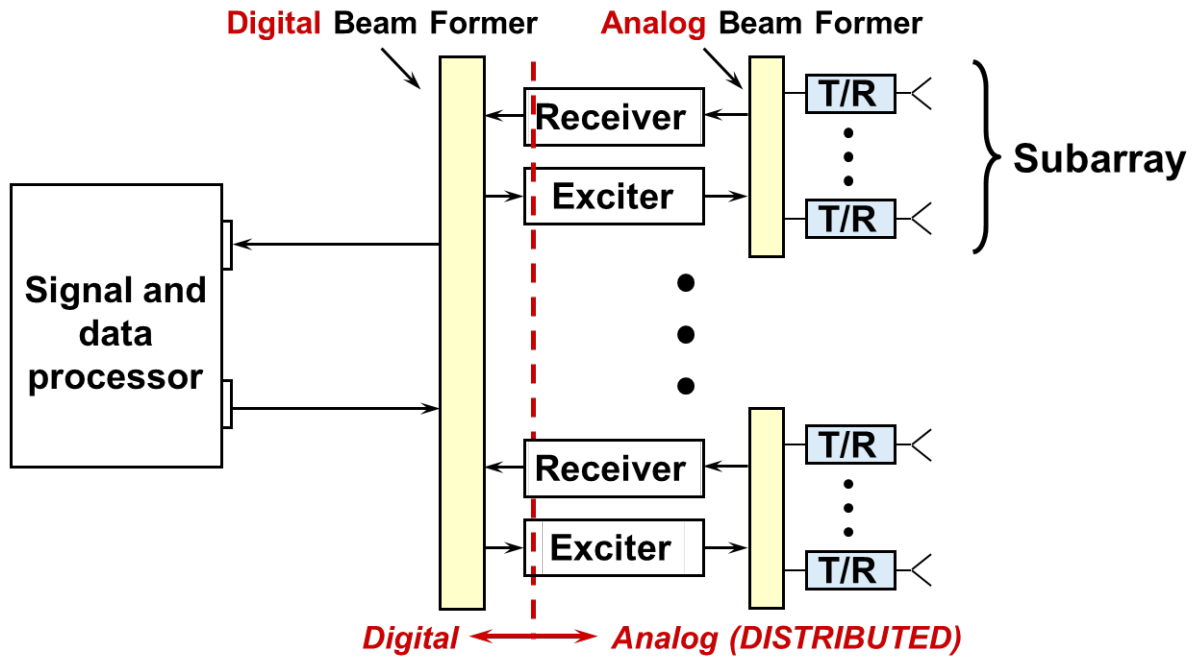


How do we achieve a large number of parallel receivers and excitors?

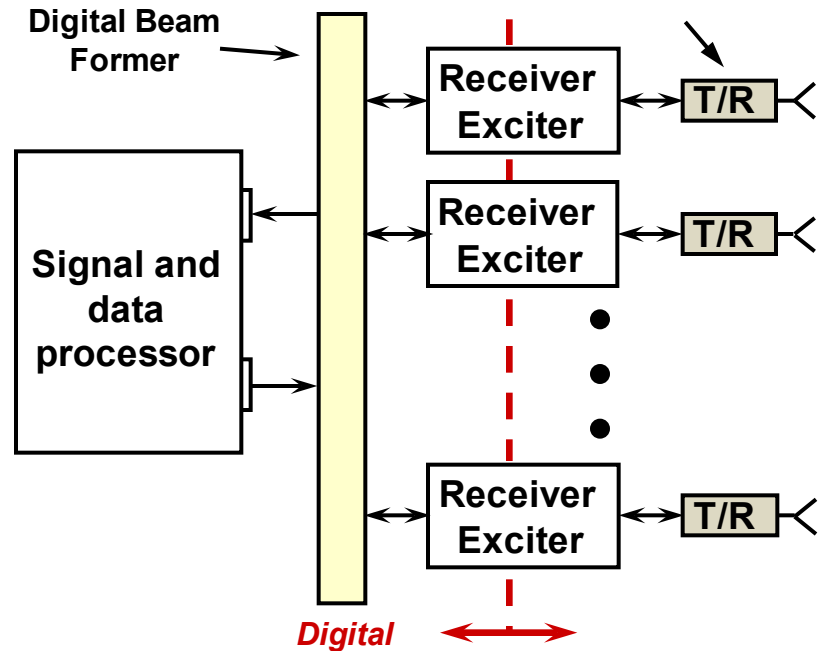
- Leverage advances in RF Silicon semiconductor technology (the march of Moore's Law).
- Leverage array scaling effects to ease the requirements of distributed receivers and excitors (Session II).

Digital Array Variations

Subarray Level



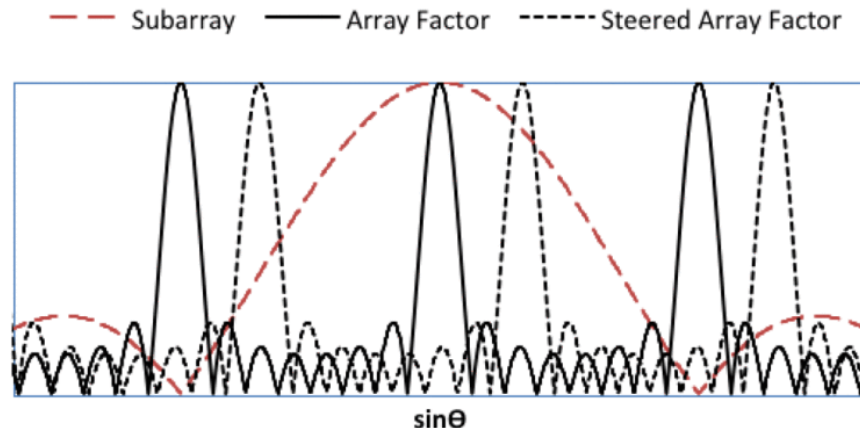
Element Level



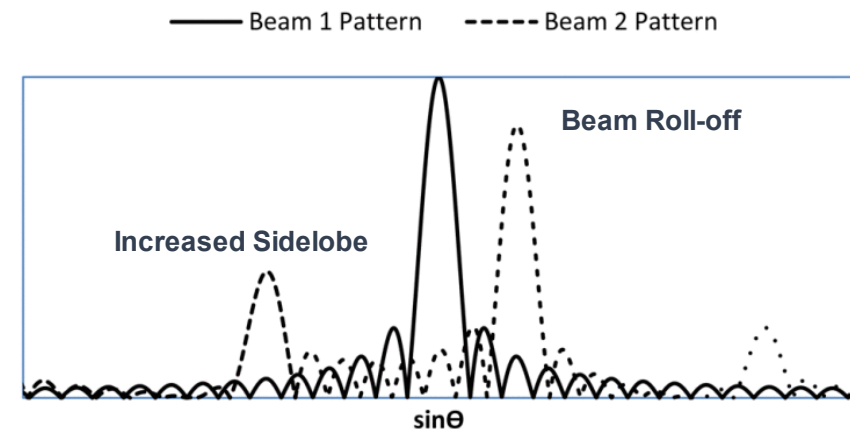
- Subarray-level digital arrays require element-level analog phased shifters; element-level digital arrays do not.
- Subarray-level digital arrays require fewer receivers and excitors, although likely with higher receiver/exciter performance.
- Both can digitally generate multiple beams, however:
 - Element-level digital arrays can provide multiple simultaneous beams at *arbitrary and independent steering angles*.
 - Subarray-level digital arrays are limited to multiple beams in a cluster around a central beam (and may require subarray overlapping).
- Other variations include 1-dimensional digital, such as azimuth (column-level) or elevation (row-level) digital.

Multiple Beams with Subarray Digital Arrays

- Element-level digital arrays can produce multiple beams unconstrained in angle.
- Subarray-level digital arrays can produce multiple beams constrained in angle (beam clusters).
 - Constrained to the steered subarray beam.
- The subarray-level digital array beam pattern is the product of the element pattern, the subarray pattern, and the array factor of the array of subarrays (right).
 - Element analog phase shifters steer the subarray pattern.
 - Multiple beams created digitally at the subarray array factor level.
- Peak gain roll-off and increased sidelobes result for beams steered off of the subarray direction (right).
- Techniques such as overlapping subarrays or subarray irregularity can reduce these effects, but add analog complexity.
- Multibeam clusters are none-the-less highly useful in improving search frame times in large search radars.



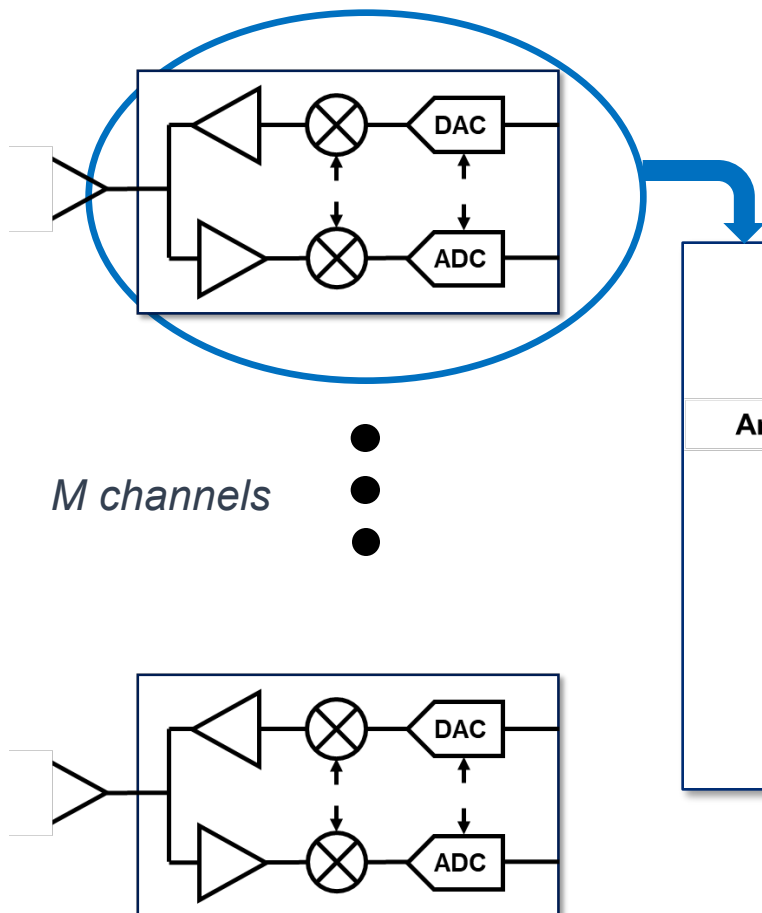
Digital re-steering at the subarray level...



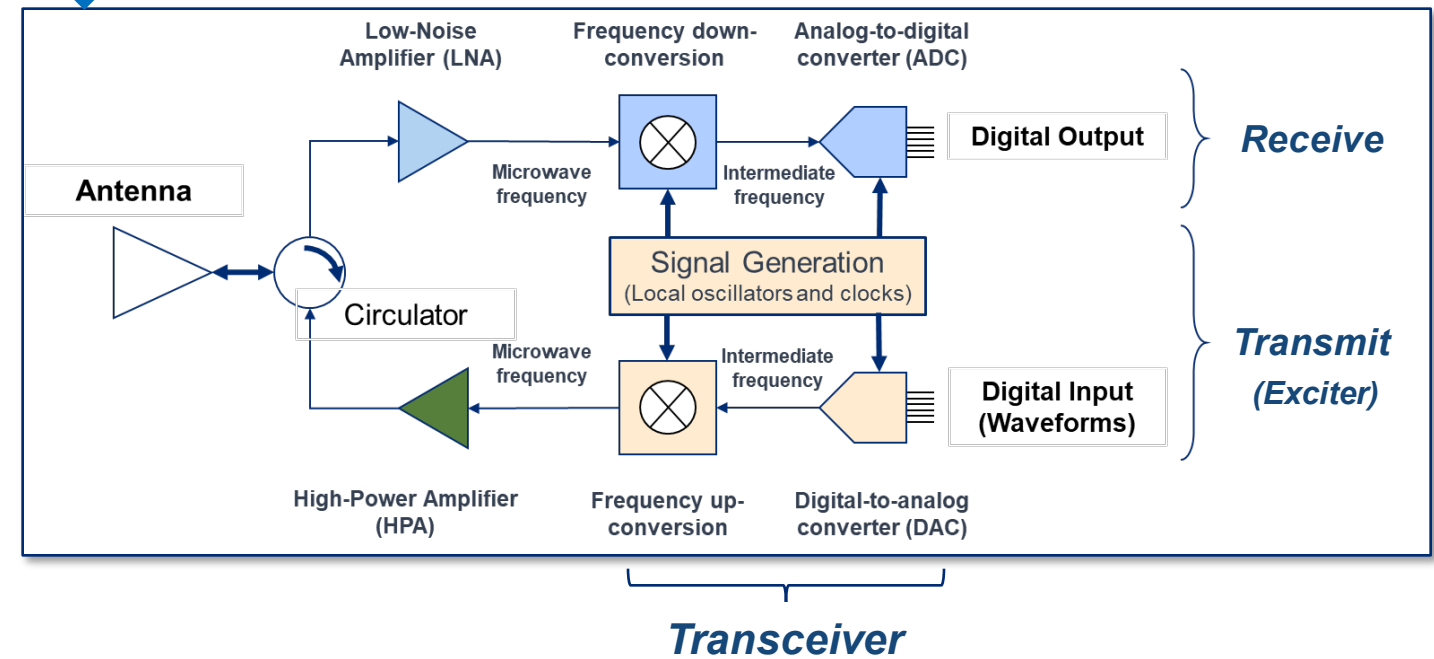
... produces beam roll-off and increased sidelobes; limiting subarray digital re-steering in angle and requiring added analog complexity such as overlapped subarrays.

Digital Array Elements and Architectural Trades

Channel HW Terminology

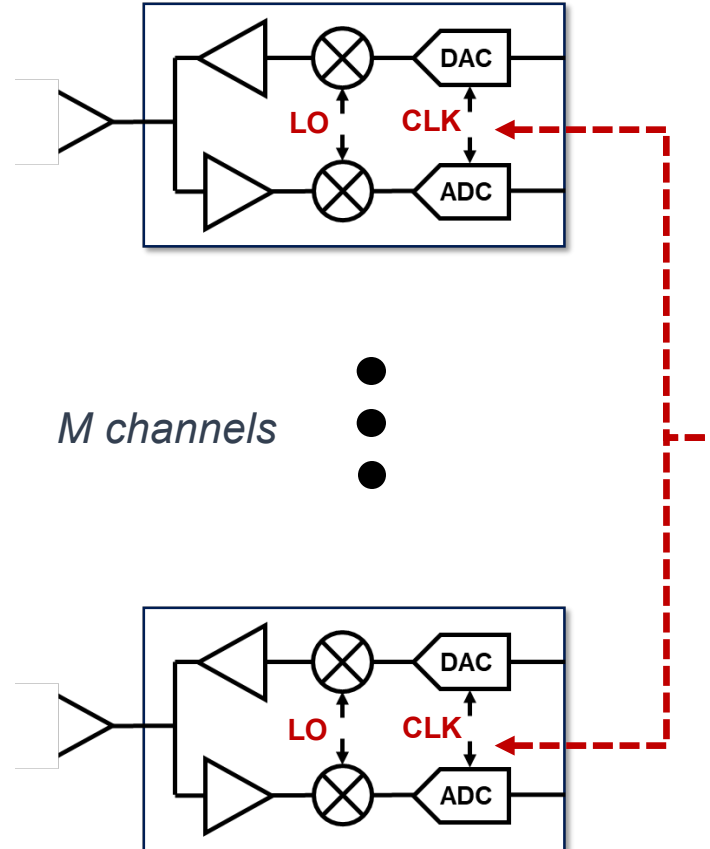


Channel Hardware Terminology



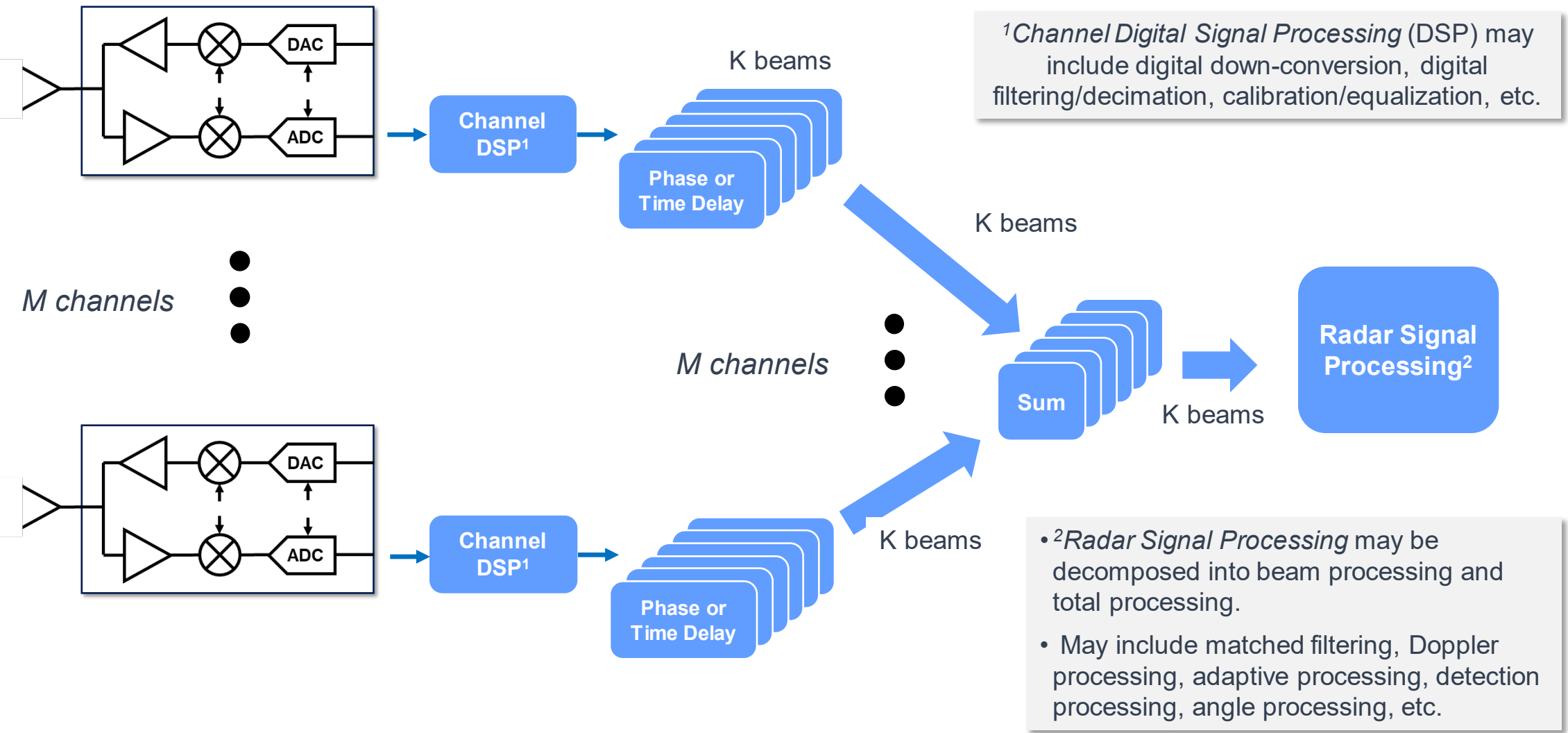
Various transceiver topologies may be used.

Synchronization and Coherence



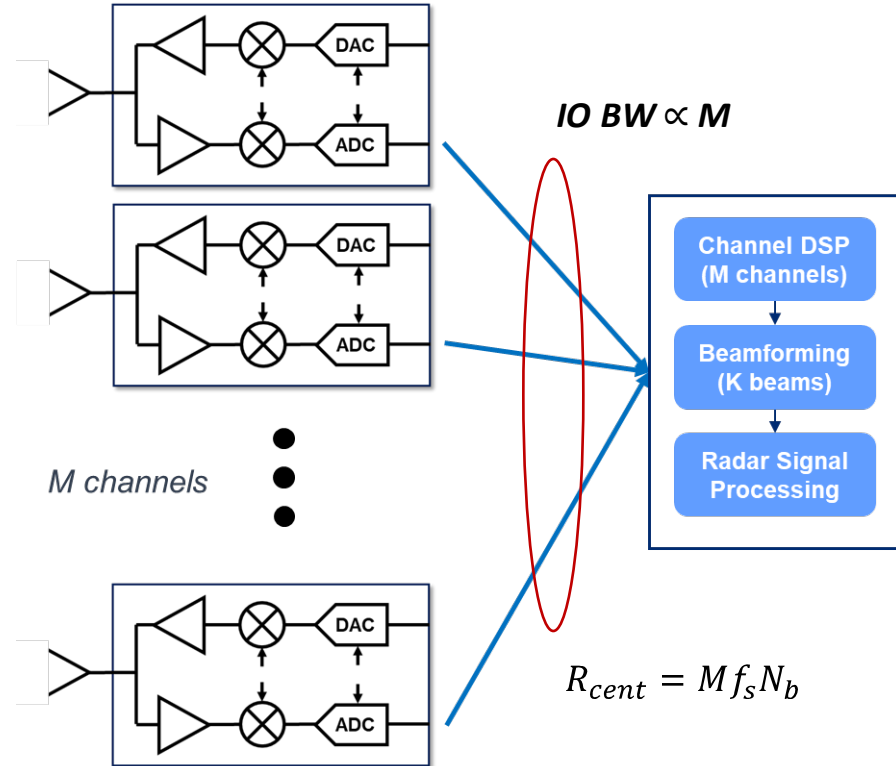
- Local Oscillator (LO) signals used in mixing must be coherent across the array.
- LO signals must be calibrated across the array to minimize phase errors.
- ADC/DAC clocks must be synchronized across the array to minimize phase errors.

Digital Array Receive Chain (Multiple Beams)



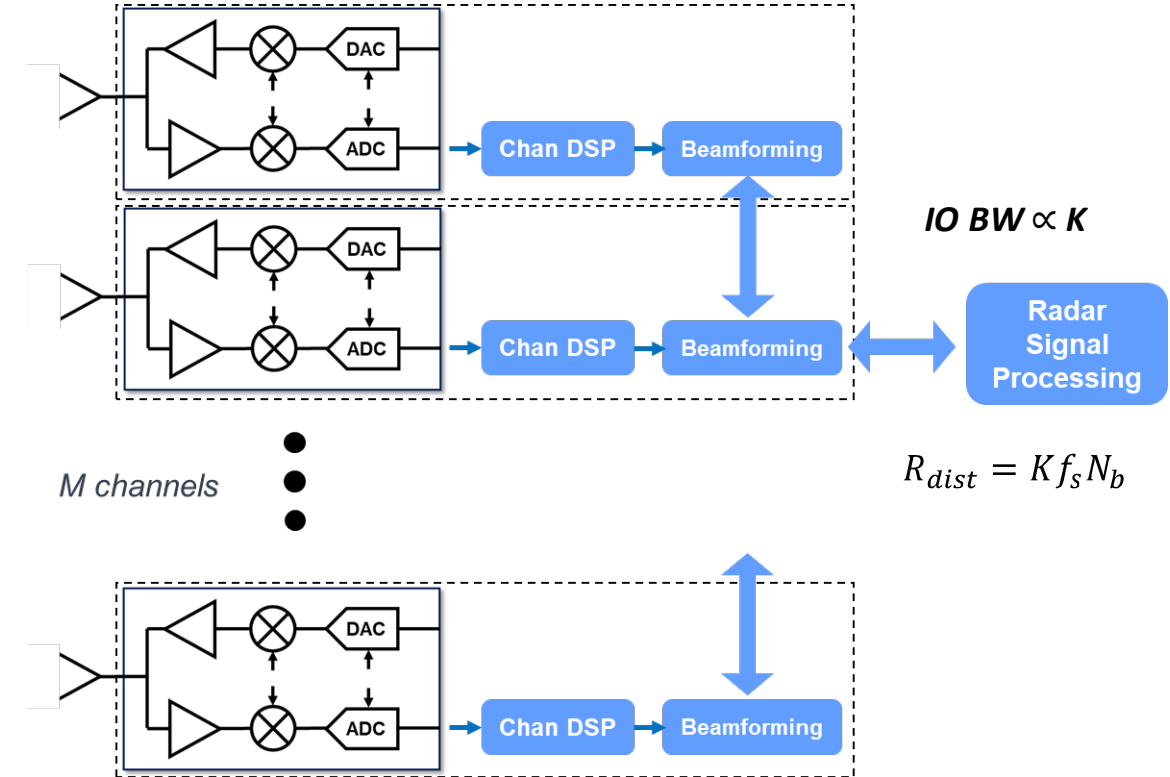
Input/Output Architecture Trades

Centralized



- R = IO data rate
- M = # of elements
- K = # of beams
- f_s = sampling rate
- N_b = # of bits

Distributed

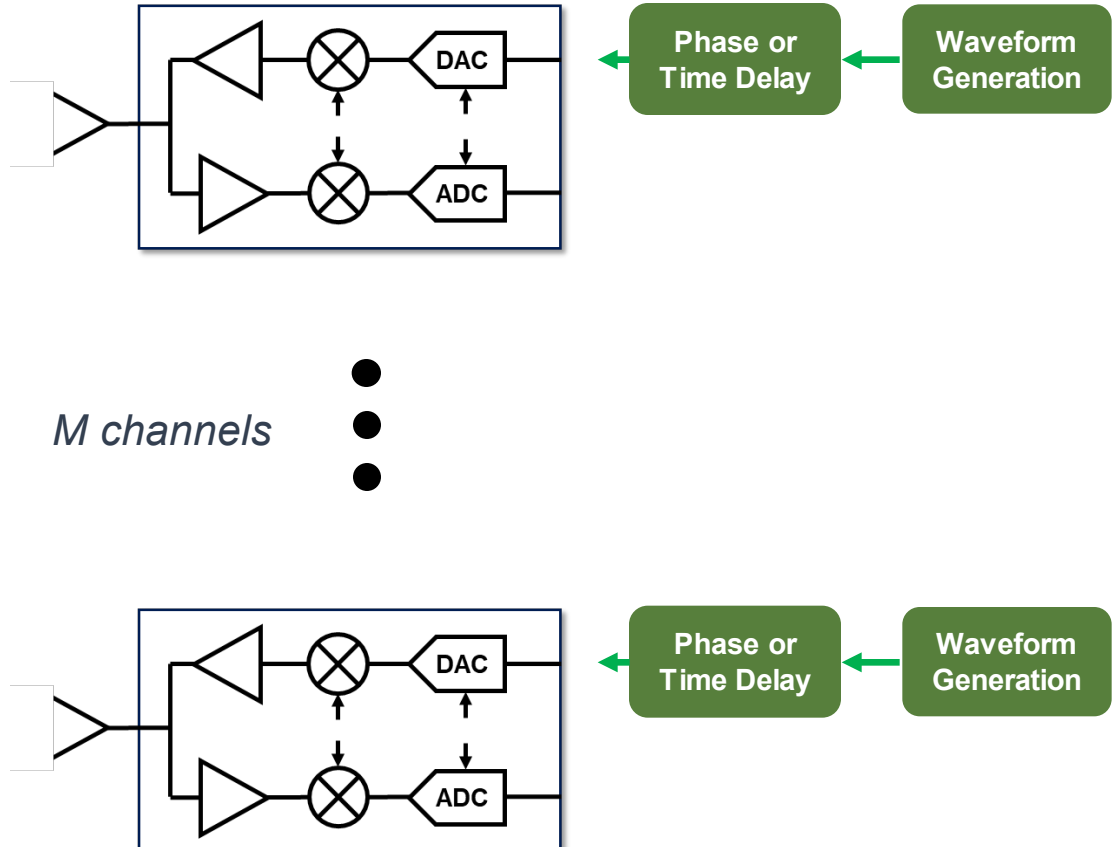


- Optimal approach depends on the number of channels, the number of beams, and the bandwidth capacity of the digital beamforming.
- Distributed architectures generally preferred for moderate to large arrays.

Beam-Bandwidth Product

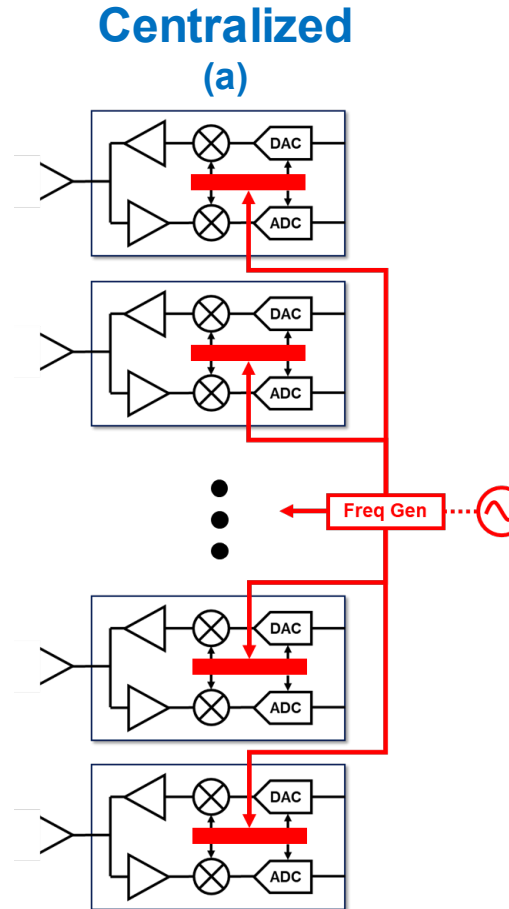
- A key metric for digital arrays is the ***Beam-Bandwidth Product*** (BBP):
 - $BBP = K * BW_{beam}$.
- The BBP represents the total amount of bandwidth that can be divided between beams in a single polarization.
- The BBP is constrained by the data rate available in the digital beamforming hardware:
- Example → Assume a Beam-Bandwidth Product of 500 MHz.
 - A radar search mode may use 50 beams at 10 MHz.
 - A high range resolution mode may use 1 beam at 500 MHz.

Digital Array Transmit Chains

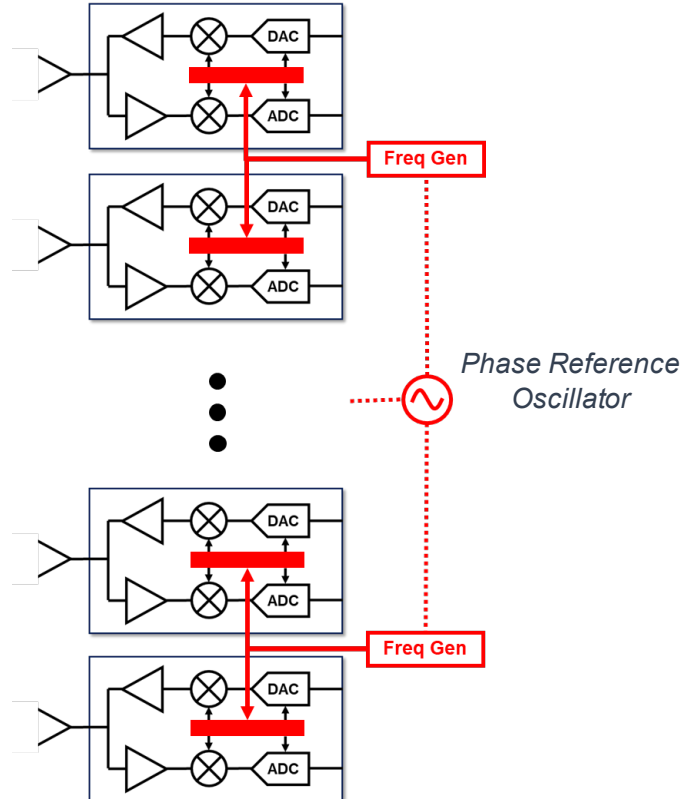


- Waveform generation may be centralized or distributed (distributed shown).
- Radars typically operate with a single beam at saturated output power.
- Distributed waveform generation allows for flexible use of the transmit aperture resource.
- Concept of arbitrary waveform generation at each channel.

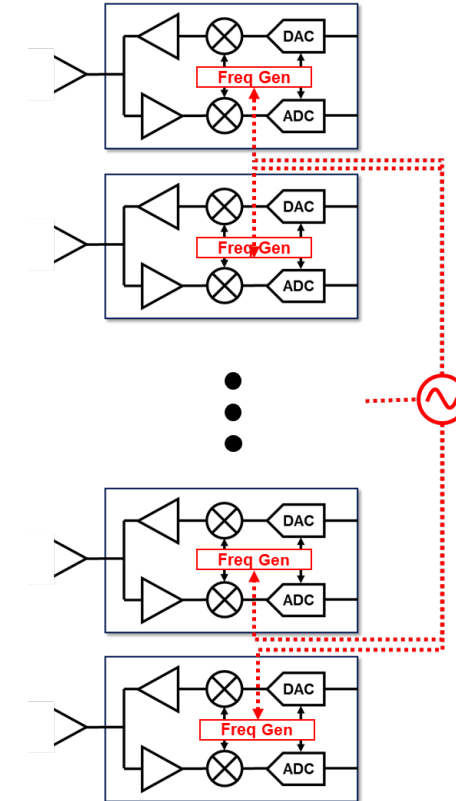
Frequency Generation and Distribution Trades



Distributed to
Multi-Channel Modules (b)

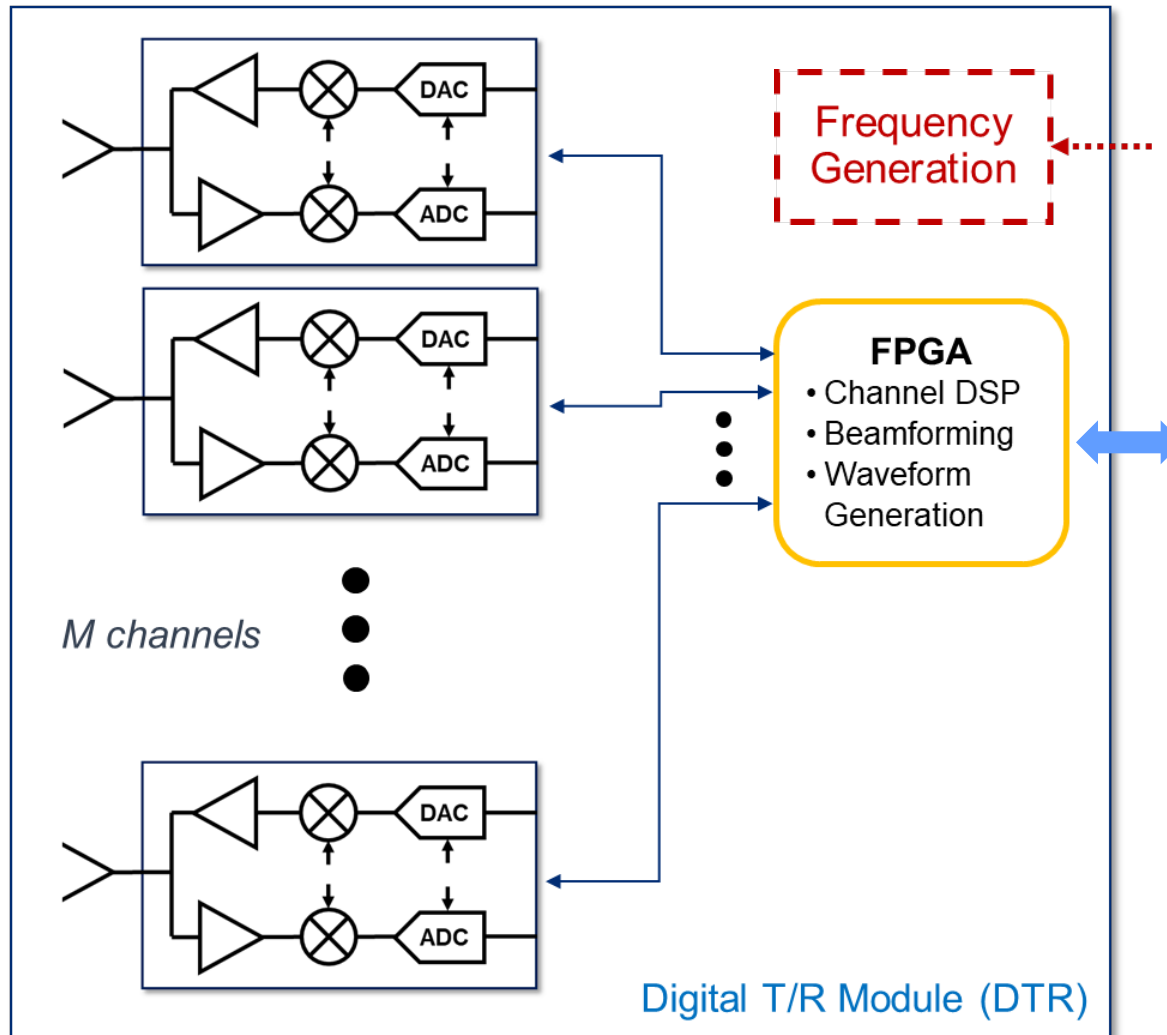


Distributed to Each Channel
(c)



- Distributing to multi-channel modules (b) balances LO power needs and HW duplication overhead.
- Provides $10 \log M$ lower phase noise than centralized, where M is the number of multi-channel modules.

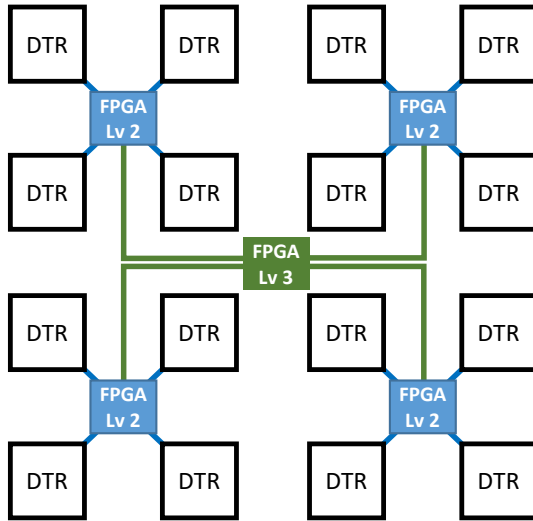
Digital Transmit/Receive Module



- Key elements:
 - Front-end amplifiers (PAs & LNAs).
 - Filters & receive protectors as needed (not shown).
 - Transceivers.
 - ADC's and DAC's.
 - FPGA (Field Programmable Gate Array).
- Common variations:
 - Amplifiers often packaged in a separate module (RF Front End).
 - ADC's and DAC's may be packaged with the FPGA (Digital Module or Antenna Processor).
- May typically have 8, 16, or more elements.

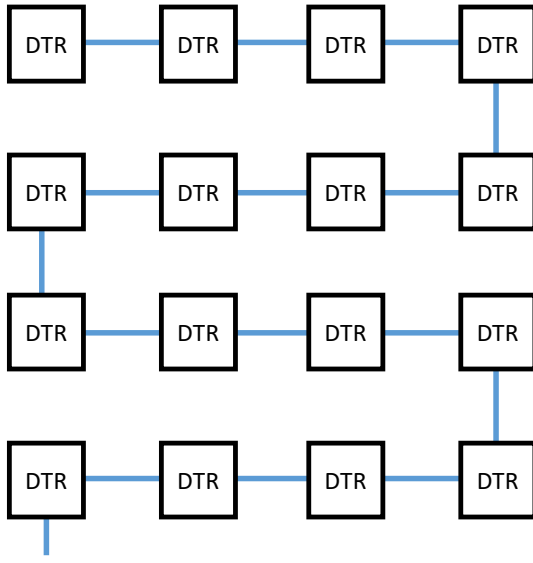
Digital Beamforming Implementation Trades

Hierarchal



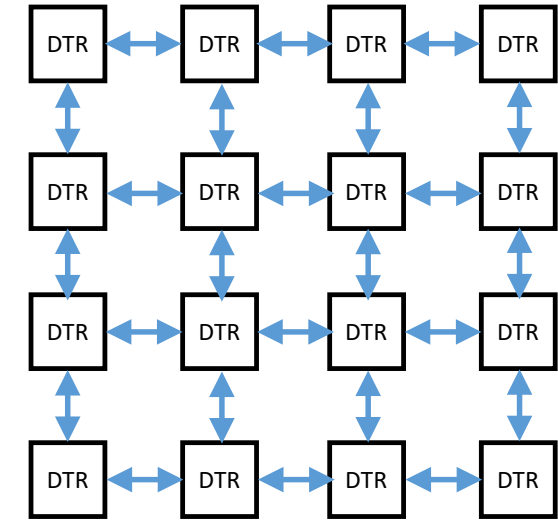
- (+) lowest latency.
- (+) supports subarray processing.
- (-) no redundancy.
- (-) increased hardware.

Serial



- (+) limits hardware.
- (~) multiple paths may provide redundancy but limit data rate.
- (-) highest latency.

Meshed

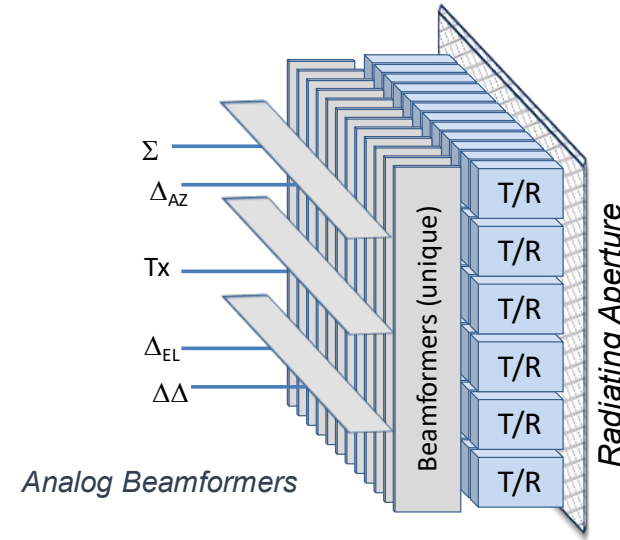


- (+) limits hardware.
- (+) multiple paths provide redundancy but limit data rate.
- (~) moderate latency.

Comparison with Analog Beamforming

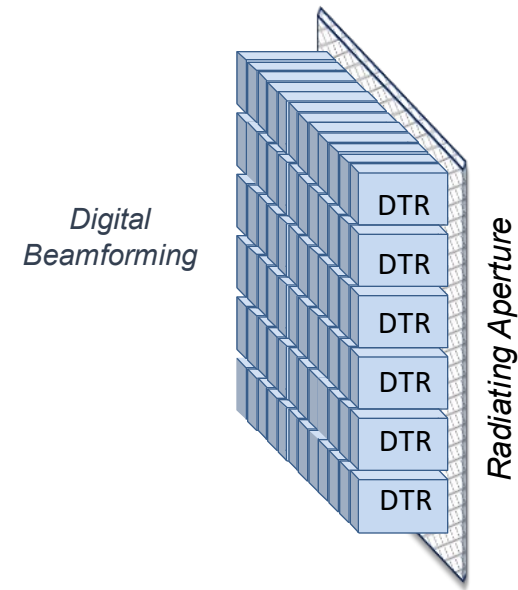
Analog AESA

- May have complex low sidelobe analog beamformers.
- Wideband requires analog time delay.
- Not suitable for multiple independently steered beams.
- Inflexible; tapers largely hard-wired in.
- Not easily scalable.



Digital Array (Element-Level)

- Flexible, adjustable tapers & array processing.
- Digital time delay for wideband (if needed).
- Multiple independent beams:
- Enables array processing algorithms.
- Highly scalable.
- Frequency agnostic digital modules may be common across applications.



RF & Mixed Signal Semiconductor Toolbox

Gallium Arsenide
(GaAs)

- Good RF (i.e. noise figure, output power, power added efficiency)
- Moderate density; lower integration; *MMIC's*
- Used in RF Front Ends

Gallium Nitride
(GaN)

- Excellent RF Power & Bandwidth (high breakdown voltage, current density)
- Moderate density; lower integration; *MMIC's*
- Used in RF Front Ends, particularly power amplifiers

Silicon Germanium
(SiGe)

- Moderate RF
- High density; medium integration; *RFIC's*
- Used in transceivers

RF CMOS (Si)

- Lower RF performance, but also lowest power consumption
- Small feature size, high density; high integration (complex SOC's)
- Used in transceivers and digital back-end modules.

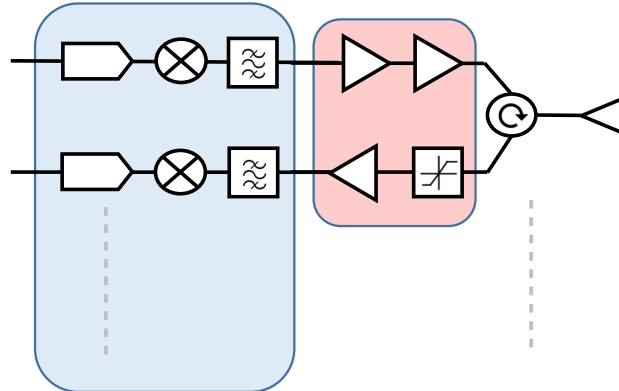
MMIC – Monolithic Microwave Integrated Circuit

RFIC – Radio Frequency Integrated Circuit

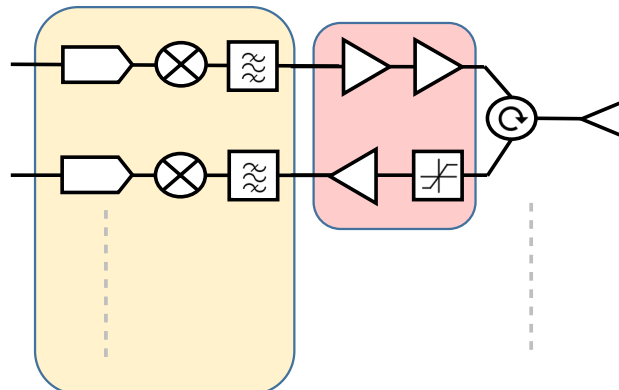
SOC – System on Chip

Semiconductor Usage

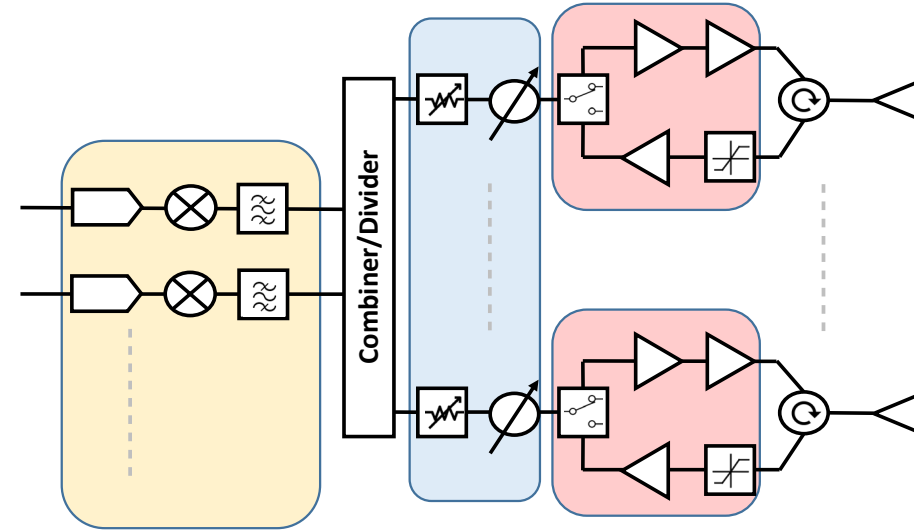
Element-Level Digital Array - SiGe



Element-Level Digital Array - CMOS



Digital Array (Subarray Level)



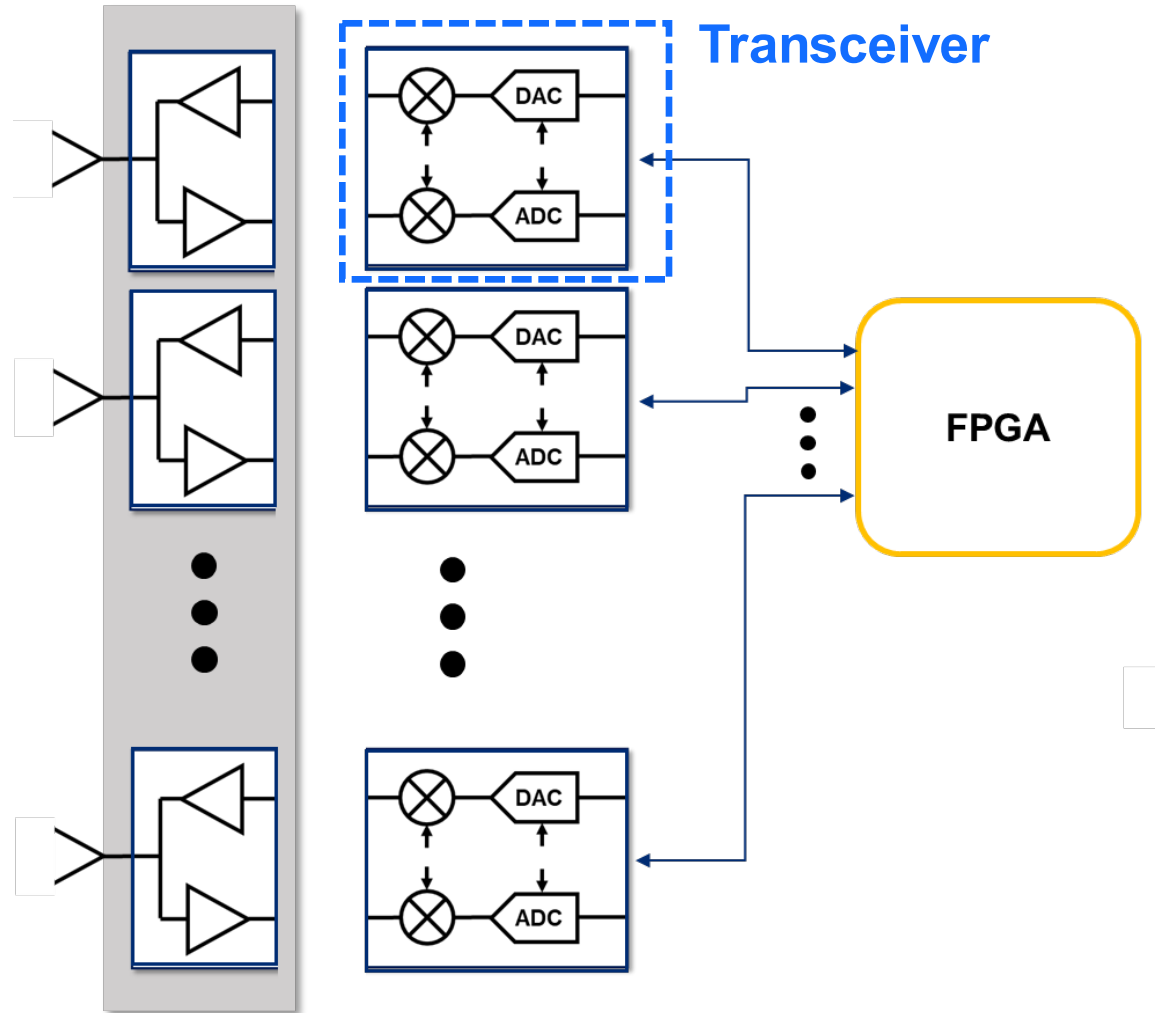
Legend

GaN
or
GaAs

SiGe

RF
CMOS

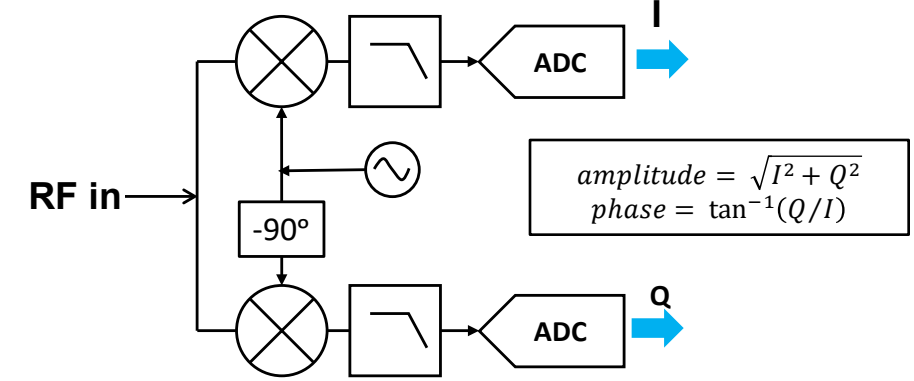
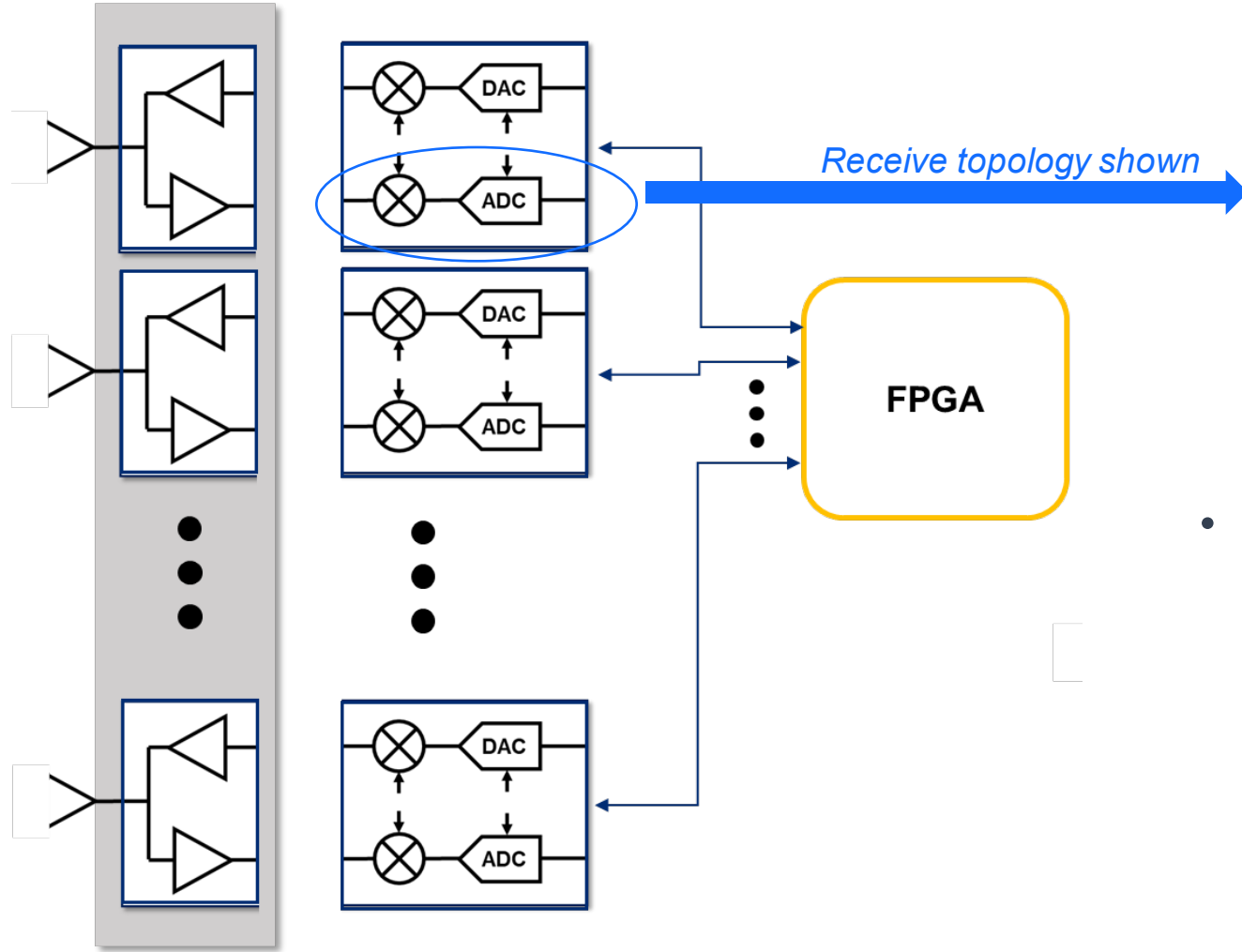
Transceiver Topologies



Transceiver Topologies

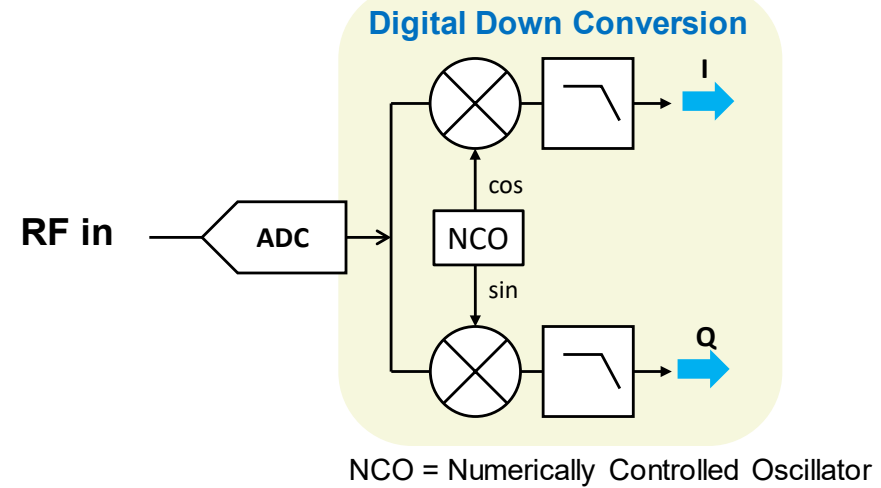
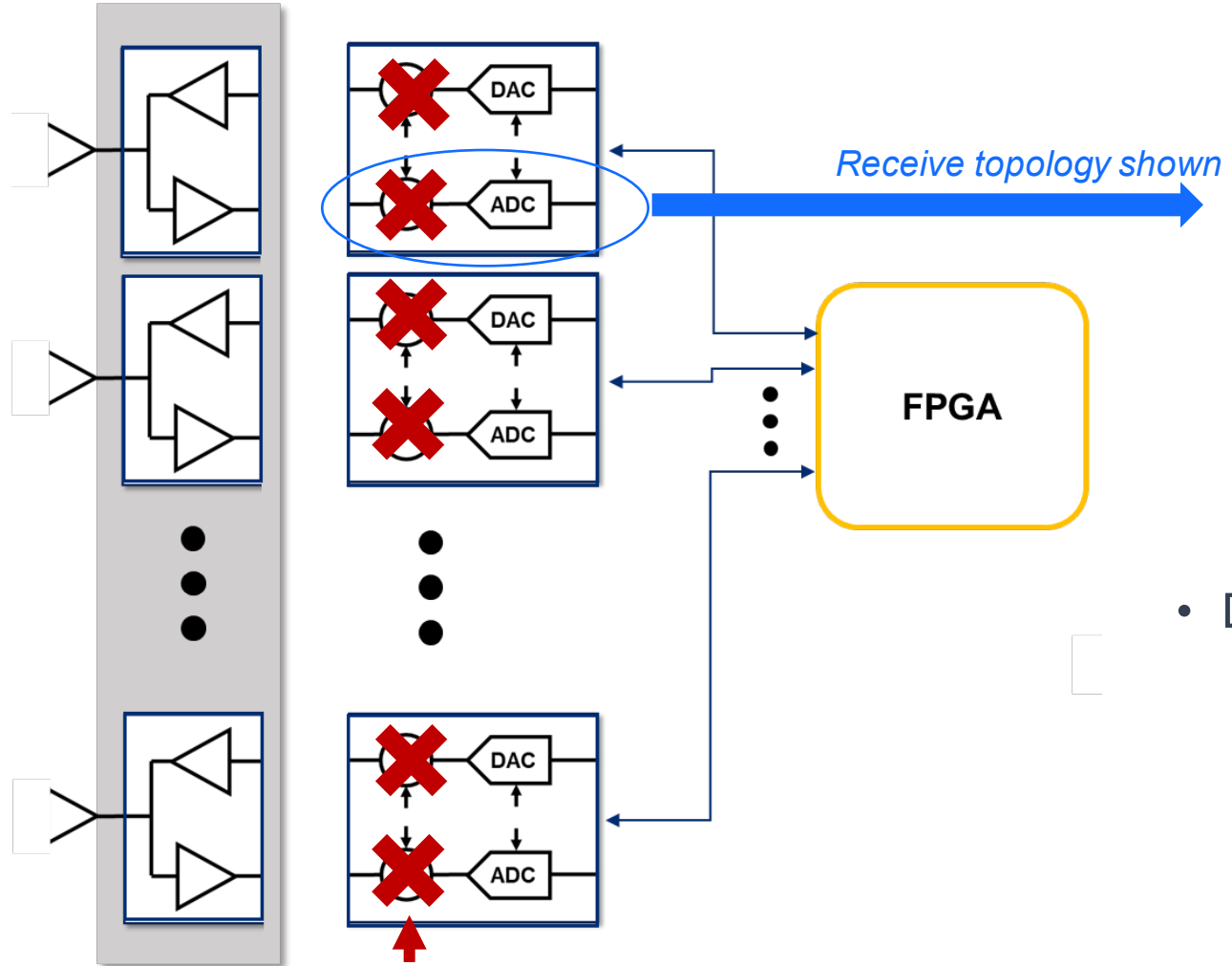
- Heterodyne (less common in Digital Arrays)
- Direct Conversion (homodyne)
- Direct Sampling

Direct Conversion Transceivers



- Direct Conversion topology:
 - (+) eases converter bandwidth requirements.
 - (+) compact for element-level use.
 - (+) low power consumption.
 - (+) good interference immunity.
 - (-) analog circuitry artifacts (DC offset, I-Q imbalance, LO leakage, etc).
 - Artifacts can be mitigated in digital arrays with many channels.

Direct Sampling Transceivers

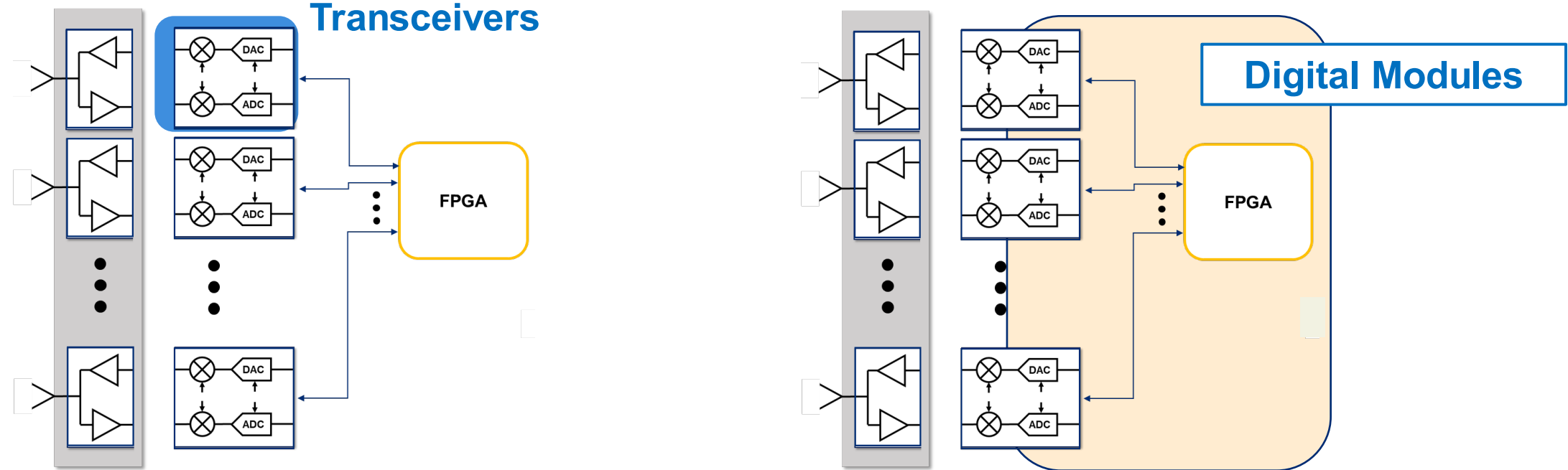


- Direct Sampling topology:
 - (+) no analog mixing or analog LO.
 - (+) digitally reconfigurable in frequency, bandwidth.
 - (+) simplest wideband operation.
 - (-) requires wider ADC input bandwidth.
 - (-) higher power consumption.

Direct Sampling implies no mixer.

(Although higher frequency applications may employ an analog down-conversion followed by Direct Sampling.)

Common Hardware Building Blocks



- SiGe or RF CMOS.
- Generally includes ADC/DAC.
- Commercial examples: Analog Devices ADRV9009, Lime Microsystems LM7002M.

- RF CMOS.
- Used w/ Direct Conversion & Direct Sampling.
- Multi-application modules.
- Commercial example: Xilinx Zynq Ultrascale-RFSoC..

Key Parameters for HW Building Blocks

Component Parameters	Transceivers	Digital Modules	Radar System Performance Relationship
Operating Frequency	🌀		Operating Frequency Band
Instantaneous Bandwidth	🌀	🌀	Range Resolution
Tx Output Power	🌀		Sensitivity driven primarily by RF Front-End power amps
Tx Phase Noise & Spurious	🌀	🌀	Clutter performance
Rcv Noise Figure	🌀	🌀	Sensitivity driven by RF Front-End LNAs
Rcv Third-Order Intercept	🌀	🌀	Linearity, Interference Mitigation
ADC # of bits	🌀	🌀	Dynamic Range
No. of Independent Tx & Rx channels	🌀	🌀	Packaging Integration & Complexity
Beam/Bandwidth Product		🌀	Multi-beam capability, mode flexibility
DC Power Consumption	🌀	🌀	Platform integration
Size and Weight	🌀	🌀	Platform integration

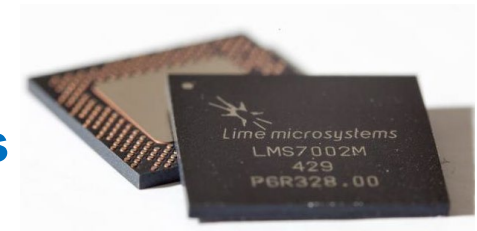
Commercial Transceiver Examples

ADRV9009
Analog Devices



- Features:
 - Dual tx and rcv channels.
 - Integrated PLL for clock & LO generation.
 - Multi-chip phase synchronization.
 - Observer receive channel.
- Key Parameters:
 - Freq: 75 MHz to 6 GHz
 - Inst BW:
 - 200 MHz receive
 - 450 MHz transmit
 - Other parameters per spec sheet:
<https://www.analog.com/media/en/technical-documentation/data-sheets/ADRV9009.pdf>

Lime 7002M
Lime Microsystems



- Features:
 - Dual tx channels; three receive channels.
 - Integrated PLL for clock & LO generation.
 - On-chip RF calibration/loopback.
- Key Parameters:
 - Freq: 100 KHz to 3.8 GHz
 - Inst BW:
 - Up to 120 MHz
 - Other parameters per spec sheet:
<https://limemicro.com/app/uploads/2017/07/LMS7002M-Data-Sheet-v3.1r00.pdf>

[7] M. Jones, et al, Integrated Transceivers Enable Small Form Factor Phased-Array Radar Platforms, Analog Devices Technical Article, June 2019.

[8] Advanced Micro Devices ADRV9009 Data Sheet (www.analog.com)

[9] Lime Microsystems LM7002M Data Sheet ([www.limemicro.com](https://limemicro.com))

Commercial Digital Back-End Example

Zynq Ultrascale+RFSoC Xilinx



RFSoC – RF System on Chip

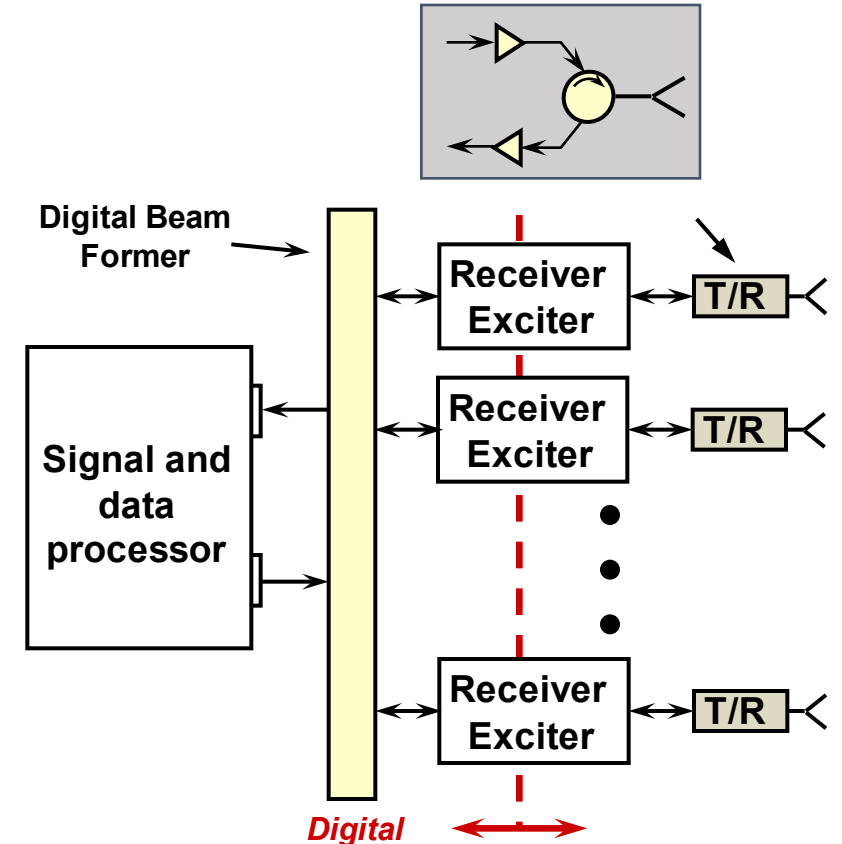
- Single chip Digital Back-End for digital arrays
 - integration of ADCs/DACs onto FPGA.
 - Software reconfigurable.
- RF in, beamformed/processed bits out.
- ZU49DR example:
 - 16 Tx and 16 Rx channels.
 - 2.5-Gsps 14-bit ADCs.
 - 10-Gsps 14-bit DACs.
- Multi-chip synchronization.
- Quadrature modulator correction.
- 4,272 DSP slices
- Eliminates Analog-FPGA interface

https://www.xilinx.com/support/documentation/data_sheets/ds889-zynq-usp-rfsooc-overview.pdf

Summary - Benefits & Challenges of Digital Arrays

- Benefits:
 - Multiple independently-steered receive beams.
 - Increased degrees of freedom for advanced processing.
 - Enhanced beam pattern performance through high precision amplitude and phase control.
 - Wideband digital True Time Delay beamforming.
 - High level of scalability and commonality.
 - Flexible, software defined arrays.
- Challenges:
 - Linearity & interference susceptibility.
 - Large degree of data transport and processing.
 - These challenges vary by specific application.

Simpler Transmit/Receive (T/R) Module



References

- 1) S. Talisa, *et. al.*, "Benefits of Digital Phased Array Radars," *Proceedings of the IEEE*, March 2016.
- 2) C. Bailey, *et al*, Design of Digital Beamforming Subarrays for a Multifunction Radar," *Proc. International Radar Conf.*, Oct. 2009.
- 3) P. Bailleul, "A New Era in Digital Beamforming for Space and Communications Arrays," *Proceedings of the IEEE*, March 2016.
- 4) A. Puglielli, "System Architecture and Signal Processing Techniques for Massive Multi-user Antenna Arrays," University of California Berkeley, 2017.
- 5) C. Fulton, *et. al.*, "Digital Arrays: Challenges and Opportunities," *Proceedings of the IEEE*, March 2016.
- 6) M. Delos, "Advanced Technologies Pave the Way for New Radar Architectures," *Analog Devices Technical Article*, November 2016.
- 7) M. Jones, *et al*, "Integrated Transceivers Enable Small Form Factor Phased-Array Radar Platforms", *Analog Devices Technical Article*, June 2019.
- 8) Advanced Micro Devices ADRV9009 Data Sheet (www.analog.com).
- 9) Lime Microsystems LM7002M Data Sheet (www.limemicro.com).
- 10) B. Farley, *et al*, "An All-Programmable 16nm RFSoC for Digital-RF Communications," *IEEE Micro*, March 2018.
- 11) Xilinx Zynq Ultrascale+RFSoC Product Specifications (www.Xilinx.com).

Good Digital Array
Reference Sources

- 
- *Proceedings of the IEEE*, vol. 104, No. 3, March 2016
 - IEEE Phased Array Systems and Technologies Conference, 2016
 - IEEE Phased Array Systems and Technologies Conference, 2019

RadarConf'22

2022 IEEE RADAR CONFERENCE



... Where Radar Innovation Never Sleeps



IEEE Region 1



LOCKHEED MARTIN



 LINCOLN LABORATORY
MASSACHUSETTS INSTITUTE OF TECHNOLOGY



Raytheon
Technologies

NORTHROP 
GRUMMAN